Investigation of novel viral vector-based influenza vaccines for broad mucosal immunity against influenza viruses in human NALT

Thesis submitted in accordance with the requirements of
the University of Liverpool for the degree of Doctor in Philosophy

By

Suttida Puksuriwong

August 2018

Abstract

Investigation of novel viral vector-based influenza vaccines for broad mucosal immunity against influenza viruses in human NALT

Suttida Puksuriwong

Influenza disease has posed a global threat by seasonal epidemics and unforeseen pandemics. The narrow protection of conventional vaccines and the unpredictable outbreaks necessitate novel influenza vaccines that provide broad protection. Since influenza virus infects humans through the nasopharyngeal mucosa, local vaccine delivery that activates cross-reactive mucosal immunity may offer an attractive vaccination strategy against virus infection and control virus transmission. Viral vector-based influenza vaccines have been currently under study and shown good safety and high systemic immunity in animal models and some in human studies. Nevertheless, the data on mucosal immunity of these vaccines in humans are still limited. The study presented here investigates the potential of *Pan paniscus* adenovirus type3- (PanAd3) and modified Vaccinia Ankara (MVA)-based influenza vaccines to induce broad T and B cell immunity against influenza subtypes in human nasopharyx-associated lymphoid tissue (NALT) using an *in vitro* cell culture system.

Firstly, influenza vaccine antigen expression was detected in adenotonsillar mononuclear cells (MNC), following stimulation by MVA-, but not PanAd3-based vaccines The MNCs, consisting of mainly lymphocytes, appeared to be refractory to PanAd3 virus infection, but susceptible to MVA virus infection. The influenza proteins (NP, M1 and HA) from MVA-NP+M1 and MVA-pdmH1HA were found predominantly in B cells and dendritic cells. Both NP and HA were intracellularly synthesised although HA later appeared to migrate to the cell membrane, whereas NP remained in the cell cytoplasm. Having shown the efficient influenza protein expression in the MNCs, the immune responses in tonsillar MNCs elicited by MVA-NP+M1 and MVA-pdmH1HA were further examined. Designed as a T cell-based vaccine, MVA-NP+M1 activated a marked increase of M1-specific cytotoxic T cell (CTL) response. The vaccine also significantly boosted $M1_{58-66}$-specific CTL responses in older children and adults, in an age-dependent manner. Besides, these cells were polyfunctional as shown by the co-expression of CD107a, IFN-γ and TNF-α in response to recall $M1_{58-66}$ peptide challenge and demonstrated the *in vitro* specific killing of peptide-pulsed target cells. In addition to MVA-NP+M1, MVA-pdmH1HA elicited cross-reactive HA-specific IgG antibodies that recognised pandemic H1N1 and heterosubtypic influenza strains in HA group1 (seasonal H1, H5 and H9), but not group 2 (H3 and H7). The stronger magnitude and the greater breadth of vaccine-induced antibodies were found in adults compared to children. Using a HAI assay, the MVA-pdmH1HA-induced antibodies were shown to bind to the head HA of pdmH1N1, but not of H5N1.

In summary, MVA-NP+M1 and MVA-pdmH1HA have the potential as mucosal vaccines to elicit cross-reactive mucosal T and B cell-mediated immune responses against a range of influenza viruses. These data provide important information for a new vaccination strategy using MVA-vectored universal influenza vaccines in intranasal vaccination against influenza in humans.

Declaration

No part of the work referred to in this thesis has been submitted in support of an application for another degree or qualification at this or any other university, or other institution of learning. All laboratory work described here has been carried out by the author at the department of Clinical Infection, Microbiology and Immunology, Institute of Infection and Global Health, University of Liverpool.

Suttida Puksuriwong

August 2018

Acknowledgement

I deeply thank my primary supervisor Dr. Qibo Zhang for his kindness and constant support throughout my 4-year study at University of Liverpool. His knowledge and advices in vaccine immunology contribute to my invaluable PhD experience. My thanks are also given to my secondary supervisor, Prof. Paul McNamara and my panel assessors; Dr. Steve Christmas and Dr. Neil Blake, for their useful guidance and suggestions.

Many many thanks to all members in Zhang's group and friends at CIMI department, who make my days at IGH full of unforgettable memories. There are some I would like to mention here; Lualuaa Zaki, Lindsay McKay, Charlene Adaken, Marion Pouget, Jeoffrey Segura and Khandaker Shadia. Moreover, this is in particular to. Dr. Muhammad Shamsher Ahmed for teaching me many immunological techniques used in my project and to Rong Xu for being the best friend and the best colleague, whom I can always discuss either personal or work issues with. Both Shamsher and Rong also provide critical feedbacks on my thesis. I would like to thank Dr. Lance Turtle for SPICE software tutorial. Also I can't forget to thank for the helpful technical supports provided by Caroline Broughton, Dr. Debbie Howarth, Dr. Carmen Martinez-Rodriguez, Dr. Victoria Sheridan and their team. I wish to thank the patients who took part in the study and the theatre staff in Alder Hey Children's Hospital, Royal Liverpool and Broadgreen University Hospitals and Aintree University Hospital for helping the collection of samples. I also thank Biodefense and Emerging Infections Research Resources Repository (BEI Resources, USA) and International Reagent Resource (IRR, USA) for providing a number of influenza reagents used in my project.

My special thanks are also given to Asso. Prof. Mullika Chomnawang for the opportunity I had to learn and carry out my first own research project many years ago when I was just a pharmacy student and that paved my way to the world of research. I cannot forget mentioning these two people; Mr. Yoshitaka Tajima and Mr. Shuro Gotou from The Chemo-Sero-Therapeutic Research Institute (Kaketsuken), whom I learned and acquired lots of knowledge of influenza vaccine development from when I was a junior researcher at GPO and that is the beginning of the more interest in the influenza vaccine research.

I also would like to thank my sponsor, the Government Pharmaceutical Organization (GPO), Thailand for the financial support and also my supportive bosses, Dr. Ponthip Wirachwong and Dr. Somchaiya Surichan.

It would not be such lovely years in Liverpool without all warm-hearted Thai friends around especially Yin (Dr. Thanalai Poonsiri), Kiang (Wasu Supharattanasitthi), P'Gluay (Phakakorn Panpho), Mai (Jiraporn Panmanee) and Pong (Panupong Thongprem) and also staff including tasty Thai foods from Chaba Chaba restaurant.

Last but not least, it can't be enough to express my gratitude to my dearest parents and my sister who always stand by me with eternal love and encouragement. You are always the wind beneath my wings.

- ขอบพระคุณพ่อและแม่ ผู้ซึ่งคอยสนับสนุนและให้กำลังใจนุ่นอยู่เสมอ -

List of Publications

Journal articles

J. Mullin, M. S. Ahmed, R. Sharma, N. Upile, H. Beer, P. Achar, **S. Puksuriwong**, F. Ferrara, N. Temperton, P. McNamara, T. Lambe, S. C. Gilbert, and Q. Zhang, "Activation of cross-reactive mucosal T and B cell responses in human nasopharynx-associated lymphoid tissue in vitro by Modified Vaccinia Ankara-vectored influenza vaccines.," *Vaccine*, vol. 34, no. 14, pp. 1688–1695, Mar. 2016.

A. Aljurayyan, **S. Puksuriwong**, M. Ahmed, R. Sharma, M. Krishnan, S. Sood, K. Davies, D. Rajashekar, S. Leong, P. S. McNamara, S. Gordon, and Q. Zhang, "Activation and induction of antigen-specific T follicular helper cells play a critical role in live-attenuated influenza vaccine-induced human mucosal anti-influenza antibody response," *J. Virol.*, vol. 92, no. 11, pp. e00114-18, Mar. 2018.

Manuscript under preparation

S. Puksuriwong, M. Ahmed, R. Sharma, M. Krishnan, S. Leong, T. Lambe, P. S. McNamara, S. C. Gilbert, Q. Zhang, "Activation of mucosal M1-specific cross-reactive cytotoxic T cell response in human nasopharynx-associated lymphoid tissue against influenza virus by MVA-NP+M1 vaccine"

Accepted abstract

S. Puksuriwong, N. Upile, C. Vaughan, P. McNamara, H. Beer, M. McCormick, T. Lambe, S. C. Gilbert and Q. Zhang, "Expression of influenza transgenes encoded in Modified Vaccinia Ankara viral vector as candidate influenza vector-based vaccines in the *in vitro* nasopharynx associated lymphoid tissues model", Institute of Infection and Global Health Research Day, November 2015 *(Poster presentation)*

S. Puksuriwong, M. S. Ahmed, R. Sharma, H. Beer, A. Markey, M. McCormick, T. Lambe, P. McNamara, S. C. Gilbert and Q. Zhang, "Activation of cross-reactive anti-influenza responses by MVA-based influenza vaccines", Institute of Infection and Global Health Research Day, November 2016 *(Oral presentation)*

S. Puksuriwong, M. S. Ahmed, R. Sharma, H. Beer, A. Markey, M. McCormick, T. Lambe, P. McNamara, S. C. Gilbert and Q. Zhang, "Novel MVA-based vaccines expressing conserved influenza antigens activate cross-reactive T and B cell responses in human NALT against influenza virus". British Society for Immunology and Dutch Society for Immunology (BSI and NVVI) conference, December 2016 *(Poster presentation)*

S. Puksuriwong, M. S. Ahmed, R. Sharma, H. Beer, A. Markey, M. McCormick, T. Lambe, P. McNamara, S. C. Gilbert and Q. Zhang, "Novel MVA-based vaccine expressing conserved influenza NP and M1 activates cross-reactive T cell responses in human NALT". British Society for Immunology (BSI) conference, December 2017 *(Poster presentation)*

S. Puksuriwong, M. S. Ahmed, R. Sharma, M. Krishnan, S. Sood, M. McCormick, S. Leong, T. Lambe, P. McNamara, S. C. Gilbert, and Q. Zhang, "Novel MVA-based vaccine expressing influenza NP and M1 activates cross-reactive T cell responses in human nasopharynx-associated lymphoid tissue (NALT)," *J. Immunol.*, vol. 200, no. 1 Supplement, 2018. *(Poster presentation)*

Table of contents

List of Tables

List of Figures

List of Abbreviations

°C	Degree Celsius
ΔFBS	Heat-inactivated Fetal Bovine Serum
µg	Microgram
µl	Microlitre
µm	Micrometre
A/PR/8	A/Puerto Rico/8/1934 (H1N1)
ADCC	Antibody-dependent cellular cytotoxicity
ADP	Antibody-mediated phagocytosis
AEC	3-amino-9-ethyl carbazole
aHP	Autologous human plasma
ANOVA	One-way analysis of variance
APC	Antigen-presenting cell
BFA	Brefeldin A
BLP	Betapropiolactone
bnAb	Broad neutralising antibody
BSA	Bovine serum albumin
CAR	Coxsackievirus and adenovirus receptor
CD	Cluster of differentiation
CDL	Complement-dependent lysis
CFDASE	Carboxyfluorescein diacetate succinimidyl ester
CFSE	Carboxyfluorescein succinimidyl ester
ChAd	Chimpanzee adenovirus
CO_2	Carbon dioxide
CTL	Cytotoxic T lymphocyte
CV-1	Monkey kidney fibroblast cell line
DC	Dendritic cell
DMEM	Dulbecco's Modified Eagle Medium
DMF	*N, N*-Dimethylformamide, anhydrous
DMSO	Dimethyl sulphoxide
DPBS	Dulbecco's Phosphate-Buffered Saline (no Calcium and Magnesium)
ELISA	Enzyme-linked Immunosorbent Assay
ELISPOT	Enzyme-linked ImmunoSpot Assay
Fcγ-R	Fc gamma receptor
FDC	Follicular dendritic cell
FFU	Fluorescent focus unit
FSC	Forward Scatter
g	Gram
GC	Germinal centre
GFP	Green Fluorescent Protein

HA	Haemagglutinin
HA1	Globular head domain of haemagglutinin
HA2	Stalk domain of haemagglutinin
hAd	Human adenovirus
HAI	Haemagglutination inhibition
HBSS	Hank's balanced salt solution
HCMV	Human cytomegalovirus
HEK 293	Human embryonic kidney cells 293
HEV	High endothelial venules
HIV	Human immunodeficiency virus
HLA	Human leukocyte antigen
HRP	Horseradish peroxidase
IAV	Influenza A virus
IBV	Influenza B virus
ICS	Intracellular staining
IFN-γ	Interferon-gamma
IgA	Immunoglobulin A
IgG	Immunoglobulin G
IgM	Immunoglobulin M
IIV	Inactivated influenza vaccine
IL	Interleukin
ISG	Interferon-stimulating genes
LAIV	Live attenuated influenza vaccine
M	Molar
M cell	Microfold cell
M1	Matrix protein 1
M1-Tm	M1 Tetramer (HLA-A02*01- GILGFVFTL ($M1_{58-66}$)-PE tetramer)
M2e	Extracellular domain of matrix protein 2
mAb	Monoclonal antibody
mDC	Myeloid dendritic cell
MFI	Median fluorescence intensity
mg	Milligram
mH5	Modified Vaccinia H5 promotor
MHC	Major histocompatibility complex
ml	Millilitre
MNC	Adenotonsillar mononuclear cell
MOI	Multiplicity of Infection
MVA	Modified Vaccinia Ankara
MW	Molecular weight
NA	Neuraminidase
nAb	Neutralising antibody
NALT	Nasopharynx-associated lymphoid tissue
NEP/NS2	Nuclear export protein/ Nonstructural protein 2

ng	Nanogram
NK cell	Natural killer cell
NLRP3	NOD-like receptor family pyrin domain containing 3
NP	Nucleoprotein
OD	Optical density
PanAd	*Pan paniscus* (bonobo) adenovirus
PBMC	Peripheral blood mononuclear cell
pDC	Plasmacytoid dendritic cell
pdm H1N1	Pandemic influenza H1N1 (2009)
PI	Propidium iodide
pIgR	Polymeric immunoglobulin receptor
PNPP	*p*-Nitrophenylphosphate
PRR	Pattern-recognition receptors
PVDF	Polyvinylidene fluoride
R10	RPMI-1640 medium containing 10% ΔFBS with HEPES, L-glutamine and penicillin/streptomycin
R10AmpB	R10 containing 0.25 µg/ml amphotericin B
rAd	Recombinant adenovirus
RBC	Red blood cell
RBS	Receptor-binding site
RDE	Receptor-destroying enzyme
RIG-I	Retinoic acid inducible gene-I
RPE	R-Phycoerythrin
RPMI-1640	Roswell Park Memorial Institute-1640 medium
SEB	Staphylococcal enterotoxin B
SEM	The standard error of the mean
SFC	Spot forming cell
SIgA	Secretory IgA antibody
SSC	Side Scatter
TCR	T-cell receptor
T_{FH}	T follicular helper cell
Th1	T helper 1
Th17	T helper 17
Th2	T helper 2
TLR	Toll-like receptor
TNF-α	Tumour necrosis factor-alpha
T_{reg}	Regulatory T cell
T_{RM}	Tissue-resident memory T cells
U/ml	Unit/millilitre
vp	Virus particle
vRNP	Viral ribonucleoprotein
VV	Vaccinia Virus
WCP	Unfractionated adenotonsillar mononuclear cells

Chapter 1

General introduction

1.1. Influenza virus

Influenza virus is a member of family *Orthomyxoviridae*. It is characterised as an eight-segmented, negative-stranded RNA, enveloped virus. The shape of influenza virus is spherical, approximately 100 nm in diameter or filamentous in excess of 300 nm in length. As shown in Figure 1.1, the virus is formed of a lipid bilayer integrated with two glycoproteins; haemagglutinin (HA) and neuraminidase (NA) and the ion-channel; matrix protein 2 (M2). Underneath the envelope overlays matrix protein 1 (M1), which encloses virion core and nuclear export protein/nonstructural protein 2 (NEP/NS2). The core of the virus is composed of eight segmented-viral RNAs, each of which is coated with nucleoprotein (NP) complex and heterotrimeric RNA-dependent RNA polymerase (PB1, PB2 and PA), called viral ribonucleoprotein (vRNP) [1].

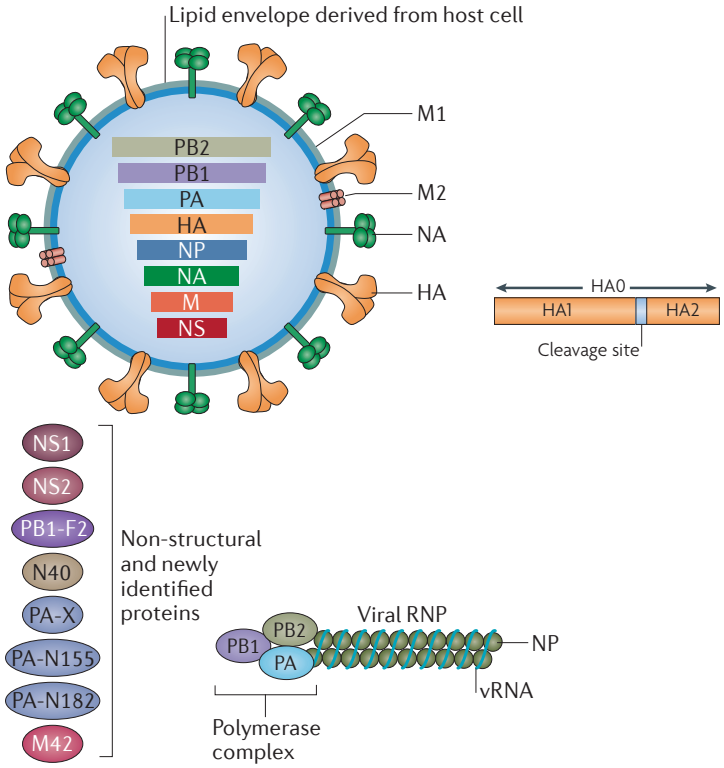

Figure 1.1 Structure of influenza virus

The envelope of influenza virus consists of haemagglutinin (HA), neuraminidase (NA) and matrix protein 2 (M2). HA0 is cleaved by host cell proteases into globular head (HA1) and stalk (HA2) and becomes active. Underneath the lipid envelope are matrix protein 1 (M1), non-structural proteins (e.g. NS1 and NS2) and eight-segmented viral ribonucleoproteins (vRNP). Each vRNP is composed of viral RNA, coated with nucleoprotein (NP) and RNA polymerase complex (PB1, PB2 and PA) (Adapted from [2], [3]).

Influenza viruses are classified into 4 types; A, B, C and D based on PB1 sequences [4]. Influenza A and B viruses are responsible for seasonal epidemics, causing human disease of any concern, while influenza C viruses causes sporadic mild illness in humans. Influenza D viruses affect cattle and are not known to infect or cause illness in people. Only influenza A viruses (IAV) are known to have caused pandemics [4]. IAVs are further classified into subtypes based on HA and NA glycoproteins [1], for example H1N1 and H3N2. To date, 18 HA and 11 NA have been identified, resulting in the large diversity of the virus. IAVs can also be classified into 2 groups based on the HA phylogeny; HA group 1 (H1, H2, H5, H6, H8, H9, H11, H12, H13, H16, H17, H18) and HA group 2 (H3, H4, H7, H10, H14, H15). Influenza B viruses (IBV) are classified into two antigenically distinct lineages; Victoria and Yamagata [5]–[7] (Figure 1.2). IAVs have a variety of hosts ranged from mammals to avian e.g. swine, cattle, equines, humans, bats, chickens and the most important one; wild waterfowl which host almost all IAV subtypes. Although each virus subtype is likely to have a restricted host, some could have multiple hosts. For example, H1, H2 and H3 virus strains could infect fowl, swine and humans. In contrast to IAVs, IBVs have limited host ranges only in humans and seals [8].

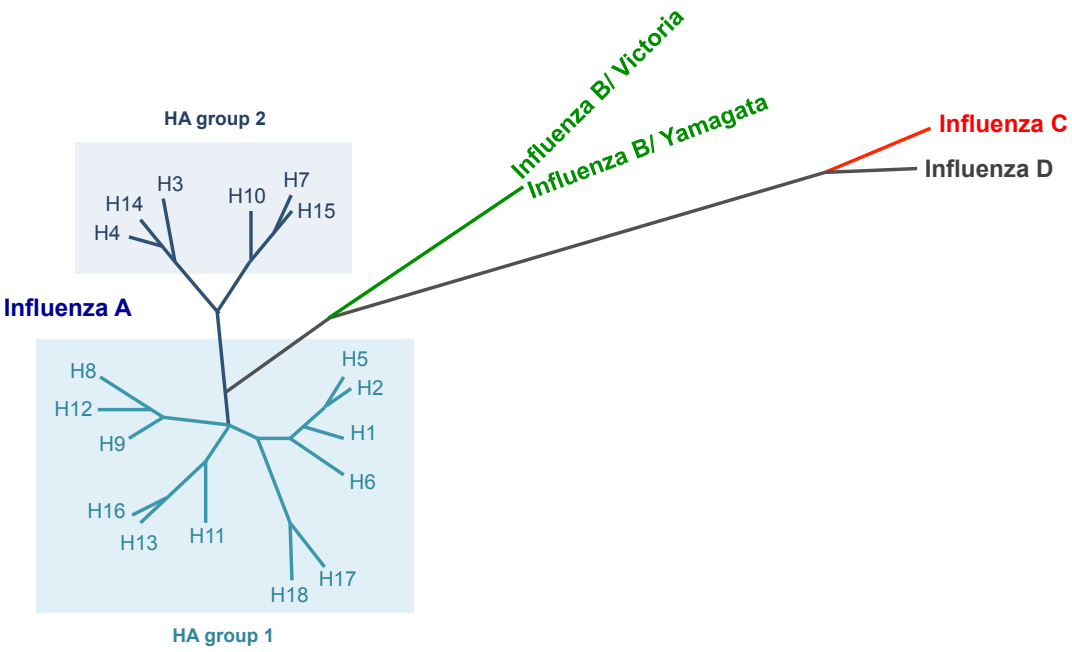

Figure 1.2 Phylogenetic tree of influenza viruses

Influenza viruses are classified into 4 types; A, B, C and D based on PB1 sequences. Influenza A viruses are further classified into 2 groups based on HA phylogeny and influenza B viruses are also separated into 2 lineages; Victoria and Yamagata (Adapted from [9]).

Influenza virus infects humans by recognising sialic acid on host cell surfaces and facilitating its HA spike to bind. Sialic acid is normally found at the terminal of glycoconjugates, which are ubiquitous on many cell types [1]. Human influenza subtypes (H1, H3) target α-2, 6 linkage of sialic acid molecules, which are commonly found on tracheal epithelial cells. In contrast, avian influenza viruses (e.g. H5), causing zoonotic infection bind to α-2, 3 linkage of sialic acid molecules in lungs, causing higher pathology and more severe symptoms [10]. Following the attachment via binding globular head of HA to sialic acid, the virus is endocytosed into host cell cytoplasm. At this stage, M2 proteins, transmembrane ion channels, pump hydrogen ions from the endosome into the virus particle. The low pH then triggers the conformational change of HA, where fusion peptide on the stalk of HA mediates the merging of virus membrane and endosomal membrane in order to release vRNP. The synthesis of viral RNA segments occurs in nucleus, which they are later exported via nucleoporins to cell cytoplasm after the interaction of M1 protein with vRNP-NEP complex. Viral proteins; HA, NA and M2 are synthesised from viral mRNA in endoplasmic reticulum and post-translationally modified in the Golgi apparatus of the cell cytoplasm. Cleavage of the HA0 into HA1 and HA2 by cellular proteases is required for viral infectivity. They are subsequently located to the cell plasma membrane for virus assembly, where HA continues to bind sialic acid at the cell membrane and M1 accumulates at the lipid bilayer of the cell membrane together with a pack of eight segmented-RNA complexes. Finally, NA cleaves the terminal sialic residues from cell-surface glycoproteins to release progeny virus [1] (Figure 1.3).

Due to the nature of RNA viruses, the error-prone RNA-dependent RNA polymerases enable the virus to undergo antigenic drift, where some amino acids of viral proteins including HA are mutated causing seasonal epidemics. Regarding their segmented genomes, it also enables the virus to undergo antigenic shift, where segmented genomes from different subtypes are reassembled, generating a novel virus strain, which could cause pandemic outbreak. This phenomenon is mainly observed among IAVs, when 2 or more virus subtypes co-infect in the same host [1]. For instance, pandemic H1N1 in 2009 is a swine origin, resulting from the reassortment of a triple reassortant (from human H3N2, North American avian and classical swine viruses) swine virus and a Eurasian avian-like swine virus [11].

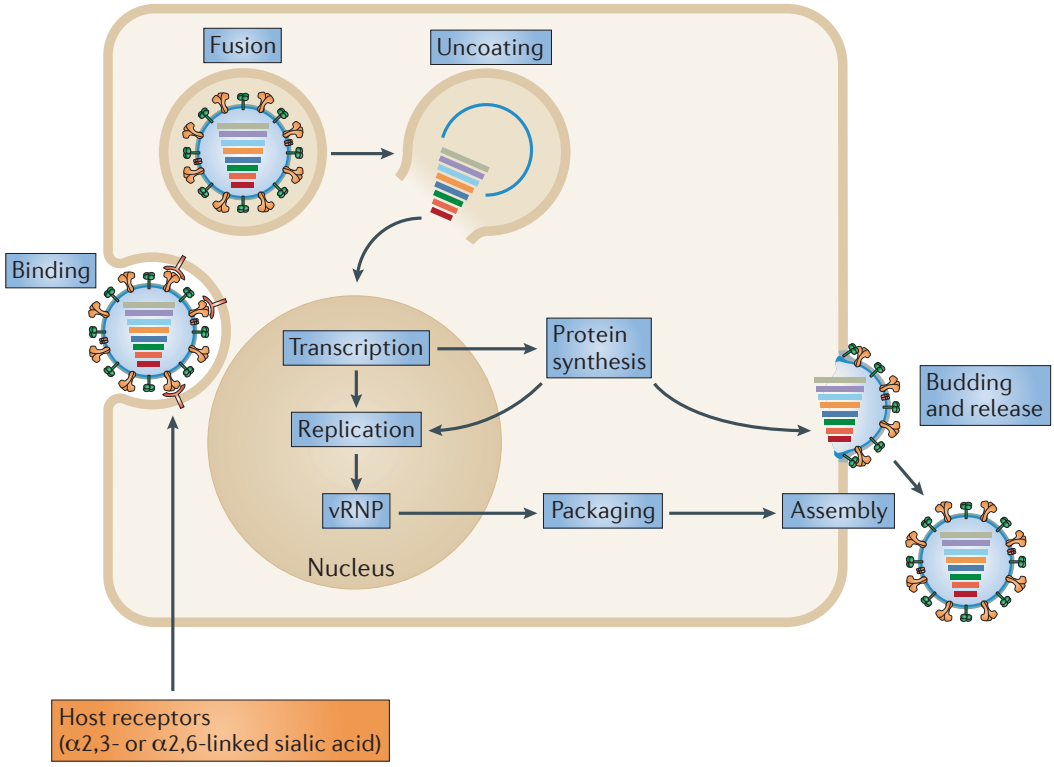

Figure 1.3 Life cycle of influenza virus

Influenza virus infects the host by facilitating its haemagglutinin (HA) to bind either α 2,3 or α 2,6 – linked sialic acid on host cells. The virus is endocytosed into the cell cytosol before becoming uncoated to release viral ribonucleoprotein (vRNP). The viral RNA is replicated in the cell nucleus before being exported to the cytosol, while viral proteins are synthesised from mRNA in the cell cytoplasm. All virus components are assembled at the cell membrane, where progeny viruses are released [2].

Influenza viruses cause respiratory disease, which is easily transmitted between humans by inhalation of virus-containing aerosols produced by sneezing or coughing. Every year, seasonal IAV epidemics cause 3-5 million cases of severe infection and up to 500,000 deaths around the world [12]. The viruses can infect all age groups and the infection rate could be as high as 40% in young children. Children under 2 years old, pregnant women and those who have underlying medical conditions are particularly at risk of hospitalisation. Moreover, mortality rate increases in the elderly over 65 years of age and immuno-compromised people [12]. Influenza pandemics on the other hand cause the higher rate of mortality and morbidity in humans due to the lack of memory immune responses to the new emerging viruses. The virus can infect people easily and rapidly spread from person to person. This has been shown during the outbreak by 1918 H1N1, 1957 H2N2, 1968 H3N2 and the recent one 2009 pdmH1N1 (Figure 1.4) [13].

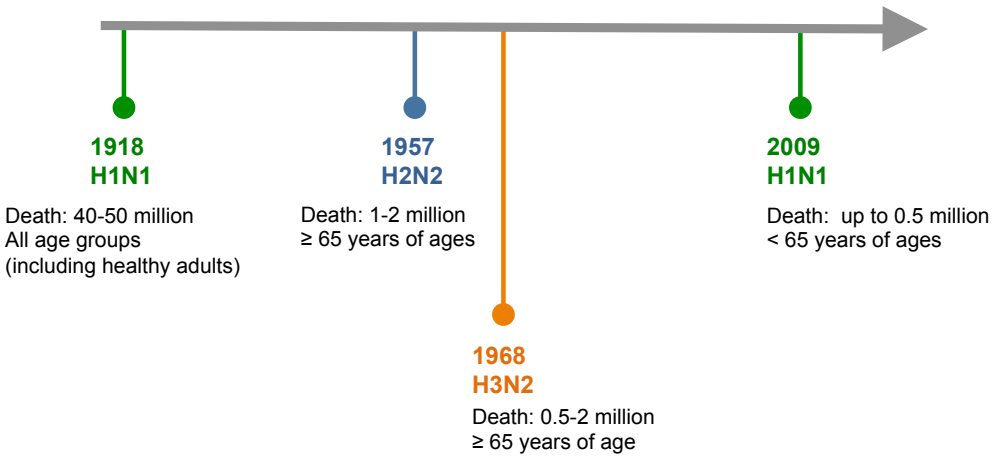

Figure 1.4 Recent influenza pandemics and their impact

The timeline shows recent influenza pandemic outbreaks in 1918, 1957, 1968 and 2009. The estimated number of deaths worldwide and the target group with the high mortality rate are shown [13].

1.2. Immune responses to influenza virus infection

Influenza virus infection induces innate and adaptive immune responses. While innate immunity provides early non-specific response to virus infection, adaptive immunity is generated later and offers a more efficient and specific response (Figure 1.5).

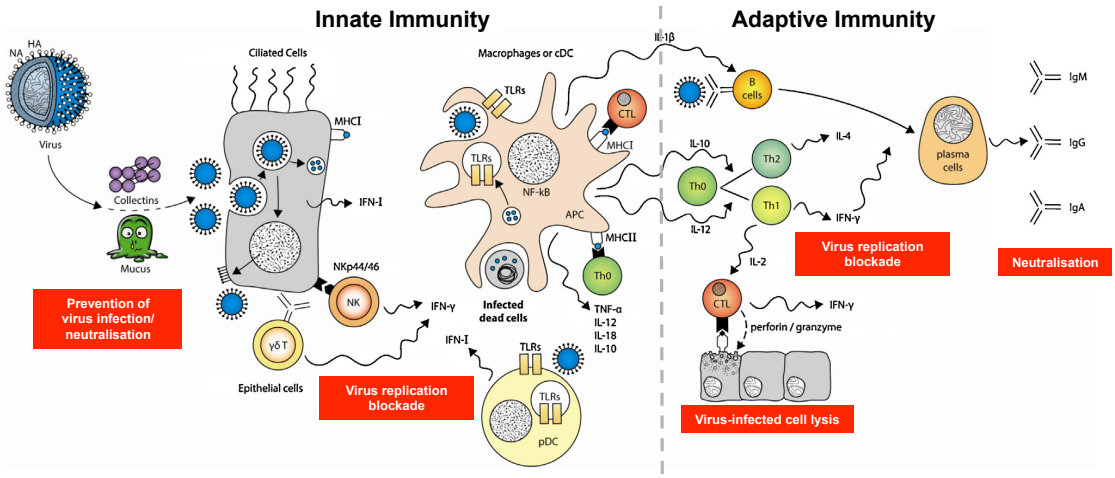

Figure 1.5 Immune responses to influenza infection

Influenza virus infection induces both innate and adaptive immune responses. Innate immunity involves mucus and collectins at the mucosal surface and innate immune cell response from macrophages, natural killer (NK) cells and dendritic cells (DC). DCs present virus antigens to T and B cells to trigger adaptive immunity, leading to the proliferation of antigen-specific T cells and the production of antibodies against influenza virus [14], [15].

1.2.1. Innate immunity

The innate immune system is the first defence mechanism to prevent the virus infection and to control the virus replication. Mucus and collectins (as antiviral agents) at the mucosal surface prevent virus infection of epithelial cells [14]. Influenza virus infection is sensed via pattern-recognition receptors (PRR) that recognise other virus-infected cells or different forms of viral RNA presented in infected cells. The PRRs are toll-like receptors (TLR), retinoic acid inducible gene-I (RIG-I) and the NOD-like receptor family pyrin domain containing 3 (NLRP3) proteins. Viral recognition by TLRs and RIG-I signals the production of proinflammatory cytokines and type I interferons. The strong antiviral activity of type I interferons inhibits the protein synthesis of host cells, limiting virus replication. Moreover, type I interferons induce interferon-stimulating genes (ISG), which also stimulate dendritic cells (DC), enhancing the viral antigen presentation to $CD4^+$ and $CD8^+$ T cells. NLPR3 as part of the inflammasome is activated by virus infection and M2 activity then converts pro-IL-1β into IL-1β, which induces Th17 differentiation and expands the antigen-specific $CD4^+$ T cells [16] (Figure 1.6).

Virus spreading could be limited by the clearance of virus-infected cells via alveolar macrophage-mediated phagocytosis as well as via cell lysis by natural killer (NK) cells upon the recognition of antibody-bound virus infected cells. Importantly, innate immune cells such as professional antigen-presenting cells including DCs, also process and present viral antigens by MHC class I or class II molecules to either $CD8^+$ or $CD4^+$ T cells to trigger the adaptive immune responses [17], [15].

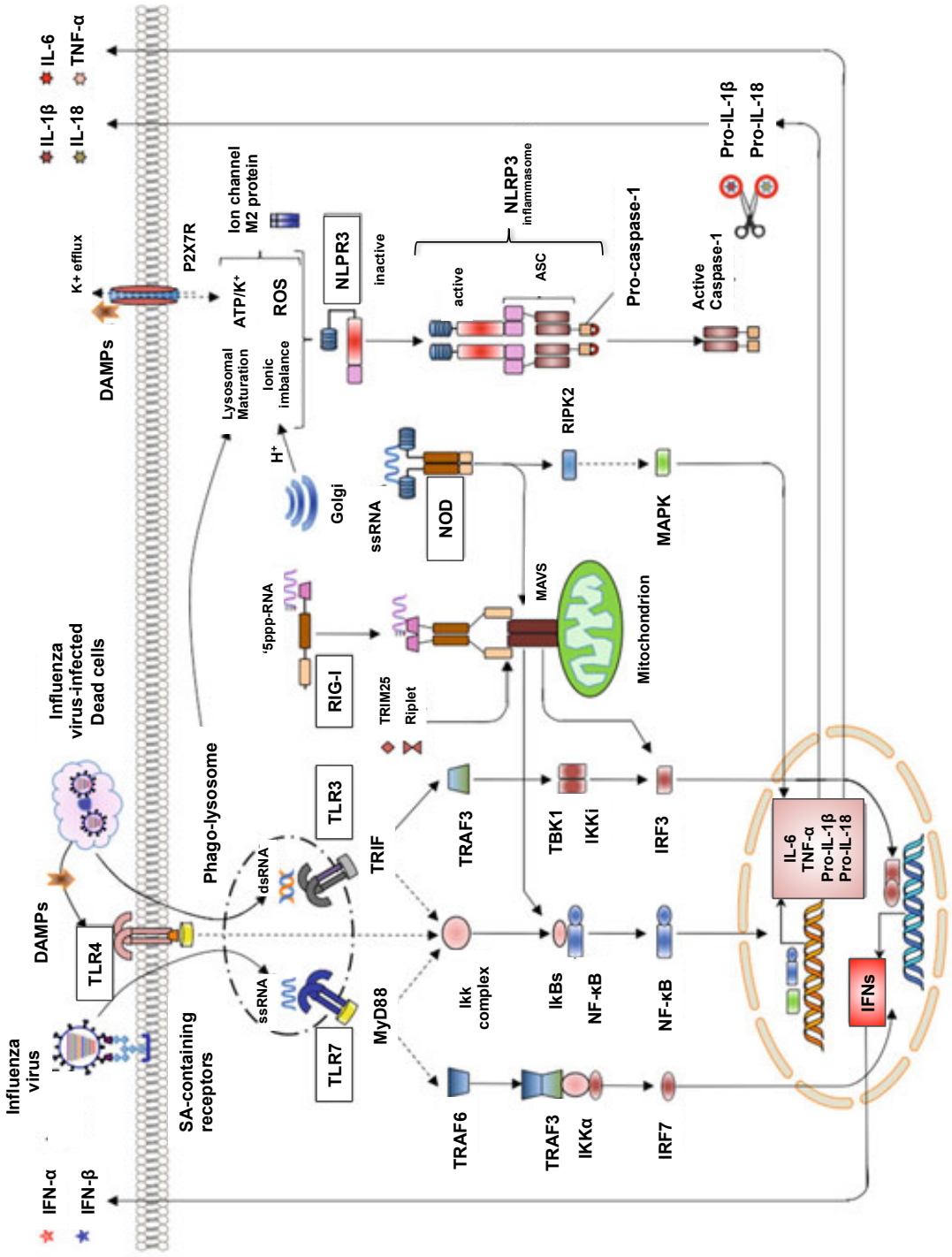

Figure 1.6 Recognition of influenza virus infection by pattern-recognition receptors and their responses

Influenza virus and influenza virus-infected cells are sensed via pattern-recognition receptors (PRR); TLRs, RIG-I, NOD2 and NLRP3 that recognise other virus-infected cells or different forms of viral RNA e.g. single-stranded RNA (ssRNA), double-stranded RNA (dsRNA) or virus proteins e.g. M2. Activation of these PRRs leads to the induction of interferon-stimulating genes (ISG) and the production of pro-inflammatory cytokines [17].

1.2.2. Adaptive immunity

The adaptive immune system is the second line of protection, which consists of humoral and cellular immunity mediated by virus-specific antibody and T cells, respectively. Both mucosal and systemic immune responses are associated with the protection against subsequent influenza virus infection.

1.2.2.1. Antibody-mediated immunity

Influenza virus infection induces virus-specific antibody response particularly towards two viral glycoproteins; HA and NA. Neutralising HA-specific antibodies are considered the most important due to the induction of sterile immunity preventing infection. The antibodies are predominantly directed to the globular HA head due to its immunodominance. Binding to the virus, they inhibit virus attachment and entry into host cells, leading to the prevention of virus infection [15], [18]. Subdominant antibodies towards the conserved HA stalk are also elicited, but at relatively lower amount [19]. However, HA stalk-specific antibodies react to a wider range of influenza viruses compared to HA head-specific ones, therefore may provide cross-reactive protection [20], [21].

Following virus infection, antibodies to other viral proteins such as NA and M2 can be also induced [15]. Anti-NA antibodies inhibit enzymatic activity of NA, resulting in limiting virus release. Although NP is a target for T cell responses, NP-specific antibodies may also contribute to the protection against influenza. These antibodies are generally considered non-neutralising and most likely to act via antibody-dependent cell lysis or complement-dependent cytotoxicity to confer protective potential [15], [18].

IgA, IgM and IgG are the main antibody isotypes elicited in response to virus infection. Secretory IgA antibodies (SIgA) are produced locally and transported to mucosal surfaces via poly Ig receptors on epithelial cell membranes. Serum IgA is rapidly produced after virus infection, while IgM antibodies are the hallmark of response to primary infection. Serum IgG antibodies are predominantly produced and can be diffused to respiratory mucosa, providing long-lived protection for subsequent influenza infection [15].

1.2.2.2. Cell-mediated immunity

Upon influenza virus infection, $CD4^+$ and $CD8^+$ T cells are activated by the recognition of viral antigens presented on either MHC class I or class II together with costimulatory signals. The majority of $CD4^+$ T cells have T helper properties. Th1 cells produce IL-2 and IFN-γ, which promote cytotoxic $CD8^+$ T cell (CTL) responses, whereas Th2 cells secrete IL-4 and IL-10 that are involved in helping B cell responses. Th17 and T_{reg} cells regulate the cellular immune responses during virus infection. CTLs play an important role in elimination of virus-infected cells, thus reducing virus shedding. Antigen-specific $CD8^+$ T cells are found in lymphoid tissues and in the circulation post infection. These memory $CD8^+$ T cells can rapidly respond to subsequent influenza infection. In humans, $CD8^+$ T cells induced by influenza viruses are mainly directed to internal viral proteins such as NP, M1 and PB. Owing to the highly conserved nature of these viral antigens, antigen-specific $CD8^+$ T cells could recognise diverse influenza strains and provide cross-reactive protection [15].

1.3. Current influenza vaccines

Vaccination is the most effective tool to prevent and control influenza infection [22]. The vaccines aim to induce adaptive immunity, providing protection against infection and disease and to induce herd immunity to restrict virus transmission within the population [22]. The current vaccines are composed of three or four virus vaccine strains; two IAVs (H1 and H3 subtypes) with one or two IBVs (Yamagata and/ or Victoria lineages). The vaccine strains are annually predicted by the World Health Organization (WHO) based on the epidemiological data of predominantly circulating strains in either northern or southern hemispheres [23]. Annual immunisation with seasonal influenza vaccines is recommended for target groups, which are children, elderly, pregnant women, and those having any underlying medical conditions such as asthma, chronic lung disease and heart disease, who are at risk of developing influenza-related complications [24]. Two types of seasonal influenza vaccines are commercially available; inactivated and live attenuated vaccines.

1.3.1. Inactivated influenza vaccines

Inactivated influenza vaccines (IIV) are available in different formulas ranging from whole virus to split virus and subunit vaccines. The vaccines are made of purified chemicals/ detergent-killed influenza viruses. While the subunit vaccine is composed of only purified HA and NA of influenza, the split one consists of other viral proteins and subviral elements such as M1 and NP. Inactivated-whole virus vaccines are mostly replaced by split and subunit ones, which provide comparable degrees of immunogenicity but less reactogenicity [22]. After intramuscular administration, IIVs predominantly induce serum IgG antibodies towards globular HA, showing positive haemagglutination inhibition (HAI), which indicates strain-specificity. 90% of vaccinees showed protective antibody titres within 2 weeks post vaccination. Nevertheless, the antibodies rapidly wane to 2-fold lower at 6 months after immunisation [25]. The vaccine effectiveness is approximately 60% in adults aged 18-65 years [26], but may reduce in young (immune-naïve) and elderly (immunosenescence) and in years of poor antigenic match [27]. IIVs are recommended for young children at 6-24 months and older children including adults 18 years of age or older and are also advised for at risk groups e.g. pregnant women and immunocompromised people. Recently, MF59C.1 adjuvanted IIVs are licensed and given in elderly 65 years of age or older to achieve protective responses [28].

1.3.2. Live attenuated influenza vaccines

Live attenuated influenza vaccines (LAIV) are the more recently developed vaccines to mimic the natural influenza infection. The virus vaccine strains are developed by subpassaging in embryonated chicken eggs under suboptimal conditions so that they are able to only grow at restricted temperature between 25°C (cold-adapted*, ca*) and 35°C (temperature sensitive, *ts*). Consequently, the virus infects and replicates only at the mucosa of the upper respiratory tract, not in the lungs after intranasal administration [29]. LAIVs also elicit serum IgG antibodies, but at a lower magnitude than IIVs. In comparison to IIVs, LAIVs induce stronger mucosal IgA antibodies and CTL response, which may provide broader immunity against circulating virus strains. SIgA antibody in nasal washes of vaccinated children may persist for at least 1 year [25]. Efficacy of LAIVs is approximately 80% in young

children aged 6 months to 7 years [26]. However, LAIVs are unlikely to boost T cell responses in adults, which may be due to the abrogation of vaccine efficacy by pre-existing antibodies that could neutralise influenza vaccine strains after administration [30]. The vaccines thus are recommended in children from 2-18 years old in European countries.

Table 1.1 Comparison of the immune response to inactivated influenza and live attenuated influenza vaccines [27]

	Inactivated influenza vaccines	**Live attenuated influenza vaccines**
HA-specific antibody		
HAI response	+++	+
Antibody secreting cells	++	+
Memory B cells	+	+
Nasal IgA	-/+	+++
NA-specific antibody	-/+	++
$CD4^+$ T cells	++	++++
$CD8^+$ T cells	-	+?
Cross protective immunity	-/+	++

1.3.3. Limits of current influenza vaccines

IIVs mainly induce systemic antibody-mediated immune responses, whereas LAIVs have superior advantage in the induction of mucosal immunity and T cell response [27] (Table 1.1). Nevertheless, both vaccines in general provide the protection against only identical or closely antigenically related influenza strains. The vaccine efficacy is still considerably variable, which depends upon how well the vaccine strains match the circulating virus strains in each season.

Various host factors including age, gender, health status, history of influenza virus infection and previous influenza vaccination and genetic differences in immune responsiveness could have impacts on the vaccine efficacy. Of them, age is likely to be of most concern [31]. Older adults with ages over 65 years old have shown declines in immune responses to the vaccines, which would result from immunosenescence [32]. This results from the decreasing numbers and function of the main immune cells e.g. dendritic cells, NK cells, B and T

lymphocytes which could result from chronic infection by Cytomegalovirus and Epstein-Barr virus [31].

In addition to the compromised efficacy of the vaccines, the zoonotic infection caused by avian influenza viruses especially high pathogenic H5N1 in the last decade and the unexpected outbreak of the pandemic in 2009 raise concerns for the need of more effective vaccines [33]. The current efforts therefore are focused on the development of new vaccines conferring broad protection against a wide range of influenza subtypes including these avian influenza viruses and unpredictable pandemics in the future.

1.4. Novel influenza vaccines

Novel influenza vaccines are being developed, aiming to elicit broadly cross-reactive immune responses across predominant IAV subtypes with the durable protection that last at least 1 year in all age groups [34]. These vaccines therefore target conserved influenza epitopes shared across influenza virus strains and novel platforms are employed to deliver the vaccine antigens.

1.4.1. Conserved protective epitopes

1.4.1.1. Ectodomain of matrix protein 2 (M2e)

M2 is formed as a homotetramer, situated on the virus envelope membrane and functions as an ion channel (Figure 1.1). The extracellular domain of M2 (M2e), a linear peptide with 23 amino acids, becomes one of the attractive targets for antibody-based vaccine owing to its highly conserved nature across human IAVs. The number of M2 molecules is normally low on the virus envelope; however, it is abundantly expressed on the surface of virus-infected cells [35]. It has been reported that protective antibodies against M2e were elicited in animals vaccinated with different forms of M2 such as recombinant M2 proteins [36], carrier-conjugated M2 peptides [37] and virus-like particle (VLP) or liposome expressing M2e [38].

1.4.1.2. The stalk region of haemagglutinin

The structure of HA is three identical copies of the HA monomer. Each monomer (HA0) is composed of a globular head (HA1) and a stalk region (HA2) (Figure 1.1). The head contains the sialic acid receptor-binding site (RBS), which is surrounded by variable antigenic sites, designated Sa, Sb, Ca1, Ca2 and Cb in H1 subtype and A, B, C and D in H3 subtypes [1] (Figure 1.7). Isolated human monoclonal antibodies directed to RBS have been shown to have broadly neutralising activity. However, RBS-recognising antibodies are not easily induced because RBS is masked by many variable regions aforementioned. The crystal structure shows that in order to bind RBS, heavy-chain complementarity determining region 3 (HCDR3) of the antibody inserts into the receptor-binding pocket which closely mimics the interaction of sialic acid with the receptor [39], [40].

The stalk region of HA shows the higher level of conservancy across influenza subtypes than the globular region. Three protective epitopes have been identified within the HA stalk. The first epitope is the centre of alpha helix A. Targeting this epitope provides protection against both IAVs and IBVs. The other two reside in the upper part of the long alpha helix CD and the base of the HA stalk including the fusion peptide and the helix-capping loop, respectively. These two epitopes are protective across HA group 2 of IAVs [41]. The boosting of HA stalk-reactive antibodies has been shown by vaccination with HA-based vaccines, whose HA molecules are modified to different forms e.g. chimeric HA, headless HA and glycosylated, from which the HA head is removed or shielded [42].

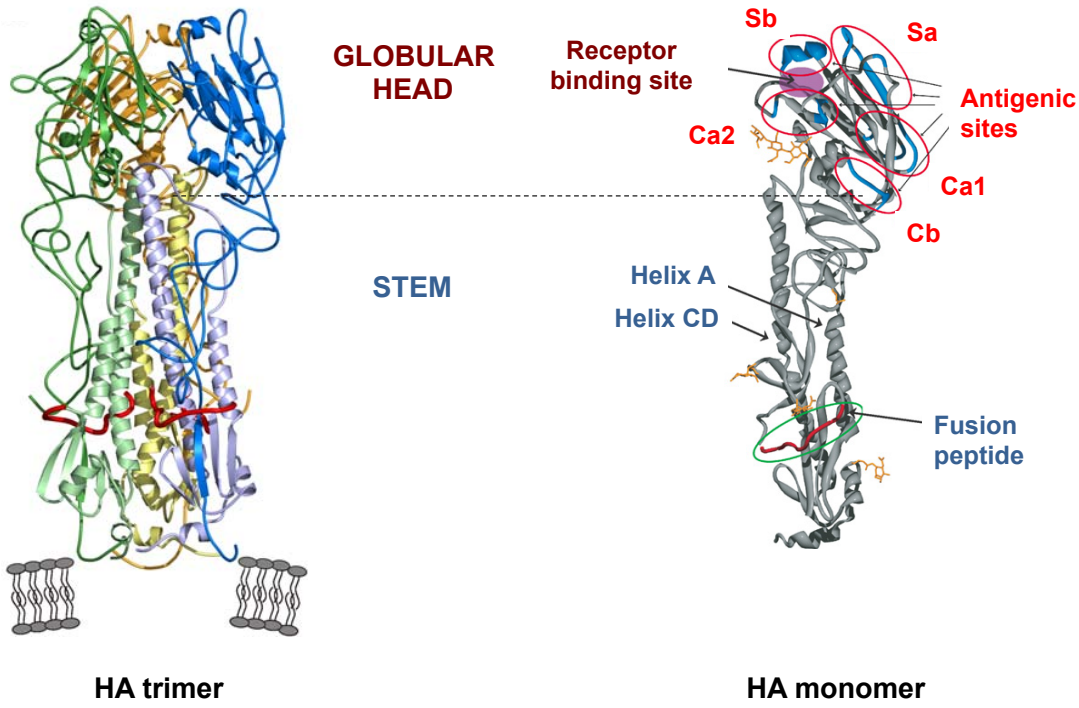

Figure 1.7 Structure of influenza haemagglutinin

Haemagglutinin (HA) is composed of three identical copies of the HA monomer. Each monomer has two regions; head and stalk. Located in the HA head are receptor-binding site (RBS) and antigenic sites which are hypervariant from strain to strain. The stem (or stalk) region includes fusion peptides and helix proteins, which are more conserved across influenza subtypes (Adapted from [1], [43]).

1.4.1.3. Internal viral proteins

Internal viral proteins such as NP, M1 and PB are the targets of T cell-based vaccines, aiming for T cell responses particularly CTL responses. During virus infection, a large number of internal viral peptides are generated in virus-infected cells. However, only a small fraction of them are bound and presented on MHC class I molecules of antigen-presenting cells (APC) to trigger CTLs. This phenomenon results from 1) the HLA haplotype and its binding affinity to individual epitopes, 2) the repertoire of T-cell receptors, 3) processing and presentation of viral peptides and 4) interaction of CTL with APC [43].

$CD8^+$ T cell IAV-specific epitopes are identified across influenza proteins [44]. One of the most frequently recognised conserved epitope is $M1_{58\text{-}66}$, which is presented in individuals with HLA-A*0201, one of the highest prevalence HLA types [43], [45]. In people who are HLA-A*0201 negative, NP has been shown to be highly immunogenic and displays 70-85%

conservancy. Five such NP peptides are HLA-A*0301-$NP_{265-273}$, HLA-B*0801-$NP_{225-233}$, HLA-B*1801-$NP_{219-226}$, HLA-B*2705-$NP_{383-391}$ and HLA-B*5701-$NP_{199-207}$ [46]. In order to protect people from all ethnic groups that have a diversity of HLA types, T cell-based vaccines should contain immunodominant epitopes restricted to those different HLA types. 80-90% population coverage can be achieved in most prominent ethnicities by focusing on only three major HLA class I supertypes (A2, A3 and B7). 100% population coverage in all major ethnicities could be reached when including two additional supertypes (A1 and A24) [47].

1.4.2. Innovative vaccine platforms

Unlike conventional vaccines, newly developed influenza vaccines often employ advanced platforms to efficiently deliver vaccine antigens [48]. These innovative approaches may be classified into two groups based on the form of immunogens [49]. The first group includes DNA vaccines and vector-based vaccines delivering influenza target genes, which are subsequently expressed to viral proteins in target cells. Another group contains virus-like particles, nanoparticles and synthesised proteins/peptides, which basically are in the form of protein or peptide antigens that could be readily recognised by immune cells when introduced into the human body.

Viral vector-based vaccines are one of the novel and promising vaccine platforms to deliver antigens, with a number of advantages over conventional vaccines. They are considered as live vaccines, but exhibit replication restriction or deficiency [50], [51]. The use of live vectors allows the *de novo* synthesis of antigenic proteins in the cytoplasm of APCs, which subsequently undergo antigen processing and presentation to T cells. Moreover, protein antigens are expressed in the native conformation, inducing potent and specific antibody. The vaccines therefore can be designed to elicit antibody and/or cell-mediated immune responses [52]. In addition, viral vector-based vaccines can be rapidly produced and upscaled for industrial production, which is beneficial during pandemic outbreaks [53], [54]. Of them, Modified Vaccinia Ankara and adenovirus vectors are lead candidates to be studied as novel influenza vaccines.

1.4.2.1. Modified Vaccinia Ankara (MVA)

MVA is an attenuated Vaccinia Virus (VV), which belongs to the family *Poxviridae* and genus *Orthopoxvirus*. It is a double-stranded DNA, enveloped virus [55]. MVA has been serial-passaged in chicken embryo fibroblast, resulting in the major deletion of genes that influence virus virulence and immune evasion and the highly restricted replication in avian cells [56]. MVA can infect mammalian cells but cannot produce new progeny virus, therefore low reactogenicity in humans. Moreover, MVA has an excellent safety profile as it has been successfully used as a vaccine to combat smallpox and has been shown to be safe even in immunodeficiencies [57]–[59]. MVA has other advantages as a viral vector; easy insertions of antigen target genes into viral genome, transient expression of recombinant antigens [60] and induction of both humoral and cellular immune responses in animals and humans [61], [62]. Due to the loss of immune evasion, MVA itself has an adjuvant-like effect due to the influx of various immune cells [63]–[66]. Importantly, anti-MVA vector antibody is unlikely to abrogate the vaccine efficacy, which allow the vaccine to be used for boosting memory responses [67].

1.4.2.2. Adenovirus

Adenovirus is a double-stranded DNA, icosahedral, non-enveloped virus and belongs to the family *Adenoviridae*. It has been initially used in gene therapy. To construct adenovirus as a viral vector, E1 and/or E3 unit of the viral genome are deleted and replaced with genes of antigens of interest. Deletion of E1 and E3 units results in deficient viral replication and loss of immune evasion, respectively. Therefore, recombinant adenovirus (rAd) can infect and replicate in target cells, but cannot release new virions. rAd has many advantages as a viral vector. The genes of antigens of interest could be easily and stably inserted into viral genomes. The virus has high tropism with a wide range of susceptible hosts, tissues and cell types, so they induce immune responses after local or parenteral administration. Moreover, they could also be produced at high titres [68].

Human and simian adenoviruses are in the same genus, *Mastadenovirus* and are classified into 6 serotypes; A-F based on their hexon (capsid protein) sequences [69] (Figure 1.8). Human adenovirus type-5 (hAd5) is one of the adenoviral vectors in species C, widely constructed as viral vector-based vaccines against a number of pathogens including human immunodeficiency virus (HIV), dengue viruses, ebola viruses and influenza viruses [70]. Although the vaccines are safe and immunogenic, their efficacy is interfered with by pre-existing antibodies to adenoviral vectors, which could be induced by natural infection or previous adenoviral-based vaccination [68]. To avoid anti-vector antibodies, hAd5 is replaced by other low prevalence human adenovirus species (e.g. species B; Ad35 and species D; Ad26, Ad28, Ad48) and also by those isolated from chimpanzee (ChAd) or bonobo (PanAd) [69].

MVA and rAd-vectored influenza vaccine candidates have been constructed with various influenza target genes of antigens such as NP, M1 and conserved HA. They showed protective responses in animal models and some have shown protection in humans, which are mediated by antibody and/or T-cell immune responses [54], [71], [72].

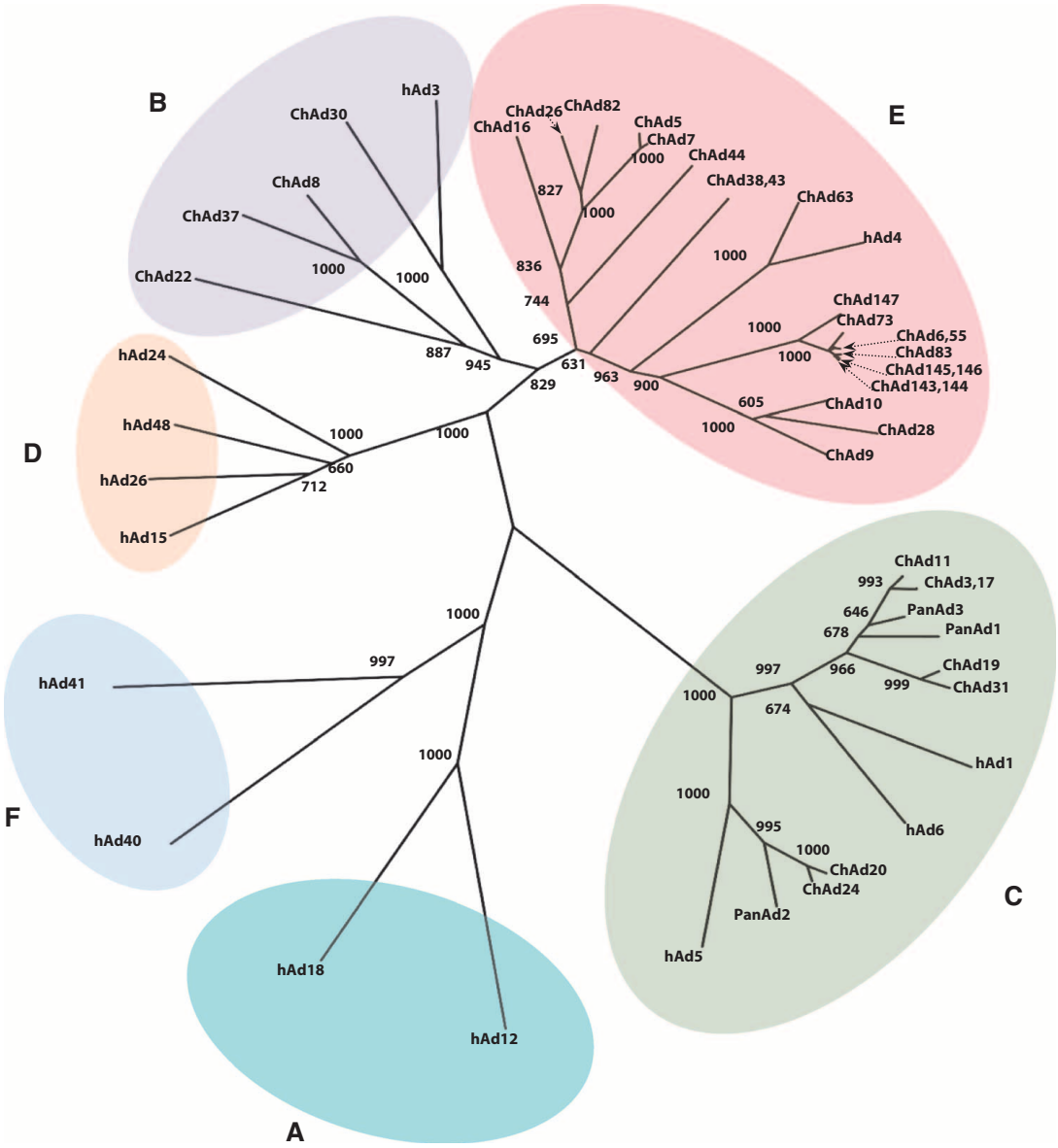

Figure 1.8 Phylogenetic tree of adenoviruses

Adenoviruses isolated from human (hAd), chimpanzee (ChAd) and bonobo (PanAd) are classified into species A-F based on their hexon capsid protein sequences [69].

1.5. Immune correlates of protection against influenza viruses

Unlike conventional vaccines that predominantly induce globular HA-specific neutralising antibodies, novel influenza vaccines could elicit various types of immune responses, whether neutralising or non-neutralising antibodies or T cell immunity depending upon the vaccine antigens. Immune correlates of protections and their functions have been extensively studied in order to assess the potential of these novel vaccines.

1.5.1. Antibodies

Vaccination with traditional vaccines dominantly elicited HA-specific neutralising antibodies (nAb), which are considered as a correlate of vaccine efficacy [18]. As these antibodies target hypervariant globular HA, the response is more likely to be strain or subtype-specific. The response has been measured by three classical immunoassays: haemagglutination inhibition (HAI), single-radial haemolysis (SRH) and virus neutralisation (VN) assays [73], [74]. The HAI assay measures the capacity of antibody to block the binding of virus to its receptor on target cells, preventing virus infection [75]. HAI antibody titre of 40 correlates with a 50% reduction in the risk of influenza infection [76]. However, this correlate of protection has been established from studies in healthy adults and is not appropriate for children [77]. The SRH assay measures antibodies that bind to the influenza virus and fix complement (usually guinea pig complement) [78]. A zone of 25 mm^2 is defined as a correlate of protection. The VN assay mainly detects functional antibodies that bind the HA globular head and block receptor binding; however it can also measure antibodies that block entry at the stage of membrane fusion. No correlate of protection has been established for the VN assay [73].

In contrast, broadly reactive antibodies (bnAb) target the stalk region of HA, which is more relatively conserved among diverse influenza subtypes. A number of HA stalk-binding monoclonal antibodies isolated from human memory B cell repertoires have been discovered to cross-react to many influenza viruses. Some only recognise subtypes in the same phylogenetic HA either group 1 (e.g. CR6261, F10) or group 2 (CR8020), while some have the cross-reactivity to both HA groups of IAV (FI6). Recently, CR9114 has been found to

react to both IAVs and IBVs [79]. The breadth of reactivity depends upon the antigenic sites that antibodies bind to [41]. Anti-HA stalk antibodies resulted in lower viral titre and delayed or no virus replication in ferrets after natural exposure to pdmH1N1 influenza virus [80]. The level of HA stalk-reactive antibodies in human sera correlated well with the reduction of weight loss in serum transfer to mice after virus challenge [81]. Recently, it was shown in humans that HA stalk-reactive antibody level correlated with a reduction in detectable viral shedding, but did not correlate with a reduction in clinical symptoms [82].

The magnitude of HA stalk-reactive antibodies in human sera is extremely low or undetectable after seasonal influenza infection or current vaccination [41]. However, these antibodies have been found to increase in patients infected with pandemic virus and in vaccinees after vaccination with pandemic H1N1 strain [20], [21], [83]–[85]. Many novel antibody-inducing vaccine candidates aim to enhance these broadly reactive HA stalk-specific antibodies to confer broad protection. Anti-HA stalk antibody has been characterised as having no HAI activity with or without neutralising activity [83]. Despite the broad neutralisation of HA stalk-specific bnAbs, their activities are generally much weaker than the ones towards the HA head [86]. It has been showed that antibody binding to the HA stalk inhibits the conformation change of HA during endocytosis, resulting in no viral genome release into host cell cytoplasm after virus infection. HA-stalk reactive antibodies may also block budding of virus and inhibit HA maturation [87].

Table 1.2 Comparisons between the features of the antibody targeting influenza HA globular head epitopes and HA stalk region epitopes (Adapted from [19])

Antibody specific to HA	Neutralisation potency	Epitope variability	Escape variants	Heterosubtypic protection
Globular head region	+++	+++	+++	+
Stalk region	++	+	+	+++

Remark: The number of (+) signs was arbitrarily determined.

Some broadly cross-reactive antibodies have no neutralising activitiy, but provide protection against influenza viruses. Without neutralisation, the antibodies confer protection by facilitating other mechanisms such as Fc-mediated cell cytotoxicity (ADCC), antibody-mediated phagocytosis (ADP) and complement-dependent lysis (CDL) [87] (Figure 1.9). ADCC has been widely studied in monoclonal antibodies isolated from animals and humans vaccinated or infected with influenza virus. ADCC-triggering antibodies bind to HA or other virus envelope proteins such as NA and M2e present on virus-infected cells and engage CD16 Fc receptor to activate innate immune cells such as NK cells, releasing potent cytotoxic molecules e.g. perforin and granzymes including anti-viral cytokines e.g. IFN-γ and TNF. A study in rhesus macaques has suggested non-neutralising antibodies with ADCC activity induced by seasonal vaccination may be associated with protection from pandemic H1N1 infection [88]. Moreover, non-neutralising anti-HA antibodies protected mice from influenza H7 virus challenge by mediating Fc-mediated effector function [89]. DiLillo *et al* have shown that human anti-HA stalk antibodies required the interaction of Fc and FcγR to mediate *in vivo* protection [90].

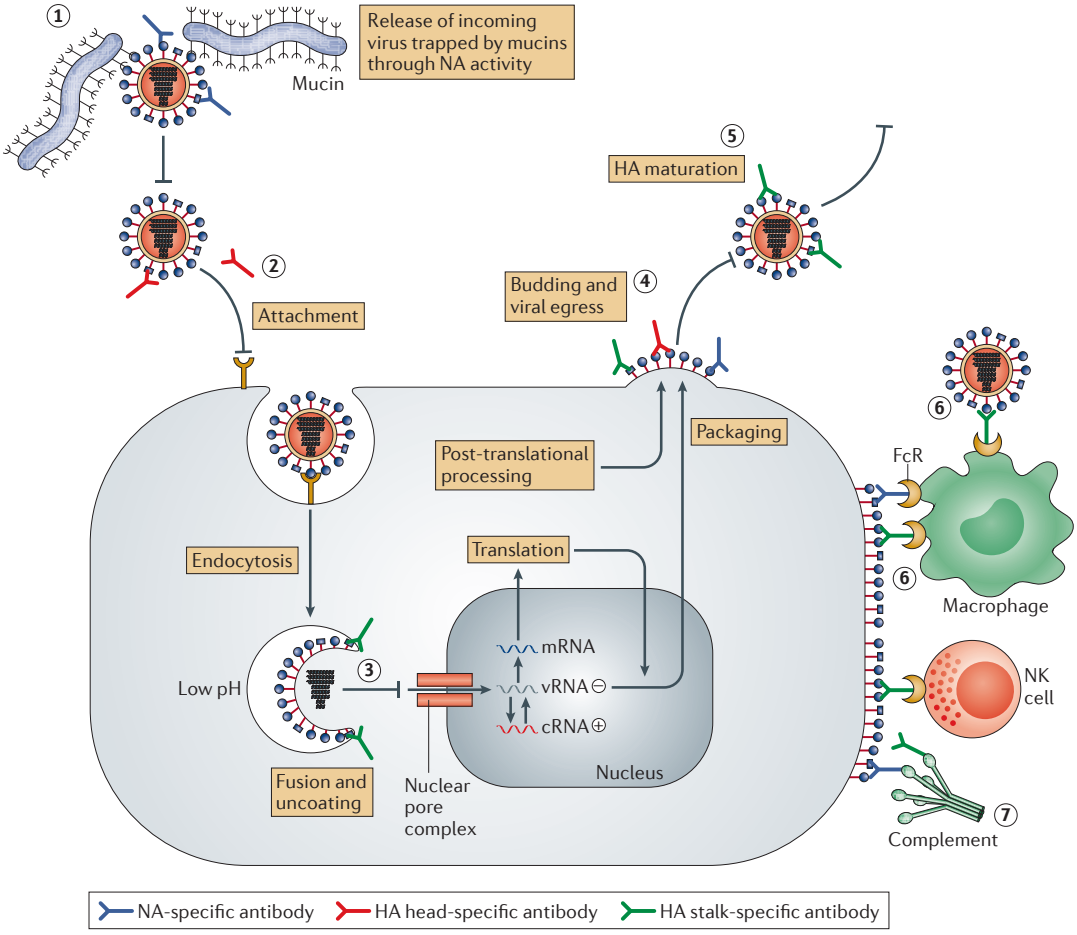

Figure 1.9 Functions of influenza virus antigen-specific antibodies

1) NA-specific antibodies promote the trapping of virus in mucins at mucosal surface. 2) Antibodies binding to the globular HA block interactions between HA and sialic acid on cellular receptors, inhibiting attachment of the virus to the cell. 3) HA stalk-specific antibodies bind to the HA on virus particles and prevent the fusion of viral and endosomal membranes by blocking the rearrangement of the HA fusion machinery. 4) Head-, stalk- and NA-specific antibodies may inhibit budding of virus. 5) HA-stalk specific antibodies may inhibit HA maturation. HA stalk and possibly NA-specific antibodies also facilitate 6) antibody-dependent cell-mediated cytotoxicity or 7) complement-dependent cytotoxicity [87].

1.5.2. T cells

The induction of T cell responses, particularly CTL responses, is the main target of novel T cell-based vaccine development. The CTL-mediated immune response plays a pivotal role in clearing virus-infected cells, resulting in the decrease of virus shedding. Although T cell response does not protect from virus infection, it reduces the disease severity [91]. As CTLs recognise most internal viral epitopes shared across IVA subtypes, they provide heterosubtypic immunity. This cross-reactive protection in the absence of virus-specific antibodies has been demonstrated in animal models, showing the correlation with cytotoxic $CD8^+$ T cells [46], [92]. There is increasing evidence in humans to support the critical role of $CD8^+$ T cell-mediated immunity. In individuals experimentally infected with influenza virus, the virus-specific cytotoxic T cell killing was shown to reduce virus shedding in the absence of specific antibodies [93]. Also, the presence of pre-existing cytotoxic $CD8^+$ T cells was associated with a decreasing severity of symptoms in patients infected with pandemic H1N1 virus during the outbreak in 2009 [94]. Moreover, rapid recovery of patients from a severe avian H7N9 infection was shown to correlate with an early onset of robust $CD8^+$ T cell response following the infection [95].

CTLs lyse virus-infected cells by facilitating different mechanisms (Figure 1.10). By recognising the viral peptide-MHC complexes presented on infected cells via T-cell receptor (TCR), CTLs release cytotoxic molecules e.g. perforin and granzymes in response. Perforin forms pores in cell membrane of virus-infected cells, where subsequently released granzymes enter into the cell cytoplasm and induce cell apoptosis. Granzyme-A and -B are the major prominent contents of cytolytic granules [96]. Moreover, the engagement of two membrane-bound TNF family ligands, FasL and TRAIL, on CTLs with their cognate receptors (Fas and TRAIL-DR) on infected cells also triggers the apoptotic-signaling cascade [97], [98].

Virus-specific CTLs also produce a range of cytokines and chemokines. IFN-γ and TNF-α are the prominent effector cytokines produced by classical CTLs. IFN-γ has a potent antiviral activity and enhances cytotoxicity of other immune cells. TNF-α is a pro-inflammatory cytokine, inducing non-specific death of infected cells and regulating the functions of other

immune cells through TNF receptors. CTLs produce a small amount of IL-2 when receiving proper co-stimulatory signals, which promote proliferation and maintain survival of them and other CTLs. CTLs differentially produce combinations of these cytokines. CTLs that co-produce IFN-γ, TNF-α and IL-2 are considered more potent than others that produce one or two cytokines. IL-10 was found to be produced by lung-resident CTLs during IVA infection. Owing to anti-inflammatory property of IL-10, CTLs producing both IFN-γ and IL-10 may balance their protective activity and tissue-pathogenic effect [99]. Both cytotoxicity and cytokine production by CTLs could contribute to protective immunity by regulating virus infection at host mucosa, resulting in virus clearance and limiting symptom severity [99].

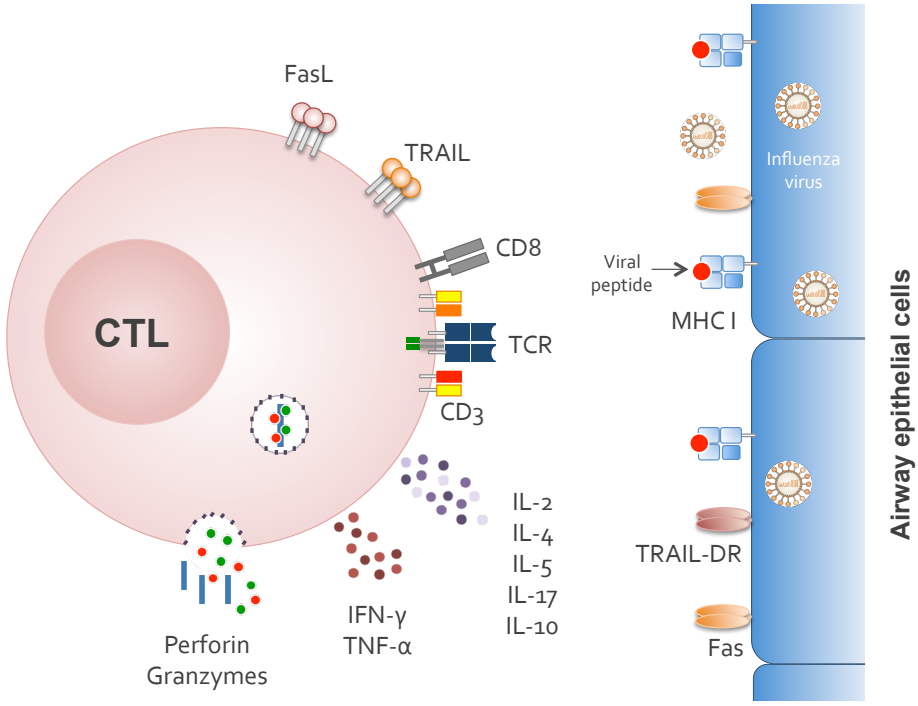

Figure 1.10 Functions of influenza virus antigen-specific cytotoxic T cells

By recognising the viral peptide-MHC complexes presented on infected cells via T-cell receptor (TCR) and CD8, CTLs release cytotoxic molecules. Perforin forms pores in cell membranes, where subsequently released granzymes enter into the cell cytoplasm and induce cell apoptosis. They also mediate two membrane-bound TNF family ligands, FasL and TRAIL, on CTLs with their cognate receptors (Fas and TRAIL-DR) on infected cells, triggering the apoptotic-signaling cascade (Adapted from [99]).

1.6. Mucosal immune responses

Mucosa could refer to the surfaces of the respiratory, gastrointestinal and urogenital tracts formed by a layer of epithelial cells. As most pathogens enter the human body at mucosal surfaces, mucosal immune responses therefore are necessary as the first line of defence. The mucosal immune system plays a pivotal role in providing mucosal protection against disease [100]. The system is composed of two functional compartments, which are inductive and effector sites (Figure 1.11). The inductive site is associated with the lymphoid tissues where the responses initially occur, in which B cells or T cells are primed or activated by pathogenic antigens presented by APCs. The antibody-secreting plasma cells and antigen-specific T cells then migrate and persist at intraepithelial layers and mucosal surface, which are effector sites [101].

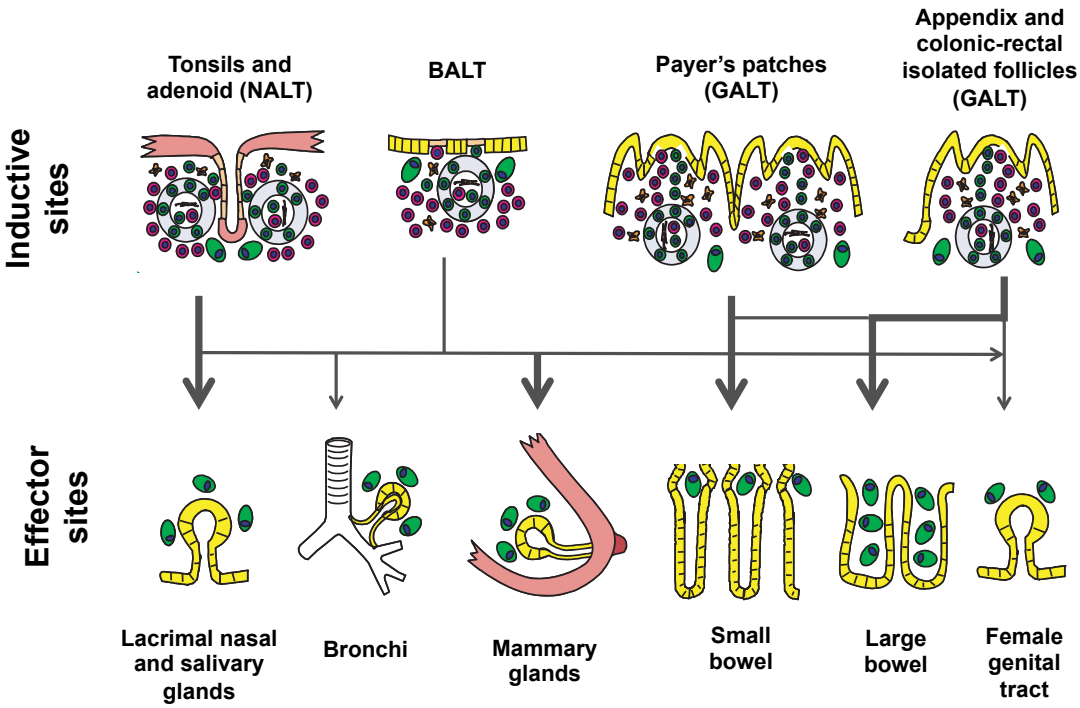

Figure 1.11 Mucosal immune system

The mucosal immune system is compartmentalised into the inductive site and the effector site. The figure shows the migration of memory B cells from inductive (top) to effector (bottom) sites, depicting the more or less preferred pathways (graded arrows) after the activation in nasopharynx-associated lymphoid tissue (NALT) represented by palatine tonsils and adenoids, bronchus-associated lymphoid tissue (BALT), and gut- associated lymphoid tissue (GALT) represented by Peyer's patches, appendix, and colonic-rectal isolated lymphoid follicles (Adapted from [102]).

In order to provide protection at the mucosa, secretory IgA (SIgA) promotes the entrapment of pathogens in the mucus, preventing pathogens from direct mucosal epithelial attachment. SIgA also has intracellular-neutralising activity, which traps and transports those epithelium-infecting pathogens back into the lumen by mediating through epithelial polymeric immunoglobulin receptor (pIgR) or by mediating ADCC to lyse the infected cells [103]. Local IgG antibody, whether locally produced or diffused from serum, can potentially neutralise pathogens that enter the mucosa [104]. It is assumed that mucosal or serum IgG diffuse across epithelial barriers by paracellular leakage or transport by mediating IgG-specific Fc receptor expressed on epithelial cells [105]. Cytotoxic T lymphocytes at the mucosa cannot prevent the infection, but could limit the infection by the clearance of virus-infected cells (Figure 1.12). These cells have been shown to persist at mucosal sites after virus infection [106]. Both antibodies and CTLs at mucosa sites contribute to protection from the infection of such pathogens including influenza viruses [101].

Mucosal immunisation becomes a more attractive strategy against pathogens invading at mucosa. It has a superior advantage compared to parental immunisation in terms of the induction of local immune responses where pathogen infection and transmission occur. Mucosal vaccination via different routes has been shown to provide protection against influenza viruses. The nasal route is among others such as oral and pulmonary routes to be rigorously studied. LAIVs are the first licensed intranasal influenza vaccines. They efficiently elicit mucosal IgA antibodies, which are thought to be the immune correlates of protection. Nonetheless, serum IgG antibodies could also be observed, indicating that mucosal immunisation induces not only mucosal but also systemic immune responses [27]. Systemic immunity after mucosal immunisation may be due to the migration of locally antigen-uptaken mucosal DCs to other systemic inductive sites such as spleen and lymph nodes [100]. The number of influenza vaccine candidates has been tested and reported to protect animals from influenza infection following intranasal vaccination. Nasal delivery of avian influenza subunit vaccines (e.g. H5N1 and H7N9) with mucosal adjuvants has enhanced both mucosal and systemic immune responses as shown in mice by the increase of virus-specific SIgA and IgG antibodies in nasal wash and serum including T cell response [107], [108].

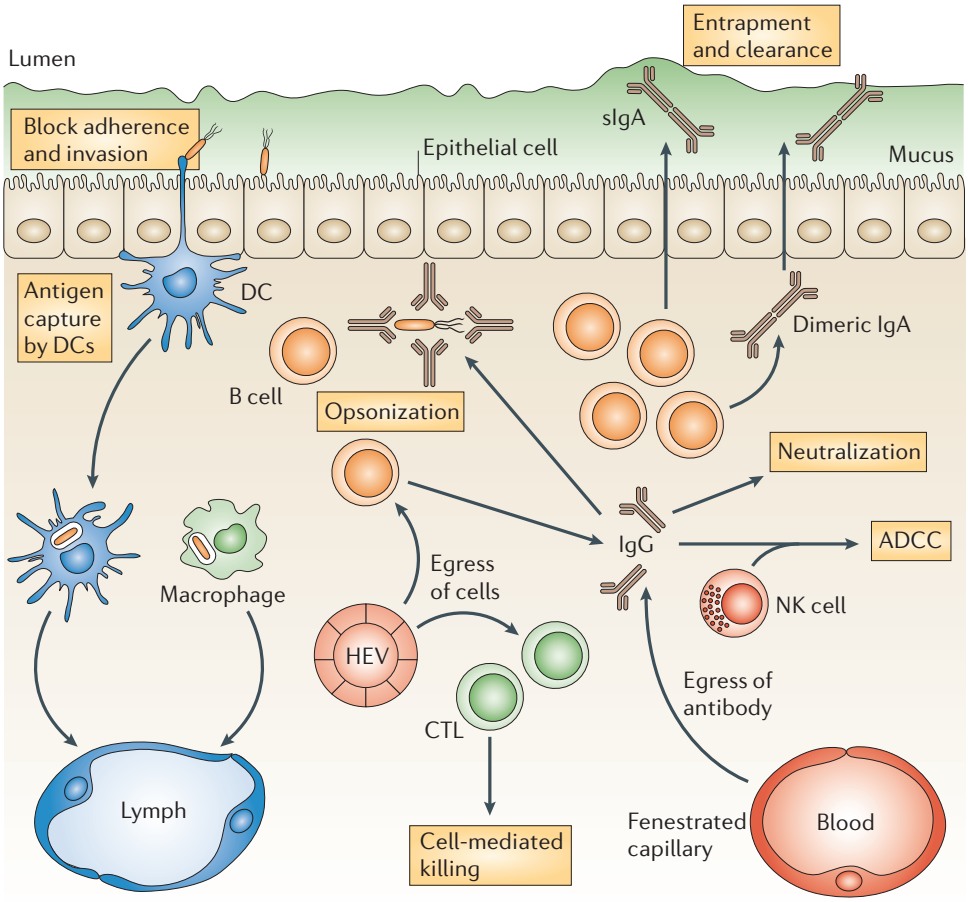

Figure 1.12 Mechanisms of immune protection at mucosal surfaces.

Multiple immune effector mechanisms contribute to protection at mucosal surfaces. Antigen-specific B and T cells from peripheral blood enter the mucosa via high endothelial venules (HEVs). Local plasma cells produce dimeric IgA that is exported along the mucus as secretory IgA (sIgA) to prevent mucosal invasion. Neutralising IgG may be derived from local plasma cells or diffused from blood. Infected cells could be lysed by antigen-specific cytotoxic T cells or by antibody-dependent cell-mediated cytotoxicity (ADCC). Pathogens can also be captured by dendritic cells and macrophages, and carried to draining lymph nodes [100].

Similarly, intranasal vaccination with whole inactivated vaccine in primed healthy individuals induced local SIgA and systemic IgG antibodies [109]–[112]. In addition to conventional vaccines, novel vaccines such as nanoparticles, VLP and virosomes intranasally delivering conserved viral proteins e.g. NP, M2e and HA also induced robust immune responses and conferred cross-protection in mice [113]–[116]. Of them, the vaccine responses were enhanced when co-delivered with mucosal adjuvants. Adenoviral vector-based vaccines expressing either HA or NP activated antigen-specific T cell responses after intranasal

administration and fully protected mice from heterologous subtypes when given as a booster dose after a prior DNA immunization [117]. These data show the potential of different forms of influenza vaccines to induce mucosal responses via intranasal immunisation.

1.7. Human nasopharyx associated lymphoid tissue (NALT)

Mucosal immune responses in the upper respiratory tract are induced in nasopharyx-associated lymphoid tissues (NALT). NALT is not only the inductive site for both T and B cell responses, but also the effector site, where primed lymphocytes frequently migrate to [101]. Human NALT, so-called Waldeyer's ring is composed of nasopharyngeal tonsil (adenoid), paired tubal tonsils, paired palantine tonsils and lingual tonsil (Figure 1.13). Of them, palatine tonsils are the major compartment as they are located at the junction of nasopharynx and oropharynx [118].

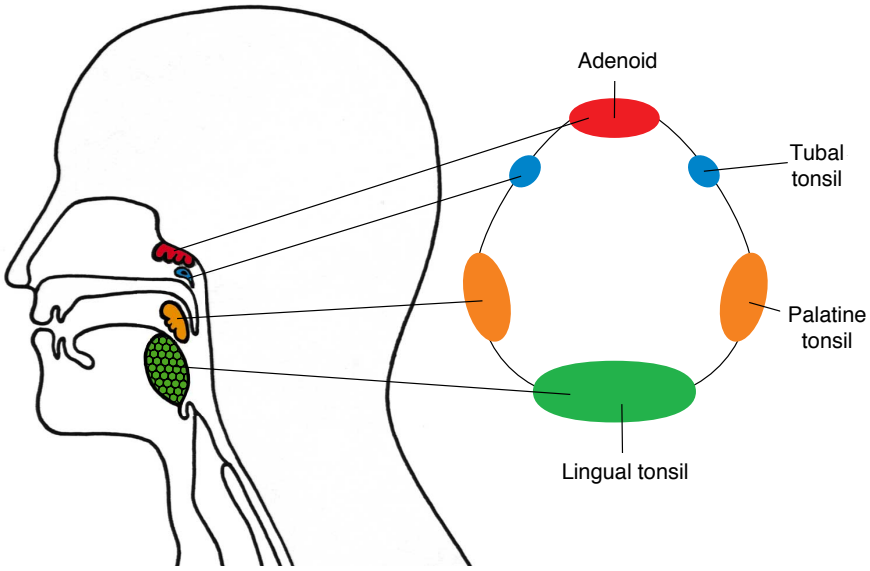

Figure 1.13 Human nasopharyx-associated lymphoid tissue (NALT)

Human NALT is composed of nasopharyngeal tonsil (adenoid), paired tubal tonsils, paired palantine tonsils and linguial tonsil [118].

Tonsils are secondary lymphoid tissues, containing a set of cellular components required for both primary and secondary immune responses. The tonsil tissues consist of three compartments; reticulated crypt epithelium, lymphoid follicles and extrafollicular regions (Figure 1.14a). The reticulated crypt epithelium or lymphoepithelium is the outer layer. There is the formation of deep tubular crypts to increase the mucosal surface. This layer comprises epithelial cells and immune cells, most of which are memory B cells followed by T cells. A small numbers of dendritic cells and macrophage are distributed in here. Lining between epithelial cells are microfold cells (M cells), which are able to transport foreign antigens to subepithelium [119]. In the subepithelial compartment, B cells are also the predominant cell population, responsible for 60-75% of cells [120]. This part contains lymphoid follicles, where B cells undergo proliferation and differentiation to memory B cells or antibody-producing plasma cells as well as T cell activation. Unlike primary lymphoid follicles, secondary ones also contain germinal centres (GC), which are composed of a dark zone of centroblasts and a light zone of centrocytes, surrounded by a mantle zone of naïve B cells (Figure 1.14b). Follicular dendritic cells (FDC) are a subset of GC dendritic cells that activates T follicular helper cells (T_{FH}) and also retains immune complexes on their plasma membrane to signal B cells during the affinity selection process in GC [119]. The extrafollicular region is the T-cell enriched area containing T cells (25-35%) with the majority of $CD4^+$ T cells together with interdigitating dendritic cells, macrophages and antibody-forming cells [120]. GCs are important for the establishment of antigen-specific memory B cell responses in a T-cell dependent manner.

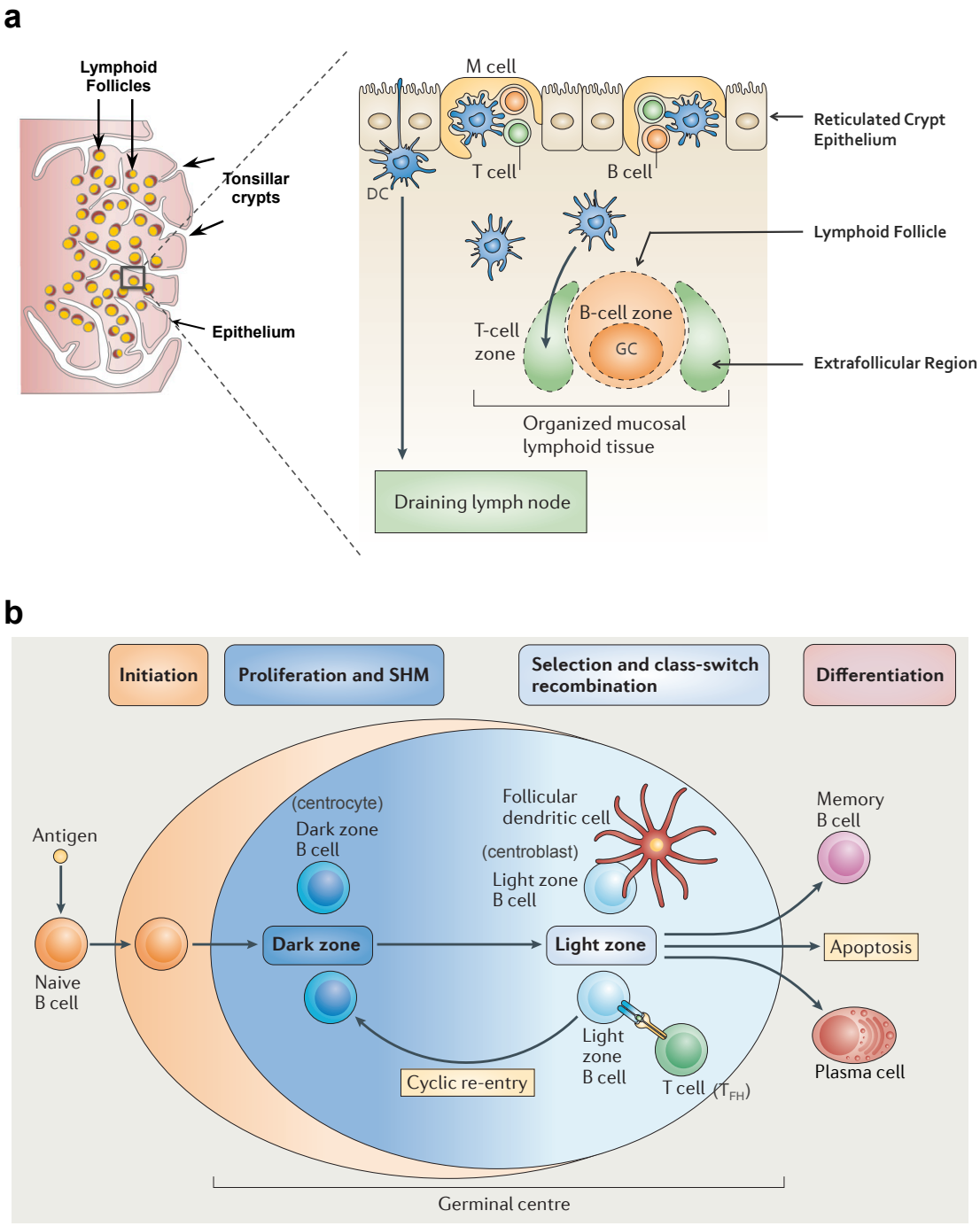

Figure 1.14 Tonsils and their compartments

Tonsils are part of the inductive sites for mucosal immune responses in the upper respiratory tract. **a)** Cross-section of tonsils shows tonsils crypts and lymphoid follicles underneath the epithelium. Enlarging the blue box in a), three compartments of tonsils are shown; reticulated crypt epithelium is a layer of epithelial cells and M cells, where immune cells (dendritic cells, B- and T-lymphocytes) reside. Subepithelial compartment located lymphoid follicles or B-cell zone and extrafollicular T-cell zone (Adapted from [100], [121]). **b)** In a germinal centre (GC) of a secondary lymphoid follicle, B cells undergo proliferation in dark zone and selection/ class switching in light zone before differentiating to memory B cells or plasma cells (Adapted from [122]).

1.8. Hypothesis

It was hypothesised that novel viral vector-based influenza vaccines have the capacity to induce mucosal immune responses if administered by the intranasal route. Since adenoid/ tonsillar tissues are parts of the mucosal immune system (NALT), known as an immune induction site for immunity against respiratory pathogens including influenza virus, using immune cells from NALT allows us to examine the mucosal immune responses to these novel viral vector-based vaccines. This project therefore aimed to study the capacity and functional properties of T cells or B cell-mediated antibodies induced by MVA- and PanAd3 vector-based influenza vaccines using the *in vitro* cell culture system containing cells from NALT of children and adults.

1.9. Objectives of the thesis

The overall objectives of the thesis are:

1. To study how the viral vector-based influenza vaccines work to induce the immune responses in human NALT.
2. To investigate the capacity of these vaccines to induce antigen-specific cross-reactive T cell responses and antibodies in human NALT.
3. To study the functional properties of these T cells and antibodies that correlate with protection.

……

Chapter 2

Materials and methods

2.1. Subjects

Subjects included in this study were children (≤15 years old) or adults (>15 years old) undergoing tonsillectomy and/or adenoidectomy due to upper airway obstruction or tonsillitis at Alder Hey Children's Hospital, Royal Liverpool and Broadgreen University Hospitals and Aintree University Hospital. Patients who received immunosuppressant within 3 weeks of surgery, or who had any known immunodeficiency were excluded from the study. Ethical approval was obtained (REC No: 14/SS/1058) and informed written consent was obtained in all cases from patients or their legal guardians.

2.2. Samples

2.2.1. Adenoidal and tonsillar tissues

After surgery, adenoidal and tonsillar tissues were stored in Hank's Balanced Salt Solution (Sigma Aldrich, UK) supplemented with 100 U/ml penicillin, 100 μg/ml streptomycin and 1% L-glutamine (all Sigma Aldrich, UK), named "HBSS" and delivered to the laboratory.

2.2.2. Peripheral blood

5-10 ml venous blood taken from the same patients as described above or 15-20 ml from healthy donors was collected into a 25-ml universal tube containing 100 μl of heparin (LEO Pharma, UK).

2.3. Vaccines/ Viruses

2.3.1. *Pan paniscus* Adenovirus type 3 virus (PanAd3) vector-based influenza vaccines

PanAd3 vector-based influenza vaccines were kindly provided by Okairòs (Rome, Italy). Briefly, PanAd3 virus was isolated from a bonobo (*Pan paniscus*) [123] and was a member of adenovirus species C based on the hexon sequences [69]. The virus was deleted in its E1 and E3 genes to obtain replication-deficient viral vector backbone, pPanAd3ΔE1ΔE3 with a human cytomegalovirus promoter (HCMV)-driven transgene expression, followed by the insertion of different conserved influenza gene cassettes; 1) nucleoprotein (NP) and matrix

protein 1 (M1) to obtain PanAd3-NPM1, 2) NP, M1 and hemagglutinin (HA) from pandemic H1N1 strain to obtain PanAd3-NPM1-pdmH1HA and 3) NP, M1 and HA from avian H5N1 strain to obtain PanAd3-NPM1-H5HA. PanAd3 vector encoding HIV gag gene (PanAd3-gag) was used as a vector control.

2.3.2. Modified Vaccinia Ankara (MVA) vector-based influenza vaccines

MVA vector-based influenza vaccines were produced by the Jenner Institute (Oxford, UK). MVA-NP-GFP expresses NP from A/Panama/2007/99 under the control of Vaccinia p7.5 early/late promoter and GFP under the control of fowlpox late FP4b promoter. MVA-pdmH1HA expresses HA of A/California/04/2009 (pdmH1N1) under the control of the modified Vaccinia H5 (mH5) promoter. MVA-NP+M1 expresses NP and M1 from A/Panama/2007/99 as a fusion protein joined by a seven amino acid linker under the control of Vaccinia p7.5 early/late promoter. MVA-wt was non-recombinant virus used as a vaccine vector control.

2.3.3. Live attenuated influenza vaccines (LAIV)

FluMist® season 2011-2012 (NR-36465, BEI resources, USA) is a trivalent live attenuated influenza vaccine, containing A/California/07/2009 (H1N1) pdm09, A/Perth/16/2009 (H3N2) and B/Brisbane/60/2008 at a concentration of $10^{6.5}$ to $10^{7.5}$ fluorescent focus units (FFU) of each of the three strains in 0.2 ml. It was used as a positive control in antibody production study.

2.3.4. Influenza viruses

Inactivated whole influenza viruses were used for hemagglutination inhibition (HAI) assay. A/California/07/2009 (pdmH1N1) were formalin-inactivated purified viruses, obtained from the Government Pharmaceutical Organization (GPO), Thailand. A/Vietnam/1203/2004 (FR-736) was BLP-inactivated virus, provided by International Reagent Resource (IRR), USA.

2.4. Recombinant influenza HA proteins and influenza peptides

Recombinant HA proteins from different influenza virus strains; A/California/04/2009 (pdm H1N1, NR-13691), A/Brisbane/59/2007 (sH1N1, NR-28607), A/Brisbane/10/2007 (H3N2, NR-19238), A/Vietnam/1203/2004 (H5N1, NR-10510), A/Hong Kong/33982/2009 (H9N2, NR-41792) and A/Anhui/1/2013 (H7N9, NR-44081) were obtained from BEI resources, USA. Unless otherwise stated, each HA was a full-length glycosylated recombinant protein that was produced in Sf9 insect cells using a baculovirus expression vector system. It was purified under conditions that preserve its biological activity and tertiary structure.

M1 peptides of influenza A viruses (NR-2667, NR-18976, NR-18977, BEI resources, USA) were reconstituted with the diluent according to manufacturer's instructions (the product information sheet). 9 to 11 of M1 peptides were pooled with a final concentration of 0.1 mg/ml. $M1_{58-66}$ (GILGFVFTL) peptide (IBA GmbH, Germany) was reconstituted in 50% dimethyl sulphoxide (DMSO) to 1 mg/ml at a final concentration. All peptides were aliquoted and kept at -20°C or colder.

2.5. Cytokines

Recombinant human interleukin (IL)-2, IL-15 and recombinant human interferon-gamma (IFN-γ) were purchased from Peprotech (UK), dissolved in sterile deionised water to 100 μg/ml and aliquoted before being kept at -80°C.

2.6. Antibodies

Fluorochrome-conjugated monoclonal antibodies used for flow-cytometry were purchased from BD Biosciences, Biolegend and eBiosciences (UK). The antibody panels for each experiment will be specified in each chapter. Antibodies against influenza subtypes used for ELISA assay were obtained from BEI Resources, USA and their details will be in chapter 5.

2.7. Tissue processing and cell isolation

2.7.1. Tissue processing

Upon receiving, adenoid and palatine tonsils were stored at 2-8°C and processed within 24 hours according to the method described previously [124]. Briefly, the adenoid/tonsils were washed with Hank's balanced salt solution (HBSS) to remove dead cells or tissue debris and contaminated blood. They then were minced in HBSS using sterile scalpel before passed through 70-μm strainer (Falcon Corning, USA) to be collected as cell suspension. The Ficoll Paque gradient (GE healthcare, Sweden) was carried out to isolate adenotonsillar mononuclear cells (MNC) by centrifugation at 400*xg* for 30 minutes with slowest acceleration and brake off settings. Adenotonsillar MNCs were collected and washed with phosphate-buffered saline (1X DPBS, Invitrogen, UK), finally resuspended in L-glutamine and HEPES modification of RPMI-1640 (Invitrogen, UK), supplemented with 100 U/ml penicillin, 100 μg/ml streptomycin (Invitrogen, UK) and 10% heat-inactivated fetal bovine serum (△FBS) (Sigma Aldrich, UK), from now on will be named "R10".

For peripheral blood mononuclear cell (PBMC) isolation, the heparinised whole blood was spun down to collect plasma (named autologous human plasma (aHP), to be used in some experiments. Blood samples were diluted in HBSS at the ratio of 1:3 and then carefully layered onto the Ficoll Paque, followed by centrifugation and the aforementioned steps as the isolation of adenotonsillar MNCs. Adenotonsillar MNCs and PBMCs were counted and suspended in R10 at $4x10^6$ cells/ml.

2.7.2. Magnetic separation of cell population

Principle

Magnetic separation is one of the methods to isolate cells of interest or deplete unwanted cell types from the cell population. The method allows separating viable and functional cells based on surface antigens. Cell separation with magnetic beads and columns is based on three steps: magnetic labeling, magnetic separation, and elution of labeled cells (Figure 2.1). The target cells are labeled via a particular surface antigen with a specific antibody

conjugated with superparamagnetic bead or in some case biotinylated, or fluorochrome-conjugated. The latter would require magnetic labeling which is achieved by the use of anti-immunoglobulin MicroBeads, anti-biotin MicroBeads, or anti-fluorochrome MicroBeads. Labeled cells then are passed through a magnetic column placed on a magnetic stand separator. The labeled cells are captured inside, while other unlabeled cells flow out of the column. Finally, the column is removed from the separator stand and the labeled cells are eluted by using a plunger [125].

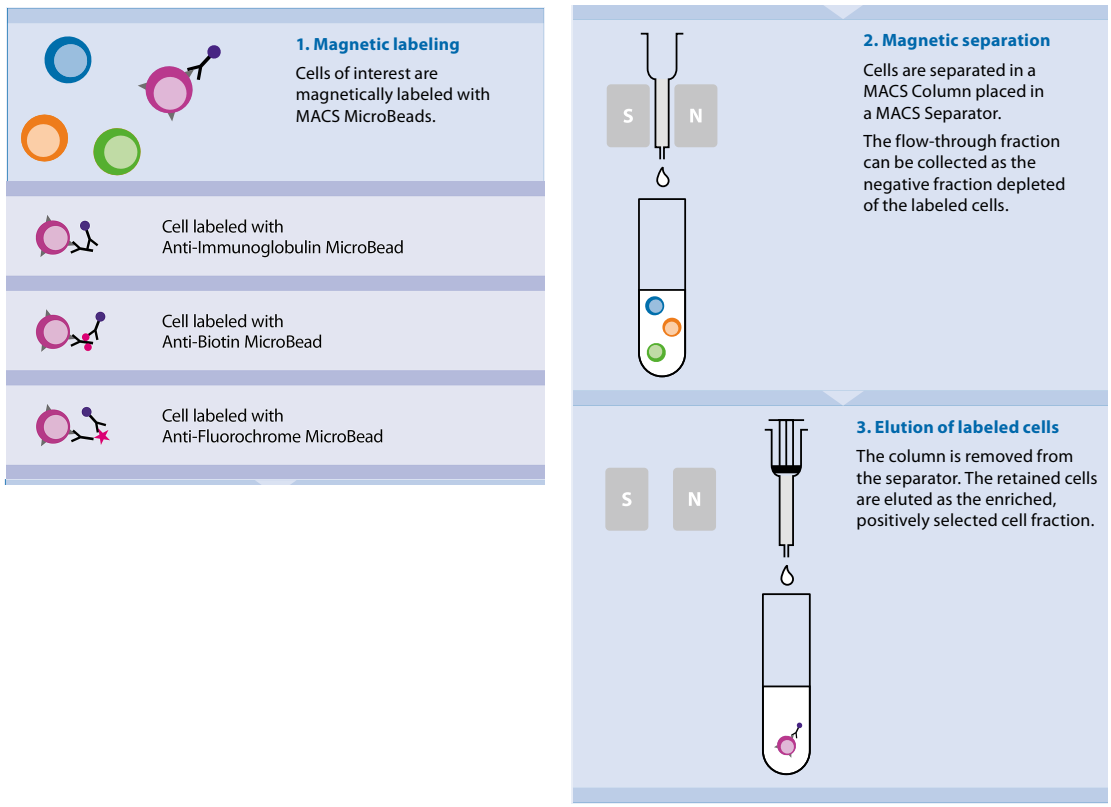

Figure 2.1 Magnetic separation of cell populations

The figure illustrates the principle of cell separation by using magnetic beads and column based on three steps; magnetic labeling, magnetic separation, and elution of labeled cells (Adapted from [125]).

2.7.2.1. Depletion of $CD69^+$ cells

For some experiments, tonsillar MNCs were depleted of activated T cells ($CD69^+$ cells) by the use of magnetic bead-based cell separation (Miltenyi Biotec, Germany) according to manufacturer's instructions. Briefly, the MNCs (5 $x10^7$-$1x10^8$ cells) were washed once with 1X DPBS (Invitrogen, UK) before being resuspended in depletion buffer (0.5% BSA in 1X DPBS). Cells were then incubated with anti-CD69-Biotin for 15 minutes at 4 °C in the refrigerator. Anti-Biotin MicroBeads were further added into the cell suspension and incubated in the fridge for 15 minutes. Cells were then washed by adding 5 ml of depletion buffer and centrifuged at 400*xg* for 5 minutes and finally resuspended in 0.5 ml of depletion buffer. A LS-column was prepared by being placed on the magnetic separator then rinsed with 2 ml of depletion buffer. MicroBead-labeled cells were passed through the column followed by adding 1 ml of depletion buffer twice. Cells coming out from the column were collected and centrifuged at 400*xg* for 5 minutes before being resuspended in R10 unless otherwise stated and counted and adjusted to $4x10^6$ cells/ml.

2.7.2.2. Positive selection of $CD8^+$ T cells and $CD19^+$ B cells

For the *in vitro* cytotoxicity assay, $CD8^+$ T cells and $CD19^+$ B cells were isolated by using magnetic bead-based cell separation (Miltenyi Biotec, Germany). $CD8^+$ T cells were extracted from MVA-NP+M1-stimulated tonsillar MNCs after 7-day culture and $CD19^+$ B cells were isolated from cryopreserved tonsillar MNCs after 1-day resting *(see 2.8)*. The MNCs (approximately $5x10^7$ cells) were washed by adding 5 ml of 1X DPBS (Invitrogen, UK) and then centrifuged at 400*xg* for 5 minutes before being resuspended in 400 μl of isolation buffer (0.5% BSA in 1X DPBS). They were labeled with either 100 μl of anti-CD8 or anti-CD19 MicroBead (Miltenyi Biotec, Germany) and incubated in the fridge for 15 minutes. Cells were washed by adding 5 ml of isolation buffer and centrifuged at 400*xg* for 5 minutes and finally resuspended in 0.5 ml of isolation buffer. Labeled cells were passed through a pre-rinsed LS-column placed on the magnetic separator stand. The column was then washed by adding 3 times of 3 ml of isolation buffer to remove non-labeled cells. Finally, 5 ml of isolation buffer were added to the column while taken away from the magnetic stand. The plunger was pushed into the column to extract the labeled-cells out into a tube. The tube

was centrifuged and cells were resuspended in 0.5 ml of R10 unless otherwise stated for $CD8^+$ T cells and 3 ml of R10 for $CD19^+$ B cells.

2.8. Cryopreservation of tonsillar MNCs

Tonsillar MNCs were cryopreserved for later $CD19^+$ B cell isolation used for cytotoxicity assays. Freezing medium (20% DMSO in △FBS) was prepared by adding 1 ml of DMSO (Sigma Aldrich, UK) in 4 ml of △FBS and pre-cooled by keeping on ice. 3 ml of pre-cooled tonsillar MNCs in R10 at $2x10^7$ cells/ml were taken into a 50-ml tube before slowly dropwise adding of 3 ml of freezing media with gentle shaking. Each 1 ml of cells in freezing medium were aliquoted in cryovials on ice before placing in a pre-cooled Mr. Frosty (Thermo scientific, UK) and frozen down at -80°C overnight and kept there until use (no more than 5 days).

To thaw the cryopreserved cells, 5 vials of cells were taken from the -80°C freezer and immediately held in a 37°C water bath with gentle shaking until a small piece of ice remained inside. 1 ml of pre-warmed R10 was added dropwise into each vial before all the cells were transferred to a centrifuge tube and pelleted by centrifuge at 400*xg* for 7 minutes. Cells were suspended in 5 ml of pre-warmed R10 and seeded in T-25 flask and incubated at 37°C, 5% CO_2 overnight for resting.

2.9. Carboxyfluorescein succinimidyl ester (CFSE) labelling

Principle

CFSE was originally developed for the purpose of *in vivo* lymphocyte tracking and also in cytotoxicity assays either *in vivo* or *in vitro*. Later, using CFSE for the tracking of lymphocyte division becomes a routine procedure in many laboratories. Initially, carboxyfluorescein diacetate succinimidyl ester (CFDASE) is a highly cell permeant, non-fluorescent dye. Rapidly influxed across cell membrane into live cells, intracellular esterase cleaves acetate groups, resulting in green fluorescent CFSE trapped inside the cells. The succinimidyl ester group reacts with intracellular free amino groups to generate highly stable covalent bonds. The result is live cells with intracellular fluorescent label that persist for months [126]. At appropriate

concentrations, CFSE is non-toxic to cells and the fluorescence is retained after formaldehyde and alcohol fixation [127]. The fluorescence intensity of CFSE is diluted between daughter cells following cell division, which allows lymphocyte proliferation to be monitored by flow-cytometry. Lymphocyte proliferation can be monitored for up to eight divisions before CFSE fluorescence decreased to the background fluorescence of unlabeled cells [126].

Method

To study T cell proliferation following vaccine stimulation, tonsillar MNCs were labeled with CFSE before vaccine stimulation and culture. If the MNCs were in R10, they needed to be washed by adding 5 ml of 1X DPBS and centrifuged at 400*xg* for 5 minutes. $1x10^6$-$1x10^8$ cells were suspended in 1 ml of 1X DPBS. 1 μl of 5mM CFSE in DMSO (Invitrogen, UK) was added into the cell supension and mixed thoroughly before incubating at 37°C for 15 minutes. After complete incubation, 5 ml of pre-warmed R10 were added into the tube and incubated at 37°C for another 5 minutes before pelleting cells by centrifuge at 400*xg* for 5 minutes. Cells were counted and finally resuspended in R10 at $4x10^6$ cells/ml. The labeled cells should be kept with minimal light exposure.

2.10. Surface and intracellular (cytoplasmic) staining

Polychromatic flow-cytometry after surface and intracellular cell staining allows to study cell phenotypes and functionality (Figure 2.2). To stain cells for flow-cytometry, freshly isolated cells or cells harvested after vaccine stimulation were transferred to 1.5–ml microtubes. Cells were pelleted to remove culture medium then washed by adding 1 ml of FACS staining buffer (0.2% BSA in 1X PBS) and centrifuged at 500*xg* for 5 minutes. Cells were then incubated for 30 minutes in the fridge with 50 μl of master mix fluorochrome-conjugated antibodies to any cell surface markers (e.g. CD19, CD3 and CD4). Cells then were washed by adding 1 ml of staining buffer and centrifuged at 500*xg* for 5 minutes. If no intracellular staining (ICS), cells were resuspended in 400-500 μl of staining buffer. If ICS was required, cells were dispersed after centrifugation then 100 μl of intracellular (IC) fixation buffer (eBioscience, UK) added with immediate vortex and incubation in the dark at room temperature for 20 minutes. To wash out fixative reagent, 1 ml of 1X permeabilisation buffer

(eBioscience, UK) was added in to the cell tube and centrifuged at 1000*xg* for 5 minutes. Supernatant was decanted as much as possible to avoid any effects of remaining fixative agent to antibodies added in the later step. Cells were then dispersed and incubated for 20 minutes at room temperature with 50 μl of master mix fluorochrome-conjugated monoclonal antibodies to any cytokines or cytoplasmic markers (e.g. IFN-γ and perforin). Cells were then washed by adding 1 ml of 1X permeabilisation buffer and centrifuged at 1000*xg* for 5 minutes. Washing was repeated with 1 ml of FACS staining buffer. Cell pellet was finally resuspended in 400-500 μl of staining buffer. Labeled cells were kept in the fridge with protection from light until flow-cytometry.

To prepare the master mix antibody, each sample required 50 μl of master mix antibodies. The volume of each antibody was calculated based on the total number of samples before mixing them together and adjusting the volume with FACS staining buffer or 1X permeabilisation buffer for surface staining and ICS, respectively. For example, if 5 samples were stained with 2 surface markers; anti-CD4-PE and anti-CD8-PECy7 and 5 μl of each antibody was required to stain each sample, the master mix antibody was prepared as following;

1. Calculate the total volume of each antibody based on the number of samples

   Total volume of anti-CD4-PE = 5 μl x 5 samples = 25 μl

   Total volume of anti-CD8-PECy7 = 5 μl x 5 samples = 25 μl
2. Calculate the total volume of FACS staining buffer to add into master mix

   Total volume of staining buffer

   = (50 μl x No. of samples) – total volume of each antibody

   = (50 μl x 5 samples) – 25 μl of anti CD4-PE – 25 μl of anti CD8-PECy7

   = 250 – 25 – 25 = 200 μl
3. In sum, mix antibodies and staining buffer as calculated to prepare master mix antibodies

Anti CD4-PE	25 μl
Anti CD8-PECy7	25 μl
Staining buffer	200 μl (or 1X permeablisation if ICS)

In case of using more than one conjugated with brilliant violent dye-conjugated antibody in the panel (e.g. BV421 together with BV650), 50 μl of brilliant stain buffer (BD Biosciences, UK) was replaced with FACS staining/ permeablisation buffer to dilute antibodies and make the master mix. The total volume of master mix added to each sample was the summed volume of all antibodies and brilliant stain buffer.

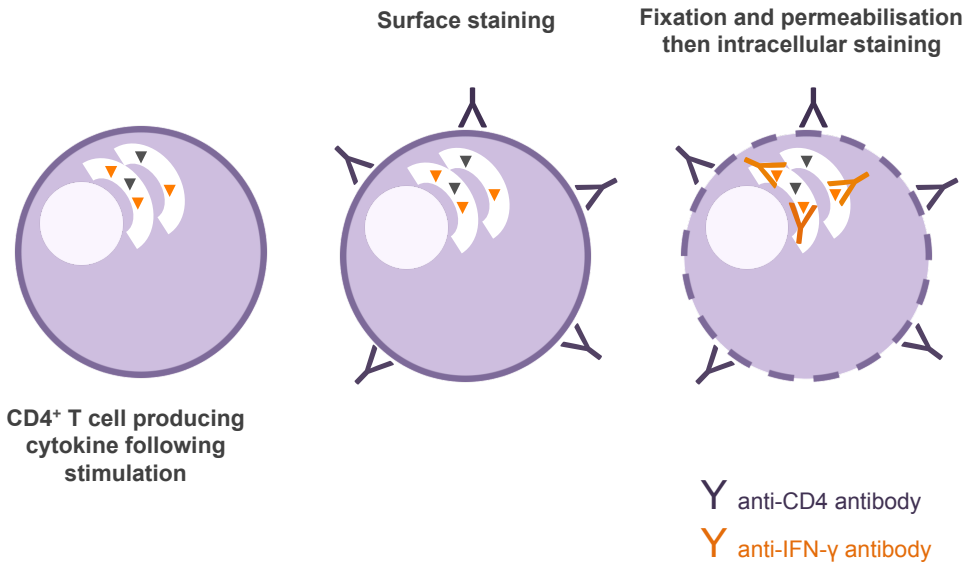

Figure 2.2 Surface and intracellular cell staining

The figure illustrates the principle of surface and intracellular cell staining using fluorescence-tagged monoclonal antibodies. Specific surface markers on the cell surface (e.g. CD4) are firstly stained. Cells then are fixed with compatible fixation agents to stabilise the cell morphology. Permeabilisation buffer generates pores on cell membrane, which allow the antibody enter into cell cytoplasm and bind to target proteins (e.g. cytokines and granzymes).

2.11. Flow-cytometry

Labeled cells were immediately analysed or kept in the fridge overnight away from light before flow-cytometry. The labeled cells were transferred to a FACS tube (Corning, UK). Flow cytometric data from each sample was acquired by FACS Calibur using CellQuest Pro software or FACS Accuri C6 or FACS Celesta using FACS Diva (BD Biosciences, USA). The number of events acquired was dependent upon each study. The data were analysed using FlowJo 8.7 software (FlowJo, LLC.) or BD AccuriC6 software (BD Biosciences, USA).

2.12. Enzyme-linked ImmunoSpot Assay (ELISPOT)

Principle

ELISPOT is a highly sensitive immunological assay to enumerate cytokines or antibody-producing cells in peripheral blood mononuclear cells or lymphoid tissue-isolated cells such as splenocytes. One of the most common applications of the assay is to quantify the frequency of IFN-γ-producing cells in response to antigenic stimulation. In the assay, cells are cultured with the target antigen in an antibody-coated membrane microtitre plate. In response to the antigen recognition, cells secrete proteins; for example IFN-γ, that being captured by specific antibodies bound in the wells. Secreted cytokines are detected by biotinylated detection antibody with streptavidin-enzyme conjugate followed by the addition of its corresponding chromogenic precipitating substrate (Figure 2.3). The end result is visible as spots, which each spot corresponds to a single secreting cell [128], [129].

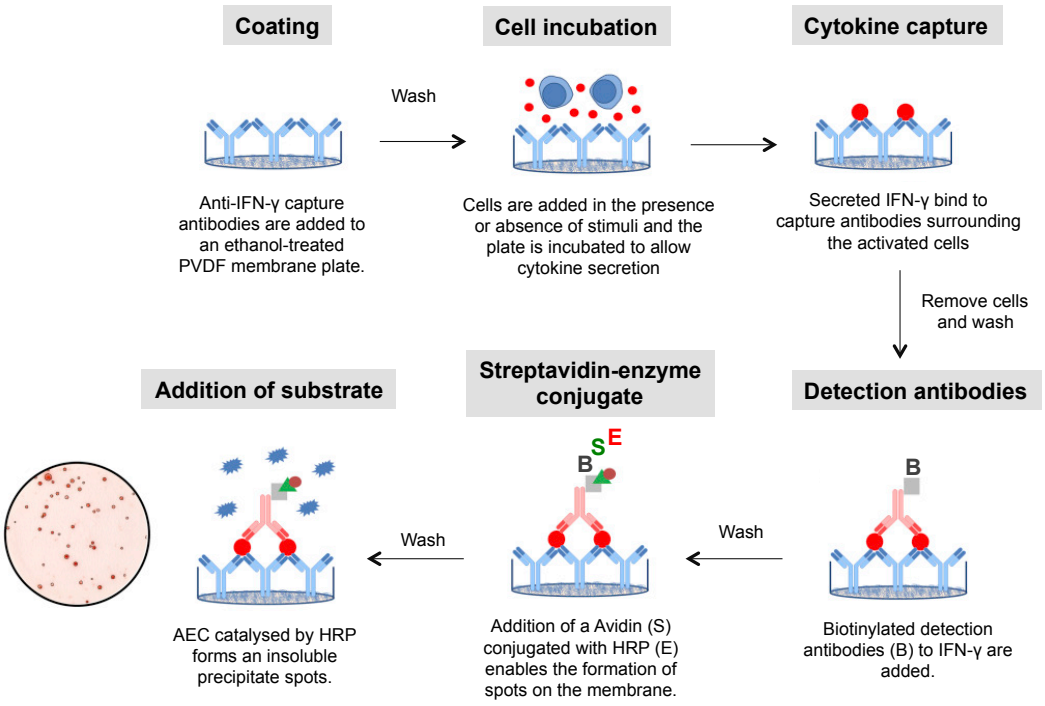

Figure 2.3 Enzyme-linked ImmunoSpot Assay (ELISPOT)

The figure illustrates the principle of IFN-γ ELISPOT assay based on six steps; antibody coating, cell incubation, cytokine capture, addition of detection antibodies, addition of streptavidin-enzyme conjugate and addition of substrate (Adapted from [130], [131]).

Method

To detect IFN-γ-producing cells in adenotonsillar MNCs following *in vitro* MVA-NP+M1 stimulation, ELISPOT was performed using human IFN-γ ELISPOT kit (eBiosciences, UK) following manufacturer's instructions. Briefly, the 96-well polyvinylidene fluoride (PVDF) membrane ELISPOT plate (MSIPN4510, Millipore, UK) was pre-wetted with 15 μl of 35% freshly prepared ethanol for 10-60 seconds. The plate was extensively washed with 200 μl of 1X PBS for five times then coated with 100 μl of 1X anti-human IFN-γ capture antibody diluted in 1X coating buffer and kept in the fridge overnight. Next day, the plate was washed twice with 1X coating buffer followed by blocking with R10 for at least 60 minutes at room temperature. In the meantime, tonsillar MNCs following *in vitro* vaccine stimulation were harvested, counted and adjusted to $2x10^6$ cells/ml. Cells were then stimulated with M1 influenza peptide pools (BEI Resources, USA; *detail see 4.3.6*). R10 was removed from the plate and 100μl of peptide-stimulated cells were seeded in triplicate. Cells without any stimulation were cell control and only R10 was used as a negative medium control. Cells stimulated with 1 μg/ml Staphylococcal enterotoxin B (SEB) (NR-44235, BEI Resources, USA) were used as positive control. The plate was incubated at 37°C, 5% CO_2 for 24 hours with minimal agitation. Following the complete incubation, cells were removed from the plate and the plate then was washed three times with washing buffer (0.05% Tween20 in 1X PBS). The plate was incubated with 100 μl of 1X anti-human IFN-γ detection antibody for 120 minutes at room temperature. It was then thoroughly washed before incubating with 100 μl of 1X Avidin-Horseradish peroxidase (Avidin-HRPO) for 45 minutes at room temperature. Finally, the plate was extensively washed with washing buffer followed by 1X PBS. Spots were developed by adding 100 μl of 3-amino-9-ethyl carbazole (AEC) substrate *(see appendix-1)* (Sigma Aldrich, UK). The plate was incubated in the dark for about 15-20 minutes before stopping the reaction by removing substrate following by rinsing with cold tap water 3-5 times and left to dry. The spots were automatically counted by an EliSpot Reader (AID).

2.13. Indirect Enzyme-linked Immunosorbent Assay (ELISA)

Principle

ELISA is a simple and rapid technique based on an enzyme-labeled antibody. It is capable of quantifying proteins immobilised to a solid surface. ELISA is traditionally performed in polystyrene microtitre plates where antigen or antibody binds via passive absorption. There are four different formats of ELISA; direct, indirect, sandwich and competitive. For the indirect ELISA, the antigen of interest is immobilised in 96- or 384-well plate. A blocking buffer is added to saturate all unbound areas; avoid any non-specific binding of analytes in the later step. Samples containing antibodies (or analytes) are then incubated in the pre-coated plate, followed by enzyme-conjugated anti-species antibody specific to the analytes (e.g. anti-human IgG antibody). The corresponding substrate is finally added, which is catalysed by the enzyme, resulting in the colour-changed solution (Figure 2.4) whose optical density (OD) can be measured by a microplate reader [132].

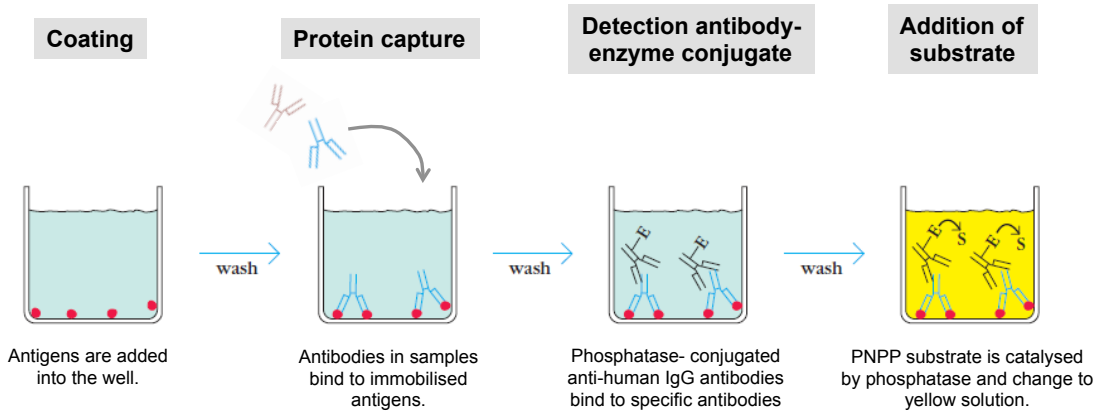

Figure 2.4 Indirect Enzyme-linked Immunosorbent Assay (ELISA)

The figure illustrates the principle of indirect ELISA to detect antigen-specific antibodies based on four steps; antigen coating, antibody capture, addition of detection antibody-enzyme and addition of substrate (Adapted from [133]).

Method

Cell culture supernatant from adenotonsillar MNCs following *in vitro* MVA-pdmH1HA stimulation was analysed for HA-specific IgG antibodies by indirect ELISA as described previously [84]. Briefly, a 96-well microplate (No. 3590, Corning, USA) was coated with 100 μl of 0.25 μg/ml HA of an influenza strain (pH1N1 or sH1N1 or H3N2 or H5N1) or 100 μl of 0.5 μg/ml HA of H7N9 or H9N2 diluted in 1X PBS (The concentration of HA of each influenza virus was pre-optimised, data not shown), then kept in the fridge overnight. Next day, the HA-coated plate was washed five times and blocked with 150 μl of blocking buffer (10%△FBS in 1X PBS) for at least 60 minutes. 50 μl of each diluted sample was applied in duplicate and incubated on a horizontal shaker at room temperature for 120 minutes. Along with the samples, human convalescent serum to H1N1 pdm09 (NR-18964) and human reference antiserum to A/Indonesia/05/2005 (H5N1) (NR-33669, both BEI resources, USA) were used as standard antiserum for specific detection of anti-pH1N1 and anti-H5N1 antibodies, respectively. Human normal immunoglobulin; Sandoglobulin (CSL, Australia) was used as the standard for the detection of anti-H3N2, anti-sH1N1, anti-H7N9 and anti-H9N2 antibodies due to unavailability of specific standard reagent. Blocking buffer was used as a negative control. After complete incubation, the plate was washed 5 times with washing buffer (0.05% Tween20 in 1X PBS) using a microplate washing machine. 50 μl of 1:2000 mouse monoclonal anti-human IgG antibody, alkaline phosphatase conjugated (Sigma Aldrich, UK) was added and incubated for 90 minutes. Finally, the plate was washed 5 times with washing buffer, before adding 50 μl of *p*-Nitrophenylphosphate (PNPP) substrate *(see appendix-1)* (Sigma Aldrich, UK). OD was read at 405 nm at 60 and 120 minutes after substrate added by microplate reader (Dynex Opsys MR™). The antibody concentration in standard antiserum (Units/ml, U/ml) was defined from its dilution that showed the OD of 1.0±0.1 at 60 minutes after adding the substrate. With the standard curve, the OD value of each sample was calculated to HA-specific IgG antibody concentration (U/ml) using DeltaSoft 1.61.0 programme (Biometallics Inc.).

2.14. Haemagglutination Inhibition (HAI) Assay

Principle

HAI assay is a gold standard to detect antibodies against a specific influenza virus strain. The assay takes advantage of the observation that HA protein of influenza virus could bind to red blood cells (RBC), causing agglutination. When antibodies specifically bind to HA of influenza virus, this antigenic site, which is around receptor-binding site (RBS) is blocked and unable to bind with RBCs, demonstrating the inhibition of haemagglutination, which is the basis of the assay (Figure 2.5). HAI assay is performed in microtitre plates. A standardised quantity of HA antigen is mixed with serially diluted samples containing virus-specific antibodies (e.g. serum), followed by the addition of RBCs to assess the degree of binding of the antibody to the HA molecule of the virus [134] .

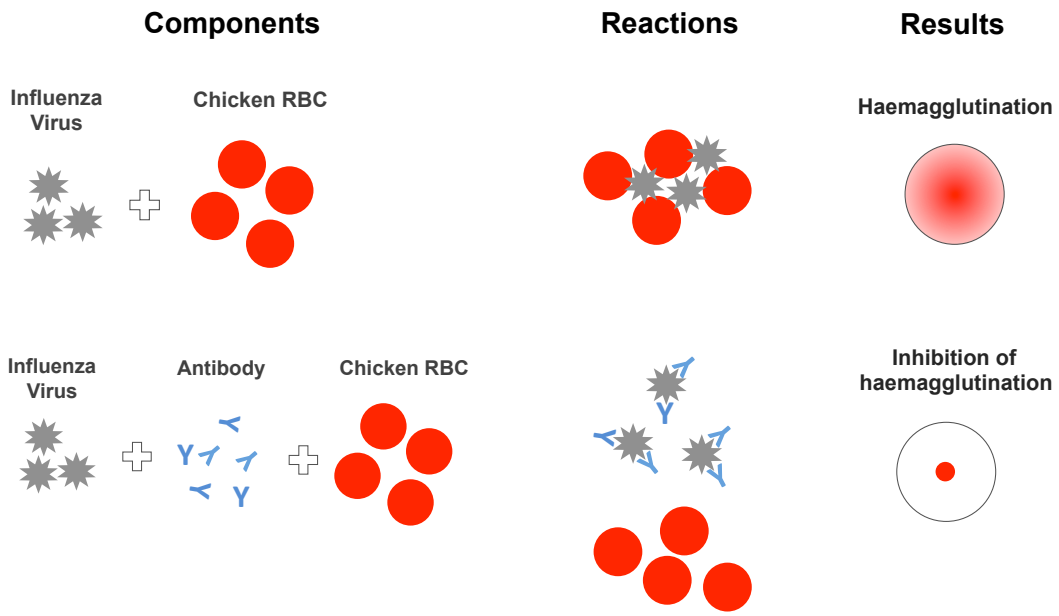

Figure 2.5 The principle of Haemagglutination Inhibition

The figure illustrates haemagglutination when co-incubating influenza and chicken red blood cells. The inhibition of haemagglutination occurs when antibodies specific to the HA epitope around the receptor binding site of the virus are introduced to the system, which block the binding of influenza viruses to RBCs (Adapted from [135]).

Method

Anti-HA antibodies in cell culture supernatant from adenotonsillar MNCs following *in vitro* MVA-pdmH1HA stimulation were also analysed by HAI assay as described previously [134]. Human serum used as positive control was treated with receptor-destroying enzyme (RDE). 100 μl of serum was added with 300 μl of 1X RDE (Denka Seiken, Japan) and incubated at 37°C for 18-24 hours. Cell culture supernatant was omitted for RDE treatment. Next day, 400 μl RDE-treated serum and 150 μl of cell supernatant samples were heated in a heat block at 56°C for 60 minutes before adding pre-cooled 1X PBS; 600 μl for serum and 150 μl for cell culture supernatant, making them 1:10 and 1:2 final dilution. 20 μl of packed chicken RBCs (First Link, UK) were added into each sample, gently mixed and incubated at room temperature for 60 minutes while inverting tubes every 15 minutes to resuspend RBCs. After centrifugation to pellet RBCs, supernatant was collected for HAI assay. To perform the assay, RDE-treated human serum was used as a positive control and PBS as a negative RBC control. 50 μl of 1X PBS was added in all wells of column 12. 50 μl of RBC-treated cell culture supernatants were added in duplicate in row A of column 1-10. The human serum was added in A11. All samples in column 1-11 were then 2-fold serial diluted by taking 25 μl of sample from row A into 25 μl of 1X PBS of successive row until row H of V-bottom 96-well plate (Nunc 249570, Thermo scientific, UK). 25 μl of 8 HA unit (HAU) standardised inactivated influenza virus antigen (pdmH1N1 or H5N1, *see appendix-1*) was added in all wells except RBC control in column 12, mixed well and incubated at room temperature for 30 minutes. 50 μl of 0.5% chicken RBCs *(see appendix-1)* was finally added in all wells and incubated at room temperature for another 30 minutes (Figure 2.6). The HAI titre of each sample was interpreted as the highest dilution showing the complete non-agglutination (Figure 2.7)

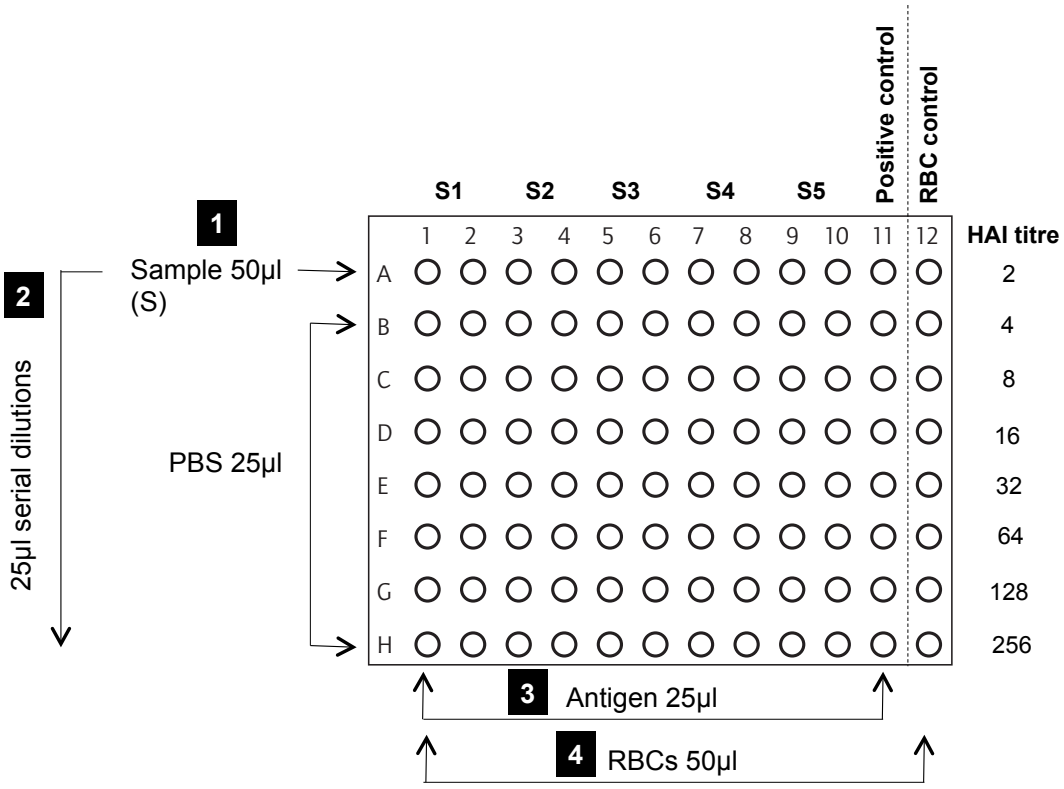

Figure 2.6 Schematic outline of haemagglutination inhibition (HAI) assay

To perform the HAI assay, 50µl of cell culture supernatants are added in duplicate from A1-A10. Positive control RDE-treated human serum is added in A11. All are then 2-fold serial diluted in 1X PBS down to row H. 25µl of influenza virus antigen is added followed by 50µl of 0.5% chicken red blood cells (RBC) to assess HAI titre. For RBC control, only 50µl of 1X PBS is added with 50µl RBCs.

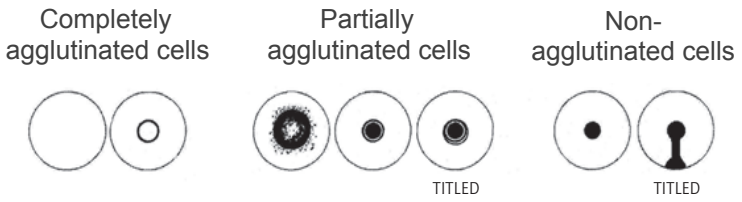

Figure 2.7 Patterns of avian red blood cell agglutination

Completely, partially and non-agglutinated chicken red blood cells are shown. Only non-agglutinated cells, which appeared as a sharp button of RBCs and flowed down when tilting the plate, were used to interpret the HAI titre [134].

2.15. Statistical analysis

All statistical analyses were performed using Graphpad Prism 5.0. The difference of two groups was analysed either by paired, non-parametric test (Wilcoxon matched-pairs singed rank test) or by unpaired, non-parametric test (Mann Whitney test). The difference among a group of more than two was analysed by one-way analysis of variance (ANOVA) and then for each pair by t-test.

…….

Chapter 3

The expression of influenza protein antigens in adenotonsillar MNCs following *in vitro* stimulation with Modified Vaccinia Ankara (MVA) and simian adenovirus (PanAd3)-vectored influenza vaccines

3.1. Introduction

Influenza has continued to cause widespread morbidity and mortality in humans, resulting in major challenges to healthcare systems. Current influenza vaccines are of limited efficacy against mismatched or emerging new virus strains [4]. The H1N1 pandemic outbreak in 2009 and the potential of future pandemics of avian influenza (e.g. H5N1, H7N9 and H9N2) highlight the urgent need for more effective vaccines. Current efforts are focused on the development of novel vaccines capable of inducing broad protection from multiple subtypes of influenza viruses including those with the potential to cause pandemics. To confer a broadly protective response, conserved viral proteins are considered as vaccine targets. These novel vaccine antigens include NP, M1, M2e and the stem region of haemagglutinin (HA2) [22], [35], [43], [136]. Moreover, a number of advanced vaccine platforms such as DNA vaccines, virus vector-based vaccines, virus-like particles, synthetic peptides and liposomes have been applied to develop novel vaccines delivering these target proteins for better and broader protection [22], [136].

Among others, virus-vectored vaccines have become one of the promising approaches owing to the favourable feasibility and capacity of transgene insertion, the precise control of target protein expression and the relative ease of production at high titres of the virus. Viral vectors are live viruses but are attenuated or deficient in replication, thus considered to be safe in general [50], [51]. Orthopoxvirus especially Modified Vaccinia Ankara (MVA) and recombinant adenovirus (rAd) vectors have been widely employed for novel influenza vaccine development. They have been constructed to express various target protein antigens, and many of them have been investigated for protective responses in either pre-clinical studies and/or clinical trials [54], [71].

Poxvirus and adenovirus can infect a wide variety of cell types and tissues [137], [138]. This advantage also allows the vectored virus to be administered via many delivery routes both parental and mucosal [139], [140]. By infecting target cells, the encoded transgenes controlled by specific promoters could be expressed to produce influenza proteins in native conformation, inducing both antigen-specific T cell responses and B cell-mediated antibody production [52]. Different types of immune cells in peripheral blood have been collectively

studied and shown to have various degrees of susceptibility to MVA [141]–[143] and some rAd vectors [144]–[146] . However, there is no such data in human NALT.

As the ultimate aim of the project is to study the immune responses elicited by MVA- and PanAd3 vector-based influenza vaccines in human NALT, it is necessary to understand how the virus-vectored vaccines behave at this mucosal inductive site. In this study, I investigated the expression of influenza proteins in different cell types in adenotonsillar MNCs and the cellular localisation of those expressed protein antigens in virus-vectored vaccine-infected cells following *in vitro* MVA- or PanAd3-vectored influenza vaccine stimulation.

3.2. Aims of the study

1. To determine the types of immune cells in adenotonsillar MNCs expressing influenza protein antigens following *in vitro* stimulation of MVA- and PanAd3-vectored influenza vaccine candidates
2. To study the cellular localisation of the influenza vaccine antigens in vectored vaccine-infected cells.

3.3. Materials and methods

3.3.1. Adenoidal and tonsillar tissues

Adenoidal and/or tonsillar tissues were obtained from patients undergoing adenotonsillectomy at local hospitals. Patients who received systemic steroids within 3 weeks prior to surgery, or who had any known immunodeficiency were excluded from the study. Adenotonsillar MNCs were isolated from the tissues following the standard protocol described in chapter 2 *(see 2.7.1)*. Cells were resuspended in R10 at $4x10^6$ cells/ml.

3.3.2. Cell lines

HEK 293T cells (kindly provided by Prof. Bill Paxton, Institute of Infection and Global Health, University of Liverpool) were cultured in T-75 flasks with Dulbecco's Modified Eagle Medium (Gibco, UK) containing 10% heat-inactivated fetal bovine serum (△FBS) and penicillin/ streptomycin (P/S), termed as "DMEM10". Cells were incubated at 37°C with 5%CO_2 and passaged when they reached approximately 80% confluence.

3.3.3. Vaccines

The following vaccines were studied for the expression of influenza vaccine antigens in adenotonsillar MNCs: MVA-wt (#1533), MVA-NP-GFP (#769), MVA-NP+M1 (#850), MVA-pdmH1HA (#1531), PanAd3-gag, PanAd3-NPM1, PanAd3-NPM1-pdmH1HA and PanAd3-NPM1-H5HA. MVA-wt and PanAd3-gag are vector only controls for MVA- and PanAd3-based vaccines, respectively. The virus titres were expressed as plaque-forming unit/ml (pfu/ml) for MVA-based vaccines and as virus particle/ml (vp/ml) for PanAd3-based vaccines.

3.3.4. Fluorochrome-conjugated monoclonal antibodies

The following fluorochrome-conjugated monoclonal antibodies were used for cell staining and flow-cytometry; CD19-PE or FITC (clone HIB19), CD3-PECy5 or PECy7 (clone UCHT1), CD11c-APC (clone B-ly6), CD123-FITC (clone 7G3) (All BD Biosciences, UK) and FITC-conjugated monoclonal antibody to influenza A NP (MA1-7322, Thermo scientific, UK).

Monoclonal antibodies to HA of A/California/04/2009 (pH1N1) (NR-42021), to HA of A/Vietnam/1203/2004 (H5N1) (NR-13444) (Both from BEI Resources, USA) and to influenza A M1 (GA2B, Abcam, UK) were in-house conjugated using R-Phycoerythrin (RPE)-LYNX conjugation kit (BioRad, UK) for measuring influenza protein expression in adenotonsillar MNCs. RPE was chosen due to its high brightness. RPE-conjugated antibodies were kept in the refrigerator and protected from light.

3.3.5. Cell stimulation and culture

Adenotonsillar MNCs were cultured with either MVA vector-based vaccines at a range of multiplicity of infection (MOI) or PanAd3 vector-based influenza vaccines at different virus particles/ cell in a 48-well cell culture plate (Corning, USA) and incubated at 37°C, 5%CO_2. Cells were harvested at different time points for a kinetic study or at 24 hours to measure influenza protein antigen expression. The MNCs without any stimulation (medium control) were used as a negative control. MVA-wt or PanAd3-gag stimulated MNCs were used as vector only controls.

MOI was calculated based on the virus titre in PFU/ml, indicating the number of infectious viruses per cell. Due to the difference in the evaluation of vaccine concentration, the number of virus particles per cell (vp/cell) was used instead of MOI for PanAd3-vectored vaccines.

To study the expression of influenza proteins in HEK 293T cell lines following *in vitro* PanAd3 vector-based vaccine stimulation, cells were seeded at 2x10^5 cells/ well in 24-well plates and cultured in DMEM10 a day before performing the experiment. Culture media was removed and 200 μl of each vaccine at the concentration of 20 vp/cell were gently added to avoid disturbing cells, then incubated at 37°C, 5%CO_2 for 90 minutes before washing out with pre-warmed DMEM. Fresh DMEM containing 2% △FBS and P/S was added to each well for a further 18-hour incubation.

3.3.6. Measurement of influenza protein expression

Following *in vitro* vaccine stimulation, adenotonsillar MNCs were harvested and washed once with FACS staining buffer prior to stain for the cell surface markers; CD19, CD3 or

CD4, CD11c and CD123. Table 3.1 described the CD markers used to identify different types of immune cells. The MNCs were fixed and permeabilised followed by intracellular staining for influenza HA of pdmH1N1 or H5N1, NP and M1 protein depending upon vaccine stimulation *(see 2.10)*. In some experiments, influenza HA of pdmH1N1 and NP was stained without cell permeabilisation, aiming to detect the proteins present on the cell surface. For GFP expression study, the MNCs were only stained for the cell surface markers.

HEK 293T cells, following PanAd3-vectored vaccine stimulation, were trypsinised by adding 100 μl of 0.25% trypsin-EDTA before tapping to detach cells from the bottom of the wells. 0.5 ml of DMEM10 was added into each well before cells were harvested in a tube and pelleted. Cells were then fixed and permeabilised followed by intracellular staining for influenza NP and HA as aforementioned.

The data for labeled MNCs or HEK 293T cells were acquired by BD FACS Calibur or Celesta. The expression of each influenza protein antigen in the MNCs was presented as the percentage of $M1^+$ or NP^+ or HA^+ cells among each cell population (T cells, B cells and dendritic cells).

Table 3.1 CD markers for immune cell identification

CD markers	Immune cells
CD3	Pan T cells (both $CD4^+$ and $CD8^+$ T cells)
CD4	$CD4^+$ T helper cells
CD19	B cells
CD11c	Myeloid dendritic cells
CD123	Plasmacytoid dendritic cells

3.3.7. Statistical analysis

The difference among a group of more than two was analysed by one-way analysis of variance (ANOVA) and then for each pair by t-test.

3.4. Results

3.4.1. The kinetic expression of MVA-encoded transgenes in adenotonsillar MNCs

The kinetics of influenza NP expression in adenotonsillar MNCs were initially studied by the use of a GFP-expressing MVA construct; MVA-NP-GFP. In this construct, as the GFP gene is linked to the promotor of the NP gene, the level of GFP expression will therefore represent the level of NP antigen expression.

Adenotonsillar MNCs were cultured with MVA-NP-GFP at MOI of 1 and GFP expression in the MNCs was examined at different time points. It was shown that GFP expression was observed mainly in $CD19^+$ B cells. The GFP expression in the MNCs was detected at as early as 6 hours following *in vitro* stimulation. The proportion of GFP^+ cells increased with time of incubation until reaching the peak, which lasted between 24 and 30 hours before decreasing. When the median fluorescence intensity (MFI) of GFP of these positive cells was analysed, the highest MFI was shown between 16 and 24 hours (Figure 3.1). Therefore, it was concluded that the optimal time to detect the expression of transgene in MVA vectored vaccine-infected cells would be at approximately 24 hours following *in vitro* stimulation.

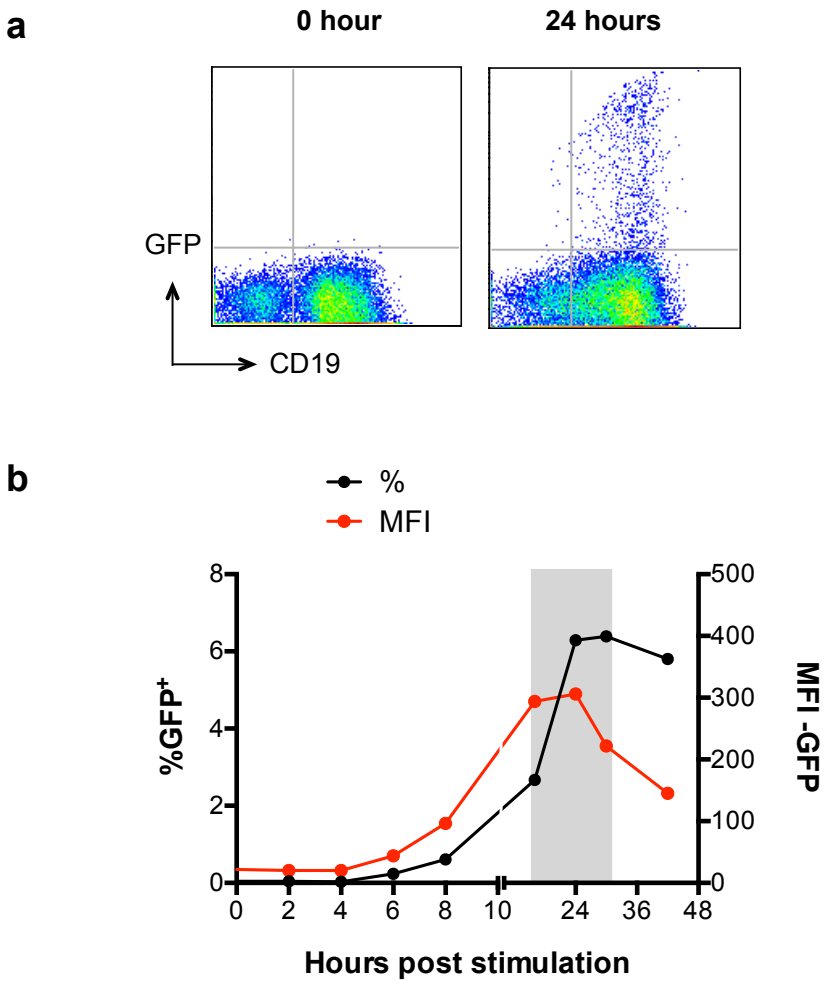

Figure 3.1 GFP expression in adenotonsillar MNCs following *in vitro* MVA-NP-GFP stimulation

Adenotonsillar MNCs were stimulated *in vitro* with MVA-NP-GFP at MOI of 1 before the measurement of the GFP expression level at different time points from 0 to 42 hours. **a)** The representative flow cytometric dot plots showed the expression of GFP at 0 and 24 hours in $CD19^+$ B cells. **b)** The kinetics of GFP expression was shown as the percentage of GFP^+ cells (black line) and the median fluorescence intensity (MFI) of GFP (red line) (n=1).

3.4.2. Specificity and sensitivity of the method based on fluorochrome-conjugated monoclonal antibody-labelling and flow-cytometry for the detection of vaccine antigen expression in adenotonsillar MNCs

Having shown the optimal 24-hour time of transgene expression after MVA vectored vaccine infection, the expression of MVA-encoded protein antigens in adenotonsillar MNCs were directly measured using the developing method based on the intracellular staining of protein antigen with fluorochrome-conjugated monoclonal antibody, followed by flow-cytometry. The range of MOIs of the vaccines was set regarding the previous study [147].

The specificity of the established method was firstly tested. Influenza M1 expression in adenotonsillar MNCs was examined following *in vitro* MVA-NP+M1 stimulation and compared with MVA-pdmH1HA (expressing HA) stimulation at the MOI of 0.025. M1 expression was detected in a significant number of the B cells in the MNCs stimulated with MVA-NP+M1, but not those with MVA-pdmH1HA and MVA-wt (Figure 3.2a,c), suggesting the high specificity of this method.

The sensitivity of this method was then assessed. Influenza HA expression in adenotonsillar MNCs was measured following *in vitro* MVA-pdmH1HA stimulation at low MOIs ranging from 0.0025 to 0.0125. HA antigen was shown to be expressed in adenotonsillar B cells with a dose-dependent manner upon MVA-pdmH1HA infection. The intermediate dose with MOI of 0.006 showed a significant difference in HA expression compared to medium control, showing 3.6 times higher positive cells. An increased proportion of HA-expressing B cells was found at the higher MOI of 0.0125. The results suggested that the method would accurately determine the protein expression in the MNCs when the proportion of protein-expressing cells was approximately 4 times higher than the background (Figure 3.2b,d).

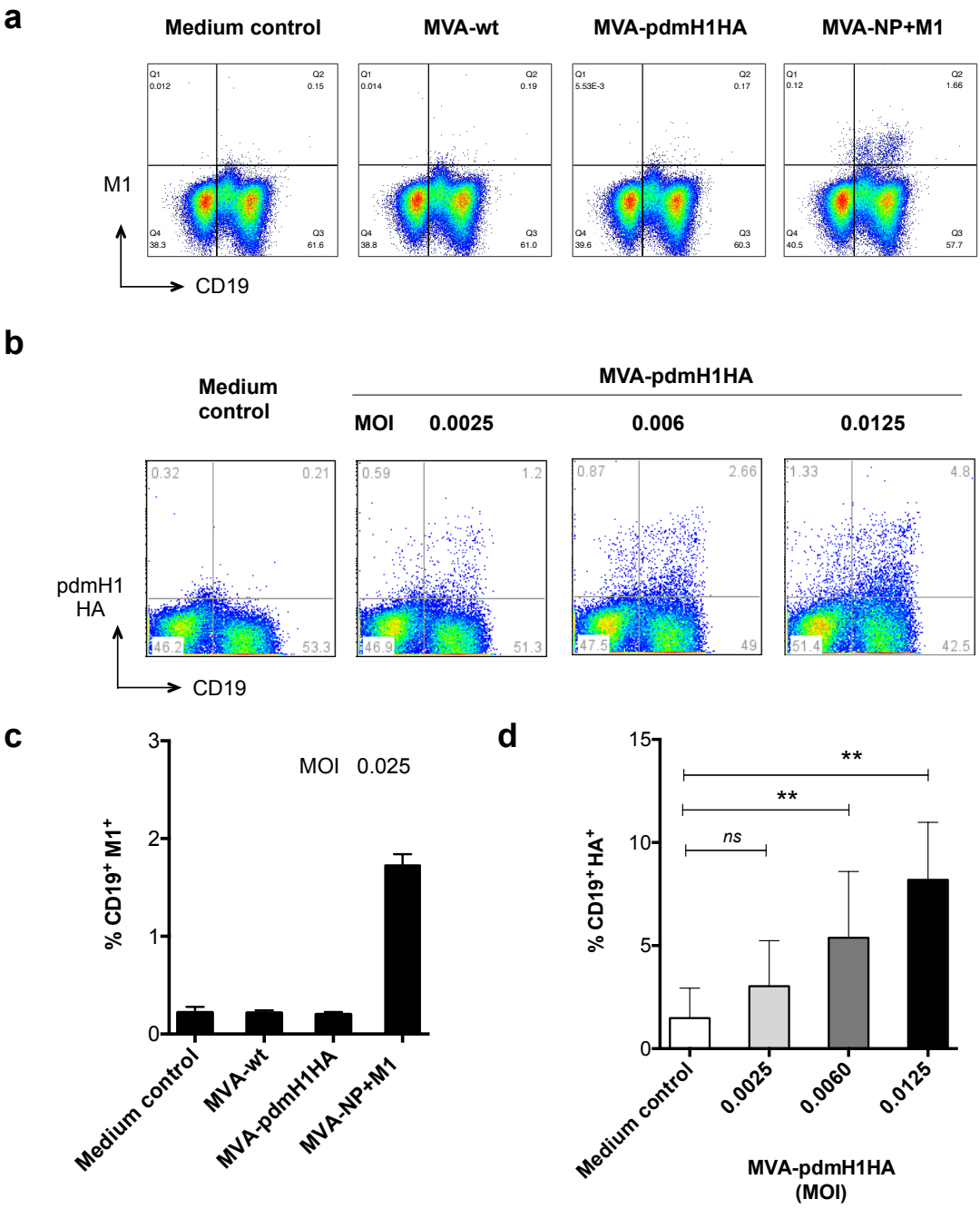

Figure 3.2 Specificity and sensitivity of the method based on fluorochrome-conjugated antibody labeling and flow-cytometry to measure the expression of influenza vaccine antigens

Adenotonsillar MNCs were stimulated *in vitro* with MVA-vectored influenza vaccines for 24 hours as compared to unstimulated MNCs (medium control). **(a,c)** The specificity of the method was shown as M1 expression was detected in $CD19^+$ B cells stimulated with MVA-NP+M1, but not with MVA-wt and MVA-pdmH1HA. Bars and error bars indicated means and SEMs (n=4). **(b,d)** The sensitivity to detect HA expression was shown following MVA-pdmH1HA stimulation. The proportion of HA-expressing B cells was shown upon stimulation with different vaccine doses (MOIs). The intermediate and highest doses showed significant HA expression compared to medium control (pair by t-test, ***p=0.0070 and **p=0.0086*, respectively). Bars and error bars indicated means and SEMs (n=4).

3.4.3. Expression of influenza NP, M1 and HA in adenotonsillar MNCs following *in vitro* MVA-vectored vaccine stimulation

Intracellular protein staining with flow-cytometry is a highly specific and sensitive method to detect influenza protein expression in virus-vectored vaccine-stimulated adenotonsillar MNCs. Thus, the types of immune cells in the MNCs targeted by MVA-vectored vaccines were then examined. Adenotonsillar MNCs were *in vitro* stimulated with either MVA-NP+M1 or MVA-pdmH1HA and the expression of influenza NP, M1 and HA was measured in different cell types including T cells, B cells and dendritic cells (DC) (Figure 3.3). To maximise the chance of MVA-vectored vaccine infection to DCs, which are in a small proportion in the isolated adenotonsillar MNCs, a relatively high titre of the vaccine (MOI of 1) was applied for cell stimulation.

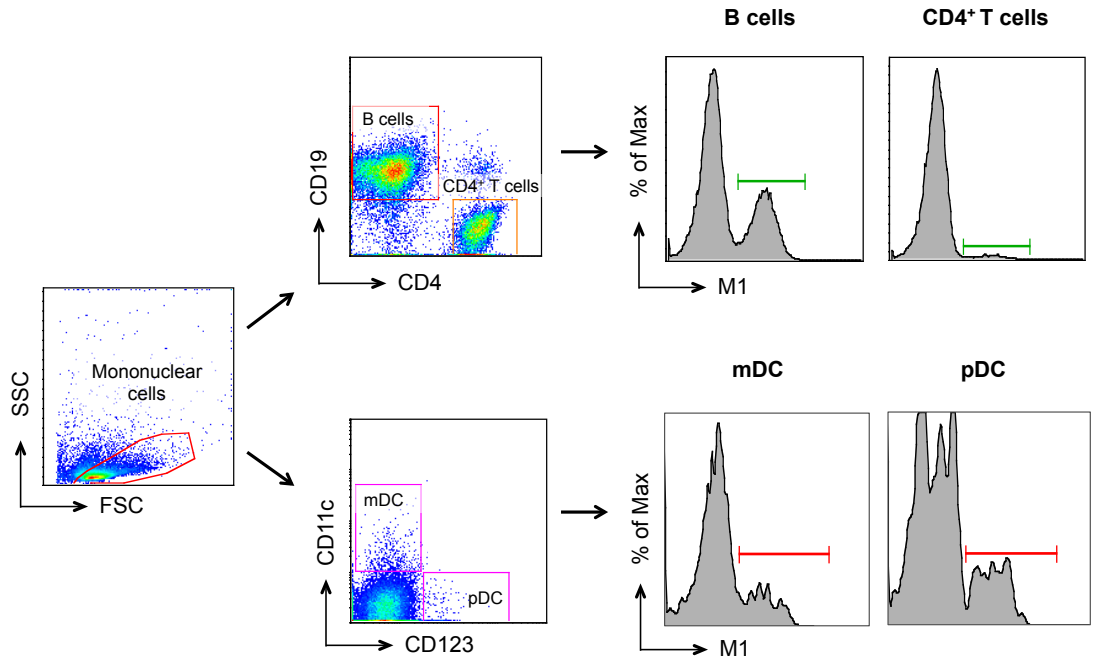

Figure 3.3 Gating strategy for the measurement of influenza protein expression

Viable adenotonsillar mononuclear cells (according to appendix-2) were gated from FSC-SSC plot. Then, either $CD19^+$ B cells or $CD4^+$ T cells as well as $CD11c^+$ myeloid DCs or $CD123^+$ plasmacytoid DCs were gated from the double antibody-stained dot plots. The influenza protein expression (e.g. M1) in each cell types was measured by gating on the histogram the population with high fluorescence intensity of influenza protein.

Following *in vitro* MVA-NP+M1 stimulation, both NP and M1 were shown to be mainly expressed in B cells (Mean ± SEM; NP 42.40 ± 6.31%, M1 35.20 ± 7.55%). Only a few positive cells were detected in $CD4^+$ T cells (NP 3.04 ± 0.91%, M1 3.56 ± 1.08%). The results from pan $CD3^+$ T cells were comparable as those from only $CD4^+$ T cells (data not shown). Most B cells showed the co-expression of both NP and M1 (Figure 3.4c), which indicated that each infected cell expressed both proteins, most likely owing to the vaccine construct where NP and M1 genes are linked to each other driven by the same promoter. According to the results, the expression of M1 could represent the expression of NP, the expression of only M1 was further examined in dendritic cells, which were a small population (<0.5%) in the MNCs. M1 expression was also detected in both myeloid dendritic cells (mDC; 21.17 ± 3.18%) and plasmacytoid dendritic cells (pDC; 22.07 ± 7.14%). By contrast, NP and M1 expressions were undetectable in any cell types following *in vitro* MVA-wt stimulation (vector control) (Figure 3.4a,b).

The expression of HA in adenotonsillar MNCs was examined following *in vitro* MVA-pdmH1HA stimulation. The vaccine dose to stimulate cells was reduced to MOI of 0.025 as cell morphology was affected when stimulated at MOI of 1 (data not shown). Similar to M1 and NP expressions, HA protein expression was also predominantly observed in B cells (21.41± 2.36%) and a few in $CD3^+$ T cells (3.51 ± 0.79%) (Figure 3.5).

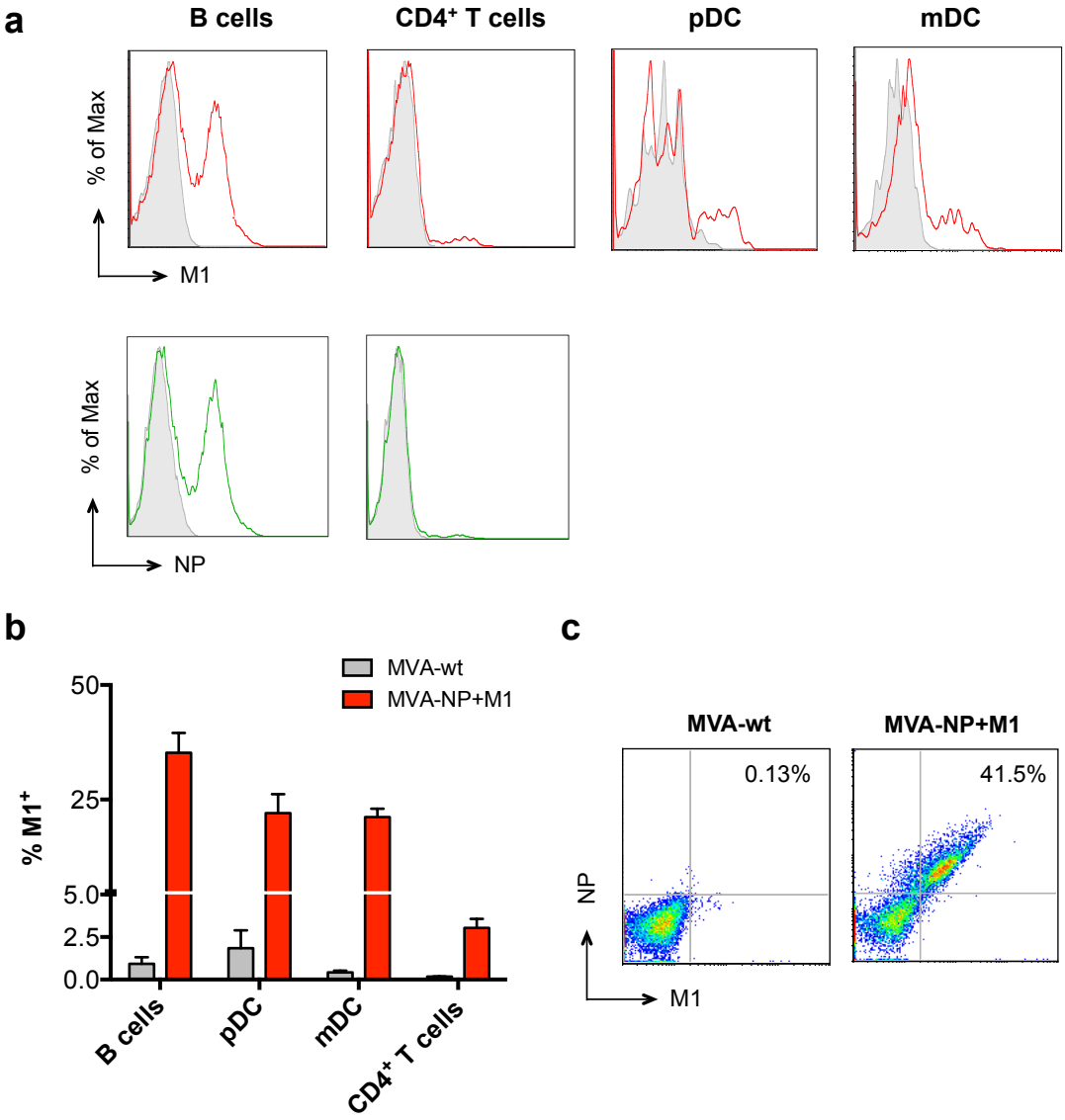

Figure 3.4 Expression of influenza nucleoprotein (NP) and matrix protein 1 (M1) following *in vitro* MVA-NP+M1 stimulation

Adenotonsillar MNCs were cultured with MVA-NP+M1 at MOI of 1 for 24 hours followed by intracellular staining for NP and M1 and flow-cytometry. **a)** The histograms showed the expression of M1 (red line) and NP (green line) in $CD19^+$ B cells, $CD4^+$ T cells, myeloid (mDC) and plasmacytoid dendritic cells (pDC) following *in vitro* MVA-NP+M1 compared to MVA-wt (grey shade) stimulation. **b)** Bar charts compared the percentage of $M1^+$ cells in each cell types between MVA-NP+M1 (red bar) and MVA-wt (grey bar) stimulation (n=3). Bars and error bars indicated means and SEMs. **c)** Gating on $CD19^+$ B cells, the representative flow cytometric dot plot showed the co-expression of NP and M1 following *in vitro* MVA-NP+M1 stimulation.

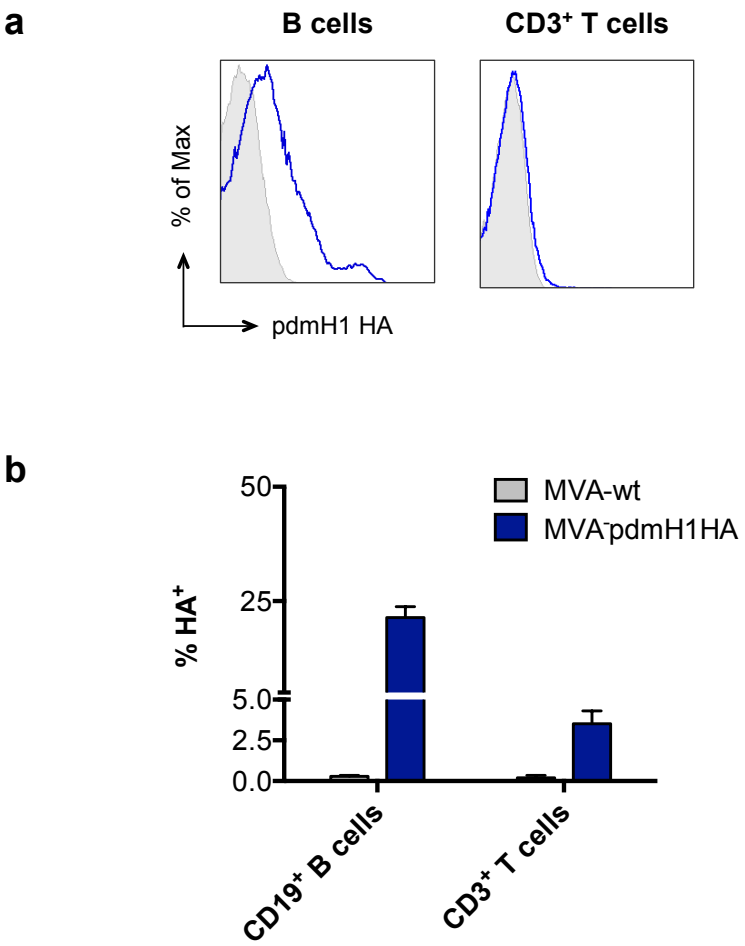

Figure 3.5 Expression of influenza haemagglutinin (HA) following *in vitro* MVA-pdmH1HA stimulation

Adenotonsillar MNCs were cultured with MVA-pdmH1HA at MOI of 0.025 for 24 hours followed by intracellular staining for HA of pandemic H1N1 strain (pdmH1HA) and flow-cytometry. **a)** The histograms showed HA protein (blue line) following *in vitro* MVA-pdmH1HA compared to MVA-wt (grey shade) stimulation in $CD19^+$ B cells and $CD3^+$ pan T cells. **b)** Bar charts compared the percentage of HA^+ cells in each cell types between MVA-pdmH1HA (blue bar) and MVA-wt (grey bar) stimulation (n=3). Bars and error bars indicated means and SEMs.

3.4.5. Cellular localisation of influenza NP and HA in MVA vector-infected adenotonsillar B cells

By using cell surface and intracellular staining to detect influenza protein antigen expression, the different localisation pattern between influenza NP and HA was observed in MVA vaccine-infected adenotonsillar B cells. At 24-hour culture, HA expression following *in vitro* MVA-pdmH1HA stimulation was detected on the B cell surface directly; but surface NP expression was not shown following *in vitro* MVA-NP+M1 stimulation. Nevertheless, both HA and NP expression were detected when these cells were intracellularly stained for HA and NP with the same antibodies (Figure 3.6a). According to the intracellular staining protocol, proteins detected are present in the cell cytoplasm rather than in the nucleus. These results suggested that following *in vitro* stimulation by the two different MVA-based vaccines, HA protein antigen localised both in the cell cytoplasm and on the cell membrane, whereas NP protein antigen remained in the cell cytosol.

As the synthesis of foreign proteins delivered by viral vectors generally occurs in the cell cytoplasm, it was queried whether HA migrated to the cell membrane after being synthesised. To examine this, the MNCs were stimulated with MVA-pdmH1HA in the presence or absence of brefeldin A (BFA), which inhibits protein transportation from the endoplasmic reticulum to the Golgi apparatus. After 6-hour culture in the absence of BFA, HA appeared on B cell surface, as shown previously. However, when BFA was introduced into the cell culture, the level of HA expression on cell surface drastically reduced, whereas no significant change in HA expression was seen in the cell cytoplasm of B cells (Figure 3.6b). This would be consistent with our hypothesis that HA encoded in MVA-pdmH1HA is initially expressed in the cytoplasm before transported to the cell surface of MVA-infected adenotonsillar B cells by the host cell protein transportation mechanism.

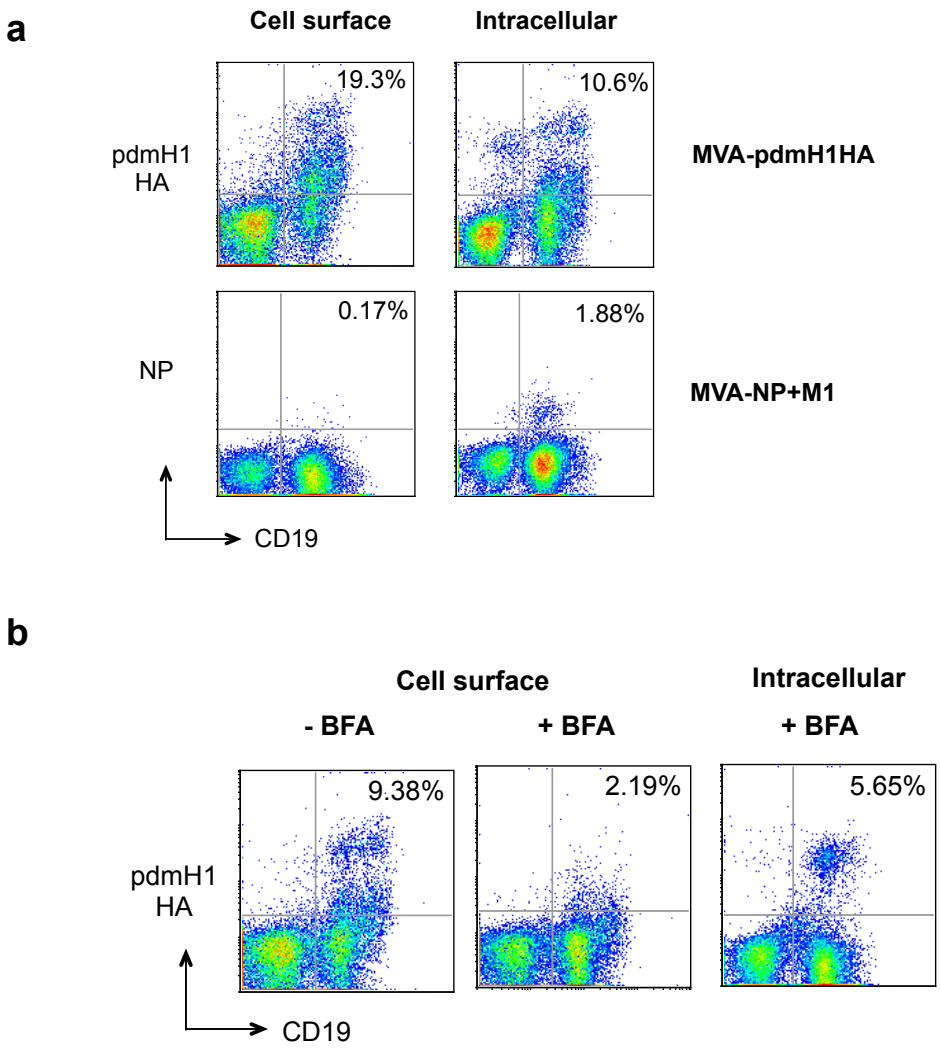

Figure 3.6 Cellular localisation of influenza NP and HA following *in vitro* MVA-vectored vaccine stimulation

Adenotonsillar MNCs were stimulated *in vitro* with either MVA-pdmH1HA or MVA-NP+M1 at MOI of 0.025. **a)** The flow cytometric dot plots showed the detection of influenza HA of pandemic H1N1 strain (pdmH1HA) on the cell surface and in the cell cytoplasm, while nucleoprotein (NP) only in the cell cytoplasm after 24-hour incubation. **b)** Following 6-hour vaccine stimulation, the reduction of influenza HA at the cell surface was seen when brefeldin A (BFA) was present. However, in the same cell sample, HA was detected in the cell cytoplasm.

3.4.6. Expression of influenza proteins in adenotonsillar MNCs following *in vitro* PanAd3-vectored vaccine stimulation

The expression of influenza proteins NP and HA in adenotonsillar MNCs was also investigated following *in vitro* stimulation with PanAd3-based influenza vaccines using the same method aforementioned. Firstly, the expression of influenza NP was measured following PanAd3-NPM1 stimulation at the ratio of one virus particle per cell (1 vp/ml). However, there was no significant NP protein expression in the MNCs either in B or T cells, which was in contrast to the prominent NP expression in B cells following *in vitro* MVA-NP+M1 stimulation (Figure 3.7).

To determine the infectivity of the PanAd3-based influenza vaccines, the expression of protein antigens from each PanAd3-based influenza vaccine was examined in a susceptible cell line, HEK293T at 20 vp/cell. NP and HA of either pandemic H1N1 or avian H5N1 were measured after the PanAd3-vectored vaccine stimulation, with MVA vaccine-stimulated cells as positive controls. Interestingly, NP and/or HA were shown to be efficiently expressed in HEK293T cells. Apart from that following PanAd3-gag (vector control) stimulation, NP expression was detectable in the cells cultured with all the PanAd3-vectored vaccines encoding NP transgene. Moreover, HA expression was shown in the cells stimulated with PanAd3-NPM1-pdmH1HA and PanAd3-NPM1-H5HA (Figure 3.8). The results indicated that these PanAd3 vector-based influenza vaccines were infectious.

Adenotonsillar MNCs were thus retested with higher doses of PanAd3-NPM1 at 10 and 50 vp/cell, but still the level of NP expression was marginal (Figure 3.7). Despite the fact that PanAd3-NPM1 vaccine was infectious, influenza NP was not found in either B or T cells, suggesting that lymphocytes are likely to be refractory to PanAd3 virus vector. Therefore, the measurement of the expression of influenza proteins from other PanAd3-vectored influenza vaccines in the MNCs was discontinued.

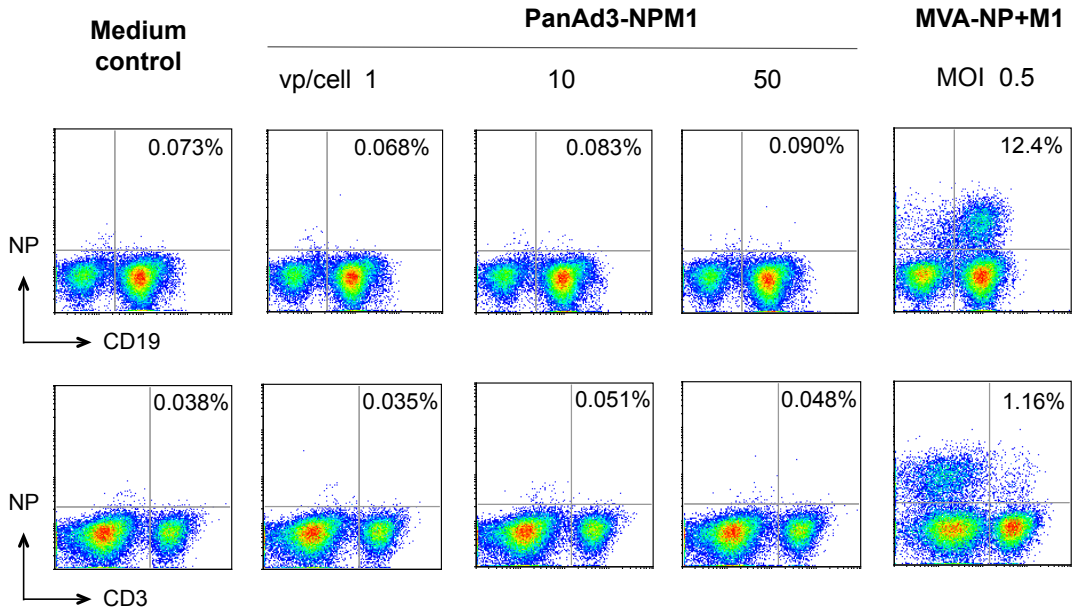

Figure 3.7 Expression of influenza nucleoprotein following *in vitro* PanAd3-NPM1 stimulation in adenotonsillar MNCs

Adenotonsillar MNCs were cultured with PanAd3-NPM1 at different virus particles per cell (vp/cell) ranging from 1 to 50 for 24 hours before intracellular staining for nucleoprotein (NP) and flow-cytometry. The flow cytometric dot plots showed the marginal expression of NP in both $CD19^+$ B cells and $CD3^+$ T cells at any vaccine doses. MVA-NP+M1-stimulated MNCs were positive control and unstimulated MNCs (medium control) were negative control.

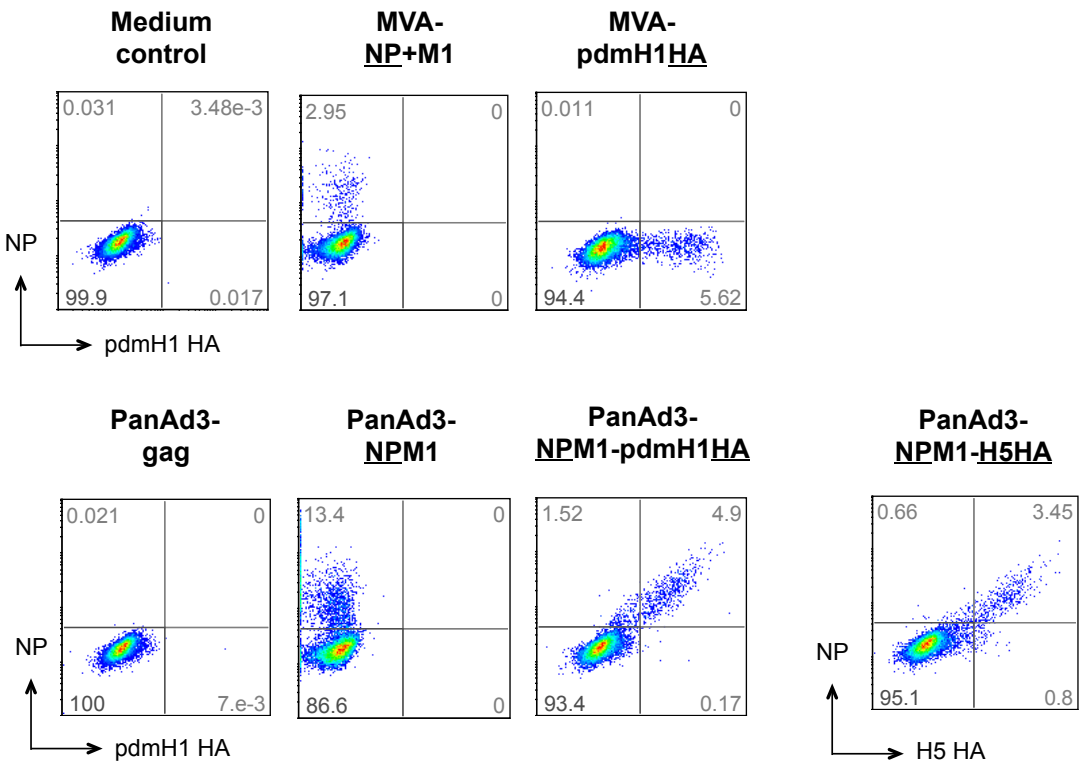

Figure 3.8 Expression of influenza proteins following *in vitro* PanAd3-based influenza vaccine stimulation in HEK293T cells

HEK293T cells were cultured with each PanAd3-based influenza vaccine encoding different influenza transgenes at 20 virus particles per cell for 24 hours before intracellular staining for influenza proteins (NP and HA). MVA-NP+M1-stimulated MNCs were positive control, whereas unstimulated MNCs (medium control) were negative control. The flow cytometric dot plots showed that the efficient expression of influenza HA and/ or NP encoded in PanAd3 vectored vaccines in HEK293T cells as compared to no protein expressions in PanAd3-gag vector only control.

3.5. Discussion and conclusion

Viral vector-based vaccines have been extensively studied in recent years to tackle cancer and infectious diseases, including influenza [50], [54], [71]. Most viral vectors are attenuated or replication-deficient viruses, hence they do not cause harmful infection while still being able to induce immunity towards foreign antigens [50], [51]. The first critical step to successfully induce immune responses by vector-based vaccines is that the transgene inserted in the vector is efficiently expressed and presented by APCs [52].

As the ultimate aim of this project is to study the immune responses activated by MVA- and PanAd3 vector-based influenza vaccines in human NALT by using an adenotonsillar cell culture system, the expression of influenza proteins in adenotonsillar MNCs was initially studied following *in vitro* vaccine stimulation. Firstly, the kinetics of influenza NP expression in the MNCs was shown following MVA-NP-GFP stimulation by the indirect measurement of GFP expression. GFP-expressing cells were detected at as early as 6 hours and peaked at 24 hours (Figure 3.1), indicating the rapid kinetics of MVA infection and transgene expression. The results were in agreement with previous studies performed in human peripheral mononuclear cells (PBMC) [141]–[143]. The reduction of GFP-expressing cells after 24 hours would result from MVA infection-induced cell apoptosis, which was also previously observed in monocytes and B cells in PBMCs [143].

In the absence of GFP expression, the detection of the protein expression from the inserted transgene in vectored-vaccines mostly relied on the use of western blotting. However, this traditional method is time-consuming and lacks the ability to identify the cell types expressing the protein of interest. A new method based on fluorescence-conjugated monoclonal antibody labeling and flow-cytometry was established to overcome those limitations. The method was shown to be highly specific and sensitive to examine the expression of influenza protein antigens in adenotonsillar MNCs following MVA-vectored vaccine stimulation (Figure 3.2).

By using the established method, the cell populations in adenotonsillar MNCs targeted by MVA-NP+M1 and MVA-pdmH1HA vaccines were assessed. Among the MNCs, B cells are

the major cell population, accounting for 60-70% in NALT followed by T cells at 20-30%. Of T cells, $CD4^+$ T cells are the majority of them. Dendritic cells are at less than 0.5% [120], [148]. Following *in vitro* culture with MVA-NP+M1 or MVA-pdmH1HA, NP, M1 or HA expression was predominantly detected in B cells (Figure 3.4 and 3.5). Further investigation showed both myeloid and plasmacytoid DCs also expressed M1 antigen following the MVA-NP+M1 stimulation (Figure 3.4). The results suggested that MVA-NP+M1 and MVA-pdmH1HA target antigen-presenting cells (APC) mainly B cells and DCs in human NALT *in vitro* and influenza proteins were efficiently expressed. As B cells are the largest proportion in NALT, they may serve as the main APCs to trigger immune responses. Previous studies indicated that poxviruses had a broad cellular tropism to PBMCs including monocytes, B cells, NK cells and also monocyte-derived DCs [141]–[143]. The lower proportion of T cells expressing influenza protein antigens may be explained as they were resistant to MVA infection, and those showing positive expression are likely to be activated T cells, which are more susceptible to MVA than resting T cells [141]. Despite the collectively available data on the susceptibility of immune cells to MVA, the major types of target cells and the percentage of MVA-infected cells may not be simply compared between studies. Of the *in vitro* experiments, there are differences in cell populations used (either single isolated cell or mixed cell populations like PBMCs), vaccine dose and time to measure the transgene expression. Likewise, differences in the cell types predominantly infected by MVA have also been found *in vivo* when different animal models and different respiratory administrations were studied, which showed that MVA targeted alveolar macrophages in lungs of mice after nasal instillation, whereas it targeted dendritic cells in lungs of cynomolgus macaques after aerosol inhalation [149]. Nonetheless, it suggests that APCs are among other immune cells to be preferentially targeted by MVA as shown in this study and previous studies.

Following the vectored-vaccine stimulation, it was demonstrated that both influenza NP and HA proteins were synthesised in the cell cytoplasm before they differently localised in MVA vaccine-infected cells. Only HA migrated to the cell membrane by using the host cell protein transportation machinery, while NP remained in the cell cytoplasm (Figure 3.6). The differences in cellular localisation of NP and HA were also shown in monkey kidney fibroblast (CV-1) upon infection with influenza protein-expressing Vaccinia virus [150]. In

influenza virus-infected host cells, HA continuously binds to sialic acid at the cell membrane, while NP binds to viral RNA in the nucleus before being transported to the cell cytoplasm for virus assembly [1]. Given that there is no gene modification of both influenza NP and HA transgenes in MVA-NP+M1 and MVA-pdmH1HA vaccines, both NP and HA proteins are considered to be expressed in the native conformation the same as generated during influenza virus infection. This may explain the mimicry of influenza protein localisation in MVA-infected cells to that in influenza-infected cells. A similar finding has been previously reported showing that non-modified influenza NP expressed from MVA vector behaved the same as the one after A/PR/8 influenza infection in Hela cells [151]. The different cellular sites of the proteins after expression would lead to different arms of immune responses being induced. The presence of intracellular foreign antigens such as NP and M1 generally results in antigen processing and presentation via MHC class I, resulting in the activation of a CTL response [52]. In contrast, it is thought that the antibody response relies on the engagement of B cell receptor to protein antigens anchored at cell membrane of infected cells [152]. In addition, the understanding of the protein localisation following viral vectored vaccine infection could lead to a better vaccine design to enhance the immune responses. By any modifications of inserted transgenes, influenza NP protein could have longer retention in the cell cytoplasm or could be highly degraded [151], while influenza HA protein could accumulate on the cell membrane or could be secreted from infected cells and captured by APCs [152].

In contrast to MVA-vectored vaccines, the expression of influenza NP from PanAd3-NPM1 was undetectable in either B cells or T cells in adenotonsillar MNCs following *in vitro* vaccine stimulation despite the use of the highest vaccine dosage at 50 vp/cell (Figure 3.7). Although the proportion of infectious particles in PanAd3-NPM1 vaccine was not determined, it was shown that the vaccine was infectious as the expression of influenza NP and/or HA was observed in permissive HEK293T cell line when the lower vaccine dose was used (Figure 3.8). This suggested that the lymphocytes may not be susceptible to PanAd3 infection. It could be explained by the similar findings reported on human adenovirus type 5 (hAd5) [153], [154], which belongs to the same species as PanAd3 [69]. The resistance of lymphocytes to hAd5 infection has been shown to be due to the lack of the surface

expression of cellular receptor for adenovirus and coxsackievirus (CAR) [155], which is the primary receptor necessary for most adenoviruses to facilitate cell attachment and infection [156]. The importance of CAR was demonstrated when adenovirus infection rate was improved in dendritic cells and T cells expressing recombinant CAR [155]. Although T and B-lymphocytes are resistant to hAd5 infection, DCs in peripheral blood have been shown to be relatively more susceptible than lymphocytes and were infected by hAd5 *in vitro* when a high titre of the virus was used [145], [157]–[160]. In this study, the expression of influenza proteins from PanAd3-vectored vaccines in DCs of adenotonsillar MNCs was not examined. It may be worthwhile to perform experiments in the future using a very high virus titre to evaluate if the mononuclear cells isolated from human NALT could be used to study the immune responses to PanAd3-vectored vaccines.

In summary, influenza protein antigens from MVA- but not from PanAd3-vectored vaccines were efficiently expressed in APCs, predominantly in B cells and DCs in the *in vitro* cell culture system modeling human NALT, hence the successful antigen delivery. Expressed from MVA vector, influenza NP accumulated in cell cytoplasm, whereas HA migrated to cell membrane of vaccine-infected cells. It suggests the different pathways of antigen processing and presentation. Based on these results, the next studies are to examine the T cell immune response to MVA-NP+M1 and the induction of antibody response to MVA-pdmH1HA, respectively.

……

Chapter 4

Activation of cross-reactive influenza antigen-specific cytotoxic T cells in human NALT *in vitro* by MVA-NP+M1

4.1. Introduction

The protection from influenza infection is mediated by virus-specific antibodies and T cells [15]. Although neutralising HA-specific antibodies are generally considered the major protective responses to the virus, there is increasing evidence to support an important role for $CD8^+$ T cell-mediated immunity in humans. In individuals experimentally infected with influenza virus, virus-specific cytotoxic T cell killing was shown to reduce virus shedding in the absence of virus-specific antibodies [93]. Also, the presence of pre-existing cytotoxic $CD8^+$ T cells was associated with decreased symptom severity in patients infected with pandemic H1N1 virus during the 2009 outbreak [94]. Moreover, rapid recovery of patients from avian H7N9 infection correlated with an early onset robust $CD8^+$ T cell response [95].

The majority of influenza virus-specific $CD8^+$ T cells recognise antigen epitopes shared among virus subtypes including internal viral protein antigens; nucleoprotein (NP) and matrix protein 1 (M1) [46], [92]. These viral antigens are highly conserved and share over 90% homology at amino acid level among different influenza strains [161]. The activation of such antigen-specific T cell response would mediate a broadly cross-reactive protection [91]. Given the potential of cytotoxic $CD8^+$ T cells for protective responses, novel T cell-based influenza vaccines are being developed [62], [162]. Of viral vectored-vaccines, Modified Vaccinia Ankara virus (MVA) is outstanding because of its excellent safety profile and immunogenicity [53], [59], [163]. MVA-NP+M1 is one of the promising vaccine candidates, showing the activation of antigen-specific T cell responses in peripheral blood of healthy donors following parenteral immunisation [164]–[167].

Since influenza virus infects humans through the nasopharyngeal mucosa, local vaccine delivery that activates cross-reactive mucosal T cell immunity may offer an attractive vaccination strategy against influenza. Intranasal live attenuated influenza vaccine (LAIV) has been shown to induce local and systemic antibodies and T cell immunity in children [30], [168], [169]. Recently, aerosol delivery of a candidate universal influenza vaccine was shown to induce local cellular immune responses associated with protection against heterosubtypic influenza A virus infection in pigs [170]. Intranasal immunisation relies on the local immune system, e.g. nasopharynx-associated lymphoid tissue (NALT) to induce T and B cell immune

responses and local draining lymph nodes [27], [171], [172]. Adenoids and tonsils are major components of human NALT and are known to be important induction sites for immunity against respiratory pathogens including influenza [171], [173], [174]. It was previously demonstrated that cross-reactive memory B cell responses in human NALT were primed following 2009 pdmH1N1 infection [84]. In order to investigate the potential of MVA-NP+M1 as a mucosal T cell-based vaccine, the activation of T cell responses in human NALT was studied. We previously showed that MVA-NP+M1 activated antigen-specific T cell responses mainly to NP in human NALT *in vitro* [147]. In this study, MVA-NP+M1 was further assessed for its capacity to elicit M1-specific T cell responses in human NALT following *in vitro* vaccine stimulation. The functional properties of vaccine-activated T cells were also studied.

4.2. Aims of the study

1. To examine the capacity of MVA-NP+M1 to elicit M1-specific T cell responses in human NALT *in vitro*
2. To compare MVA-NP+M1-activated T cell responses in children and adults
3. To examine the functionality of MVA-NP+M1-elicited M1-specific $CD8^+$ T cells

4.3. Materials and methods

4.3.1. Adenoidal/ tonsillar tissues and peripheral blood

Adenoidal and/or tonsillar tissues were obtained from patients undergoing adenotonsillectomy at local hospitals. Patients who received systemic steroids within 3 weeks prior to surgery, or who had any known immunodeficiency were excluded from the study.

Adenotonsillar MNCs were isolated from the tissues as in the standard protocol described in chapter 2 *(see 2.7.1)*. In some experiments, the MNCs needed screening for the positivity of HLA-A2 type by cell surface staining with mouse anti-human HLA-A2-PE followed by flow-cytometry (Figure 4.1). $CD69^+$ cell depletion was performed using magnetic anti-CD69 microbeads (Miltenyi Biotec, Germany), which removed pre-existing activated T cells expressing high levels of CD69 *(see 2.7.2.1)* and $CD69^+$cell-depleted MNCs were resuspended in R10 medium containing 0.25 µg/ml amphotericin B– named "R10AmpB" at $4x10^6$ cells/ml. Peripheral blood taken from the same patient was spun down to collect its plasma, from now termed "autologous human plasma (aHP)".

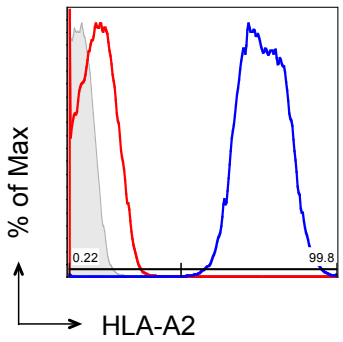

Figure 4.1 Cell surface staining for HLA-A2 type screening

Adenotonsillar MNCs were stained for HLA-A2 on their surface followed by flow-cytometry. The histogram shows HLA-A2 negative (red line) and HLA-A2 positive (blue line) samples compared to unstained cells (grey shade).

4.3.2. Vaccines

MVA-NP+M1 (#850) is Modified Vaccinia Ankara (MVA) virus expressing NP and M1 from A/Panama/2007/99 as a fusion protein joined by a seven amino acid linker under the control of the Vaccinia p7.5 early/late promoter. MVA-wt (#1533) was non-recombinant MVA used as a vector control. The vaccines are provided by the Jenner Institute, University of Oxford (UK).

4.3.3. Influenza peptides

MHC class I-restricted 9-mer synthetic peptides of influenza M1 proteins (NR-2667, Table 4.1) and MHC class II-restricted 15-mer synthetic peptides of influenza M1 proteins (NR-18977, Table 4.2) were obtained from BEI resources, USA. Some 15-mer peptides were selected from all peptides spanning across M1 protein based on their conservancy among IAVs [44], [175]. Each individual peptide was reconstituted in 50% acetonitrile or DMSO according to manufacturer's instructions. 10 to 11 peptides were then pooled at the concentration of 0.1 mg/ml per peptide for subsequent cell stimulation. $M1_{58-66}$ (GILGFVFTL) was purchased from IBA GmbH, Germany and was reconstituted in 50% DMSO at a final concentration of 1 mg/ml.

4.3.4. Fluorochrome-conjugated monoclonal antibodies and M1-tetramer

The following fluorochrome-conjugated antibodies were used in cell staining and flow-cytometric analysis including HLA-A2-PE (clone BB7.2), CD8-FITC (clone RPA-T8), CD103-PE (clone Ber-ACT8), CD45RO-FITC (clone UCHL1), granzymeB-BV510 or AlexaFluor® 647 (clone GB11), CD107a-BV421 (clone H4A3), IFN-γ-APC-R700 (clone B27), TNF-α-PE-CF594 (clone MAb11), IL-2-BV650 (clone MQ1-17H12) and IL-10-APC (clone JES3-19F1) (BD Bioscience, UK); IFN-γ-PECy7 (clone 4S.B3), granzymeA-PECy7 (clone CB9) (eBioscience, UK); and perforin-APC (clone B48), granzymeA-PerCPCy5.5 (clone CB9), CD8-PerCPCy5.5 (clone SK1), CD4-Pacific blue (clone RPA-T4) and CD69-APC (clone FN50) (Biolegend, UK).

HLA-A02*01- GILGFVFTL ($M1_{58-66}$)-PE tetramer (T01011, MBL, USA), termed as "M1-Tm" was used for surface staining to detect M1-specific $CD8^+$ T cells.

Table 4.1 List of 9-mer M1 peptides (NR-2667) and their HLA restriction

Influenza proteins	Pool No.	Amino acid sequences (9)	HLA restriction [44], [175]
M1	1	29-EDVFAGKNT-37	HLA-A*03
		31-VFAGKNTDL-39	HLA-A*2402, HLA-B*08
		37-TDLEALMEW-45	HLA-A*01
		49-RPILSPLTK-57	HLA-A*03
		51-ILSPLTKGI-59	HLA-A*0201
		56-TKGILGFVF-64	HLA-A*02
		58-GILGFVFTL-66	HLA-A*02, HLA-A*2402
		60-LGFVFTLTV-68	HLA-A*02
		66-LTVPSERGL-74	HLA-A*02
		68-VPSERGLQR-76	HLA-A*02
	2	71-ERGLQRRRF-79	HLA-A*02
		75-QRRRFVQNA-83	HLA-A*02
		76-RRRFVQNAL-84	HLA-A*02
		122-GALASCMGL-130	HLA-B*35
		123-ALASCMGLI-131	HLA-B*35
		124-LASCMGLIY-132	HLA-B*35
		126-SCMGLIYNR-134	HLA-B*35
		177-NRMVLASTT-185	HLA-A*0301, HLA-A*11
		179-MVLASTTAK-187	HLA-A*0301, HLA-A*11
		180-VLASTTAKA-188	HLA-A*0301, HLA-A*11
		181-LASTTAKAM-189	HLA-A*0301, HLA-A*11

Table 4.2 List of 15-mer M1 peptides (NR-18977) and their HLA restriction

Influenza proteins	Pool No.	Amino acid sequences (15)	HLA restriction [44], [175]
M1	1	13-SIIPSGPLKAEIAQR-27	HLA-DR1, DR3
		17-SGPLKAEIAQRLESV-31	HLA-DR1, DR3
		37-TDLEALMEWLKTRPI-51	HLA-DP4
		41-ALMEWLKTRPILSPL-55	HLA-DP4
		57-KGILGFVFTLTVPSE-71	HLA-DR4
		77-RRFVQNALNGNGDPN-91	HLA-DR7, DR1
		229-LKDDLLENLQA YQKR-243	HLA-DR1
		233-LLENLQA YQKRMGVQ-247	HLA-DR1
		237-LQAYQKRMGVQMQRF-251	HLA-DR1
		242-KRMGVQMQRFK-252	HLA-DR1

4.3.5. Cell stimulation for T cell assays

$CD69^+$ cell-depleted tonsillar MNCs were cultured with either MVA-NP+M1 or MVA-wt at a final concentration of $1x10^5$ pfu/ml then incubated in 48-well cell culture plates (Corning, USA) at 37°C, 5%CO_2. The MNCs without any stimulation (medium control) were used as negative control. Culture medium was supplemented with 2%v/v aHP and 5 ng/ml interleukin (IL)-15. At day 2, 0.5 ml pre-warmed fresh R10AmpB medium with 2%v/v aHP and 5 ng/ml IL-15 were added in each well. Unless otherwise stated, cells were then incubated for another 5 days (7 days in total) before performing any further experiments. Non-HLA typed tonsillar MNCs were used for quantifying M1-specific T cell responses by IFN-γ ELISPOT assay or intracellular cytokine staining, whereas the MNCs from HLA-A2 positive individuals were used for analysing M1-specific $CD8^+$ T cell responses by tetramer staining.

4.3.6. IFN-γ ELISPOT and intracellular cytokine staining

At day 7 following *in vitro* stimulation with MVA-wt or MVA-NP+M1 *(see 4.3.5)*, tonsillar MNCs were rested in R10AmpB medium for 2 days before performing IFN-γ ELISPOT assays (eBiosciences, UK). At day 9, the MNCs from each stimulation were separately harvested from culture plates and pelleted. Cells were then resuspended in R10AmpB and adjusted to $2x10^6$ cells/ml and aliquoted at 350 µl per tube. SEB (NR-44235, BEI Resources, USA) and M1 peptide pools were pre-diluted in R10AmpB at the ratio of 1:10 and 1:5, respectively. MVA-wt and MVA-NP+M1-stimulated MNCs were restimulated with diluted M1 peptide pools at final concentration of 10 µg/ml per peptide (No.1-3, Table 4.3). Some cells were left without peptide stimulation as background control (No.4, Table 4.3). Unstimulated MNCs were restimulated with SEB at a final concentration of 1 µg/ml for positive control (No.5, Table 4.3). R10AmpB medium without MNCs was used as negative control. 100 µl of peptide-restimulated MNCs (containing $2x10^5$ cells) were seeded in triplicate into a pre-coated ELISPOT plate as shown in the layout (Figure 4.2). The plate was then incubated at 37°C, 5% CO_2 for 24 hours with minimal agitation. Next day, spots were developed according to the ELISPOT protocol *(see 2.12)*.

To analyse the data, the number of spots in each stimulation (No.1-5 according to Table 4.3) in triplicate was averaged and adjusted to the spot forming cells per $1x10^6$ cells (SFC/ million cells) by multiplying by 5. Of either MVA-wt or MVA-NP+M1 stimulated MNCs, the SFC/ million from each peptide restimulation (No.1-3) was subtracted from the one without peptide stimulation (No.4 as background). The background-subtracted SFC/ million from pool No. 1 and 2 of 9-mer M1 peptides were added together (No.1+2). Finally, the SFC/ million from MVA-wt and MVA-NP+M1-stimulated MNCs from each individual towards 9-mer or 15-mer M1 peptides were compared.

Table 4.3 Peptide restimulation for IFN-γ ELISPOT assay

No.	Peptides/ protein		MNCs and peptide/protein volume (µl)		
			Unstimulated MNCs	MVA-wt stimulated MNCs	MVA-NP+M1 stimulated MNCs
1	MHC class I-restricted 9-mer peptides (1:5) (Table 4.1)	M1 Pool 1	N/A	17.7	17.7
2		M1 Pool 2	N/A	19.5	19.5
3	MHC class II-restricted 15-mer peptides (1:5) (Table 4.2)	M1 Pool 1	N/A	17.7	17.7
4	No peptides		N/A	0.0	0.0
5	SEB (1:10); positive control		7.0	N/A	N/A

Note: N/A means no sample

	1	2	3	4	5	6	7	8	9	10	11	12
A	+ (5)	MVA-wt (1)	MVA-wt (2)	MVA-wt (3)								
B	+ (5)											
C	+ (5)											
D	(-)	MVA-NP+M1 (1)	MVA-NP+M1 (2)	MVA-NP+M1 (3)								
E	(-)											
F	(-)											
G	(-)	MVA-wt (4)										
H	(-)	MVA-NP+M1 (4)										

Figure 4.2 Sample layout for IFN-γ ELISPOT assay

The layout illustrates the position of each sample in the plate from column 1 to 4. MVA-wt or MVA-NP+M1-stimulated MNCs were restimulated with peptide pools indicated as No.1-3 in Table 4.3. SEB-stimulated MNCs (+) as No.5 in Table 4.3 is a positive control and R10AmpB medium without cells (-) is a negative control. Cells were then seeded in triplicate in the pre-coated ELISPOT plates.

In the parallel experiment, the type of T cells responding to M1 peptides was also examined by intracellular cytokine staining. The MNCs following *in vitro* vaccine stimulation (the same as the ones analysed by ELISPOT assay) were also restimulated with the peptide pools (Table 4.3) at final concentration of 10 μg/ml per peptide in the presence of brefeldin A and incubated at 37°C, 5%CO_2 for 6 hours. Cells were then stained for surface CD4 and CD8 and intracellular staining for IFN-γ, followed by flow-cytometry.

4.3.7. Detection of $M1_{58-66}$-specific $CD8^+$ T cells and intracellular cytotoxic molecules

Following *in vitro* 7-day MVA-NP+M1 or MVA-wt stimulation *(see 4.3.5)*, tonsillar MNCs were harvested before co-incubation with anti-CD8 antibody and M1-Tm at 4°C for 30 minutes to detect $M1_{58-66}$-specific $CD8^+$ T cells. In some experiments, cells were further intracellularly stained for perforin, granzyme-A and granzyme-B, followed by flow-cytometry. T cell responses in the MNCs from each individual to MVA-wt and MVA-NP+M1 were then compared.

4.3.8. Measurement of T cell proliferation

$CD69^+$cell-depleted tonsillar MNCs from HLA-A2 positive individuals were labelled with CFSE *(see 2.9)*. CFSE-labeled cells were resuspended in R10AmpB medium supplemented with 2%aHP and 5 ng/ml IL-15 before stimulation with either $1x10^5$ pfu/ml of MVA-NP+M1 or MVA-wt or without stimulation *(see 4.3.5)* then incubated at 37°C, 5% CO_2 for 5 days. Cells were then harvested and stained for CD8 and M1-Tm, followed by flow-cytometry. T cell proliferation in the MNCs from each individual to MVA-wt and MVA-NP+M1 were then compared.

4.3.9. Detection of surface CD107a expression and intracellular cytokines

Following *in vitro* 7-day MVA-NP+M1 stimulation *(see 4.3.5)*, tonsillar MNCs were harvested, pelleted and resuspended in pre-warmed R10AmpB medium then pulsed with 0.25 μg/ml $M1_{58-66}$ peptide and co-cultured with anti-CD107a antibody (CD107a-BV421) in the presence of brefeldin A (BFA) and monensin (eBiosciences, UK) and incubated at 37°C, 5% CO_2 with light protection. Cells were collected at every hour for 5 hours followed by staining for

surface CD8 and M1-Tm with intracellular IFN-γ to study the kinetics of surface CD107a expression and IFN-γ cytokine production. In another experiment, cells were collected at 5 hours post peptide restimulation before staining for CD8, M1-Tm and a set of cytokines; IFN-γ, TNF-α, IL-2 and IL-10, followed by flow-cytometry. The functional profile of M1-Tm$^+$ cells was then analysed using SPICE 5.0 software (NIH, NIAID, USA).

4.3.10. *In vitro* cytotoxicity assay

Isolated CD8$^+$ T cells following MVA-NP+M1 stimulation *(see 4.3.5)* were co-cultured with $M1_{58-66}$-pulsed autologous B cells before measuring the number of B cells being killed (Figure 4.3) as described previously [176]. Briefly, autologous B cells were isolated from cryopreserved tonsillar MNCs *(see 2.8)* using a CD19 isolation kit *(see 2.7.2.2)* (Miltenyi Biotec, Germany) and incubated overnight with 40 ng/ml recombinant human IFN-γ (Peprotech, UK) to increase the expression of MHC-I and CD86 on the B cells, limiting the variability of B cells from different donors and also to enhance B cell viability. Autologous B cells were labelled with CFSE *(see 2.9)* at a final concentration of either 0.02 μM (T_{low}) or 0.2 μM (T_{high}). T_{low} were further pulsed with 5 μg/ml $M1_{58-66}$ peptide for 45 minutes at 37°C, 5%CO_2, while some T_{low} were left without peptide pulsing. Both T_{low} with or without peptide pulsing and T_{high} were adjusted to 2x10^5 cells/ml. $T_{low,\ pulsed}$ and T_{high} were mixed at the ratio of 1:1. $T_{low,\ unpulsed}$ and T_{high} were also mixed at the ratio of 1:1. CD8$^+$ T cells were isolated from tonsillar MNCs following *in vitro* 7-day MVA-NP+M1 stimulation using a CD8 isolation kit *(see 2.7.2.2)* (Miltenyi Biotec, Germany). Isolated CD8$^+$ T cells were resuspended in 0.7 ml R10AmpB medium, containing 4-10x10^6 cells/ml and 2-fold serial dilutions made from 1:1 to 1:32. 100 μl of CD8$^+$ T cells at different serial dilutions were co-cultured with 100 μl of mixed $T_{low,\ pulsed}$ and T_{high} in a round-bottom 96-well plate (Corning, USA) for 6 hours at 37°C, 5%CO_2. Only 100 μl of mixed $T_{low,\ pulsed}$ and T_{high} were cultured in 100 μl of R10 as negative control. 100 μl of undiluted isolated CD8$^+$ T cells co-cultured with 100 μl of mixed $T_{low,\ unpulsed}$ and T_{high} for peptide pulsing control. After complete incubation, cells were harvested from each well and washed once before staining with LIVE/DEAD Far red (Invitrogen, UK) at room temperature for 30 minutes followed by surface staining for CD8 and M1-Tm. 4,000 events of T_{high} were acquired during flow-cytometry for each sample. Effector T cells (E)

were the number of M1-Tm$^+$ cells, while target cells (T) were the total numbers of T_{low} in the culture. The percentage of specific lysis at different E/T ratio was calculated by the following formula, which was based on the reduction of the fraction of T_{low}/ T_{high} cells after co-culturing with CD8$^+$ T cells compared from that without CD8$^+$ T cells.

$$\% \text{ Specific lysis} = 100 \times [(T_{low}/T_{high})_{alone} - (T_{low}/T_{high})_{effector}] \times (T_{low}/T_{high})_{alone}^{-1}$$

T_{low}	the number of $CFSE_{low}$ B cells
T_{high}	the number of $CFSE_{high}$ B cells
$(T_{low}/T_{high})_{alone}$	the number of T_{low}/ the number of T_{high} of negative control
$(T_{low}/T_{high})_{effector}$	the number of T_{low}/ the number of T_{high} of a well, co-cultured with CD8$^+$ T cells

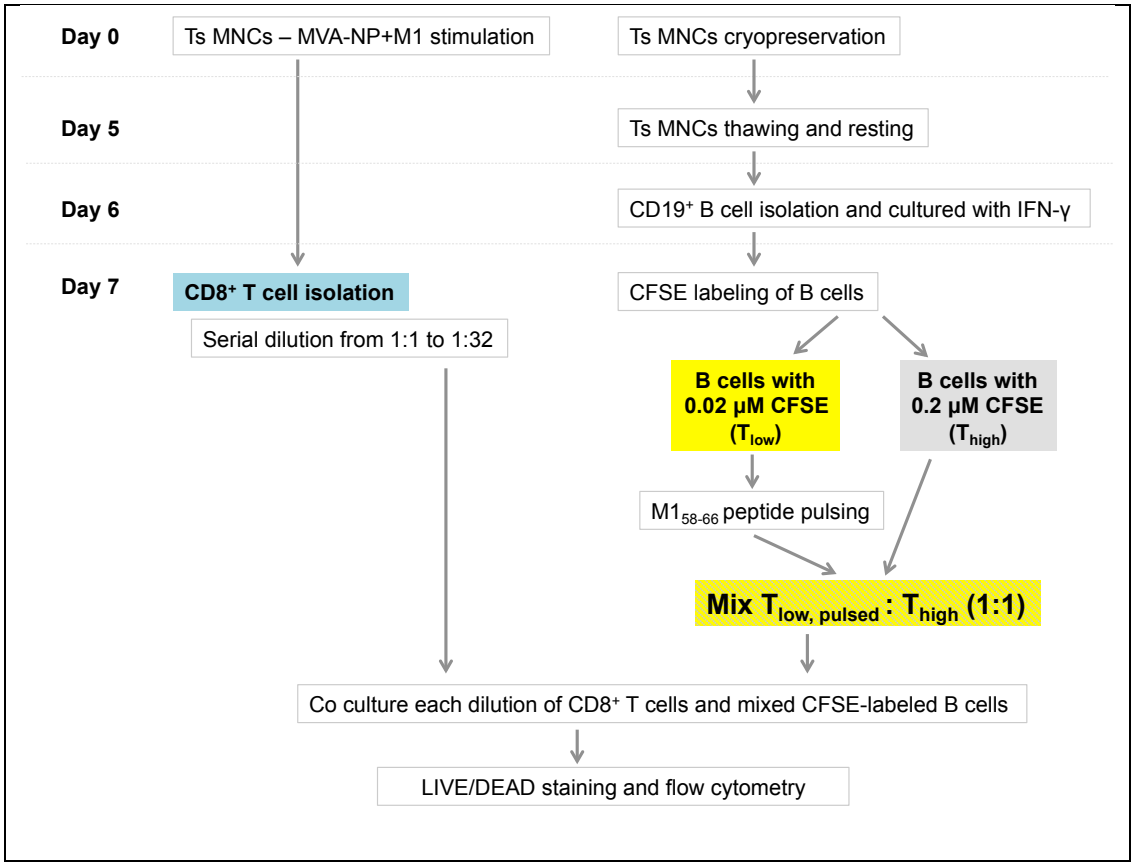

Figure 4.3 Diagram of *in vitro* cytotoxicity assay

The figure depicts the steps of *in vitro* cytotoxicity assay along with the timeline started from day 0 to day 7. The assay is composed of two main parts, which are 1) CD8$^+$ T cell isolation from MVA-NP+M1-stimulated adenotonsillar mononuclear cells (MNCs) and 2) B cell isolation from the MNCs followed by CFSE labeling and peptide pulsing. Isolated CD8$^+$ T cells are co-cultured with labeled B cells at different ratios and the number of dead B cells is measured by live/dead staining and flow-cytometry.

4.3.11. Flow-cytometry

Flow cytometric data was acquired by FACS Calibur using CellQuest Pro software or FACS Celesta using FACS Diva (BD Biosciences, USA). Otherwise stated, $2x10^5$ or more events of lymphocytes were required. The data were analysed using FlowJo 8.7 software (FlowJo, LLC.).

4.3.12. Statistical analysis

For two-group comparisons, based on the normality of distribution of data, parametric paired-t test, nonparametric Wilcoxon matched-pairs signed rank test and nonparametric Mann-Whitney test were performed using GraphPad Prism. $p<0.05$ was considered as statistically significant.

4.4. Results

4.4.1. Optimisation of *in vitro* cell stimulation with MVA-NP+M1 vaccine

To start with, some key parameters of the *in vitro* cell culture with MVA-NP+M1, which were incubation time, vaccine dose and cytokine supplement were optimised for the detection of antigen-specific $CD8^+$ T cells. The frequency of $CD8^+$ M1-Tm^+ cells was measured using M1 tetramer. PBMCs from a HLA-A2 positive healthy donor were used to perform this experiment initially.

Incubation time was firstly optimised. The MVA-NP+M1 dose at $5x10^4$ pfu/ml was used regarding the previous study [147] to stimulate PBMCs. As shown in Figure 4.4a, the number of $CD8^+$ M1-Tm^+ cells in PBMCs following *in vitro* vaccine stimulation detectably increased compared to medium control at day 7 (9.63% vs 0.13%), but not at day 3 (0.062% vs 0.067%).

To optimise vaccine stimulation concentration, PBMCs were stimulated with MVA-NP+M1 at a range of doses of $5x10^4$, $1x10^5$ and $5x10^5$ pfu/ml, respectively for 7 days. The frequency of $CD8^+$ M1-Tm^+ cells was in a dose-dependent manner, showing 9.63%, 19.5% and 24.6%, respectively compared to medium control at 0.15%. Cell viability was roughly obtained from gating the viable cell population from the FSC-SSC plot based on the data from propidium iodide staining *(see appendix-2).* The MNCs stimulated with MVA-NP+M1 at any dose showed lower cell viability at day 7 compared to medium control (88.5%). However, using the highest vaccine dose demonstrated noticeably decreasing cell viability (76%) than the other two doses (80.7% and 80.6%) (Figure 4.4b). Therefore, the intermediate vaccine dose at $1x10^5$ pfu/ml was chosen for cell stimulation.

Finally, the effect of cytokines; interleukin (IL)-2 and IL-15, on cell culture was studied following *in vitro* stimulation of MVA-NP+M1 at $1x10^5$ pfu/ml. As shown in Figure 4.4c, PBMCs stimulated with MVA-NP+M1 with the supplement of 5 ng/ml IL-15 activated the highest number of $CD8^+$ M1-Tm^+ cells (23.09%), followed by those supplemented with 20U/ml IL-2 (20.36%) and those with no cytokine supplement (18.82%). $CD8^+$ M1-Tm^+ cells in unstimulated MNCs (medium control) remained low and comparable in the absence and the presence of IL-2 or IL-15, showing 0.15, 0.14 and 0.13%, respectively. In addition, cell viability was likely to be

improved by the supplement of IL-15 (86.2%) and IL-2 (81.1%) compared to no cytokine supplement (80.6%). Therefore, 5 ng/ml of IL-15 (as manufacturer recommended dose) was supplemented in the culture of tonsillar MNCs stimulated with MVA-NP+M1.

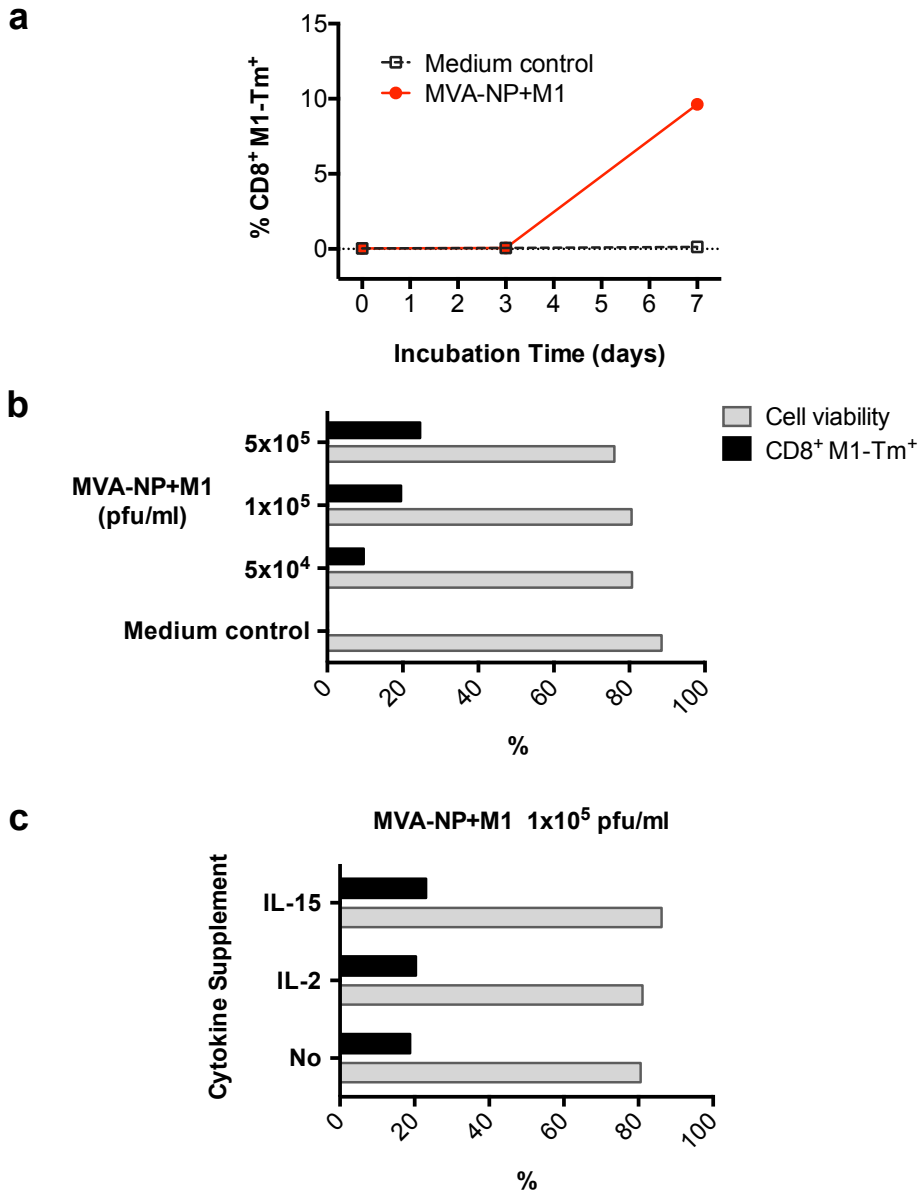

Figure 4.4 Optimisation for MVA-NP+M1 vaccine-cell stimulation

Incubation period, vaccine dose and cytokine supplement were optimised in *in vitro* MVA-NP+M1-cell stimulation for the detection of antigen-specific $CD8^+$ T cells, peripheral blood mononuclear cells (PBMCs) were stimulated with MVA-NP+M1 and $CD8^+$ $M1\text{-}Tm^+$ cells and cell viability were assessed. **a)** Using $5x10^4$ pfu/ml of vaccine without cytokine supplement, $CD8^+$ $M1\text{-}Tm^+$ cells were measured at day 3 and 7. **b)** Following 7-day incubation without cytokine supplement, $CD8^+$ $M1\text{-}Tm^+$ cells and cell viability were compared in three different concentrations of the vaccine used. **c)** Following $1x10^5$ pfu/ml of MVA-NP+M1 stimulation, $CD8^+$ $M1\text{-}Tm^+$ cells and cell viability were compared when cell culture was supplemented with interleukin (IL)-15 or IL-2 or left without any cytokine supplement.

Having obtained such optimal parameters, further optimisation was performed using tonsillar MNCs on cell preparation and vaccine concentration. Unlike PBMCs, tonsillar MNCs contain a larger number of $CD69^+$ activated cells. They are most likely to die because of *in vitro* over stimulation, which may have an impact on other viable cells during the culture. $CD69^+$ cell depletion removed pre-existing activated T cells expressing high levels of CD69 from both $CD4^+$ and $CD8^+$ T cells, but retained naïve and memory T cells including $CD45RO^+$ $CD103^+$ tissue-resident memory $CD8^+$ T cells in the MNCs (Figure 4.5). The comparable frequency of $CD8^+$ M1-Tm^+ cells was observed in the MNCs between before (0.23%) and after (0.25%) the depletion. As $CD69^+$ cell depletion removed a number of $CD4^+$ T cells, which resulted in an increased proportion of $CD8^+$ T cells in the MNCs, this may explain the comparable number of $CD8^+$ M1-Tm^+ cells observed. Following *in vitro* vaccine stimulation, the frequency of $CD8^+$ M1-Tm^+ cells was higher with the use of $CD69^+$cell-depleted MNCs (10.72%) than that of unfractionated MNCs (8.59%).

Besides, the optimal MVA-NP+M1 vaccine dose to stimulate $CD69^+$cell-depleted tonsillar MNCs was also shown at $1x10^5$ pfu/ml among three concentrations as same as previously titrated in PBMCs. The frequency of $CD8^+$ M1-Tm^+ cells was comparable between the use of $1x10^5$ and $5x10^5$ pfu/ml vaccine (0.67% vs 0.81%). However, the higher cell viability was observed at the former dose (78.1%) compared to the latter dose (71.4%). The MNCs without stimulation showed 0.04% $CD8^+$ M1-Tm^+ cells with 81.6% cell viability.

All optimised parameters were shown in Table 4.4.

Table 4.4 Optimised parameters for MVA-NP+M1-tonsillar mononuclear cell stimulation

Parameters	Results
Cell preparation	$CD69^+$cell-depleted MNCs
Vaccine dose	$1x10^5$ pfu/ml
Cytokine supplement	5 ng/ml Interleukin (IL)-15
Incubation time	7 days

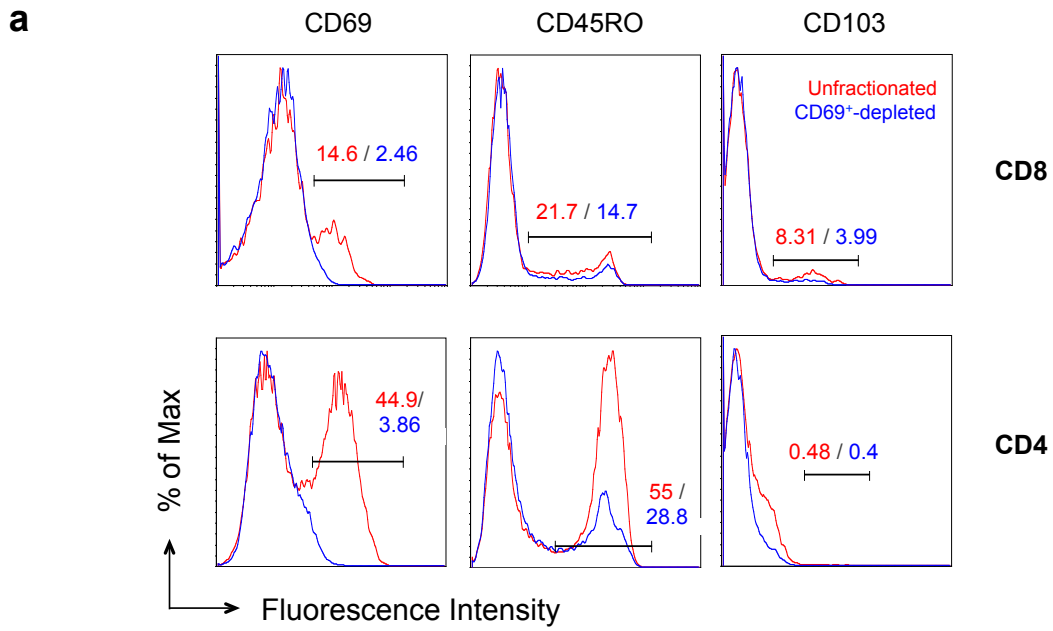

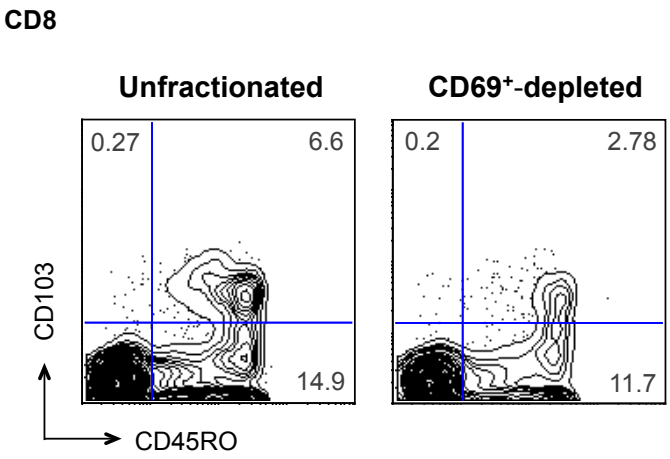

Figure 4.5 Cell phenotypes in unfractionated and CD69$^+$cell-depleted MNCs

Phenotypic study was performed before and after CD69$^+$ cells depletion of tonsillar MNCs by surface staining a panel of CD4, CD8, CD69, CD45RO and CD103. **a)** Comparison of the expression of CD69, CD45RO and CD103 of either CD8$^+$ or CD4$^+$ T cells in unfractionated (red) and CD69$^+$cell-depleted MNCs (blue). **b)** Gating on CD8$^+$ T cells, flow cytometric dot plot compared CD45RO and CD103-expressing cells in unfractionated and CD69$^+$cell-depleted MNCs.

4.4.2. MVA-NP+M1 activated conserved M1-specific T cell responses.

In chapter 3, it was shown that MVA-NP+M1 efficiently expressed influenza NP and M1 proteins in adenotonsillar MNCs following *in vitro* vaccine stimulation. The use of lower vaccine dose ($1x10^5$ pfu/ml or MOI at 0.025) to stimulate the MNCs for T cell response study still demonstrated that approximately 3% of lymphocytes mainly B cells expressed M1 protein, indicating that vaccine antigen is present in the cell culture system. MVA-NP+M1 was then investigated whether it would be able to activate cell-mediated immunity in human NALT *in vitro*, particularly focusing on $CD8^+$ T cells (CTL) recognising M1 epitopes.

To assess the capacity of MVA-NP+M1 to elicit M1-specific cross-reactive T cell responses, tonsillar MNCs from non HLA-typed subjects following 7-day MVA-wt or MVA-NP+M1 *in vitro* stimulation were restimulated with 9-mer synthetic conserved M1 peptide pools. IFN-γ-producing cells in response to the peptides were analysed by ELISPOT assay and intracellular cytokine staining (ICS). The magnitude of M1-specific T cell responses to 9-mer peptides were highly variable in individuals; however, all of them exhibited an increasing proportion of IFN-γ-secreting cells following MVA-NP+M1 compared to MVA-wt stimulation (n=7, p=0.0156). A set of longer 15-mer M1 peptides was also selected from peptide library for the assessment of $CD4^+$ T cell response. The increasing T cell response to 15-mer M1 peptides was also observed in MVA-NP+M1 stimulated MNCs, but could not reach significance (n=3, p=0.25) (Figure 4.6b). However, ICS data demonstrated that the responses to both 9-mer and 15-mer M1 peptide pools were generated from $CD8^+$ rather than $CD4^+$ T cells (Figure 4.6c,d).

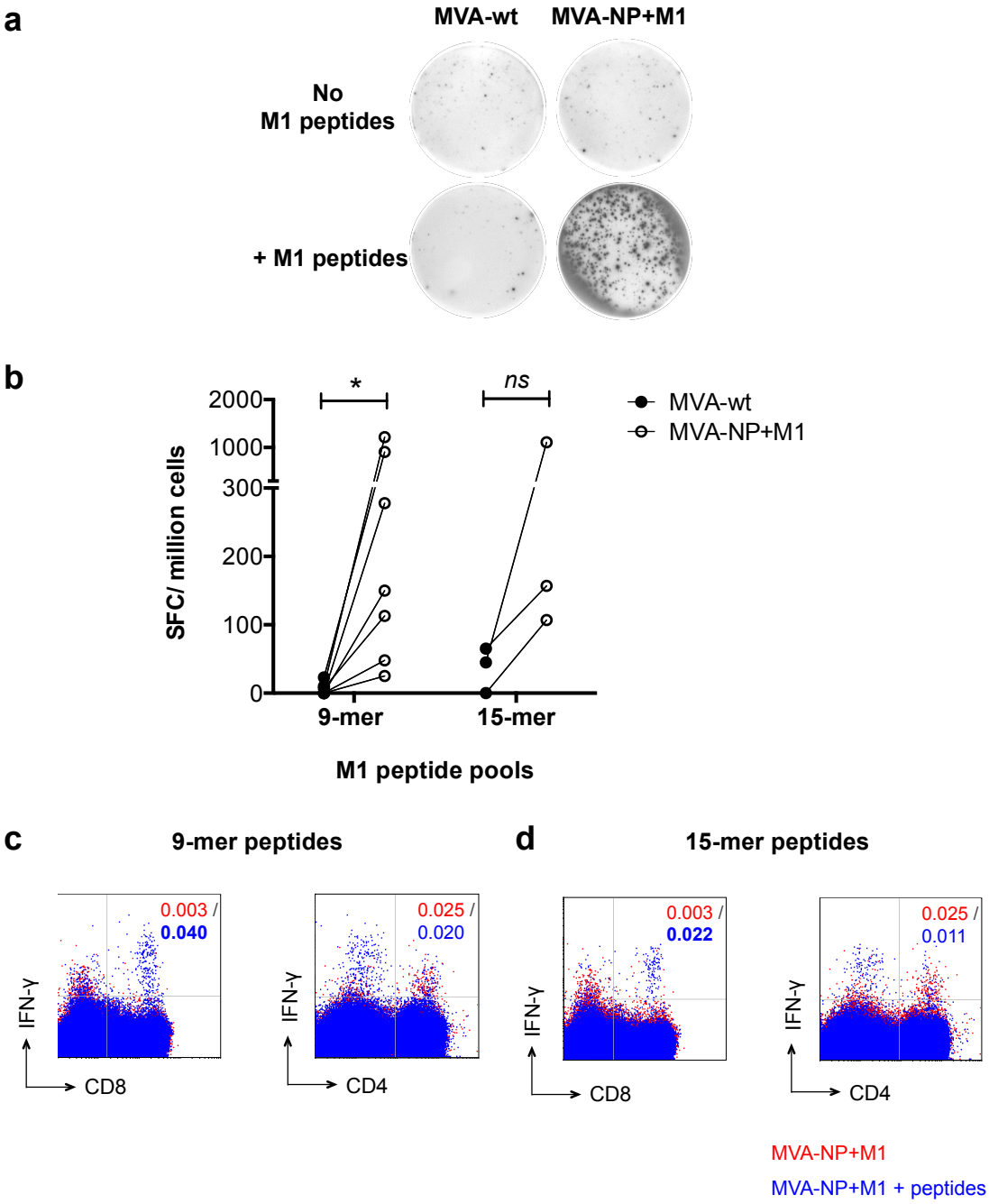

Figure 4.6 MVA-NP+M1 activated T cell responses to conserved M1 peptides

Following 7-day MVA-NP+M1 or MVA-wt *in vitro* stimulation, $CD69^{+}$cell-depleted tonsillar MNCs were rested for 2 days before restimulating with conserved M1 peptide pools (either 9-mer or 15-mer) followed by measuring the frequency of IFN-γ producing cells by ELISPOT assay and intracellular cytokine staining (ICS). **a)** A representative sample showed spots in MVA-NP+M1 compared to MVA-wt stimulated cells at day 9 before and after M1 peptide restimulation. **b)** Comparison of each individual spot forming cells (SFC)/ a million cells in MVA-wt and MVA-NP+M1-stimulated MNCs towards 9-mer (n=7, **p=0.0156*) and 15-mer M1 (n=3, *p=0.25*). Wilcoxon matched-pairs signed rank test was used for comparison between two groups. **c,d)** The overlay of flow cytometric dot plots showing IFN-γ producing $CD8^{+}$ or $CD4^{+}$ T cells before (red) and after (blue) **c)** 9-mer or **d)** 15-mer M1 peptide pool restimulation.

4.4.3. MVA-NP+M1 activated $M1_{58-66}$-specific $CD8^+$ T cells in HLA-matched individuals.

Having shown that MVA-NP+M1 activated CTLs in human NALT *in vitro* directed to conserved M1 peptides, the further study was to examine $M1_{58-66}$-specific $CD8^+$ T cell responses following *in vitro* MVA-NP+M1 stimulation using M1 tetramer staining. From now on, " M1-Tm^+ " cell refers to the frequency of $M1_{58-66}$-specific T cells of total $CD8^+$ T cells (Figure 4.7).

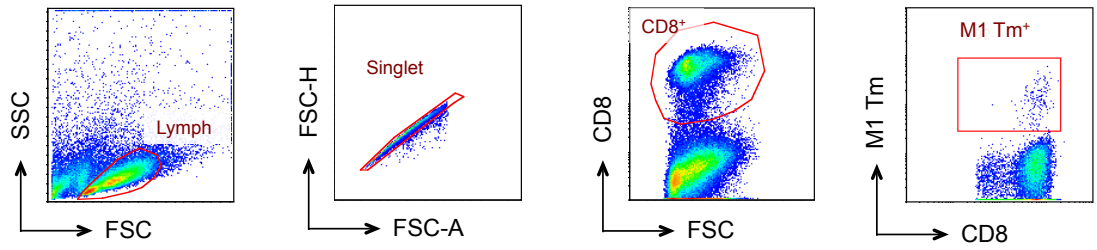

Figure 4.7 Gating strategy for M1-Tm^+ cell analysis

To measure M1-Tm^+ cells following *in vitro* MVA-NP+M1 stimulation, lymphocytes were firstly gated from the FSC-SSC plot (the gate referred to viable cells according to the data from propidium iodide (PI) staining in Appendix-2). Only singlet cells were selected by plotting FSC-H against FSC-A. Then $CD8^+$ T cells were gated. Among $CD8^+$ T cells, M1-Tm^+ cells were gated from the plot of CD8 against M1-Tm.

As each antigen epitope is differently restricted to the HLA haplotype, the specificity of the use of M1 tetramer to detect M1-Tm^+ cells following *in vitro* MVA-NP+M1 stimulation was tested in tonsillar MNCs from subjects who were either HLA-A2 positive or negative. Among the subjects of comparable age, M1-Tm^+ cells were only detected in individuals who were HLA-A2 positive (Figure 4.8), suggesting that these $M1_{56-88}$-specific T cell responses are elicited in only HLA-matched individuals.

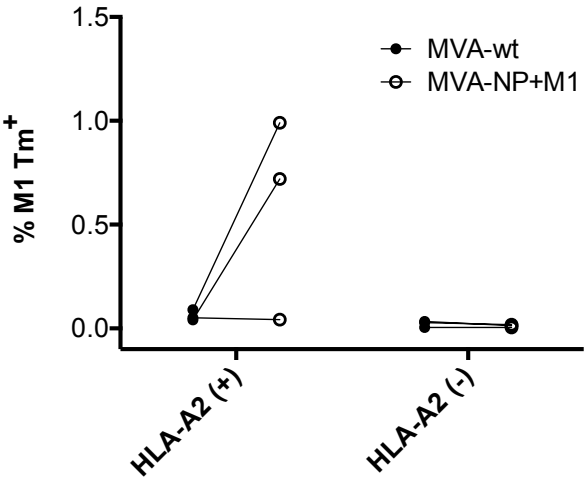

Figure 4.8 $M1_{58-66}$-specific T cell responses needed HLA-A2 restriction.

Adenotonsillar MNCs from either HLA-A2 positive or negative subjects at similar ages (ranging from 2 to 16 years olds) were stimulated with MVA-wt or MVA-NP+M1 for 7 days and the frequency of M1-Tm^+ cells was measured. The number of M1-Tm^+ cells following MVA-NP+M1 stimulation was compared to those after MVA-wt stimulation in subjects who have either HLA-A2 positive or HLA-A2 negative.

The pre-existing M1-Tm^+ cells were firstly measured in each individual. The frequency of M1-Tm^+ cells in freshly isolated tonsillar MNCs varied, but were generally low (0.03-0.16%, median 0.1%). Only one adult sample showed as high as 0.25%. Following *in vitro* stimulation, MVA-NP+M1 elicited a significant increase in M1-Tm^+ cells in tonsillar MNCs (median 0.37%), compared to MVA-wt (vector alone) (median 0.05%) (n=22, $p<0.0006$) and medium control (median 0.05%) (Figure 4.9a).

When M1-Tm^+ T cell responses were compared among different age groups (Table 4.5), an age-dependent increase was shown in the magnitude of M1-Tm^+ cell response. Children <4 years of age in general showed very low response to the vaccine (0.00-0.03%, median 0.00%), while the older children had significantly higher responses ($p=0.0413$) with the variable magnitude of M1-Tm^+ cells (0.01-1.44%, median 0.22%). All adults responded to the vaccine with significantly higher numbers of M1-Tm^+ cells (0.29-4.47%, median 0.60%) than younger ($p=0.0025$), but not older children (Figure 4.9b).

Table 4.5 Study subjects information

Subjects		Average age (Range)	n
Children	Group 1	2.5 (2-3.5)	5
	Group 2	5.7 (4-9)	10
Adults		20.6 (16-34)	7

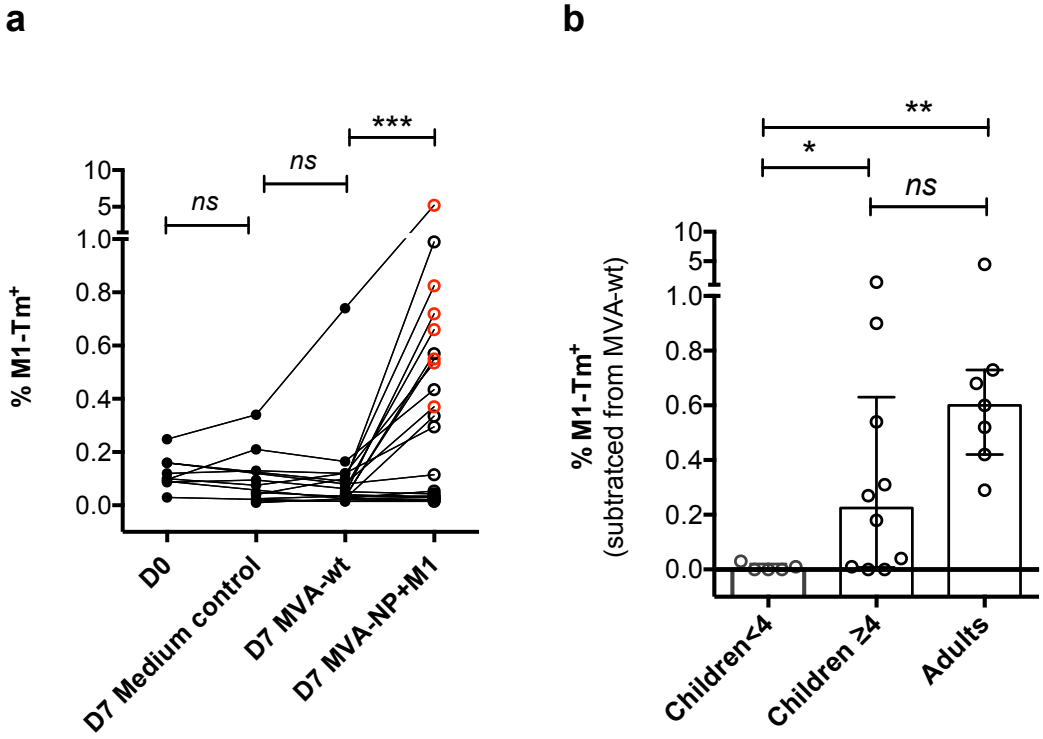

Figure 4.9 $M1_{58-66}$-specific $CD8^+$ T cells activated by MVA-NP+M1.

M1-Tm^+ cells were measured in $CD69^+$cell-depleted tonsillar MNCs following *in vitro* MVA-wt or MVA-NP+M1 stimulation or left without any stimulation (medium control). **a)** The proportion of M1-Tm^+ cells was shown in freshly isolated cells from tonsils at day 0 (D0) and at day 7 (D7) after vaccine stimulation. MVA-NP+M1 activated an significant increase in M1-Tm^+ cells in both children (black open circles) and adults (red open circles) compared to MVA-wt (Wilcoxon matched-paired signed rank test, n=22, ****p=0.0006*). At day7, MVA-wt showed a similar number of M1-Tm^+ cells as medium control. **b)** Comparison of the frequency of M1-Tm^+ cells among different age groups. Older children and adults had a stronger response than younger children (Mann Whitney test, **p=0.0431*, ***p=0.0025*). Bars and error bars indicated medians with interquartile ranges.

Further analysis with CFSE cell tracing demonstrated that MVA-NP+M1 activated a proliferative M1-Tm$^+$ cell response in tonsillar MNCs *in vitro*, compared to the absence of such response in MVA vector-stimulated MNCs (n=3, p=0.0475) (Figure 4.10).

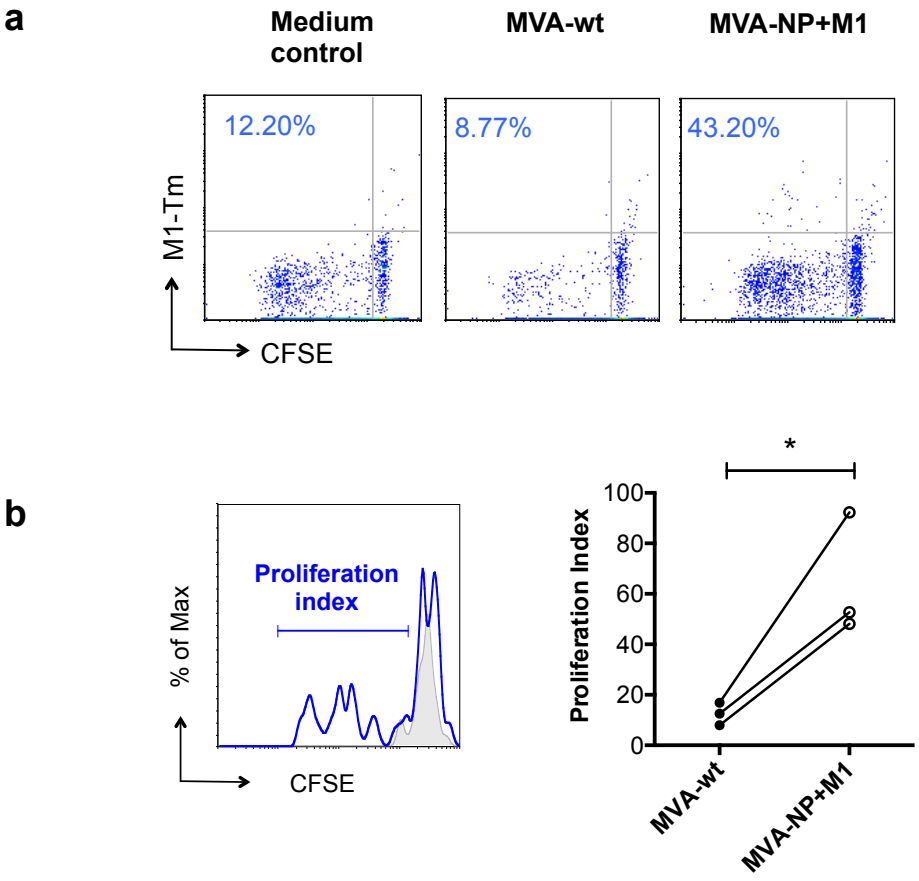

Figure 4.10 Proliferation of M1$_{58-66}$-specific CD8$^+$ T cells following *in vitro* MVA-NP+M1 stimulation.

M1-Tm$^+$ cells were measured in CFSE-labelled CD69$^+$cell-depleted tonsillar MNCs following *in vitro* MVA-wt or MVA-NP+M1 stimulation or left without any stimulation. **a)** Gating on CD8$^+$ T cells, the flow cytometric dot plots showed newly proliferating M1-Tm$^+$ cells defined as M1-Tm$^+$ CFSE$_{low}$ cells (top left quadrant) in each stimulation. **b)** The histogram overlaid the M1-Tm$^+$ cells following MVA-NP+M1 (blue line) compared to MVA-wt (grey shade) stimulation. Proliferation index was the proportion of M-Tm$^+$ cells having the low intensity of CFSE (or the proportion of proliferating cells). MVA-NP+M1 activated the significant higher number of newly proliferating M1-Tm$^+$ compared to MVA-wt (Paired-t test, n=3, **p=0.0475*).

4.4.4. $M1_{58-66}$-specific $CD8^+$ T cells exhibited effector functions and *in vitro* killing capacity

To determine whether MVA-NP+M1-activated $M1_{58-66}$-specific $CD8^+$ T cells were functionally active, the expression of cytotoxic effector molecules and cytokines in M1-Tm^+ cells was examined. Following 7-day *in vitro* vaccine stimulation, MVA-NP+M1 activated a significantly higher number of M1-Tm^+ cells expressing perforin (p=0.0098), granzyme-A (p=0.0078) and granzyme-B (p=0.0313) compared to MVA-wt (Figure 4.11a). Besides, MVA-NP+M1-stimulated MNCs contained substantial amounts of M1-Tm^+ cells that intracellularly stored perforin, granzyme-A and granzyme-B (92%, 62% and 69% of M1-Tm^+ cells, respectively) (Figure 4.11b).

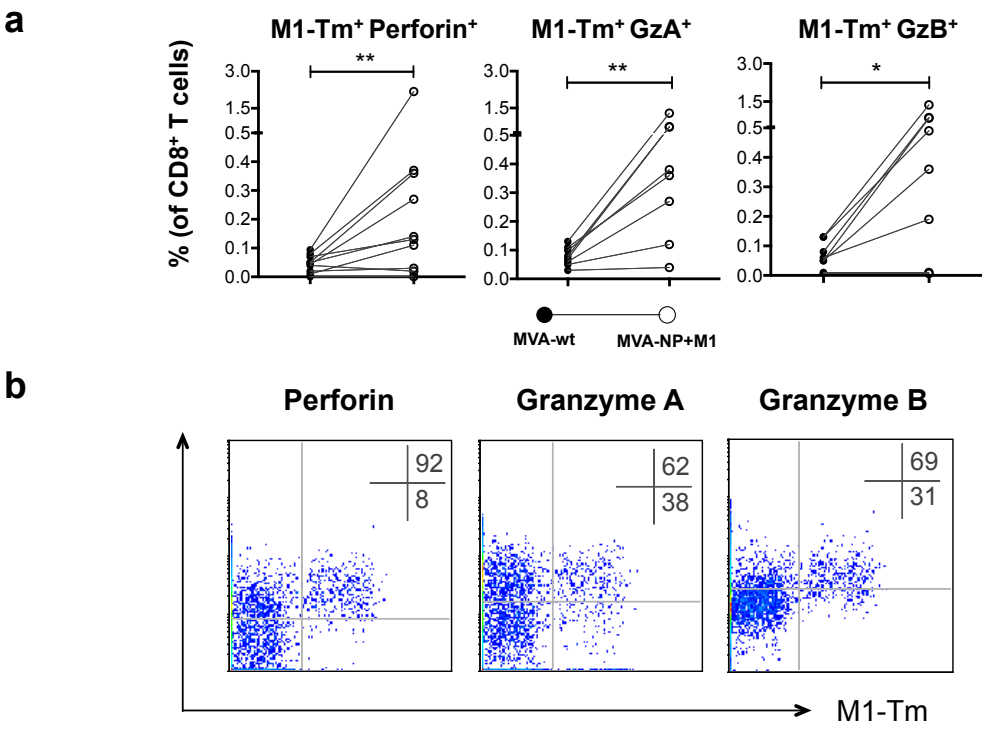

Figure 4.11 Expression of cytotoxic effector molecules in $M1_{58-66}$ specific $CD8^+$ T cells.

$CD69^+$cell-depleted tonsillar MNCs following 7-day *in vitro* stimulation with either MVA-wt or MVA-NP+M1 were measured for frequency of M1-Tm^+ cells and the expression of cytotoxic molecules. **a)** MVA-NP+M1, compared to MVA-wt, activated M1-Tm^+ cells that expressed perforin (n=10, ***p=0.0098*), granzyme A (n=8, ***p=0.0078*) and granzyme B (n=8, **p=0.0313*). Wilcoxon matched-paired signed rank was used for comparison between two groups. **b)** Gating on $CD8^+$ T cells, the representative flow cytometric dot plots showed the expression of perforin, granzyme-A and -B in M1-Tm^+ cells following MVA-NP+M1 stimulation. The number on the top right corner indicated the percentages of each cytotoxic molecule-expressing M1-Tm^+ cells of total M1-Tm^+ cells.

MVA-NP+M1-stimulated MNCs were then restimulated with $M1_{58-66}$ peptide followed by the detection of surface CD107a (a marker for cytotoxic degranulation) and cytokine expression. As shown in Figure 4.12a, surface CD107a expression was markedly upregulated in M1-Tm^+ cells after $M1_{58-66}$ peptide restimulation. Similarly, as shown in Figure 4.12b, cytokine expression was also upregulated. IFN-γ was produced by most activated M1-Tm^+ cells compared to the lower expression in non-M1-specific $CD8^+$ T cells (M1-Tm^-). The kinetics of surface CD107a and IFN-γ expression was further studied and a similar pattern was shown (Figure 4.12c, d). Notably, a more rapid upregulation in the expression of CD107a than IFN-γ was clearly seen at one hour after peptide pulsing. Approximately 40% of M1-Tm^+ cells expressed surface CD107a, compared to 10% producing IFN-γ (n=4, p=0.0155). Both surface CD107a expression and IFN-γ production appeared to peak at 3 hours (Figure 4.12d). As shown in Figure 4.12e, IFN-γ and TNF-α were abundantly expressed in M1-Tm^+ cells following peptide pulsing. A modest number of M1-Tm^+ cells were also shown to express IL-2, but a few expressed IL-10. Due to the marginal expression of IL-10, IL-10 was not included in the functional profile analysis of M1-Tm^+ cells as shown in Figure 4.12f. The most frequently detected M1-Tm^+ cells were those expressing CD107a with IFN-γ and TNF-α (45%), following by those that co-expressed of IFN-γ and TNF-α (10%), CD107a and either IFN-γ (9%) or TNF-α (4%). Some M1-Tm^+ cells (3%) were shown to express CD107a and all three cytokines (IFN-γ, TNF-α and IL-2). Approximately 20% of these cells did not express any of CD107a and cytokines.

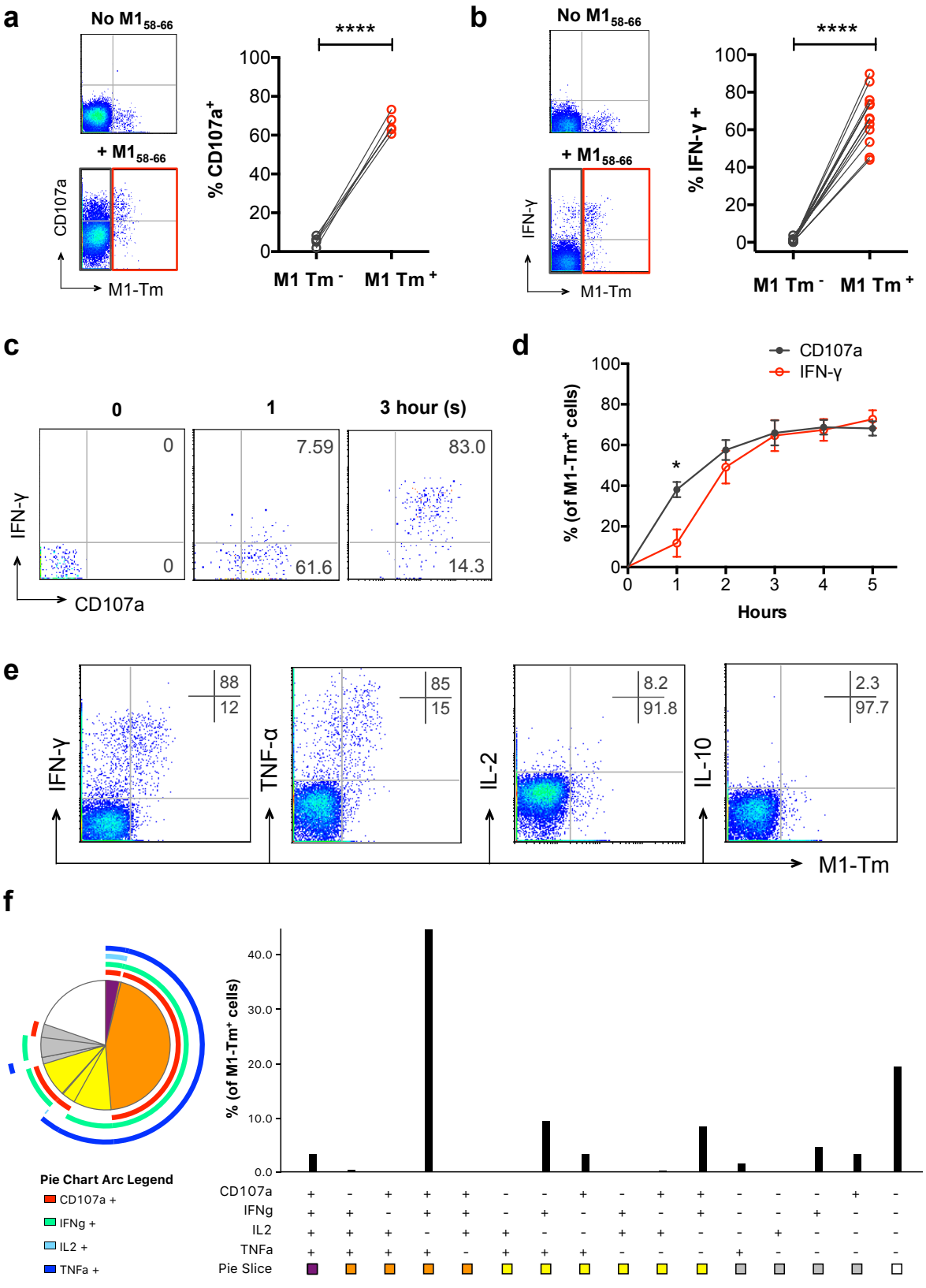

Figure 4.12 Functional properties of $M1_{58-66}$-specific $CD8^+$ T cells

Following 7-day *in vitro* MVA-NP+M1 stimulation, tonsillar MNCs were pulsed with $M1_{58-66}$ peptide for 6 hours followed by detection of surface CD107a expression and intracellular cytokines by flow-

cytometry. Levels of CD107a and IFN-γ expression were compared between M1-Tm$^+$ and M1-Tm$^-$ cells. **a)** Surface CD107a was highly expressed in M1-Tm$^+$ as compared to the lower level in M1-Tm$^-$ cells (Paired-t test, n=6, ****$p<0.0001$). **b)** IFN-γ expression was also significantly higher in M1-Tm$^+$ compared to M1 Tm$^-$ cells (Paired-t test, n=13, ****$p<0.0001$). **c)** Representative flow cytometric dot plots and **d)** the kinetic curves showed the co-expression of surface CD107a and intracellular IFN-γ in M1-Tm$^+$ cells following peptide pulsing. At 1 hour, the percentages of CD107a$^+$ cells were significantly higher than those of IFN-γ$^+$ cells (Paired-t test, n=4, *$p=0.0155$). Means and SEMs were shown at each time point. **e)** Representative flow cytometric dot plots showed the expression of IFN-γ, TNF-α, IL-2 and IL-10 in M1-Tm$^+$ cells. The number on the top right corner indicated the proportion of M1-Tm$^+$ cells expressing each cytokine of total M1-Tm$^+$ cells. **f)** The functional profile of M1-Tm$^+$ cells was analysed using SPICE 5.0 software (n=2). With the pie chart, the different colours of arcs around showed the proportion of M1-Tm$^+$ cells expressing each marker; CD107a (red), IFN-γ (green), IL-2 (light blue) and TNF-α (dark blue). The pie slices were shown in five different colours, which referred to the number of CD107a/ cytokines co-expressed; 4 in purple, 3 in orange, 2 in yellow, 1 in grey and 0 in white. These same coloured pie slices were also appeared in the bar chart together with the legend below informing different combinations of the CD107a/cytokine expression, where (+) referred to positive and (-) to negative expression of each marker. Black bars demonstrated the proportion of M1-Tm$^+$ cells in different functional profiles. For example, the first bar showing in the purple pie slice demonstrated approximately 3% of M1-Tm$^+$ cells expressing all four markers; CD107a, IFN-γ, IL-2 and TNF-α.

Having shown that M1-Tm$^+$ cells mobilised CD107a to their cell surface after peptide restimulation, implying degranulation, the expression of cytotoxic molecules including perforin and granzyme-A and –B were then measured in CD107a$^+$ M1-Tm$^+$ cells in tonsillar MNCs at every hour until 5 hours after $M1_{58-66}$ peptide restimulation. Median fluorescence intensity (MFI) of perforin and granzyme-A gradually increased in the first three hours, while the decrease of granzyme-B was observed in the first two hours. All three cytotoxic molecules stabilised at 4 hours before increasing at 5 hours (Figure 4.13a). It was convinced that the tiny fraction of M1-Tm$^+$ cells (less than 1% of total CD8$^+$ T cells) resulted in the very low absolute number of M1-Tm$^+$ cells among large number of total events being acquired for analysis and the kinetics of cytotoxic effector molecule release observed may not be truly representative.

As a much higher number of M1-Tm$^+$ cells could be detected in PBMCs upon MVA-NP+M1 stimulation (~20% of total CD8$^+$ T cells), the same experiment was carried out using PBMCs to further identify the degranulation kinetics of CTLs activated by MVA-NP+M1. In accordance with tonsillar MNCs, the majority of these cells contained perforin and granzymes in their

cytoplasm. After the $M1_{58-66}$ peptide pulsing, the kinetics of surface CD107a expression was in a similar pattern (data not shown) to that in tonsillar MNCs. Interestingly, both granzyme-A and -B in $CD107a^+$ M1-Tm^+ cells of PBMCs were shown to continuously decrease in the first three hours before increasing in at 5 hours. However, perforin gradually increased at all times as similarly observed in tonsillar MNCs (Figure 4.13b).

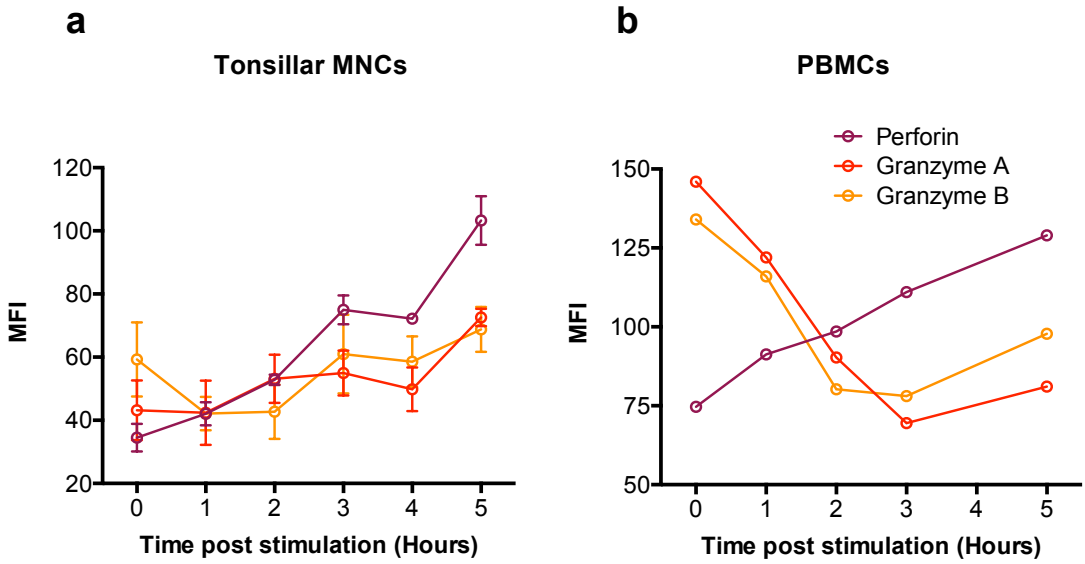

Figure 4.13 The kinetics of cytotoxic molecule release of M1-Tm^+ cells following $M1_{58-66}$ peptide restimulation.

a) $CD69^+$cell-depleted tonsillar MNCs (n=3) or **b)** peripheral blood mononuclear cells (PBMCs) following 7-day *in vitro* stimulation with MVA-NP+M1 were pulsed with $M1_{58-66}$ peptide in the presence of anti-human CD107a antibodies (CD107a-BV421) and brefeldin A plus monensin during culture. The expression of cytotoxic molecules; perforin (purple line), granzyme A (red line) and granzyme B (orange line) in $CD107a^+$ M1-Tm^+ cells was measured in different time points. Dots and error bars indicated means and SEMs at each time point.

Finally, the capacity of M1-Tm^+ cells in tonsillar MNCs to mediate cytotoxic killing of target cells was examined *in vitro*. Isolated $CD8^+$ T cells following *in vitro* MVA-NP+M1 stimulation containing M1-Tm^+ cells were used as effector T cells (E) and co-cultured at different ratios with $M1_{58-66}$ peptide-pulsed autologous B cells (as target cells, T), followed by the analysis of target cell lysis using LIVE/DEAD staining followed by flow-cytometry. The proportion of M1-Tm^+ cells in total isolated $CD8^+$ T cells following vaccine stimulation varied from 1 to 3% among samples, resulting in the highest E/T ratio that also varied from 0.77 to 1.57.

Representative data as demonstrated in Figure 4.14a showed there was a significant decrease in peptide-pulsed B cells (T_{low}), but not B cells without peptide pulsing (T_{high}) following co-culture with $CD8^+$ T cells, indicating specific lysis of peptide-pulsed B cells. Of three individuals tested, the capacity of lysis killing at the highest E/T ratio was shown at 24, 26 and 56%. All of them showed linear regression with R^2 over 0.85, where the increase of target cell-lysis correlated with the increase in effector to target cell (E/T) ratio (Figure 4.14b).

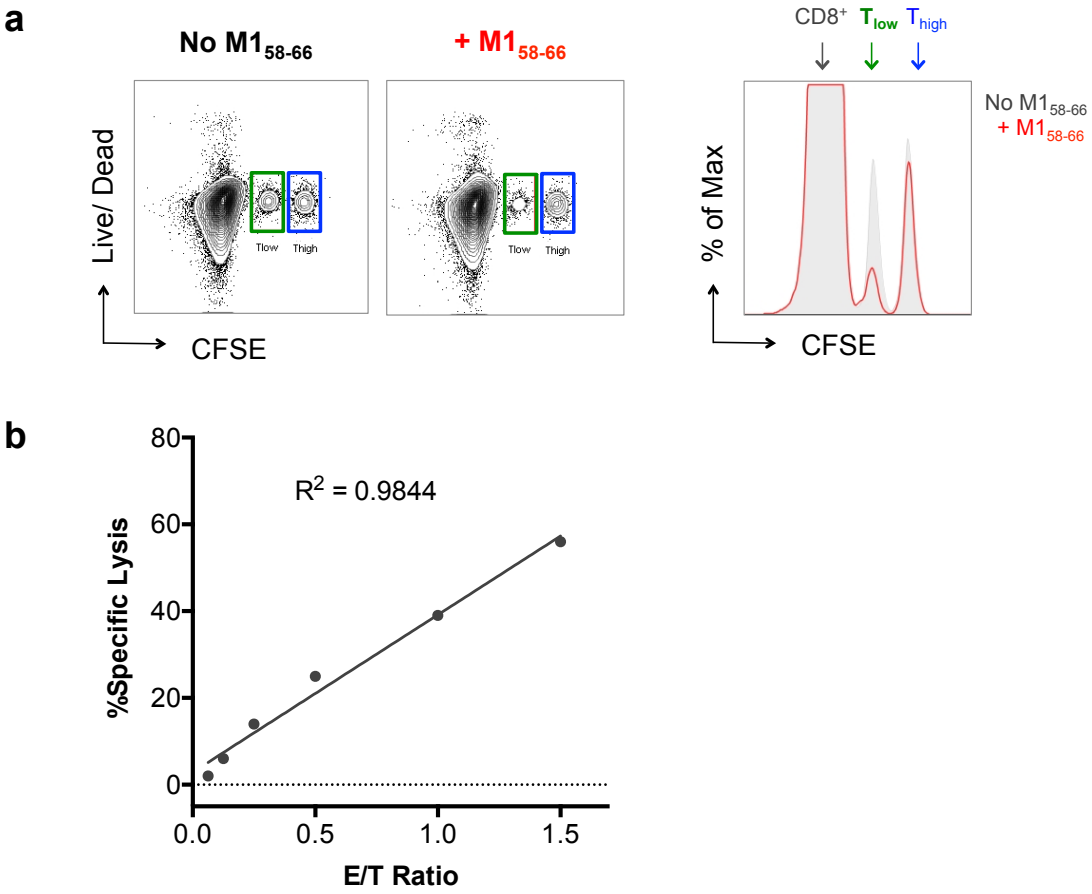

Figure 4.14 Specific killing capacity of $M1_{58-66}$-specific $CD8^+$ T cells

Isolated $CD8^+$ T cells following MVA-NP+M1 stimulation were co-cultured at different ratios with autologous B cells labeled with low (T_{low}) and high CFSE intensities (T_{high}) for 6 hours. T_{low} were either pulsed with $M1_{58-66}$ peptide or left without pulsing, while T_{high} were always left without pulsing. **a)** The representative flow cytometric plot and the histogram showed the decreasing number of T_{low} after peptide pulsing (green box or red middle peak on histogram) compared to non-pulsing (blue box or middle grey shade on histogram), which indicated specific target cells being killed. **b)** Graph plotted between % specific lysis and E/T ratio exhibited the linear regression. E was referred to M1-Tm^+ cells of isolated $CD8^+$ T cells, whereas T was referred to the total number of T_{low}.

4.5. Discussion and conclusion

MVA-NP+M1 has been designed to confer broadly protective cellular immunity as the vaccine antigens contain widely conserved $CD8^+$ T cell epitopes among influenza A viruses [35]. Since intranasal vaccination (e.g. LAIV) is considered a biologically more relevant and effective vaccination strategy against respiratory pathogens [30], [168], [169], the potential of MVA-NP+M1 as a mucosal vaccine to activate cross-reactive T cell responses was investigated in human NALT *in vitro*.

The optimisation of *in vitro* cell stimulation with MVA-NP+M1 vaccine was initially performed and it was shown that the highest magnitude of M1-specific $CD8^+$ T cell response was obtained following the stimulation of PBMCs or $CD69^+$cell-depleted tonsillar MNCs with the final concentration of $1x10^5$ pfu/ml MVA-NP+M1 vaccine with IL-15 supplement followed by a 7-day incubation period (Figure 4.4 and 4.5). As MVA infection could induce cell apoptosis [143], the optimal vaccine dose would result in the balance of cell viability and T cell response. IL-15 has the essential roles to induce human naïve and memory $CD8^+$ T cells proliferation and is also involved in maintaining memory $CD8^+$ T cells [177]. Moreover, IL-15 producing cells were found in T cell areas and the squamous epithelial cells lining human tonsils [178]. Therefore, IL-15 supplement may provide physiological environment for the cell culture. Although $CD8^+$ T cells in the MNCs without stimulation (medium control) seemed to proliferate during the culture, there was no increase of antigen-specific $CD8^+$ T cells observed, suggesting that the IL-15 dose used in this study does not cause non-specific T cell induction. Finally, the detectable T cell response was shown at day-7 following *in vitro* stimulation. Within this period of time, it would allow antigen-specific CTLs to expand after the recognition of influenza NP/M1 antigens. Similarly, it was previously shown that T cell responses in healthy volunteers were detectable in peripheral blood as early as 1 week following MVA-NP+M1 vaccination [167].

CTLs have been shown to positively correlate with protection from different subtypes of influenza virus [91], [179]. In this study, the capacity of MVA-NP+M1 to activate antigen-specific $CD8^+$ T cell responses was examined in human NALT *in vitro*. Data from IFN-γ ELISPOT assay and ICS demonstrated that MVA-NP+M1 activated a marked increase in

IFN-γ-secreting $CD8^+$ T cells in tonsillar MNCs specific to conserved influenza M1 epitopes (Figure 4.6). This was in accordance with previous studies showing the increasing magnitude of T cell responses to the epitopes spanned across NP and M1 in peripheral blood of MVA-NP+M1-vaccinated healthy people [165], [167].

$CD4^+$ T cells as T helper cells also play an important role in enhancing $CD8^+$ T cell response. By using 15-mer peptides, T cell response to M1 peptides was observed in an ELISPOT assay; however, the data from ICS showed that the responses were likely to be originated from $CD8^+$ T cells rather than $CD4^+$ T cells. The 15-mer peptides should be principally presented by MHC class II molecules to $CD4^+$ T cells; however, the peptides may be able to bind to the MHC class I if there is carboxy terminus at both ends of them [180], activating $CD8^+$ T cell response instead. A study suggested that the use of 17-mer rather than 15-mer peptides to stimulate splenocytes gave more optimal respiratory syncytial virus (RSV)-specific $CD4^+$ T cell response [181]. To this point, the optimal peptide length and sequences may be considered for the study of $CD4^+$ T cell response to the vaccine.

$M1_{58-66}$–specific $CD8^+$ T cell responses were further examined using HLA-A2-restricted $M1_{58-66}$ tetramer staining. $M1_{58-66}$ is one of the immunodominant M1 epitopes, which is conserved among influenza A viruses including H1, H3 and H5 [44], [182], [183]. The epitope is restricted to HLA-A2, which is among the highest frequencies in most ethnic groups, responsible for 20-30% overall and 50% in Caucasians [184], [185]. The frequency of pre-existing M1-Tm^+ cells was generally low in tonsillar MNCs. A similar finding has been observed in peripheral blood from young adults and elderly, and in whom these M1-specific T cells had central memory T cell phenotypes [186]. Following *in vitro* stimulation, MVA-NP+M1 elicited M1-Tm^+ T cell response in tonsillar MNCs from HLA-matched individuals (Figure 4.9a). The similar finding was previously shown that the frequency of M1-Tm^+ cells in peripheral blood tended to be in higher in MVA-NP+M1-vaccinated donors than controls although it did not reach significance. However, it should be noted that the measurement of M1-Tm^+ cells in this study was not performed at the peak time of T cell response (week 3), but 1 week later when the T cells showed contraction. Despite the insignificant increase of M1-Tm^+ cells, they showed that these cells in vaccinees were highly activated [187]. The

results in this study showed that the CTL response was age-dependent (Figure 4.9b). The markedly increased response was observed for the first time in older children and the response was strongest in adults. The results in this study support the hypothesis that MVA-NP+M1 has the capacity to boost M1-specific mucosal $CD8^+$ T cell responses in addition to systemic T cell responses in adults [165], [167] and elderly [164]. This is likely via activating the memory $CD8^+$ T cells primed by previous natural exposure to influenza viruses or vaccination. MVA-vectored vaccines have been shown to induce memory T cells in other studies. Clonality studies in vaccinated-elderly showed MVA-NP+M1 expanded pre-existing epitope-specific T cells [164]. MVA expressing HIV-1 genes also predominantly induced central memory $CD8^+$ T cells specific to HIV-1 Gag [188].

Having shown the activation of $M1_{58-66}$-specific $CD8^+$ T cell responses, the functionality of these cells was then studied. It is generally thought that cytotoxic $CD8^+$ T cells exert their effector activities to limit virus infection and disease severity [46], [91] through cytotoxic effector molecule release and pro-inflammatory cytokine secretion [99]. It was demonstrated herein that many M1-Tm^+ cells in tonsillar MNCs activated by MVA-NP+M1 *in vitro* expressed perforin, granzyme-A and –B (Figure 4.11), which were subsequently released upon the recognition of $M1_{58-66}$ peptide, as implied from the rapid upregulation of surface CD107a expression. In addition, it was also shown that the kinetics of surface CD107a expression correlated well with that of cytokine (IFN-γ) production in M1-Tm^+ cells (Figure 4.12c,d). However, the more rapid upregulation of surface CD107a than IFN-γ expression at the first hour after peptide challenge suggests a rapid or perhaps an immediate degranulation and cytotoxic molecule release rather than cytokine secretion at the initial stage of $CD8^+$ T responses. This was supported by the results demonstrating that perforin and granzymes were already stored intracellularly in M1-Tm^+ cells before peptide challenge. In contrast, IFN-γ was not detected in M1-Tm^+ cells and was likely to be produced *de novo* following antigen challenge.

Many M1-Tm^+ cells co-expressed CD107a with anti-viral cytokines; IFN-γ and TNF-α (Figure 4.12f). In addition to these two cytokines, some of these cells also co-expressed IL-2, which may exhibit more potent cytotoxic functions than those producing only one or two cytokines

[99]. Similar functional profiles showing the co-expression of CD107a and pro-inflammatory cytokines of human cytotoxic T cells in peripheral blood were reported previously following *in vitro* influenza virus infection [189] and after MVA-NP+M1 vaccination [167]. The results suggest that M1-Tm$^+$ cells produce both cytotoxic effector molecules and inflammatory cytokines upon specific antigen recognition. The functional profile suggests that M1-Tm$^+$ cells are likely to be short-lived effector and effector memory CD8$^+$ T cells [190], [191]. Despite the fact that the majority of $M1_{58-66}$-specific CTLs were functionally active, it was noteworthy that some of these CTLs seemed to be unresponsive upon the recalled peptide restimulation. Future study may answer whether or not these cells are dysfunctional.

As surface CD107a expression implies degranulation, the release of cytotoxic molecules was also assessed (Figure 4.13). Although a consistent reduction of cytotoxic molecules in the responding CTLs (M1-Tm$^+$ CD107a$^+$) was not observed in tonsillar MNCs, the pattern was observed in PBMCs. It is likely that the low number of M1-Tm$^+$ cells in tonsillar MNCs tested and the gradual loss of these cells over the course of peptide restimulation in the experiment may have affected the consistency of this observation. By performing the same experiment in PBMCs containing larger number of M1-Tm$^+$ cells, the continuous decrease of granzyme-A and –B in CD107a$^+$ M1-Tm$^+$ cells was obviously displayed at the first 3 hours upon the peptide restimulation. The rising level of granzymes at 5 hours may be explained as the accumulation of newly synthesised granzyme molecules [192]. In contrast, the gradual increase of perforin seemed to result from the use of clone B-D48 antibody for staining, which sensitively detects different conformations of perforin (both pre-existing and *de novo* synthesised) [193], [194].

Having shown that MVA-NP+M1-activated M1-Tm$^+$ cells in tonsillar MNCs were polyfunctional, the *in vitro* cytotoxic killing assay was finally performed and the results supported that MVA-NP+M1-activated M1-Tm$^+$ cells possessed a potent cytotoxic killing activity capable of specific target cell lysis in human NALT (Figure 4.14).

In conclusion, the results demonstrated that MVA-NP+M1 had the capacity to activate a cross-reactive M1-specific mucosal CD8$^+$ T cell response in an age-dependent manner. These M1-specific CTLs exhibited classical cytotoxic effector markers and produced pro-

inflammatory cytokines leading to specific killing of target cells in human NALT *in vitro*. It suggests that this novel vaccine has the potential to act as a mucosal vaccine to activate a broadly cross-reactive cytotoxic T cell response against a range of influenza subtypes.

.....

Chapter 5

Activation of cross-reactive HA-specific IgG antibody response in human NALT *in vitro* by MVA-pdmH1HA

5.1. Introduction

Neutralising antibodies (nAb) are considered as the benchmark of protective immune responses to influenza viruses [18]. This type of antibody can be induced by seasonal influenza vaccines, either inactivated or live attenuated, and provide the protection from circulating viruses that are identical or closely antigenically matched to vaccine strains [22]. On the other hand, the broader protective responses across influenza subtypes could be mediated by broadly neutralising antibodies (bnAb), in addition to cytotoxic T cell immunity [35], [136].

Broadly neutralising monoclonal antibodies to influenza viruses have been discovered from isolated human memory B cells. They target the more relatively conserved HA stalk instead of the HA globular head. Binding to different epitopes on the HA stalk results in the difference in the breadth of reactivity. Most antibodies have been shown to cross-react to either phylogenetic HA group 1 or group 2. A few have the cross-reactivity to both HA groups, and recently, one has been found to recognise HA of both influenza A and B viruses [41], [79], [195]. The anti-HA stalk antibodies are found in some individuals following seasonal vaccination or natural infection [196], [197]. Nevertheless, the frequencies of the HA stalk specific antibody-producing B cells are relatively rare, which results from the subdominant activation of HA stalk-reactive memory B cells during seasonal epidemics [19]. Although the magnitude of anti-HA stalk antibody response is low during seasonal vaccination, the HA stalk-reactive antibodies were found to increase markedly in people infected with pandemic H1N1 virus during the outbreak in 2009 [20], [21], [83]–[85]. It was hypothesised that the significant changes in the immunodominant globular head epitopes of the pandemic H1 HA compared to the contemporary seasonal H1 HAs lead to decreased competition for antigen among pre-existing memory B cells, which in turn allowed for the expansion of the subdominant stem-specific memory B cells [19]. Later, it has been also shown that the HA stalk reactive antibodies could be more efficiently boosted by sequential immunisation with divergent HAs [41], [42]. Vaccination with the subunit pandemic H1N1 vaccine also boosted the HA stalk-specific antibodies in healthy adults; however, the antibodies waned faster than those induced by natural infection [198]. The HA stalk-reactive

antibodies have been characterised as having no haemagglutination inhibition (HAI) activity as they do not bind to the globular HA head [198]. HA stalk-reactive antibody-mediated protection is most likely via neutralising activity by trapping an internalised virus in the endosome or by inhibiting HA maturation of virus or via requiring Fcγ-R interaction for cell-mediated cytotoxicity [87], [199], [200] as shown in Figure 1.9.

Given the cross-reactivity of anti-HA stalk antibodies, recent efforts are focused on the use of novel vaccines and vaccination strategies to boost these antibodies in order to confer broadly protective response to multiple subtypes of influenza viruses [201], [202]. Various vaccine platforms such as DNA vaccines, vector-based vaccines and modified HA protein vaccines have been employed together with or without the use of adjuvants. Of them, MVA expressing influenza HA is one of the candidate vaccines and have been reported to induce cross-reactive protection in different animal models [54]. MVA-expressing HA of A/Vietnam/1194/2004 (H5N1) has been shown to induce cross-clade neutralising antibodies to different H5N1 subtypes in animal models [203], [204] and in humans [67].

Despite the accumulative findings of the protective responses induced by MVA-vectored vaccines, a few have shown the potential of the vaccines to induce mucosal antibody responses, which may provide superior protection from virus infection in humans. We have previously shown that MVA-pdmH1HA elicits the mucosal cross-reactive HA-specific IgG antibodies to influenza subtypes in human NALT following *in vitro* vaccine stimulation [147]. In this study, the potential of MVA-pdmH1HA to activate such B cell-mediated antibody response was further studied. The MVA-pdmH1HA-elicited antibodies were assessed for the magnitude and the breadth of cross-reactivity to heterologous subtypes including seasonal H1, H3, H5, H7 and H9 and the antibodies were also characterised for the HA-binding site.

5.2. Aims of the study

1. To measure the capacity of MVA-pdmH1HA to elicit HA-specific IgG antibodies against influenza A viruses in HA group 1 and group 2 in human NALT *in vitro*
2. To compare the magnitude and the breadth of cross-reactive antibody response between children and adults

5.3. Materials and methods

5.3.1. Adenoidal/ tonsillar tissues and peripheral blood

Adenoidal and tonsillar tissues were obtained from children (average age 6.2, 2-15) and adults (average age 27.4, 16-54) undergoing adenotonsillectomy at local hospitals. Patients who received systemic steroids within 3 weeks prior to surgery, or who had any known immunodeficiency were excluded from the study.

Adenotonsillar MNCs were then isolated from the tissues as the standard protocol described in chapter 2 *(see 2.7.1)* and were resuspended in R10 at $4x10^6$ cells/ml. Peripheral blood taken from the same patient was spun down to collect its plasma, termed "autologous human plasma (aHP)".

5.3.2. Vaccines/ Viruses

MVA-pdmH1HA (#1531) is a recombinant Modified Vaccinia Ankara (MVA) expressing full-length HA of A/California/04/2009 (pdmH1N1) under the control of the modified Vaccinia H5 (mH5) promoter. MVA-wt (#1533) was a non-recombinant virus used as a vector control.

FluMist® season 2011-2012 (NR-36465, BEI resources, USA) is a trivalent live attenuated influenza vaccine (LAIV), containing A/California/07/2009 (pdmH1N1), A/Perth/16/2009 (H3N2) and B/Brisbane/60/2008. It was used as a positive control for the antibody production study.

The following two inactivated whole influenza viruses were used as antigens for haemagglutination inhibition assay; A/California/07/2009 (GPO, Thailand) and A/Vietnam/ 1203/2004 (FR-736, IRR, USA).

5.3.3. Influenza recombinant proteins

Recombinant HA protein from influenza subtypes; A/California/04/2009 (pdmH1N1, NR-13691), A/Brisbane/59/2007 (sH1N1, NR-28607), A/Brisbane/10/2007 (H3N2, NR-19238), A/Vietnam/1203/2004 (H5N1, NR-10510), A/Hong Kong/33982/2009 (H9N2, NR-41792) and

A/Anhui/1/2013 (H7N9, NR-44081) were obtained from BEI resources, USA and used for enzyme-linked immunosorbent assay (ELISA) to detect HA-specific IgG antibodies. Unless otherwise stated, each HA was a full-length glycosylated recombinant protein that was produced in Sf9 insect cells using a baculovirus expression vector system. It was purified under conditions that preserve its biological activity and tertiary structure.

5.3.4. Measurement of HLA-DR expression

To measure the expression of HLA-DR on MVA-pdmH1HA-infected adenotonsillar B cells, the MNCs were cultured with MVA-pdmH1HA at a final concentration of $5x10^4$ pfu/ml (or MOI of 0.00125) for 18-20 hours. The MNCs were harvested and stained for surface CD19-FITC (clone HIB19) and HLA-DR-APC (clone G46-6) (Both BD Biosciences, UK) before intracellular staining with RPE-conjugated monoclonal anti-pandemic H1N1 HA antibody, followed by flow-cytometry.

5.3.5. Cell stimulation and culture for antibody production study

Adenotonsillar MNCs were cultured with either MVA-wt or MVA-pdmH1HA at the final concentration of $5x10^4$ pfu/ml unless otherwise stated or left without any stimulation (medium control). The MNCs stimulated with FluMist® season 2011-2012 at the final concentration of 2 µl/ml (approximately 10^5 FFU/ml per each virus) were used as positive control [205]. Cell culture media was additionally supplemented with 2%aHP and seeded in 96-well plate. The plate was incubated for 10 days before cell culture supernatant was collected and stored at -20°C until analysis.

5.3.6. Detection of HA-specific IgG antibodies by indirect ELISA

Cell culture supernatant following 10-day *in vitro* vaccine stimulation *(see 5.3.5)* was analysed for HA-specific IgG antibodies by ELISA assay *(see 2.13).* The cell culture supernatant was thawed at room temperature and pre-diluted in ELISA blocking buffer (10%ΔFBS in 1XPBS) at different ratio before tested. If the sample showed the optical density (OD) out of the standard range, the sample dilution needed to be adjusted either higher or lower than the previous one and retested. Nevertheless, the lowest sample dilution

of all samples was 1:5, due to the limit of sample volume. The antibody concentration (Units/ml; U/ml) of each sample was calculated based on the standard curve with four-parameter logistic curve fit using DeltaSoft 1.61.0 programme. Any sample demonstrating an antibody concentration lower than the limit of detection of the assay (undetectable value by DeltaSoft programme) was re-calculated its concentration based on the standard curve with polynomial regression using Microsoft Excel programme.

Due to the background caused by the pre-existing anti-influenza antibodies in aHP, the antibody concentration in cell culture supernatants following *in vitro* MVA-wt or MVA-pdmH1HA stimulation was subtracted from that of medium control unless otherwise stated before being used for any statistical analysis.

For qualitative analysis to determine the breadth of cross-reactive antibody, the positive antibody response was defined when the subtracted antibody concentration of the MVApdmH1HA-stimulated cell culture supernatant was higher than that of the MVA-wt-stimulated one and was not below the lowest limit of detection of the assay (The value was obtained from DeltaSoft programme).

5.3.7. Haemagglutination inhibition (HAI) assay

Antibodies in cell culture supernatants following *in vitro* MVA-wt and MVA-pdmH1HA stimulation and medium control were characterised by HAI assay *(see 2.14)* to homologous (pdmH1N1) and heterologous virus strains (H5N1) (Figure 5.7). Briefly, cell culture supernatant was heated followed by chicken red blood cell treatment to remove non-specific haemagglutinin before performing the HAI assay. The HAI titre in cell culture supernatants from each individual after MVA-wt and MVA-pdmH1HA stimulations was compared. HAI conversion was defined as 2 or more fold change when the HAI titre of MVA-pdmH1HA-stimulated cell culture supernatant was divided by that of the MVA-wt-stimulated one.

5.3.8. Statistical analysis

For two-group comparisons, based on the normality of distribution of data. Nonparametric Wilcoxon matched-pairs signed rank test and nonparametric Mann-Whitney test were performed using GraphPad Prism. $p<0.05$ was considered as statistically significant.

5.4. Results

5.4.1. Optimisation of *in vitro* cell stimulation with MVA-pdmH1HA

Optimisation was initially performed on the cell culture supplement and MVA-pdmH1HA vaccine doses. Cell culture was routinely supplemented with 10% ΔFBS. In order to enhance antibody production, autologous human plasma (aHP) was also added to cell culture medium and the concentration of aHP was optimised. The use of aHP increased HA-specific IgG antibodies to pdmH1N1 detected by ELISA assay as seen in medium control. The higher the aHP concentration added, the higher the anti-pdmH1N1 antibody were detected, suggesting that pre-existing anti-influenza antibodies were contained in aHP. 2% aHP supplement was shown among other aHP concentrations to maximally enhance the amount of HA-specific IgG anti-pdmH1 antibodies in the MNCs following *in vitro* MVA-pdmH1HA stimulation (Figure 5.1).

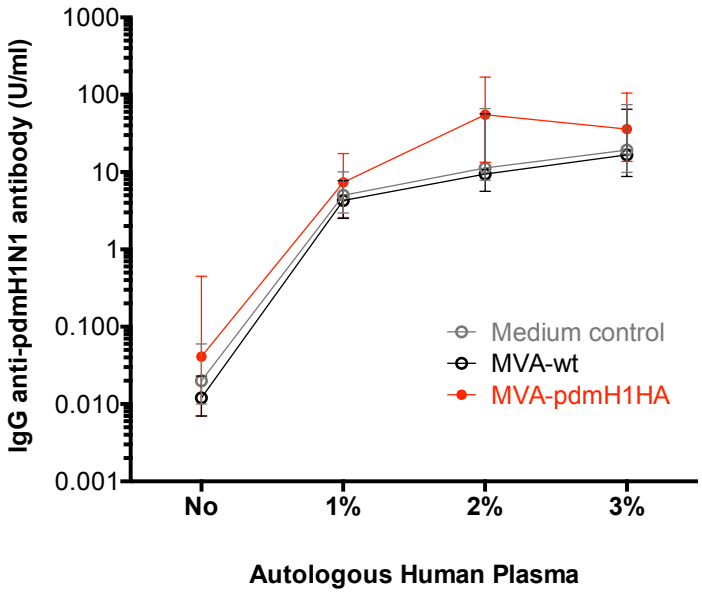

Figure 5.1 Optimisation of autologous human plasma concentration

Adenotonsillar mononuclear cells were cultured with either MVA-wt or MVA-pdmH1HA at $5x10^4$ pfu/ml or left without any stimulation (medium control) without or with autologous human plasma (aHP) supplement, varied from 1-3%v/v. HA-specific anti-pdmH1N1 IgG antibody was measured in cell culture supernatant by enzyme-linked immunosorbent assay. The antibodies were shown in medium control (grey line), MVA-wt (black line) and MVA-pdmH1HA (red line) stimulation. Dots and error bars indicated medians and interquartile ranges (n=7).

With 2% aHP supplement, adenotonsillar MNCs were then stimulated with MVA-pdmH1HA doses ranging from $2.5x10^4$, $5x10^4$ and $1x10^5$ pfu/ml and anti-pdmH1HA antibody was measured. The antibody concentration in medium control and MVA-wt-stimulated cell culture supernatant was comparable for each vaccine dose tested. Following the *in vitro* stimulation of MVA-pdmH1HA, the highest antibody response was shown with the use of vaccine at the concentration of $5x10^4$ pfu/ml. The use of the higher vaccine dose decreased the magnitude of the antibody response (Figure 5.2).

Therefore, for the antibody production study, adenotonsillar MNCs would be stimulated with MVA-pdmH1HA at a final concentration of $5x10^4$ pfu/ml and incubated for 10 days before the cell culture supernatant was analysed for HA-specific IgG antibodies to influenza subtypes.

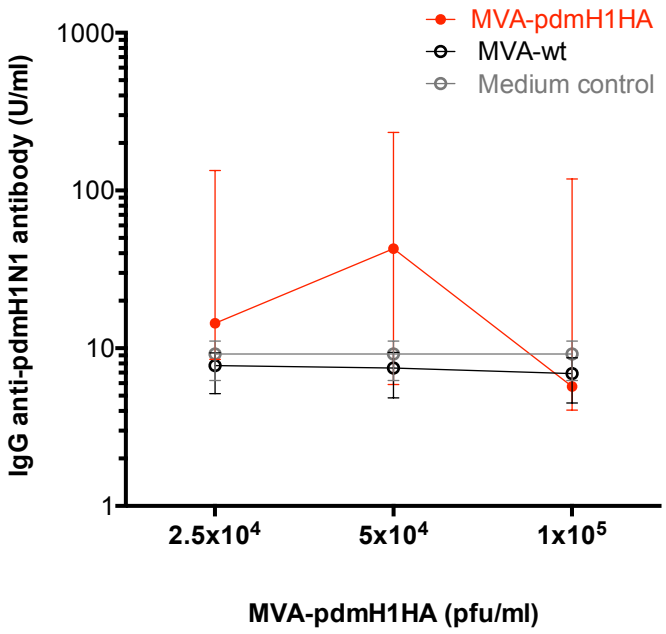

Figure 5.2 Optimisation of MVA-pdmH1HA vaccine dose

Adenotonsillar mononuclear cells were stimulated with either MVA-wt or MVA-pdmH1HA at different concentrations with 2% autologous human plasma supplement. HA-specific anti-pdmH1N1 antibody was measured by enzyme-linked immunosorbent assay. The antibody concentration in medium control (grey) and MVA-wt - (black) and MVA-pdmH1HA (red) -stimulated cell culture supernatant at different vaccine doses were compared (n=4). Dot and error bars indicated medians and interquartile ranges.

5.4.2. HLA-DR upregulation in influenza HA-expressing tonsillar B cells

Having shown in chapter 3 that influenza HA was abundantly expressed in B cells, it was questioned whether there was an upregulation of HLA class II molecules, which are important for antigen presentation to activate $CD4^+$ T cell responses, helping the B cell-mediated antibody response. The use of MVA-pdmH1HA dose at $5x10^4$ pfu/ml resulted in approximately 8% of the MNCs mainly B cells to express HA. The expression of HLA-DR was measured in adenotonsillar B cells following *in vitro* MVA-pdmH1HA stimulation. It was observed that HLA-DR was upregulated in influenza HA-expressing B cells. The higher fluorescence intensity of HA antigen was shown, the higher HLA-DR was expressed. Of $CD19^+$ B cells, the median fluorescence intensity (MFI) of HLA-DR was 419, 258 and 139 in HA^{high}, HA^{int} and HA^{neg} cells, respectively, while the MFI of $CD19^-$ non-B cells was as low as 5.79 (Figure 5.3).

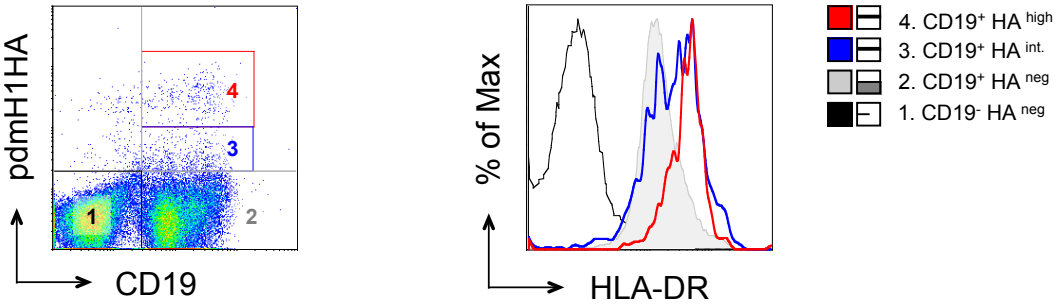

Figure 5.3 The upregulation of HLA-DR in HA-expressing B cells.

Adenotonsillar mononuclear cells were stimulated with MVA-pdmH1HA at $5x10^4$ pfu/ml for 18-20 hours. Cells were harvested and stained for CD19 and HLA-DR on the cell surface before intracellular staining for HA of pandemic H1N1. The flow cytometry dot plot showed 1) $CD19^-$ HA^{neg} (black line) 2) $CD19^+$ HA^{neg} (grey shade) 3) $CD19^+$ HA^{int} (blue line) and 4) $CD19^+$ HA^{high} (red line) and the histogram compared the median fluorescent intensity (MFI) of HLA-DR between the four cell populations as described above.

5.4.3. MVA-pdmH1HA elicited cross-reactive HA-specific IgG antibodies to influenza subtypes

MVA-pdmH1HA was then assessed for its capacity to elicit HA-specific IgG antibodies in adenotonsillar MNCs to homologous (pandemic H1N1) and heterologous influenza subtypes (Figure 5.4). Following 10-day *in vitro* stimulation with MVA-wt and MVA-pdmH1HA, HA-specific anti-pdmH1N1 antibodies in cell culture supernatant was analysed by ELISA. The MNCs stimulated with LAIV was used as positive control. Only MNCs that showed positive anti-pdmH1N1 antibody response to LAIV were included in the study, as they seemed to respond well in antibody production. The quality of tissues and the MNCs after isolation may affect the response of cells to the vaccine. Over half of children and almost all adults responded to LAIV, showing the higher anti-pdmH1N1 antibody compared to medium control.

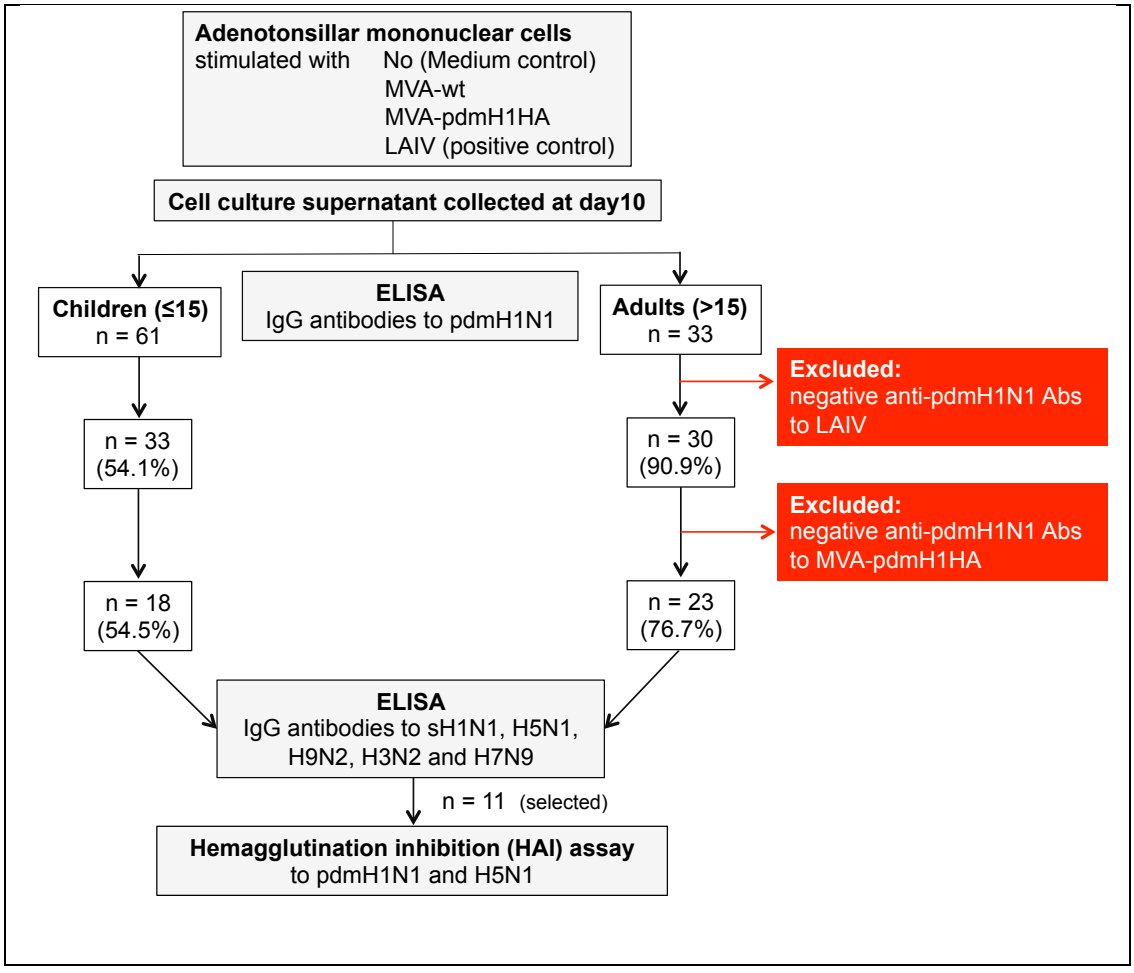

Figure 5.4 Experimental and analysis flow of the antibody production study

The diagram shows the experimental flow for the antibody production study of MVA-pdmH1HA vaccine including the criteria to exclude any data from the analysis.

The MNCs showing positive antibody responses to LAIV were then measured for the HA-specific IgG antibody response to MVA-pdmH1HA. It was shown that *in vitro* stimulation by MVA-pdmH1HA elicited a significant increase in anti-pdmH1N1 HA antibody levels compared to the MVA-wt control in adenotonsillar MNCs from both children (n=33, $p<0.0001$) and adults (n=30, $p<0.0001$) (Figure 5.5a).

The cell culture supernatant that demonstrated the positive anti-pdmH1N1 antibody response following MVA-pdmH1HA stimulation were further measured HA-specific IgG antibodies to heterologous influenza viruses in HA group 1 (sH1N1, H5N1, H9N2) and HA group 2 (H3N2 and H7N9) then the magnitude and breadth of reactivity antibody were assessed in children and adults. Following *in vitro* MVA-pdmH1HA stimulation, adenotonsillar MNCs from both children and adults were shown to produce IgG antibodies recognising influenza in HA group 1. The antibodies to HA group 2 viruses were only observed in adults towards H3N2. No antibodies to H7N9 were observed in both children and adults (Figure 5.5b). The magnitude of antibody response was highest towards pdmH1N1, followed by to HA group1 viruses. The antibodies to HA group 2 viruses were generally low, although they were detectable in a few samples.

When compared between 2 age groups, adults were shown to produce a higher level of antibodies than children to both homologous and heterologous influenza strains particularly in HA group1. The median IgG antibodies (U/ml) to pdmH1N1, sH1N1, H5N1, H9N2 were 13.65, 0.47, 0.81 and 0.26 in adults and were 1.58, 0.04, 0.04 and 0.00 in children, respectively (Figure 5.6a). In addition to the higher magnitude of antibody, adenotonsillar MNCs from adults in general produced antibodies with the greater breadth of reactivity than that from children. Approximately 40% of children were shown to produce HA-specific IgG antibodies to only homologous pdmH1N1 without cross-reactivity to other viruses tested, whereas the MNC from almost all adults produced cross-reactive antibodies to other virus strains. The majority of adults (~50%) produced antibodies that cross-reacted to 2 or 3 virus subtypes, mainly in HA group 1. There were approximately 15% of adults produced cross-reactive antibodies to the tested virus strains in both HA group 1 and group 2 (Figure 5.6b,c).

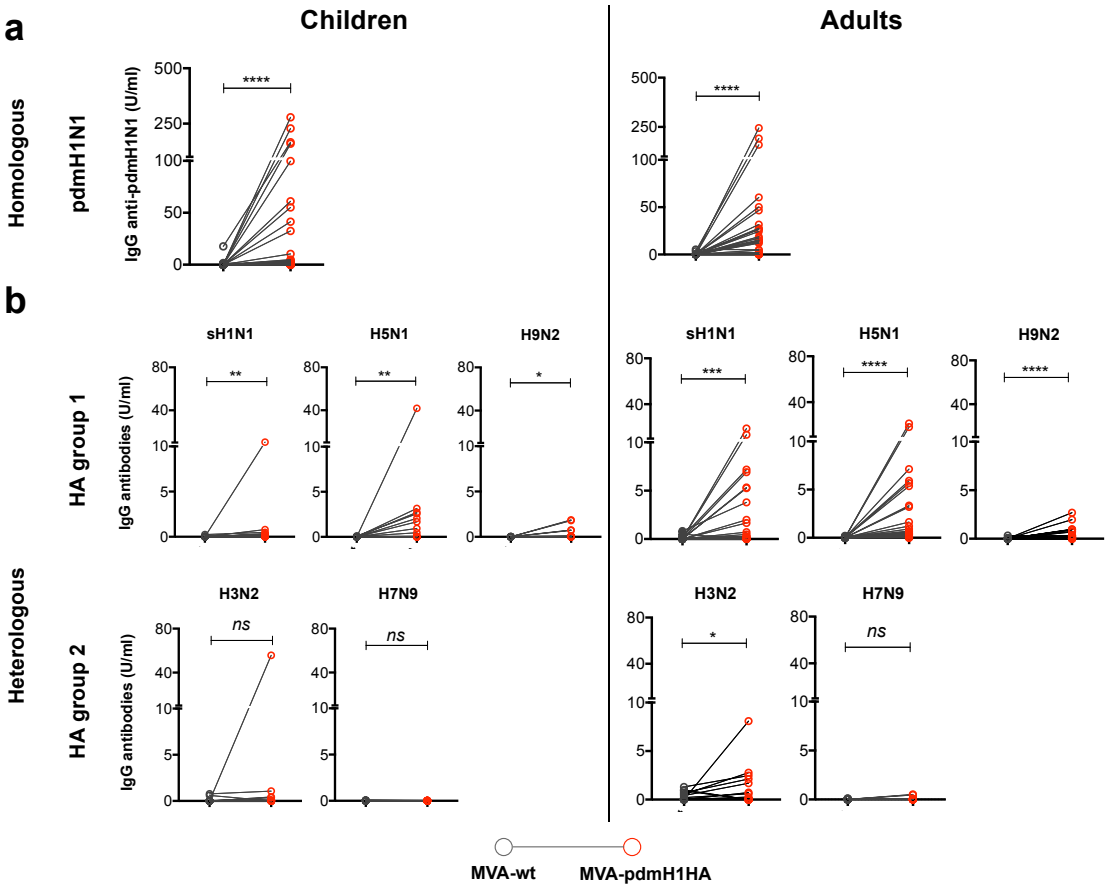

Figure 5.5 Cross-reactive HA-specific IgG antibodies to homologous and heterologous influenza subtypes elicited by MVA-pdmH1HA

Adenotonsillar mononuclear cell culture supernatants following 10-day stimulation with either MVA-wt or MVA-pdmH1HA or left without stimulation (medium control) were analysed for HA-specific IgG antibodies to pdmH1N1 and other heterologous subtypes by enzyme-linked immunosorbent assay (ELISA). Background-subtracted antibody concentrations (U/ml) were compared between MVA-wt (grey circle) and MVA-pdmH1HA stimulation (red open circle). **a)** MVA-pdmH1HA significantly elicited higher IgG anti-pdmH1N1 antibodies in both children (n=33, ****$p<0.0001$) and adults (n=30, ****$p<0.0001$). **b)** MVA-pdmH1HA significantly elicited higher IgG antibodies to sH1N1 (**$p=0.002$), H5N1 (**$p=0.0026$) and H9N2 (*$p=0.0259$), but not HA group 2; H3N2 ($p=0.1484$) and H7N9 ($p=0.0640$) in children (n=18). The vaccine also significantly elicited higher IgG antibodies to sH1N1 (***$p=0.0007$), H5N1 (****$p<0.0001$) and H9N2 (****$p<0.0001$) and HA group 2; H3N2 (*$p=0.0417$) but not H7N9 ($p=0.2078$) in adults (n=23). Wilcoxon matched-pair signed rank test was used for comparison between the two groups.

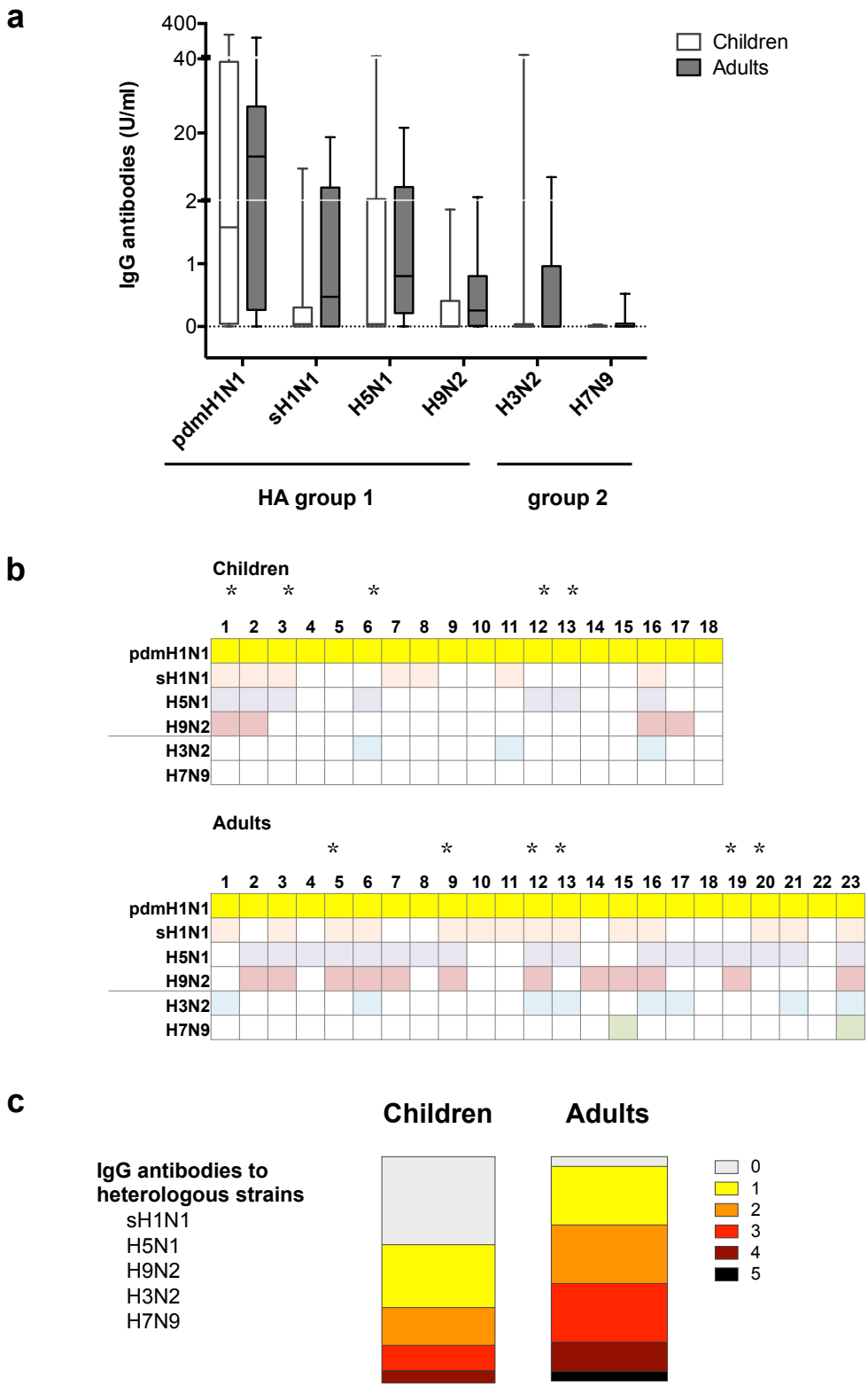

Figure 5.6 The magnitude and the breadth of reactivity of antibodies elicited by MVA-pdmH1HA in children and adults

Following 10-day *in vitro* MVA-pdmH1HA stimulation, adenotonsillar mononuclear cell culture supernatants that showed positive IgG anti-pdmH1N1 antibody response were analysed for HA-specific IgG antibodies to five heterologous influenza subtypes. **a)** The magnitude of antibody response

to all six influenza strains was compared between children (n=18) and adults (n=23). Bar and error bars indicated medians and interquartile ranges. **b)** Colour indicated the positive antibody response to each virus strain (yellow – pdmH1N1, orange – sH1N1, purple – H5N1, pink – H9N2, blue – H3N2, green – H7N9) in each individual. The subjects were in the order of ages from young to old. Star (*) over the number indicated the sample selected for haemagglutination inhibition assay. **c)** The breadth of reactivity of antibodies between children (n=18) and adults (n=23) was compared based on the positive antibody response to heterosubtypic viruses. The bar in different colours illustrated the number of heterologous subtypes that the antibodies cross-reacted to, ranging from zero (0) to five (5). Zero meant the antibodies only reacted to homologous pdmH1N1.

5.4.4. Haemagglutination inhibition (HAI) activity of MVA-pdmH1HA-elicited antibodies

Having shown that MVA-pdmH1HA elicited cross-reactive HA-specific IgG antibodies against homologous (pdmH1N1) and heterologous viruses in HA group 1 (sH1N1, H5N1 and H9N2), it was then characterised whether these antibodies were HA-stalk specific by performing HAI assay. Cell culture supernatants showing positive anti-pdmH1N1 and anti-H5N1 antibodies were selected to perform the HAI assay against inactivated pdmH1N1 and H5N1 viruses (Figure 5.7).

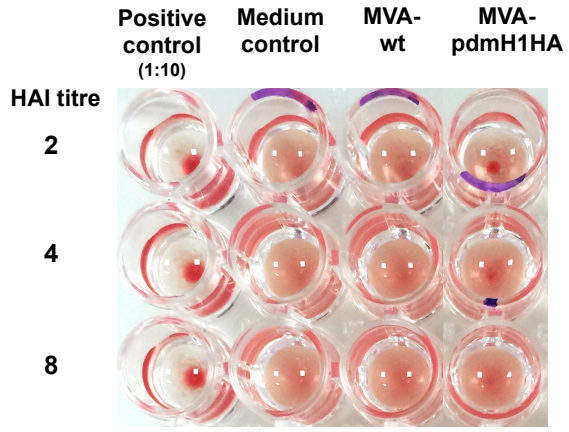

Figure 5.7 Haemagglutination inhibition (HAI) assay.

Representative data from a sample showing HAI activity against pdmH1N1 virus interpreting as a red button. Cell culture supernatant following *in vitro* MVA-pdmH1HA stimulation showed an HAI titre of 2, while that following MVA-wt stimulation and medium control did not show any inhibition, shown as HAI titre less than 2. This sample therefore showed HAI conversion with a 2-fold change. Human serum as a positive control had HAI titre higher than 80.

Adenotonsillar MNC culture supernatant following *in vitro* LAIV stimulation was used to perform the preliminary test and the HAI titre to pdmH1N1 virus was determined. Median anti-pdmH1N1 antibody titre were 32.4 (8-145) and 164.4 (85-893) U/ml in medium control and LAIV-stimulated cell culture supernatant, respectively. Almost all samples (12 of 14; 85.7%) showed HAI conversion upon LAIV stimulation as compared to medium control (p=0.0005) with 2-16-fold change (Figure 5.8a).

The HAI assay was then performed to measure the HAI titre in the cell culture supernatant following *in vitro* MVA-wt and MVA-pdmH1HA stimulation. Of selected 11 samples, anti-pdmH1N1 and anti-H5N1 antibodies were shown in Table 5.1.

Table 5.1 Antibody concentration (U/ml) in cell culture supernatant samples selected for HAI assay

Antibodies to	Median (range) antibody concentration (U/ml)		
	Medium control	**MVA-wt**	**MVA-pdmH1HA**
pdmH1N1	36.2 (7-131)	36.0 (6-125)	148.8 (9-339)
H5N1	1.3 (0.4-4.4)	1.3 (0.4-4.0)	5.1 (0.8-8)

Low HAI titre (between 1 and 4) was detected against pdmH1N1 and H5N1 in medium control and MVA-wt-stimulated cell culture supernatant. Following MVA-pdmH1HA stimulation, 5 of 11 (45.5%) were observed HAI conversion with 4-16-fold change against pdmH1N1, but did not reach significance, whereas no HAI conversion was observed against H5N1 (Figure 5.8b).

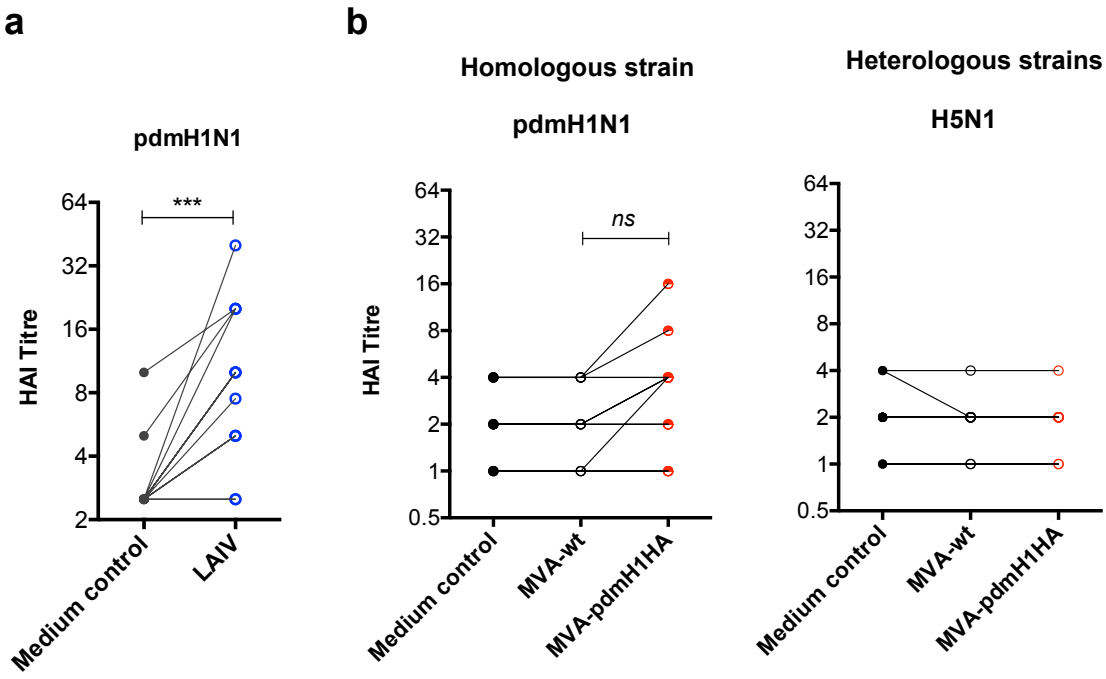

Figure 5.8 Hemagglutination inhibition (HAI) titre against influenza viruses.

HAI assay was performed to measure the HAI titre in adenotonsillar MNC culture supernatants following *in vitro* live attenuated influenza vaccine (LAIV), MVA-wt, MVA-pdmH1HA stimulation and no stimulation (medium control) **a)** LAIV-induced antibodies showed significant HAI conversion to pdmH1N1 virus (n=14, ****p=0.0005*). **b)** MVA-pdmH1HA-elicited antibodies in some individuals showed HAI conversion to pdmH1N1 (n=11, *p=0.0625*), but no HAI conversion to H5N1 (n=11) was observed. Wilcoxon matched-pair signed rank test was used for 2-group comparison

5.5. Discussion and conclusion

HA stalk-reactive antibodies recognise multiple influenza subtypes and therefore could mediate the broadly protective responses [195], [202]. These cross-reactive antibodies were shown to be efficiently boosted in humans after pandemic H1N1 infection [20], [21], [83]–[85], raising the possibility of developing novel vaccines to confer such antibody-mediated broad protection from a range of influenza subtypes. In this study, a MVA-pdmH1HA vaccine candidate was assessed for its potential to elicit cross-reactive HA-specific IgG antibodies in human NALT *in vitro*.

The cell culture system was firstly optimised. 2%v/v aHP supplement in cell culture media appeared to enhance antibody induction in adenotonsillar MNCs following *in vitro* vaccine stimulation (Figure 5.1). The addition of aHP may provide a more favourable physiological environment and essential nutrients or cytokines that would be beneficial for cell signaling and enhance the T-helper cell activity [206], [207]. Although the supplement of aHP in cell culture media resulted in increased anti-influenza HA antibodies detected in cell culture supernatant, the presence of such antibodies was unlikely to interfere with the detection of antibodies induced following *in vitro* MVA-pdmH1HA stimulation. Those pre-existing anti-influenza antibody in aHP could be subtracted so that the antibody newly produced upon MVA-pdmH1HA stimulation was obtained. In addition, there may be concern about the impact of anti-MVA vector antibody in aHP on the induction of antibody. Although the anti-MVA antibody in aHP was not measured, influenza HA expression in tonsillar MNCs upon the MVA-pdmH1HA stimulation was less likely to be affected by aHP (data not shown). This is consistent with the previous report showing that pre-existing antibodies to MVA in human serum did not compromise the efficacy of MVA-expressing H5N1 HA vaccine [67]. The optimal MVA-pdmH1HA vaccine dose was shown at the final concentration of $5x10^4$ pfu/ml. The use of higher vaccine dose led to a decrease of antibody response (Figure 5.2). This may be explained in that the use of the high vaccine dose to stimulate the MNCs could cause a larger number of MVA-infected B cells, which were subsequently induced to apoptosis [143] and this may abrogate the antibody induction.

Upon vaccine stimulation, the expression of influenza HA from the MVA-pdmH1HA was previously shown. It was also shown here that HA-expressing B cells upregulated the expression of HLA-DR (Figure 5.3), indicating the occurrence of antigen processing and presentation within these B cells. HLA-DR is one of the HLA class II molecules that are essential for antigen presentation to $CD4^+$ T-helper cells and the activation of T-helper cells could help B cell-mediated antibody responses [208]. We have recently demonstrated that T_{FH} is a T-helper cell subset, having a critical role in the antibody induction in response to LAIV in human NALTs *in vitro* [209]. Circulating influenza-specific T_{FH} were also shown to positively correlate with the antibody response in humans following immunisation with split seasonal influenza vaccine [210]. The results suggested that the induction of antibody responses by MVA-pdmH1HA may be T-cell dependent and this finding needed further investigation on the activation of HA-specific T_{FH}.

In addition to SIgA, IgG antibodies at respiratory mucosa were also shown to protect mice from influenza infection [211]. Our previous finding showed that IgG antibodies were the predominant isotype of antibodies induced by LAIV in human NALT *in vitro* [212]. Regarding its importance, mucosal IgG antibody production was examined in human NALT following *in vitro* MVA-pdmH1HA stimulation. MVA-pdmH1HA elicited a significant HA-specific IgG antibody response in adenotonsillar MNCs to pdmH1N1 (homologous strain) and also to a number of heterosubtypic influenza viruses, including A/Brisbane/59/2007 (seasonal H1N1), A/Vietnam/1203/2004 (avian H5N1) and A/Hong Kong/33982/ 2009 (avian H9N2), which were HA group 1 viruses. Cross-reactive antibodies to HA group 2 viruses (A/Brisbane/10/2007; H3N2 and A/Anhui/1/2013; H7N9) were observed only in some individuals (Figure 5.5). These extended results support our previous finding [147] and indicate that the vaccine-elicited antibodies are more likely to cross-react to only HA-group 1 viruses. This may not be surprising as pdmH1N1 belongs to the HA group 1, thus the antibody induced by its HA antigen is mainly towards other viruses within the same HA phylogeny [79]. Similar finding were also reported on the limited breadth of reactivity of antibodies towards group 1 haemagglutinins in animals and humans following vaccination with HA antigens from pdmH1N1 and H5N1 [67], [203], [204], [213]–[216]. Cross-reactive antibodies to both HA groups were even rarely found as the antibody needed to adopt

multiple binding sites to cope with the high amino acid diversity and structural constraint by the presence of glycans surrounding the target epitopes [200]. The breadth of cross-reactivity of antibodies was extended to divergent influenza A viruses by sequential immunisation of HA from both phylogenetic groups as shown in mice [217]. Recently, antibodies that broadly reacted to both HA group 1 and 2 were discovered in people following H7N9 vaccination [218].

Having shown that MVA-pdmH1HA elicited cross-reactive antibodies in adenotonsillar MNCs, the antibody response was compared between children and adults. The MNCs from adults produced stronger responses than those from children in terms of the magnitude and the breadth of reactivity of antibody towards a range of influenza viruses (Figure 5.6). Our previous study demonstrated the broader and stronger cross-reactive anti-HA antibodies in adults compared to children following 2009 pdmH1N1 infection [85]. Moreover, an age-dependent induction of HA stalk-reactive antibodies by recombinant chimeric HA-based vaccine was also shown [219]. These may explain the broader cross-reactive antibodies produced in adults upon MVA-pdmH1HA stimulation. Adults in general develop memory B cells recognising a wider range of influenza viruses compared to children via seasonal vaccination or natural infection through their lifetime [19]. Anti-HA stalk antibodies are also likely to be generated from pre-existing memory B cells [41], which are differentiated to plasma cells for anti-influenza antibody responses [220]. Taken together, age and the exposure history to influenza would have an impact on the induction of cross-reactive antibody responses.

Heterosubtypic protective responses are mediated by the antibodies targeting conserved HA stalk region rather than the hypervariant globular head region [35], [136]. The antibodies detected by ELISA assay could be either HA head- or HA stalk-reactive, due to the use of full-length HA. Thus, MVA-pdmH1HA-elicited cross-reactive antibodies in cell culture supernatant were characterised regarding whether they were HA stalk-specific or not by HAI assay. The undetectable HAI activity to H5N1 as shown in Figure 5.8b could imply that the antibodies recognising H5N1 by binding to its HA stalk [198]. However, since the level of antibodies to H5N1 was relatively low in the cell culture supernatant, one may argue on the

sensitivity of the assay to detect the HAI activity in these samples. A recent study has reported that the species of erythrocytes have a significant impact on the titres obtained from haemagglutination (HA) and haemagglutination inhibition (HAI) assays. Chicken and turkey erythrocytes seem to be the most appropriate for both assays with seasonal influenza strains, in addition to pigeon erythrocytes, particularly for the B strains. In the case of the avian strain, chicken erythrocytes are suitable for HA assay and horse erythrocytes for HAI assay [221]. It was also found that the sensitivity of HAI assay against H5N1 avian virus was significantly improved by the use of the horse erythrocytes instead of the chicken erythrocytes as they exclusively showed α-2, 3 linkage of sialic acid molecules, which avian strains preferentially bind [222]. Therefore, the HAI assay against H5N1 strain needed repeating with the use of horse erythrocytes.

Furthermore, the antibody responses to influenza HA stalk domain needed analysing by other assays. HA-stalk reactive antibodies could be directly determined by ELISA when the plate coated with stable trimeric HA stalk or chimeric HA proteins [81], [82], [223], [224]. Moreover, the broadly neutralising activity of the antibodies can be measured by using influenza virus or pseudotyped virus expressing chimeric HA molecules [225]–[227].

On the other hand, the observation of positive HAI activity to pdmH1N1 in some individuals (Figure 5.8b) suggested that MVA-pdmH1N1 elicited HA head-reactive antibodies to pdmH1N1. Anti-HA head antibodies to pdmH1N1 in tonsillar MNCs were detectable upon MVA-pdmHN1 stimulation as previously reported [147]. As all subjects were recruited during 2015-2017 when pdmH1N1 predominantly circulated, their MNCs were most likely to contain the virus-specific memory B cells. Upon the recognition of the head domain of HA in the vaccine antigen expressed from MVA-pdmH1HA, HA head-specific antibodies could be elicited by activation of the pre-existing pdmH1N1-specific memory B cells in the MNCs.

In general, memory B cells are likely to be trained to react predominantly to the head rather than the stalk part of HA following exposure to the same or antigenically close influenza virus strains [228]. Although the infection or the vaccination by pdmH1N1 virus, having a distinct HA head region, efficiently enhanced anti-HA stalk antibodies in people during the outbreak, it was later shown that re-immunisation with inactivated pdmH1N1 vaccines resulted in

modest anti-HA stalk antibody production as the response preferentially targeted immunodominant globular head HA epitopes [228], [229]. Although the presence of the pdmH1N1 HA head domain as the vaccine antigen in MVA-pdmH1HA could lead to the activation of anti-HA head specific antibody responses, the broadly cross-reactive anti-HA stalk antibody response by the vaccine may result from the self-adjuvant effect as one of the advantages of the MVA vector, which allows the influx of various immune cells due to the lose of immunoevasive factors of MVA [63]–[66]. The adjuvant effect could broaden the antibody response by the more efficient recruitment of a broader repertoire of influenza-specific memory B cells [19]. The MVA-based vaccines thus may confer the cross-reactive antibody response by the activation of memory B cells specific to cross-reactive HA epitopes. It would be valuable in the future to study the impact of these pre-existing pdmH1N1 HA head-specific memory B cells in humans on the capacity of MVA-pdmH1HA to boost cross-reactive anti-HA stalk antibodies.

In conclusion, the study showed that MVA-pdmH1HA vaccine had the capacity to elicit cross-reactive HA-specific IgG antibodies to homologous virus (pdmH1N1) and to heterologous subtypes in phylogenetic HA group1 viruses (seasonal H1, H5 and H9) in human NALT *in vitro*, although the response to group 2 viruses (H3 and H7) was limited. The magnitude and breadth of cross-reactive antibodies elicited by the vaccine may be affected by age and history of exposure to influenza. This vaccine candidate may have the potential to be used as a mucosal vaccine to activate cross-reactive antibody response, providing broad protection against a range of influenza subtypes.

……

Chapter 6

General discussion and conclusion

6.1. Discussion

Influenza virus infection causes widespread morbidity and mortality in humans, despite the available vaccines. IIV provides narrow protection, mediated by serum HA-specific neutralising antibodies against circulating viruses that matched or are closely antigenically related to vaccine strains. The vaccine efficacy therefore markedly reduces in some seasons due to mismatching vaccine strains [26]. Despite lower serum IgG antibody induction, LAIV is considered to be superior to IIV as it elicits mucosal IgA and T cell responses, resulting in broader protection [25], [230]. However, for safety reasons, LAIV is only recommended for children at 2 years of age and over and adults less than 50 years old [231]. Besides the modest efficacy and limitation of current available vaccines, the H1N1 pandemic outbreak in 2009 and the potential of future pandemics of avian influenza (e.g. H5N1, H7N9 and H9N2) [232] also highlight the urgent need for more effective vaccines that confer broad immunity against multiple types of influenza viruses including those with the potential to cause pandemics.

Mucosal immunity is considered as the frontline defence against pathogenic infection and transmission at mucosal sites [100], [233], [234]. As influenza virus is a respiratory pathogen that infects humans through the nasopharyngeal mucosa, local vaccine delivery that activates cross-reactive mucosal immunity may offer an attractive vaccination strategy against influenza. The first licensed intranasal LAIV has been shown to induce local and systemic antibodies and T cell immunity in children [30], [168], [169], [235]. Intranasal immunisation relies on the local immune system such as nasopharynx-associated lymphoid tissue (NALT) to induce T and B cell immunity [236]. Adenoids and tonsils are major components of human NALT [173], [174], [171] and are known to be important inductive sites for mucosal immunity against respiratory pathogens including influenza [235], [236].

Viral vector-based vaccines have been widely studied recently as novel and promising vaccines against cancer and infectious diseases such as malaria, HIV, tuberculosis and influenza [50], [51], [54]. We hypothesised that some novel viral vector-based influenza vaccines expressing conserved influenza proteins have the capacity to induce mucosal

immune responses if administered by the intranasal route. So in this project, I investigated the potential of MVA- and PanAd3-vectored influenza vaccine candidates as intranasal vaccines to induce either T cell or B cell-mediated broad immunity against a range of influenza subtypes in human NALT.

6.1.1. Influenza transgene expression and protein localisation in NALT

The first critical step to successfully induce immune responses by vector-based vaccines is that the transgene inserted in the vector is efficiently expressed and presented by APCs [52].

In chapter 3, the vaccine antigen expression in adenotonsillar MNCs was studied following *in vitro* MVA- and PanAd3-vectored vaccine stimulation using the established method based on fluorochrome-conjugated monoclonal antibody-labeling and flow-cytometry. The expression of influenza NP and M1 from MVA-NP+M1 and that of influenza HA from MVA-pdmH1HA were detected in the adenotonsillar MNCs predominantly in B cells and DCs. The results suggest that MVA targets APCs which is in accordance to previous studies [141]–[143], [149] and the vaccine antigens could be efficiently expressed in NALT if administered intranasally. In contrast, the expression of influenza NP from PanAd3-NPM1 was not observed in the T and B cells of adenotonsillar MNCs, despite the fact that it was detected in the permissive HEK293 T cell line following vaccine stimulation. This indicates that the PanAd3 virus vectored vaccine may not be able to infect human NALT lymphocytes, similar to human adenovirus type 5, which is in the same species as previously reported [153]–[155]. Unless PanAd3-vectored vaccines infect DCs in the MNCs when used at the high dose, which remains to be answered, the vaccines may not have the capacity to induce significant immune responses in NALT. Subsequent studies are therefore focused on MVA-based vaccines; MVA-NP+M1 and MVA-pdmH1HA.

The expression of influenza proteins in MVA-infected B cells was observed as early as 6 hours and peaked at about 24 hours following vaccine stimulation, suggesting rapid kinetics of MVA infection and transgene expression, which is in agreement with previous studies [141]–[143]. MVA-based vaccines were also shown to have shorter time of antigen

presentation, which resulted in a rapid peak time of T cell response to the antigens [188], [237].

In addition to the expression of influenza proteins from the MVA-vectored vaccines, it was observed that influenza NP accumulated in the cell cytoplasm, whereas influenza HA migrated to cell membrane of MVA-infected tonsillar B cells, despite the fact that both proteins were initially synthesised in the cell cytosol. The different cellular localisation patterns of two influenza proteins was reported previously [150]. Without transgene modification, influenza NP and HA are most likely to be expressed in the native structure, and the localisation of both proteins may mimic that occurring during influenza virus infection, where HA continuously binds to sialic acid at the cell membrane, while NP binds to viral RNA in the nucleus before being imported to the cell cytoplasm for the virus assembly [1]. The results suggest each vaccine protein antigen may have different sites of localisation after expression from the vector. The findings would be useful for better vaccine design, which allows the antigen proteins to have longer retention in the cell cytoplasm or are highly degraded [151] to enhance the T cell immune responses. In addition, a well-designed antigen could increase the accumulation of antigens on cell membranes or could enable the secretion of the antigen from infected cells to be captured by APCs [152], inducing antibody production.

Having shown the efficient expression of the influenza vaccine antigens from either MVA-NP+M1 or MVA-pdmH1HA in human NALT immune cells, I further investigated the potential of both vaccines to induce mucosal cross-reactive T cell and B cell-mediated antibody immune responses towards influenza viruses, respectively.

6.1.2. Activation of cross-reactive CTL response by MVA-NP+M1

There is increasing evidence supporting the critical role of CTLs in protection against influenza virus infection, including in individuals who lack virus-specific antibodies [93]–[95]. Heterosubtypic T cell immunity is mainly generated by CTLs, which recognise conserved epitopes of NP, M1 and PB. The magnitude and functional quality of $CD8^+$ T cell responses are critical for the efficacy of T cell-based vaccines.

In chapter 4, I examined the CTL response, focusing on the M1 antigen-specific CTL response and the functional properties of the CTLs in adenotonsillar MNCs induced by MVA-NP+M1 *in vitro* stimulation. MVA-NP+M1 activated a marked increase of M1-specific $CD8^+$ T cells in human NALT, as shown by IFN-γ ELISPOT assay and a significant increase of $M1_{58-66}$-specific $CD8^+$ T cells, which recognise one of the most conserved M1 epitopes shared across influenza A viruses [44], [182], [183] as shown by $M1_{58-66}$ tetramer staining. These results on the significant response to M1 protein in particular suggest the vaccine would at least benefit approximately 50% of Caucasians [185] or 20-30% of all ethnicities [184], who have HLA-A2, which is restricted for $M1_{58-66}$ presentation.

In addition, the most frequently detected $M1_{58-66}$-specific CTLs were $CD107a^+$ IFN-γ^+ TNF-α^+, demonstrating their functionality with the release of cytotoxic molecules (perforin and granzymes) and the production of multiple potent pro-inflammatory cytokines, in response to recall antigen challenge. This functional profile of these CTLs seemed to reflect the phenotypes of short-lived effector and effector memory $CD8^+$ T cells [190], [191] and similar findings have been also reported [167], [189]. In addition to the effector functional properties, $M1_{58-66}$-specific CTLs were able to kill M1-peptide-pulsed target cells *in vitro*.

The $M1_{58-66}$-specific T cell response was shown in an age-dependent manner, where significant T cell responses were observed in children over 4 years olds and in adults. The results support the hypothesis that MVA-NP+M1 has the capacity to boost M1-specific mucosal $CD8^+$ T cell response in addition to systemic T cell responses in adults [165], [167] and elderly [164]. This is likely via activating the memory $CD8^+$ T cells primed by previous natural exposure to influenza viruses or vaccination. The activation of memory T cells by MVA-vectored vaccines has been shown in other studies [164], [188]. The results also suggests that a single dose vaccination of MVA-NP+M1 would benefit those whose immune cells are already primed for influenza including older children, adults and elderly. Young children may need a heterologous prime-boost regime to enhance the response.

6.1.3. Activation of broadly reactive antibody-mediated response by MVA-pdmH1HA

In addition to cytotoxic T cell immunity, the broadly protective response across influenza subtypes could be mediated by broadly neutralising antibodies [35], [136], which target the highly conserved stalk domain of HA [41], [200]. HA stalk-reactive antibodies therefore can recognise multiple influenza virus strains and could provide broad protection [195], [202].

In chapter 5, antibody responses in adenotonsillar MNCs to HA antigens following *in vitro* MVA-pdmH1HA stimulation were studied. It was shown that MVA-pdmH1HA elicited cross-reactive HA-specific IgG antibodies in human NALT recognising homologous (pdmH1N1) and heterologous influenza in HA group 1 (sH1N1, H5 and H9), but not those in HA group 2 (H3 and H7) as shown by ELISA assay. The magnitude of antibody response activated by MVA-pdmH1N1 was dominant towards the homologous pdmH1N1 strain, followed by that to other HA group 1 viruses which showed relatively lower response. The results extend our previous finding [147] and indicate that MVA-pdmH1HA elicits antibodies that cross-react to primarily HA group 1 viruses. Many isolated broadly neutralising monoclonal antibodies discovered so far showed cross-reactivity to HA group 1 viruses [79]. Moreover, the breadth of reactivity of antibodies tends to toward other influenza subtypes within the same HA phylogeny of vaccine antigen as previously reported in many studies [67], [203], [204], [213]–[216].

When the cross-reactive antibody responses were compared, both the magnitude and the breadth of the responses in adults were shown to be higher than in children. The age-dependent increase in the cross-reactive antibody response was also reported in other studies [85], [219]. These cross-reactive antibodies were most likely to be derived from the activation of HA stalk-specific memory B cells [41] generated from previous exposure to influenza through their lifetime [19]. The results support the hypothesis that the MVA-pdmH1HA vaccine activates cross-reactive memory B cells specific to conserved HA regions including the stalk, thus boosting the cross-reactive antibodies. It is possible that age and the exposure history to influenza may affect the cross-reactive antibody response in NALT immune cells by the MVA-pdmH1HA vaccine.

6.1.4. MVA-vectored influenza vaccines as mucosal vaccines

It has been generally considered that mucosal immunisation has the capacity to generate a superior local immune response, thus can efficiently prevent infection and control transmission of pathogens including influenza [25], [100]. To be effective, a mucosal vaccine needs to be immunogenic and capable of activating local mucosal immune tissue [234]. In this project, I have shown that MVA-NP+M1 and MVA-pdmH1HA candidate vaccines are capable of eliciting mucosal cross-reactive T cell and B cell antibody responses respectively in human NALT, using our *in vitro* cell culture system.

The results from this project also support the concept that MVA is a good virus vector for boosting memory responses in humans, as the MVA-vectored vaccines demonstrated the capacity to significantly enhance both T cell and B cell antibody responses in older children and adults who are most likely to be primed by previous exposure/ infection. MVA has been employed as a boosting vector following either homologous/heterologous vector or protein priming in many prime-boost studies against malaria and HIV, showing the synergistic effect on the magnitude of immune responses [238]–[240]. It has been shown previously that MVA-NP+M1 as a booster enhanced the frequency of antigen-specific $CD8^+$ T cells in bronchoalveolar lavage and lungs of hAd5-primed mice, and intranasal compared to other routes of administration showed the highest T cell responses [241].

In addition to immunogenicity, MVA has an excellent safety profile as it has been used for smallpox vaccination without problems in humans [242]. Moreover, it did not show any virulence in immunodeficient animals after virus injection [163]. MVA was also shown to be safe in mice following intranasal administration as MVA mainly targeted NALT, lungs and draining lymph nodes and no inflammatory reactions were detected in the central nervous system as well as the upper and lower airways [243]. The study in rhesus macaques has shown that aerosol delivery of MVA-vectored vaccines was safe and there was no vaccine-associated pathology, including in the brain and lungs [244].

Taken together, the results from this study support that intranasal administration of MVA-NP+M1 and MVA-pdmH1HA in humans can elicit mucosal immunity, involving the activation of T cell and B cell memory responses in human NALT.

6.2. Conclusion

In this project, I studied two MVA-vectored vaccines; MVA-NP+M1 and MVA-pdmH1HA in our *in vitro* human cell culture system modeling NALT. I firstly demonstrated that influenza vaccine antigens (NP, M1 and HA) were efficiently expressed in the NALT immune cells, predominantly in adenotonsillar B cells and DCs. Following *in vitro* vaccine stimulation, MVA-NP+M1 was shown to activate cross-reactive polyfunctional M1-specific CTLs, exhibiting specific target killing. MVA-pdmH1HA vaccine elicited HA-specific IgG antibodies that broadly reacted to influenza subtypes in phylogenetic HA group 1. The magnitude of both CTL and antibody responses were shown in an age-dependent manner, supporting the capacity of these MVA-vectored vaccines to elicit memory T and B cell responses. Our results suggest that both MVA-NP+M1 and MVA-pdmH1HA have the potential as intranasal mucosal vaccines to boost cross-reactive mucosal T and B cell-mediated immune responses against a range of influenza viruses. These data provide important supporting information for a potential new vaccination strategy using MVA-vectored universal influenza vaccines in intranasal vaccination against influenza in humans.

6.3. Future directions

6.3.1. Phenotypes of M1-specific CTLs

Having shown that MVA-NP+M1 induced a prominent and functional $M1_{58-66}$-specific T cell response in this project, it will be useful to further characterise these cells, in terms of their memory phenotypes, particularly on how they relate to tissue-resident memory T cells (T_{RM}). T_{RM} in human lungs have been suggested to mount a rapid response and kill influenza-infected epithelial cells and contribute to protection [245], [246]. Recent studies have shown that T_{RM} are also found in secondary lymphoid tissues, including tonsils [178], [247], [248].

6.3.2. Mechanisms of action of MVA-pdmH1HA-elicited antibodies

The functional properties of MVA-pdmH1HA-elicited antibodies were not investigated in this study. However, we have shown in the previous study that the antibodies had neutralising activity to heterologous H1N1 subtypes (A/Brisbane/59/2007 and A/South Carolina/1918) and to H5N1 (A/Vietnam/1203/2004) [147]. In addition to neutralisation, there is increasing evidence supporting that HA stalk-reactive antibodies could mediate *in vivo* protection via Fc-mediated cytotoxicity [87], [200], [249]. The interaction of Fc of antibody with Fc receptors on immune cells (e.g. NK cells) or complement could induce cell cytotoxicity or phagocytosis by macrophages [88], [90], [250], [251]. It was shown in mice that MVA-expressing modified HA of H5N1 induced neutralising antibodies, correlating with the protection against H5N1 viruses in different clades, while antibody-dependent cellular cytotoxicity (ADCC) [252] and cytotoxic T cell immunity [211] were associated with protection from heterologous virus strains such as pdmH1N1. Thus, it would be useful in future studies to determine other mechanisms of action in MVA-pdmH1HA-elicited antibodies that may correlate with protection.

6.3.3. Activation of HA-specific T follicular helper cells by MVA-pdmH1HA

In addition to antibody induction, it was shown that HA-expressing adenotonsillar B cells upregulated their HLA-DR, which indicates the antigen processing and presentation capacity via HLA class II. The antigen presented by HLA class II can activate $CD4^+$ T cells. We have shown that the induction of antigen-specific T_{FH} by LAIV in human NALT *in vitro* correlated with the antibody response [209]. Circulating influenza-specific T_{FH} were also shown to correlate with the antibody response in humans following immunisation with split seasonal influenza vaccine [210]. Since the upregulation of HLA-DR suggests the activation of $CD4^+$ T cells, it will be valuable to investigate the correlation between T_{FH} activation and antibody production following MVA-pdmH1HA stimulation.

……

References

[1] N. M. Bouvier and P. Palese, “The biology of influenza viruses,” *Vaccine*, vol. 26S, pp. D49–D53, Sep. 2008.

[2] Y. Shi, Y. Wu, W. Zhang, J. Qi, and G. F. Gao, “Enabling the ‘host jump’: Structural determinants of receptor-binding specificity in influenza A viruses,” *Nat. Rev. Microbiol.*, vol. 12, no. 12, pp. 822–831, 2014.

[3] K. Subbarao and T. Joseph, “Scientific barriers to developing vaccines against avian influenza viruses,” *Nat. Rev. Immunol.*, vol. 7, no. 4, pp. 267–278, 2007.

[4] World Health Organization, “Influenza Fact Sheet,” 2018. [Online]. Available: http://www.who.int/en/news-room/fact-sheets/detail/influenza-(seasonal). [Accessed: 27-Apr-2018].

[5] J. Y. Noh and W. J. Kim, “Influenza vaccines: Unmet needs and recent developments,” *Infect. Chemother.*, vol. 45, no. 4, pp. 375–386, 2013.

[6] S. Tong, X. Zhu, Y. Li, M. Shi, J. Zhang, M. Bourgeois, H. Yang, X. Chen, S. Recuenco, J. Gomez, L.-M. Chen, A. Johnson, Y. Tao, C. Dreyfus, W. Yu, R. McBride, P. J. Carney, A. T. Gilbert, J. Chang, Z. Guo, C. T. Davis, J. C. Paulson, J. Stevens, C. E. Rupprecht, E. C. Holmes, I. A. Wilson, and R. O. Donis, “New world bats harbor diverse influenza A viruses,” *PLoS Pathog.*, vol. 9, no. 10, p. e1003657, 2013.

[7] M. L. Shaw and P. Palese, “Orthomyxoviridae,” 2007. [Online]. Available: https://basicmedicalkey.com/orthomyxoviridae/. [Accessed: 28-Jun-2018].

[8] U. Joseph, Y. C. F. Su, D. Vijaykrishna, and G. J. D. Smith, “The ecology and adaptive evolution of influenza A interspecies transmission,” *Influenza Other Respi. Viruses*, vol. 11, no. 1, pp. 74–84, Jan. 2017.

[9] G. W. Carnell, F. Ferrara, K. Grehan, C. P. Thompson, and N. J. Temperton, “Pseudotype-based neutralization assays for influenza: A systematic analysis,” *Front. Immunol.*, vol. 6, no. MAR, 2015.

[10] M. de Graaf and R. A. M. Fouchier, “Role of receptor binding specificity in influenza A virus transmission and pathogenesis.,” *EMBO J.*, vol. 33, no. 8, pp. 823–41, Apr. 2014.

[11] G. Neumann, T. Noda, and Y. Kawaoka, “Emergence and pandemic potential of swine-origin H1N1 influenza virus,” *Nature*, vol. 459, no. 7249, pp. 931–939, 2009.

[12] A. S. Monto, “Epidemiology of influenza,” *Vaccine*, vol. 26S, pp. D45–D48, Sep. 2008.

[13] Centers for Disease Control and Prevention, “Past Pandemics,” 2018. [Online]. Available: https://www.cdc.gov/flu/pandemic-resources/basics/past-pandemics.html. [Accessed: 28-Apr-2018].

[14] E. Crisci, T. Mussá, L. Fraile, and M. Montoya, “Review: Influenza virus in pigs,” *Mol. Immunol.*, vol. 55, no. 3–4, pp. 200–211, 2013.

[15] J. H. C. M. Kreijtz, R. A. M. Fouchier, and G. F. Rimmelzwaan, “Immune responses to influenza virus infection,” *Virus Research*, vol. 162, no. 1–2. pp. 19–30, 2011.

[16] A. Iwasaki and P. S. Pillai, “Innate immunity to influenza virus infection.,” *Nat. Rev. Immunol.*, vol. 14, no. 5, pp. 315–28, 2014.

[17] B. Pulendran and M. S. Maddur, “Innate immune sensing and response to influenza,” *Curr. Top. Microbiol. Immunol.*, vol. 386, pp. 23–71, 2015.

[18] G. F. Rimmelzwaan and J. E. McElhaney, “Correlates of protection: Novel generations of influenza vaccines,” *Vaccine*, vol. 26S, pp. D41–D44, Sep. 2008.

[19] A. H. Ellebedy and R. Ahmed, “Re-engaging cross-reactive memory B cells: The influenza puzzle,” *Front. Immunol.*, vol. 3, p. 53, 2012.

[20] N. Pica, R. Hai, F. Krammer, T. T. Wang, J. Maamary, D. Eggink, G. S. Tan, J. C. Krause, T. Moran, C. R. Stein, D. Banach, J. Wrammert, R. B. Belshe, A. Garcia-Sastre, and P. Palese, “Hemagglutinin stalk antibodies elicited by the 2009 pandemic influenza virus as a mechanism for the extinction of seasonal H1N1 viruses,” *Proc. Natl. Acad. Sci.*, vol. 109, no. 7, pp. 2573–2578, 2012.

[21] J. Wrammert, D. Koutsonanos, G.-M. Li, S. Edupuganti, J. Sui, M. Morrissey, M. McCausland, I. Skountzou, M. Hornig, W. I. Lipkin, A. Mehta, B. Razavi, C. Del Rio, N.-Y. Zheng, J.-H. Lee, M. Huang, Z. Ali, K. Kaur, S. Andrews, R. R. Amara, Y. Wang, S. R. Das, C. D. O’Donnell, J. W. Yewdell, K. Subbarao, W. A. Marasco, M. J. Mulligan, R. Compans, R. Ahmed, and P. C. Wilson, “Broadly cross-reactive antibodies dominate the human B cell response against 2009 pandemic H1N1 influenza virus infection,” *J. Exp. Med.*, vol. 208, no. 1, pp. 181–193, 2011.

[22] S.-S. Wong and R. J. Webby, “Traditional and new influenza vaccines,” *Clin. Microbiol. Rev.*, vol. 26, no. 3, pp. 476–492, Jul. 2013.

[23] World Health Organization, “Influenza vaccine viruses and reagents,” 2018. [Online]. Available: http://www.who.int/influenza/vaccines/virus/en/. [Accessed: 27-Apr-2018].

[24] Centers for Disease Control and Prevention, “People at High Risk of Developing Flu–Related Complications,” 2018. [Online]. Available: https://www.cdc.gov/flu/about/disease/high_risk.htm. [Accessed: 27-Apr-2018].

[25] R. J. Cox, K. A. Brokstad, and P. Ogra, “Influenza virus: Immunity and vaccination strategies. Comparison of the immune response to inactivated and live attenuated influenza vaccines,” *Scand. J. Immunol.*, vol. 59, no. 1, pp. 1–15, 2004.

[26] M. T. Osterholm, N. S. Kelley, A. Sommer, and E. A. Belongia, “Efficacy and effectiveness of influenza vaccines: A systematic review and meta-analysis,” *Lancet. Infect. Dis.*, vol. 12, no. 1, pp. 36–44, Jan. 2012.

[27] S. Sridhar, K. Brokstad, and R. Cox, “Influenza vaccination strategies: Comparing inactivated and live attenuated influenza vaccines,” *Vaccines*, vol. 3, no. 2, pp. 373–389, Apr. 2015.

[28] Seqirus Inc., “Package insert FLUAD®,” 2017. [Online]. Available: https://www.fda.gov/downloads/biologicsbloodvaccines/safetyavailability/vaccinesafety/ucm474387.pdf. [Accessed: 27-Apr-2018].

[29] H. F. Maassab and M. L. Bryant, “The development of live attenuated cold-adapted influenza virus vaccine for humans,” *Rev. Med. Virol.*, vol. 9, no. 4, pp. 237–244, 1999.

[30] X.-S. He, T. H. Holmes, C. Zhang, K. Mahmood, G. W. Kemble, D. B. Lewis, C. L. Dekker, H. B. Greenberg, and A. M. Arvin, “Cellular immune responses in children and adults receiving inactivated or live attenuated influenza vaccines.,” *J. Virol.*, vol. 80, no. 23, pp. 11756–11766, 2006.

[31] C. Mameli, E. D’auria, P. Erba, P. Nannini, and G. V. Zuccotti, “Influenza vaccine response: Future perspectives,” *Expert Opin. Biol. Ther.*, vol. 18, no. 1, pp. 1–5, Jan. 2018.

[32] J. E. McElhaney, “Influenza vaccine responses in older adults,” *Ageing Res. Rev.*, vol. 10, no. 3, pp. 379–388, Jul. 2011.

[33] L. A. Reperant, F. M. Moesker, and A. D. M. E. Osterhaus, “Influenza: from zoonosis to pandemic,” *ERJ open Res.*, vol. 2, no. 1, p. 13, Jan. 2016.

[34] E. J. Erbelding, D. J. Post, E. J. Stemmy, P. C. Roberts, A. D. Augustine, S. Ferguson, C. I. Paules, B. S. Graham, and A. S. Fauci, “A universal influenza

vaccine: The strategic plan for the national institute of allergy and infectious diseases," *J. Infect. Dis.*, vol. 218, no. 3, pp. 347–354, 2018.

[35] S. C. Gilbert, "Advances in the development of universal influenza vaccines," *Influenza Other Respi. Viruses*, vol. 7, no. 5, pp. 750–758, Sep. 2013.

[36] V. A. Slepushkin, J. M. Katz, R. A. Black, W. C. Gamble, P. A. Rota, and N. J. Cox, "Protection of mice against influenza A virus challenge by vaccination with baculovirus-expressed M2 protein," *Vaccine*, vol. 13, no. 15, pp. 1399–1402, 1995.

[37] J. Fan, X. Liang, M. S. Horton, H. C. Perry, M. P. Citron, G. J. Heidecker, T. M. Fu, J. Joyce, C. T. Przysiecki, P. M. Keller, V. M. Garsky, R. Ionescu, Y. Rippeon, L. Shi, M. A. Chastain, J. H. Condra, M. E. Davies, J. Liao, E. A. Emini, and J. W. Shiver, "Preclinical study of influenza virus a M2 peptide conjugate vaccines in mice, ferrets, and rhesus monkeys," *Vaccine*, vol. 22, no. 23–24, pp. 2993–3003, 2004.

[38] C. B. Turley, R. E. Rupp, C. Johnson, D. N. Taylor, J. Wolfson, L. Tussey, U. Kavita, L. Stanberry, and A. Shaw, "Safety and immunogenicity of a recombinant M2e-flagellin influenza vaccine (STF2.4xM2e) in healthy adults," *Vaccine*, vol. 29, no. 32, pp. 5145–5152, 2011.

[39] J. R. Whittle, R. Zhang, S. Khurana, L. R. King, J. Manischewitz, H. Golding, P. R. Dormitzer, B. F. Haynes, E. B. Walter, M. A. Moody, T. B. Kepler, H. X. Liao, and S. C. Harrison, "Broadly neutralizing human antibody that recognizes the receptor-binding pocket of influenza virus hemagglutinin," *Proc Natl Acad Sci U S A*, vol. 108, no. 34, pp. 14216–14221, 2011.

[40] M. Hong, P. S. Lee, R. M. B. Hoffman, X. Zhu, J. C. Krause, N. S. Laursen, S.-I. Yoon, L. Song, L. Tussey, J. E. Crowe, A. B. Ward, and I. A. Wilson, "Antibody recognition of the pandemic H1N1 Influenza virus hemagglutinin receptor binding site.," *J. Virol.*, vol. 87, no. 22, pp. 12471–12480, 2013.

[41] K. E. Neu, C. J. Henry Dunand, and P. C. Wilson, "Heads, stalks and everything else: how can antibodies eradicate influenza as a human disease?," *Curr. Opin. Immunol.*, vol. 42, pp. 48–55, 2016.

[42] F. Krammer, "Novel universal influenza virus vaccine approaches," *Curr. Opin. Virol.*, vol. 17, pp. 95–103, 2016.

[43] Z. Staneková and E. Varečková, "Conserved epitopes of influenza A virus inducing protective immunity and their prospects for universal vaccine development.," *Virol. J.*, vol. 7, no. 1, p. 351, Jan. 2010.

[44] H.-H. Bui, B. Peters, E. Assarsson, I. Mbawuike, and A. Sette, “Ab and T cell epitopes of influenza A virus, knowledge and opportunities.,” *Proc. Natl. Acad. Sci. U. S. A.*, vol. 104, no. 1, pp. 246–251, Jan. 2007.

[45] G. F. Rimmelzwaan, J. H. C. M. Kreijtz, R. Bodewes, R. A. M. Fouchier, and A. D. M. E. Osterhaus, “Influenza virus CTL epitopes, remarkably conserved and remarkably variable.,” *Vaccine*, vol. 27, no. 45, pp. 6363–6365, Oct. 2009.

[46] E. J. Grant, S. M. Quiñones-Parra, E. B. Clemens, and K. Kedzierska, “Human influenza viruses and CD8 + T cell responses,” *Curr. Opin. Virol.*, vol. 16, pp. 132–142, 2016.

[47] A. Sette, M. Newman, B. Livingston, D. McKinney, J. Sidney, G. Ishioka, S. Tangri, J. Alexander, J. Fikes, and R. Chestnut, “Optimizing vaccine design for cellular processing, MHC binding and TCR recognition,” *Tissue Antigens*, vol. 59, no. 6, pp. 443–451, 2002.

[48] A. Kumar, T. S. Meldgaard, and S. Bertholet, “Novel platforms for the development of a universal influenza vaccine,” *Front. Immunol.*, vol. 9, p. 600, 2018.

[49] F. Berlanda Scorza, V. Tsvetnitsky, and J. J. Donnelly, “Universal influenza vaccines: Shifting to better vaccines,” *Vaccine*, vol. 34, no. 26, pp. 2926–2933, 2016.

[50] S. J. Draper and J. L. Heeney, “Viruses as vaccine vectors for infectious diseases and cancer,” *Nat. Rev. Microbiol.*, vol. 8, no. 1, pp. 62–73, Jan. 2010.

[51] T. Ura, K. Okuda, and M. Shimada, “Developments in viral vector-based vaccines,” *Vaccines*, vol. 2, no. 3, pp. 624–641, Jul. 2014.

[52] M. A. Liu, “Immunologic basis of vaccine vectors,” *Immunity*, vol. 33, no. 4, pp. 504–515, 2010.

[53] A. F. Altenburg, J. H. C. M. Kreijtz, R. D. de Vries, F. Song, R. Fux, G. F. Rimmelzwaan, G. Sutter, and A. Volz, “Modified Vaccinia virus Ankara (MVA) as production platform for vaccines against influenza and other viral respiratory diseases,” *Viruses*, vol. 6, no. 7, pp. 2735–2761, Jul. 2014.

[54] R. D. de Vries and G. F. Rimmelzwaan, “Viral vector-based influenza vaccines,” *Hum. Vaccines Immunother.*, vol. 12, no. 11, pp. 2881–2901, 2016.

[55] L. H. McCurdy, B. D. Larkin, J. E. Martin, and B. S. Graham, “Modified Vaccinia Ankara: Potential as an alternative smallpox vaccine,” *Clin. Infect. Dis.*, vol. 38, no. 12, pp. 1749–1753, 2004.

[56] H. Meyer, G. Sutter, and A. Mayr, “Mapping of deletions in the genome of the highly attenuated vaccinia virus MVA and their influence on virulence,” *J. Gen. Virol.*, vol. 72, no. 5, pp. 1031–1038, 1991.

[57] M. W. Carroll and B. Moss, “Host range and cytopathogenicity of the highly attenuated MVA strain of vaccinia virus: Propagation and generation of recombinant viruses in a nonhuman mammalian cell line,” *Virology*, vol. 238, no. 2, pp. 198–211, 1997.

[58] I. Drexler, K. Heller, B. Wahren, V. Erfle, and G. Sutter, “Highly attenuated modified vaccinia virus Ankara replicates in baby hamster kidney cells, a potential host for virus propagation, but not in various human transformed and primary cells,” *J. Gen. Virol.*, vol. 79, no. 2, pp. 347–352, 1998.

[59] T. J. Blanchard, A. Alcamí, P. Andrea, and G. L. Smith, “Modified vaccinia virus Ankara undergoes limited replication in human cells and lacks several immunomodulatory proteins: Implications for use as a human vaccine,” *J. Gen. Virol.*, vol. 79, no. 5, pp. 1159–1167, 1998.

[60] G. Sutter and B. Moss, “Nonreplicating vaccinia vector efficiently expresses recombinant genes.,” *Proc. Natl. Acad. Sci.*, vol. 89, no. 22, pp. 10847–10851, 1992.

[61] S. J. Draper, A. C. Moore, A. L. Goodman, C. A. Long, A. A. Holder, S. C. Gilbert, F. Hill, and A. V. S. Hill, “Effective induction of high-titer antibodies by viral vector vaccines,” *Nat. Med.*, vol. 14, no. 8, pp. 819–821, 2008.

[62] S. C. Gilbert, “T-cell-inducing vaccines - what’s the future,” *Immunology*, vol. 135, no. 1, pp. 19–26, 2012.

[63] J. Delaloye, T. Roger, Q. G. Steiner-Tardivel, D. Le Roy, M. K. Reymond, S. Akira, V. Petrilli, C. E. Gomez, B. Perdiguero, J. Tschopp, G. Pantaleo, M. Esteban, and T. Calandra, “Innate immune sensing of modified vaccinia virus Ankara (MVA) is mediated by TLR2-TLR6, MDA-5 and the NALP3 inflammasome,” *PLoS Pathog.*, vol. 5, no. 6, p. e1000480, 2009.

[64] R. Förster, G. Wolf, and A. Mayr, “Highly attenuated poxviruses induce functional priming of neutrophils in vitro,” *Arch. Virol.*, vol. 136, no. 1–2, pp. 219–226, 1994.

[65] Z. Waibler, M. Anzaghe, H. Ludwig, S. Akira, S. Weiss, G. Sutter, and U. Kalinke, “Modified Vaccinia virus Ankara induces Toll-like receptor-independent type I interferon responses,” *J. Virol.*, vol. 81, no. 22, pp. 12102–12110, 2007.

[66] M. H. Lehmann, W. Kastenmuller, J. D. Kandemir, F. Brandt, Y. Suezer, and G. Sutter, “Modified vaccinia virus ankara triggers chemotaxis of monocytes and early respiratory immigration of leukocytes by induction of CCL2 expression,” *J. Virol.*, vol. 83, no. 6, pp. 2540–52, 2009.

[67] J. H. C. M. Kreijtz, M. Goeijenbier, F. M. Moesker, L. van den Dries, S. Goeijenbier, H. L. M. De Gruyter, M. H. Lehmann, G. D. de Mutsert, D. A. M. C. van de Vijver, A. Volz, R. A. M. Fouchier, E. C. M. van Gorp, G. F. Rimmelzwaan, G. Sutter, and A. D. M. E. Osterhaus, “Safety and immunogenicity of a modified-vaccinia-virus-Ankara-based influenza A H5N1 vaccine: A randomised, double-blind phase 1/2a clinical trial,” *Lancet Infect. Dis.*, vol. 14, no. 12, pp. 1196–1207, 2014.

[68] N. Tatsis and H. C. J. Ertl, “Adenoviruses as vaccine vectors,” *Mol. Ther.*, vol. 10, no. 4, pp. 616–629, Oct. 2004.

[69] S. Colloca, E. Barnes, A. Folgori, V. Ammendola, S. Capone, A. Cirillo, L. Siani, M. Naddeo, F. Grazioli, M. L. Esposito, M. Ambrosio, A. Sparacino, M. Bartiromo, A. Meola, K. Smith, A. Kurioka, G. A. O’Hara, K. J. Ewer, N. Anagnostou, C. Bliss, A. V. S. Hill, C. Traboni, P. Klenerman, R. Cortese, and A. Nicosia, “Vaccine vectors derived from a large collection of simian adenoviruses induce potent cellular immunity across multiple species,” *Sci. Transl. Med.*, vol. 4, no. 115, p. 115ra2, Jan. 2012.

[70] M. O. Lasaro and H. C. J. Ertl, “New insights on adenovirus as vaccine vectors,” *Mol. Ther.*, vol. 17, no. 8, pp. 1333–1339, Aug. 2009.

[71] R. A. Tripp and S. M. Tompkins, “Virus-vectored influenza virus vaccines,” *Viruses*, vol. 6, no. 8, pp. 3055–79, Aug. 2014.

[72] S. Sebastian and T. Lambe, “Clinical advances in viral-vectored influenza vaccines,” *Vaccines*, vol. 6, no. 2, 2018.

[73] S. Pavlova, F. D’Alessio, S. Houard, E. J. Remarque, N. Stockhofe, and O. G. Engelhardt, “Workshop report: Immunoassay standardisation for ‘universal’ influenza vaccines,” *Influenza Other Respi. Viruses*, vol. 11, no. 3, pp. 194–201, 2017.

[74] C. Trombetta, D. Perini, S. Mather, N. Temperton, and E. Montomoli, “Overview of serological techniques for influenza vaccine evaluation: Past, present and future,” *Vaccines*, vol. 2, no. 4, pp. 707–734, 2014.

[75] J. C. de Jong, A. M. Palache, W. E. P. Beyer, G. F. Rimmelzwaan, A. C. M. Boon, and A. D. M. E. Osterhaus, “Haemagglutination-inhibiting antibody to influenza virus,” *Dev. Biol. (Basel).*, vol. 115, pp. 63–73, 2003.

[76] D. Hobson, R. L. Curry, A. S. Beare, and A. Ward-Gardner, “The role of serum haemagglutination-inhibiting antibody in protection against challenge infection with influenza A2 and B viruses,” *J. Hyg. (Lond).*, vol. 70, no. 4, pp. 767–777, 1972.

[77] S. Black, U. Nicolay, T. Vesikari, M. Knuf, G. Del Giudice, G. Della Cioppa, T. Tsai, R. Clemens, and R. Rappuoli, “Hemagglutination Inhibition Antibody Titers as a Correlate of Protection for Inactivated Influenza Vaccines in Children,” *Pediatr. Infect. Dis. J.*, vol. 30, no. 12, pp. 1081–1085, 2011.

[78] S. M. Russell, D. McCahon, and A. S. Beare, “A single radial haemolysis technique for the measurement of influenza antibody,” *J. Gen. Virol.*, vol. 27, no. 1, pp. 1–10, 1975.

[79] S. Quiñones-Parra, L. Loh, L. E. Brown, K. Kedzierska, and S. A. Valkenburg, “Universal immunity to influenza must outwit immune evasion,” *Front. Microbiol.*, vol. 5, p. 285, 2014.

[80] R. Nachbagauer, M. S. Miller, R. Hai, A. B. Ryder, J. K. Rose, P. Palese, A. García-Sastre, F. Krammer, and R. A. Albrecht, “Hemagglutinin stalk immunity reduces influenza virus replication and transmission in ferrets,” *J. Virol.*, vol. 90, no. 6, pp. 3268–3273, 2016.

[81] H. Jacobsen, M. Rajendran, A. Choi, H. Sjursen, K. A. Brokstad, R. J. Cox, P. Palese, F. Krammer, and R. Nachbagauer, “Influenza virus hemagglutinin stalk-specific antibodies in human serum are a surrogate marker for in vivo protection in a serum transfer mouse challenge model,” *MBio*, vol. 8, no. 5, pp. e01463-17, 2017.

[82] J. K. Park, A. Han, L. Czajkowski, S. Reed, R. Athota, T. Bristol, L. A. Rosas, A. Cervantes-Medina, J. K. Taubenberger, and M. J. Memoli, “Evaluation of preexisting anti-hemagglutinin stalk antibody as a correlate of protection in a healthy volunteer challenge with influenza A/H1N1pdm virus,” *MBio*, vol. 9, no. 1, pp. e02284-17, 2018.

[83] C. Chiu, J. Wrammert, G.-M. Li, M. McCausland, P. C. Wilson, and R. Ahmed, “Cross-reactive humoral responses to influenza and their implications for a universal vaccine,” *Ann. N. Y. Acad. Sci.*, vol. 1283, no. 1, pp. 13–21, Apr. 2013.

[84] W. H. Mahallawi, A. V Kasbekar, M. S. McCormick, K. Hoschler, N. Temperton, S. C. Leong, H. Beer, F. Ferrara, P. S. McNamara, and Q. Zhang, “Infection with 2009 H1N1 influenza virus primes for immunological memory in human nose-associated lymphoid tissue, offering cross-reactive immunity to H1N1 and avian H5N1 viruses,” *J. Virol.*, vol. 87, no. 10, pp. 5331–5339, 2013.

[85] M. S. Ahmed, L. C. Jacques, W. Mahallawi, F. Ferrara, N. Temperton, N. Upile, C. Vaughan, R. Sharma, H. Beer, K. Hoschler, P. S. McNamara, and Q. Zhang, “Cross-reactive immunity against influenza viruses in children and adults following 2009 pandemic H1N1 infection,” *Antiviral Res.*, vol. 114, pp. 106–112, 2015.

[86] W. He, C. E. Mullarkey, J. A. Duty, T. M. Moran, P. Palese, and M. S. Miller, “Broadly neutralizing anti-influenza virus antibodies: Enhancement of neutralizing potency in polyclonal mixtures and IgA backbones,” *J. Virol.*, vol. 89, no. 7, pp. 3610–3618, 2015.

[87] F. Krammer and P. Palese, “Advances in the development of influenza virus vaccines,” *Nat. Rev. Drug Discov.*, vol. 14, no. 3, pp. 167–182, 2015.

[88] S. Jegaskanda, J. T. Weinfurter, T. C. Friedrich, and S. J. Kent, “Antibody-dependent cellular cytotoxicity is associated with control of pandemic H1N1 influenza virus infection of macaques,” *J. Virol.*, vol. 87, no. 10, pp. 5512–5522, 2013.

[89] G. S. Tan, P. E. Leon, R. A. Albrecht, I. Margine, A. Hirsh, J. Bahl, and F. Krammer, “Broadly-reactive neutralizing and non-neutralizing antibodies directed against the H7 influenza virus hemagglutinin reveal divergent mechanisms of protection,” *PLoS Pathog.*, vol. 12, no. 4, p. e1005578, 2016.

[90] D. J. DiLillo, P. Palese, P. C. Wilson, and J. V. Ravetch, “Broadly neutralizing anti-influenza antibodies require Fc receptor engagement for in vivo protection,” *J. Clin. Invest.*, vol. 126, no. 2, pp. 605–610, 2016.

[91] G. F. Rimmelzwaan, R. A. Fouchier, and A. D. Osterhaus, “Influenza virus-specific cytotoxic T lymphocytes: a correlate of protection and a basis for vaccine development,” *Curr. Opin. Biotechnol.*, vol. 18, no. 6, pp. 529–536, 2007.

[92] A. C. L. Tan, G. Deliyannis, M. Bharadwaj, L. E. Brown, W. Zeng, and D. C. Jackson, “The design and proof of concept for a CD8+ T cell-based vaccine inducing cross-subtype protection against influenza A virus,” *Immunol. Cell Biol.*, vol. 91, no. 1, pp. 96–104, Jan. 2013.

[93] A. J. McMichael, F. M. Gotch, G. R. Noble, and P. A. Beare, “Cytotoxic T-cell immunity to influenza,” *N. Engl. J. Med.*, vol. 309, no. 1, pp. 13–17, 1983.

[94] S. Sridhar, S. Begom, A. Bermingham, K. Hoschler, W. Adamson, W. Carman, T. Bean, W. Barclay, J. J. Deeks, and A. Lalvani, “Cellular immune correlates of protection against symptomatic pandemic influenza,” *Nat. Med.*, vol. 19, no. 10, pp. 1305–1312, 2013.

[95] Z. Wang, Y. Wan, C. Qiu, S. Quiñones-Parra, Z. Zhu, L. Loh, D. Tian, Y. Ren, Y. Hu, X. Zhang, P. G. Thomas, M. Inouye, P. C. Doherty, K. Kedzierska, and J. Xu, "Recovery from severe H7N9 disease is associated with diverse response mechanisms dominated by CD8+ T cells," *Nat. Commun.*, vol. 6, p. 6833, 2015.

[96] S. P. Cullen and S. J. Martin, "Mechanisms of granule-dependent killing," *Cell Death Differ.*, vol. 15, no. 2, pp. 251–262, 2008.

[97] D. J. Topham, R. a Tripp, and P. C. Doherty, "CD8+ T cells clear influenza virus by perforin or Fas-dependent processes," *J. Immunol.*, vol. 159, no. 11, pp. 5197–5200, 1997.

[98] E. L. Brincks, A. Katewa, T. A. Kucaba, T. S. Griffith, and K. L. Legge, "CD8 T cells utilize TRAIL to control influenza virus infection," *J. Immunol.*, vol. 181, no. 7, pp. 4918–4925, 2008.

[99] S. Duan and P. G. Thomas, "Balancing immune protection and immune pathology by CD8+ T-cell responses to influenza infection," *Front. Immunol.*, vol. 7, p. 25, Feb. 2016.

[100] M. R. Neutra and P. A. Kozlowski, "Mucosal vaccines: The promise and the challenge," *Nat. Rev. Immunol.*, vol. 6, no. 2, pp. 148–158, 2006.

[101] S. Tamura and T. Kurata, "Defense mechanisms against influenza virus infection in the respiratory tract mucosa," *Jpn. J. Infect. Dis.*, vol. 57, pp. 236–247, 2004.

[102] P. Brandtzaeg, "Mucosal immunity: Induction, dissemination, and effector functions," *Scand. J. Immunol.*, vol. 70, no. 6, pp. 505–515, 2009.

[103] M. E. Lamm, "Interation of antigens and antibodies at mucosal surfaces," *Annu. Rev. Microbiol.*, vol. 51, no. 1, pp. 311–340, Oct. 1997.

[104] R. Ito, Y. A. Ozaki, T. Yoshikawa, H. Hasegawa, Y. Sato, Y. Suzuki, R. Inoue, T. Morishima, N. Kondo, T. Sata, T. Kurata, and S. I. Tamura, "Roles of anti-hemagglutinin IgA and IgG antibodies in different sites of the respiratory tract of vaccinated mice in preventing lethal influenza pneumonia," *Vaccine*, vol. 21, no. 19–20, pp. 2362–2371, 2003.

[105] M. Yoshida, S. M. Claypool, J. S. Wagner, E. Mizoguchi, A. Mizoguchi, D. C. Roopenian, W. I. Lencer, and R. S. Blumberg, "Human neonatal Fc receptor mediates transport of IgG into luminal secretions for delivery of antigens to mucosal dendritic cells," *Immunity*, vol. 20, no. 6, pp. 769–783, 2004.

[106] J. A. Wiley, R. J. Hogan, D. L. Woodland, and A. G. Harmsen, “Antigen-specific CD8(+) T cells persist in the upper respiratory tract following influenza virus infection,” *J. Immunol.*, vol. 167, no. 6, pp. 3293–3299, 2001.

[107] W. Cao, J. H. Kim, A. J. Reber, M. Hoelscher, J. A. Belser, X. Lu, J. M. Katz, S. Gangappa, M. Plante, D. S. Burt, and S. Sambhara, “Nasal delivery of Protollin-adjuvanted H5N1 vaccine induces enhanced systemic as well as mucosal immunity in mice,” *Vaccine*, vol. 35, no. 25, pp. 3318–3325, 2017.

[108] L. Song, D. Xiong, H. Song, L. Wu, M. Zhang, X. Kang, Z. Pan, and X. Jiao, “Mucosal and systemic immune responses to influenza H7N9 antigen HA1-2 co-delivered intranasally with flagellin or polyethyleneimine in mice and chickens,” *Front. Immunol.*, vol. 8, p. 326, 2017.

[109] A. Ainai, T. Suzuki, S. Tamura, and H. Hasegawa, “Intranasal administration of whole inactivated influenza virus vaccine as a promising influenza vaccine candidate,” *Viral Immunol.*, vol. 30, no. 6, pp. 451–462, 2017.

[110] E. Greenbaum, D. Engelhard, R. Levy, M. Schlezinger, A. Morag, and Z. Zakay-Rones, “Mucosal (SIgA) and serum (IgG) immunologic responses in young adults following intranasal administration of one or two doses of inactivated, trivalent anti-influenza vaccine,” *Vaccine*, vol. 22, no. 20, pp. 2566–2577, 2004.

[111] T. G. Boyce, H. H. Hsu, E. C. Sannella, S. D. Coleman-Dockery, E. Baylis, Y. Zhu, G. Barchfeld, A. DiFrancesco, M. Paranandi, B. Culley, K. M. Neuzil, and P. F. Wright, “Safety and immunogenicity of adjuvanted and unadjuvanted subunit influenza vaccines administered intranasally to healthy adults,” *Vaccine*, vol. 19, no. 2–3, pp. 217–226, Sep. 2000.

[112] J. Treanor, C. Nolan, D. O’Brien, D. Burt, G. Lowell, J. Linden, and L. Fries, “Intranasal administration of a proteosome-influenza vaccine is well-tolerated and induces serum and nasal secretion influenza antibodies in healthy human subjects,” *Vaccine*, vol. 24, no. 3, pp. 254–262, 2006.

[113] C. Wang, W. Zhu, Y. Luo, and B.-Z. Wang, “Gold nanoparticles conjugating recombinant influenza hemagglutinin trimers and flagellin enhanced mucosal cellular immunity,” *Nanomedicine*, vol. 14, no. 4, pp. 1349–1360, Apr. 2018.

[114] M. Qi, X. E. Zhang, X. Sun, X. Zhang, Y. Yao, S. Liu, Z. Chen, W. Li, Z. Zhang, J. Chen, and Z. Cui, “Intranasal nanovaccine confers homo- and hetero-subtypic influenza protection,” *Small*, vol. 14, no. 13, p. e1703207, 2018.

[115] Y.-T. Lee, E.-J. Ko, Y. Lee, K.-H. Kim, M.-C. Kim, Y.-N. Lee, and S.-M. Kang, “Intranasal vaccination with M2e5x virus-like particles induces humoral and cellular immune responses conferring cross-protection against heterosubtypic influenza viruses,” *PLoS One*, vol. 13, no. 1, p. e0190868, Jan. 2018.

[116] T. Ebensen, J. Debarry, G. K. Pedersen, P. Blazejewska, S. Weissmann, K. Schulze, K. C. McCullough, R. J. Cox, and C. A. Guzmán, “Mucosal administration of cycle-di-nucleotide-adjuvanted virosomes efficiently induces protection against influenza H5N1 in mice,” *Front. Immunol.*, vol. 8, p. 1223, 2017.

[117] D. Lapuente, Z. Ruzsics, C. Thirion, and M. Tenbusch, “Evaluation of adenovirus 19a as a novel vector for mucosal vaccination against influenza A viruses,” *Vaccine*, vol. 36, no. 19, pp. 2712–2720, May 2018.

[118] M. Perry and A. Whyte, “Immunology of the tonsils,” *Immunol. Today*, vol. 19, no. 9, pp. 414–421, 1998.

[119] H. Nave, A. Gebert, and R. Pabst, “Morphology and immunology of the human palatine tonsil,” *Anat. Embryol. (Berl).*, vol. 204, no. 5, pp. 367–373, Nov. 2001.

[120] P. N. Boyaka, P. F. Wright, M. Marinaro, H. Kiyono, J. E. Johnson, R. A. Gonzales, M. R. Ikizler, J. A. Werkhaven, R. J. Jackson, K. Fujihashi, S. Di Fabio, H. F. Staats, and J. R. McGhee, “Human nasopharyngeal-associated lymphoreticular tissues. Functional analysis of subepithelial and intraepithelial B and T cells from adenoids and tonsils,” *Am. J. Pathol.*, vol. 157, pp. 2023–2035, 2000.

[121] S. Y. C. Kang, N. Kannan, L. Zhang, V. Martinez, M. P. Rosin, and C. J. Eaves, “Characterization of epithelial progenitors in normal human palatine tonsils and their HPV16 E6/E7-induced perturbation,” *Stem cell reports*, vol. 5, no. 6, pp. 1210–1225, Dec. 2015.

[122] K. Basso and R. Dalla-Favera, “Germinal centres and B cell lymphomagenesis,” *Nat. Rev. Immunol.*, vol. 15, no. 3, pp. 172–184, 2015.

[123] A. Vitelli, M. R. Quirion, C.-Y. Lo, J. A. Misplon, A. K. Grabowska, A. Pierantoni, V. Ammendola, G. E. Price, M. R. Soboleski, R. Cortese, S. Colloca, A. Nicosia, and S. L. Epstein, “Vaccination to conserved influenza antigens in mice using a novel Simian adenovirus vector, PanAd3, derived from the bonobo Pan paniscus,” *PLoS One*, vol. 8, no. 3, p. e55435, Jan. 2013.

[124] Q. Zhang, J. Bernatoniene, L. Bagrade, J. C. Paton, T. J. Mitchell, S. Hammerschmidt, D. A. Nunez, and A. Finn, “Regulation of production of mucosal antibody to pneumococcal protein antigens by T-cell-derived gamma interferon and

interleukin-10 in children," *Infect. Immun.*, vol. 74, no. 8, pp. 4735–4743, Aug. 2006.

[125] Miltenyi Biotec, "MACS® Cell Separation," 2018. [Online]. Available: https://www.miltenyibiotec.com/_Resources/Persistent/b5349effdd595b72195e588aff033be3e24706bd/IM0020021.pdf. [Accessed: 28-Jul-2018].

[126] B. J. C. Quah, H. S. Warren, and C. R. Parish, "Monitoring lymphocyte proliferation in vitro and in vivo with the intracellular fluorescent dye carboxyfluorescein diacetate succinimidyl ester," *Nat. Protoc.*, vol. 2, no. 9, pp. 2049–2056, 2007.

[127] T. Scientific, "eBioscience™ CFSE," 2018. [Online]. Available: https://www.thermofisher.com/order/catalog/product/65-0850-84. [Accessed: 06-Jun-2018].

[128] M. A. Navarrete, "ELISpot and DC-ELISpot assay to measure frequency of antigen-specific IFNγ-secreting cells," in *ELISA Methods and Protocols*, R. Hnasko, Ed. Humana Press, New York, NY, 2015, pp. 79–86.

[129] Mabtech, "Find 1 cell in 100,000 with ELISpot," 2017. [Online]. Available: https://www.mabtech.com/sites/default/files/2016-elispot-web.pdf. [Accessed: 06-Jun-2018].

[130] "ELISPOT," 2018. [Online]. Available: http://ars.els-cdn.com/content/image/1-s2.0-S0022202X16310594-gr1.jpg%0D%0A. [Accessed: 21-Sep-2017].

[131] Mabtech, "ELISpot Step-by-step," 2018. [Online]. Available: https://www.mabtech.com/knowledge-center/assay-principles/elispot-assay-principle/elispot-step-step. [Accessed: 07-Jun-2018].

[132] A. V. Lin, "Indirect ELISA," in *ELISA Methods and Protocols*, vol. 1318, Humana Press, New York, NY, 2015, pp. 51–59.

[133] "ELISA," 2018. [Online]. Available: http://laboratoryinfo.com/wp-content/uploads/2015/12/Indirect-elisa.png%0D%0A. [Accessed: 21-Sep-2017].

[134] World Health Organization, "Identification of the haemagglutinin subtype of viral isolates by haemagglutination inhibition testing," in *Manual for the laboratory diagnosis and virological surveillance of influenza*, WHO Press, 2011, pp. 43–57.

[135] T. Acharya, "Hemagglutination Inhibition Test (HAI): Principle, procedure, result and interpretations," 2014. [Online]. Available: https://microbeonline.com/wp-content/uploads/2014/12/Hemagglutination-Inhibition-image.jpg%0D%0A. [Accessed: 07-Nov-2017].

[136] L. Reperant, G. Rimmelzwaan, and A. Osterhaus, "Advances in influenza vaccination," *F1000Prime Rep.*, vol. 6, 2014.

[137] R. M. Buller and G. J. Palumbo, “Poxvirus pathogenesis,” *Microbiol. Rev.*, vol. 55, no. 1, pp. 80–122, 1991.

[138] J. Cook and J. Radke, “Mechanisms of pathogenesis of emerging adenoviruses,” *F1000Research*, vol. 6, p. 90, 2017.

[139] K. Xiang, G. Ying, Z. Yan, Y. Shanshan, Z. Lei, L. Hongjun, and S. Maosheng, “Progress on adenovirus-vectored universal influenza vaccines,” *Hum. Vaccines Immunother.*, vol. 11, no. 5, pp. 1209–1222, 2015.

[140] M. M. Gherardi and M. Esteban, “Recombinant poxviruses as mucosal vaccine vectors,” *J. Gen. Virol.*, vol. 86, no. 11, pp. 2925–2936, Nov. 2005.

[141] A. Chahroudi, R. Chavan, N. Kozyr, N. Koyzr, E. K. Waller, G. Silvestri, and M. B. Feinberg, “Vaccinia virus tropism for primary hematolymphoid cells is determined by restricted expression of a unique virus receptor,” *J. Virol.*, vol. 79, no. 16, pp. 10397–10407, Aug. 2005.

[142] J. M. Sánchez-Puig, L. Sánchez, G. Roy, and R. Blasco, “Susceptibility of different leukocyte cell types to Vaccinia virus infection,” *Virol. J.*, vol. 1, no. 1, p. 10, Jan. 2004.

[143] C. Flechsig, Y. Suezer, M. Kapp, S. M. Tan, J. Löffler, G. Sutter, H. Einsele, and G. U. Grigoleit, “Uptake of antigens from modified vaccinia Ankara virus-infected leukocytes enhances the immunostimulatory capacity of dendritic cells,” *Cytotherapy*, vol. 13, no. 6, pp. 739–752, 2011.

[144] T. Kessler, K. Hamprecht, T. Feuchtinger, and G. Jahn, “Dendritic cells are susceptible to infection with wild-type adenovirus, inducing a differentiation arrest in precursor cells and inducing a strong T-cell stimulation,” *J. Gen. Virol.*, vol. 91, no. Pt 5, pp. 1150–1154, May 2010.

[145] K. Loré, W. C. Adams, M. J. E. Havenga, M. L. Precopio, L. Holterman, J. Goudsmit, and R. A. Koup, “Myeloid and plasmacytoid dendritic cells are susceptible to recombinant adenovirus vectors and stimulate polyfunctional memory T cell responses,” *J. Immunol.*, vol. 179, no. 3, pp. 1721–1729, Aug. 2007.

[146] C. Richardson, P. Brennan, M. Powell, S. Prince, Y.-H. Chen, O. B. Spiller, and M. Rowe, “Susceptibility of B lymphocytes to adenovirus type 5 infection is dependent upon both coxsackie-adenovirus receptor and alphavbeta5 integrin expression.,” *J. Gen. Virol.*, vol. 86, no. Pt 6, pp. 1669–79, Jun. 2005.

[147] J. Mullin, M. S. Ahmed, R. Sharma, N. Upile, H. Beer, P. Achar, S. Puksuriwong, F. Ferrara, N. Temperton, P. McNamara, T. Lambe, S. C. Gilbert, and Q. Zhang, “Activation of cross-reactive mucosal T and B cell responses in human nasopharynx-associated lymphoid tissue in vitro by Modified Vaccinia Ankara-vectored influenza vaccines,” *Vaccine*, vol. 34, no. 14, pp. 1688–1695, Mar. 2016.

[148] L. P. Titov, A. M. Dashkevich, V. L. Chekan, and L. M. DuBuske, “Phenotypic characterization of immune cells isolated from adenoids and tonsils of children with adenoid and tonsil hypertrophy,” *J. Allergy Clin. Immunol.*, vol. 129, no. 2, p. AB13, Feb. 2012.

[149] A. F. Altenburg, C. E. Van De Sandt, B. W. S. Li, R. J. MacLoughlin, R. A. M. Fouchier, G. Van Amerongen, A. Volz, R. W. Hendriks, R. L. De Swart, G. Sutter, G. F. Rimmelzwaan, and R. D. De Vries, “Modified vaccinia virus Ankara preferentially targets antigen presenting cells in vitro, ex vivo and in vivo,” *Sci. Rep.*, vol. 7, no. 1, p. 8580, 2017.

[150] G. L. Smith, J. Z. Levin, P. Palese, and B. Moss, “Synthesis and cellular location of the ten influenza polypeptides individually expressed by recombinant vaccinia viruses,” *Virology*, vol. 160, no. 2, pp. 336–345, Oct. 1987.

[151] A. F. Altenburg, C. E. van de Sandt, S. E. van Trierum, H. L. M. De Gruyter, P. R. W. A. van Run, R. A. M. Fouchier, K. Roose, X. Saelens, A. Volz, G. Sutter, R. D. de Vries, and G. F. Rimmelzwaan, “Increased protein degradation improves influenza virus nucleoprotein-specific CD8+ T cell activation in vitro but not in C57BL/6 mice,” *J. Virol.*, vol. 90, no. 22, pp. 10209–10219, Nov. 2016.

[152] S. J. Draper, M. G. Cottingham, and S. C. Gilbert, “Utilizing poxviral vectored vaccines for antibody induction—Progress and prospects,” *Vaccine*, vol. 31, no. 39, pp. 4223–4230, Sep. 2013.

[153] M. Lyons, D. Onion, N. K. Green, K. Aslan, R. Rajaratnam, M. Bazan-Peregrino, S. Phipps, S. Hale, V. Mautner, L. W. Seymour, and K. D. Fisher, “Adenovirus type 5 interactions with human blood cells may compromise systemic delivery,” *Mol. Ther.*, vol. 14, no. 1, pp. 118–128, Jul. 2006.

[154] C. Richardson, P. Brennan, M. Powell, S. Prince, Y.-H. Chen, O. B. Spiller, and M. Rowe, “Susceptibility of B lymphocytes to adenovirus type 5 infection is dependent upon both coxsackie-adenovirus receptor and alphavbeta5 integrin expression,” *J. Gen. Virol.*, vol. 86, no. Pt 6, pp. 1669–1679, Jun. 2005.

[155] R. P. Leon, T. Hedlund, S. J. Meech, S. Li, J. Schaack, S. P. Hunger, R. C. Duke, and J. DeGregori, “Adenoviral-mediated gene transfer in lymphocytes,” *Proc. Natl.*

Acad. Sci. U. S. A., vol. 95, no. 22, pp. 13159–13164, Oct. 1998.

[156] Y. Zhang and J. M. Bergelson, “Adenovirus receptors,” *J. Virol.*, vol. 79, no. 19, pp. 12125–12131, Oct. 2005.

[157] C. A. Smith, L. S. Woodruff, G. R. Kitchingman, and C. M. Rooney, “Adenovirus-pulsed dendritic cells stimulate human virus-specific T-cell responses in vitro,” *J. Virol.*, vol. 70, no. 10, pp. 6733–6740, Oct. 1996.

[158] L. A. Lyakh, “Adenovirus type 5 vectors induce dendritic cell differentiation in human CD14+ monocytes cultured under serum-free conditions,” *Blood*, vol. 99, no. 2, pp. 600–608, Jan. 2002.

[159] A. Benlahrech, J. Harris, A. Meiser, T. Papagatsias, J. Hornig, P. Hayes, A. Lieber, T. Athanasopoulos, V. Bachy, E. Csomor, R. Daniels, K. Fisher, F. Gotch, L. Seymour, K. Logan, R. Barbagallo, L. Klavinskis, G. Dickson, and S. Patterson, “Adenovirus vector vaccination induces expansion of memory CD4 T cells with a mucosal homing phenotype that are readily susceptible to HIV-1,” *Proc. Natl. Acad. Sci. U. S. A.*, vol. 106, no. 47, pp. 19940–19945, Nov. 2009.

[160] W. William and K. Lor, “Recombinant adenovirus vector infection of human dendritic cells,” in *Viral Gene Therapy*, K. Xu, Ed. InTech, 2011, pp. 149–168.

[161] L. Y. H. Lee, D. L. A. Ha, C. Simmons, M. D. De Jong, N. V. V. Chau, R. Schumacher, C. P. Yan, A. J. McMichael, J. J. Farrar, G. L. Smith, A. R. M. Townsend, B. A. Askonas, S. Rowland-Jones, and T. Dong, “Memory T cells established by seasonal human influenza A infection cross-react with avian influenza A (H5N1) in healthy individuals,” *J. Clin. Invest.*, vol. 118, no. 10, pp. 3478–3490, 2008.

[162] J. Spitaels, K. Roose, and X. Saelens, “Influenza and memory T cells: How to awake the force,” *Vaccines*, vol. 4, no. 4, p. 33, 2016.

[163] G. T. Werner, U. Jentzsch, E. Metzger, and J. Simon, “Studies on poxvirus infections in irradiated animals,” *Arch. Virol.*, vol. 64, no. 3, pp. 247–256, 1980.

[164] R. D. Antrobus, P. J. Lillie, T. K. Berthoud, A. J. Spencer, J. E. McLaren, K. Ladell, T. Lambe, A. Milicic, D. A. Price, A. V. S. Hill, and S. C. Gilbert, “A T cell-inducing influenza vaccine for the elderly: Safety and immunogenicity of MVA-NP+M1 in adults aged over 50 years,” *PLoS One*, vol. 7, no. 10, p. e48322, Oct. 2012.

[165] P. J. Lillie, T. K. Berthoud, T. J. Powell, T. Lambe, C. Mullarkey, A. J. Spencer, M. Hamill, Y. Peng, M.-E. Blais, C. J. A. Duncan, S. H. Sheehy, T. Havelock, S. N.

Faust, R. L. Williams, A. Gilbert, J. Oxford, T. Dong, A. V. S. Hill, and S. C. Gilbert, “Preliminary assessment of the efficacy of a T-cell-based influenza vaccine, MVA-NP+M1, in humans,” *Clin. Infect. Dis.*, vol. 55, no. 1, pp. 19–25, Jul. 2012.

[166] R. D. Antrobus, T. K. Berthoud, C. E. Mullarkey, K. Hoschler, L. Coughlan, M. Zambon, A. V. Hill, and S. C. Gilbert, “Coadministration of seasonal influenza vaccine and MVA-NP+M1 simultaneously achieves potent humoral and cell-mediated responses,” *Mol. Ther.*, vol. 22, no. 1, pp. 233–238, Jan. 2014.

[167] T. K. Berthoud, M. Hamill, P. J. Lillie, L. Hwenda, K. A. Collins, K. J. Ewer, A. Milicic, H. C. Poyntz, T. Lambe, H. A. Fletcher, A. V. S. Hill, and S. C. Gilbert, “Potent CD8+ T-cell immunogenicity in humans of a novel heterosubtypic influenza a vaccine, MVA-NP+M1,” *Clin. Infect. Dis.*, vol. 52, no. 1, pp. 1–7, 2011.

[168] T. G. Boyce, W. C. Gruber, S. D. Coleman-Dockery, E. C. Sannella, G. W. Reed, M. Wolff, and P. F. Wright, “Mucosal immune response to trivalent live attenuated intranasal influenza vaccine in children,” *Vaccine*, vol. 18, no. 1/2, pp. 82–88, 1999.

[169] K. G. I. Mohn, F. Zhou, K. A. Brokstad, S. Sridhar, and R. J. Cox, “Boosting of cross-reactive and protection-associated T cells in children after live attenuated influenza vaccination,” *J. Infect. Dis.*, vol. 215, no. 10, pp. 1527–1535, 2017.

[170] S. B. Morgan, J. D. Hemmink, E. Porter, R. Harley, H. Shelton, M. Aramouni, H. E. Everett, S. M. Brookes, M. Bailey, A. M. Townsend, B. Charleston, and E. Tchilian, “Aerosol delivery of a candidate universal influenza vaccine reduces viral load in pigs challenged with pandemic H1N1 virus,” *J. Immunol.*, vol. 196, no. 12, pp. 5014–5023, 2016.

[171] P. Brandtzaeg, “Immune functions of nasopharyngeal lymphoid tissue,” *Adv. Otorhinolaryngol.*, vol. 72, pp. 20–24, Jan. 2011.

[172] A. Pizzolla, Z. Wang, J. R. Groom, K. Kedzierska, A. G. Brooks, P. C. Reading, and L. M. Wakim, “Nasal-associated lymphoid tissues (NALTs) support the recall but not priming of influenza virus-specific cytotoxic T cells,” *Proc. Natl. Acad. Sci.*, vol. 114, no. 20, pp. 5225–5230, May 2017.

[173] H. Y. Wu, H. H. Nguyen, and M. W. Russell, “Nasal lymphoid tissue (NALT) as a mucosal immune inductive site.,” *Scand. J. Immunol.*, vol. 46, no. 5, pp. 506–513, 1997.

[174] A. W. Zuercher, S. E. Coffin, M. C. Thurnheer, P. Fundova, and J. J. Cebra, “Nasal-associated lymphoid tissue is a mucosal inductive site for virus-specific humoral and cellular immune responses,” *J. Immunol.*, vol. 168, no. 4, pp. 1796–1803, 2002.

[175] D. F. Hoft, E. Babusis, S. Worku, C. T. Spencer, K. Lottenbach, S. M. Truscott, G. Abate, I. G. Sakala, K. M. Edwards, C. Buddy Creech, M. A. Gerber, D. I. Bernstein, F. Newman, I. Graham, E. L. Anderson, and R. B. Belshe, “Live and inactivated influenza vaccines induce similar humoral responses, but only live vaccines induce diverse T-cell responses in young children,” *J. Infect. Dis.*, vol. 204, no. 6, pp. 845–853, 2011.

[176] F.-M. Mbitikon-Kobo, M. Bonneville, R.-P. Sekaly, and L. Trautmann, “Ex vivo measurement of the cytotoxic capacity of human primary antigen-specific CD8 T cells,” *J. Immunol. Methods*, vol. 375, no. 1–2, pp. 252–257, 2012.

[177] K. S. Schluns and L. Lefrançois, “Cytokine control of memory T-cell development and survival,” *Nat. Rev. Immunol.*, vol. 3, no. 4, pp. 269–279, Apr. 2003.

[178] H. G. Woon, A. Braun, J. Li, C. Smith, J. Edwards, F. Sierro, C. G. Feng, R. Khanna, M. Elliot, A. Bell, A. D. Hislop, S. G. Tangye, A. B. Rickinson, T. Gebhardt, W. J. Britton, and U. Palendira, “Compartmentalization of total and virus-specific tissue-resident memory CD8+ T Cells in human lymphoid organs,” *PLoS Pathog.*, vol. 12, no. 8, p. e1005799, 2016.

[179] S. Sridhar, “Heterosubtypic T-cell immunity to influenza in humans: Challenges for universal T-cell influenza vaccines,” *Front. Immunol.*, vol. 7, p. 195, May 2016.

[180] Murphy, Kenneth P. Travers, Paul, M. Walport, C. A. Janeway, A. Mowat, and C. Weaver, *Janeway’s immunobiology*, 8th ed. New York ; Garland Science, 2012., 2012.

[181] D. S. McDermott, C. J. Knudson, and S. M. Varga, “Determining the breadth of the respiratory syncytial virus-specific T cell response,” *J. Virol.*, vol. 88, no. 6, pp. 3135–3143, Mar. 2014.

[182] J. Liu, B. Wu, S. Zhang, S. Tan, Y. Sun, Z. Chen, Y. Qin, M. Sun, G. Shi, Y. Wu, M. Sun, N. Liu, K. Ning, Y. Ma, B. Gao, J. Yan, F. Zhu, H. Wang, and G. F. Gao, “Conserved epitopes dominate cross-CD8 $^{+}$ T-cell responses against influenza A H1N1 virus among Asian populations,” *Eur. J. Immunol.*, vol. 43, no. 8, pp. 2055–2069, Aug. 2013.

[183] A. C. M. Boon, G. de Mutsert, Y. M. F. Graus, R. A. M. Fouchier, K. Sintnicolaas, A. D. M. E. Osterhaus, and G. F. Rimmelzwaan, “The magnitude and specificity of influenza A virus-specific cytotoxic T-lymphocyte responses in humans is related to HLA-A and -B phenotype,” *J. Virol.*, vol. 76, no. 2, pp. 582–590, 2002.

[184] T. A. Peterson, T. Bielawny, P. Lacap, R.-A. Hardie, C. Daniuk, L. Mendoza, S. Thavaneswaran, T. Kariri, J. Kimani, C. Wachihi, M. Kimani, T. B. Ball, F. A. Plummer, and M. Luo, “Diversity and frequencies of HLA class I and class II genes of an east African population,” *Open J. Genet.*, vol. 4, no. 2, pp. 99–124, Apr. 2014.

[185] The Royal Liverpool and Broadgreen University Hospitals and University of Liverpool, “Allele Frequencies in Worldwide Populations.” [Online]. Available: http://www.allelefrequencies.net/default.asp. [Accessed: 19-Jan-2018].

[186] G. Almanzar, D. Herndler-Brandstetter, S. V. Chaparro, B. Jenewein, M. Keller, and B. Grubeck-Loebenstein, “Immunodominant peptides from conserved influenza proteins – A tool for more efficient vaccination in the elderly?,” *Wiener Medizinische Wochenschrift*, vol. 157, no. 5–6, pp. 116–121, Mar. 2007.

[187] T. J. Powell, Y. Peng, T. K. Berthoud, M.-E. Blais, P. J. Lillie, A. V. S. Hill, S. L. Rowland-Jones, A. J. McMichael, S. C. Gilbert, and T. Dong, “Examination of influenza specific T cell responses after influenza virus challenge in individuals vaccinated with MVA-NP+M1 vaccine,” *PLoS One*, vol. 8, no. 5, p. e62778, May 2013.

[188] V. K. B. Pillai, S. Kannanganat, P. Penaloza-MacMaster, L. Chennareddi, H. L. Robinson, J. Blackwell, and R. R. Amara, “Different patterns of expansion, contraction and memory differentiation of HIV-1 Gag-specific CD8 T cells elicited by adenovirus type 5 and modified vaccinia Ankara vaccines,” *Vaccine*, vol. 29, no. 33, pp. 5399–5406, 2011.

[189] A. C. M. Boon, G. de Mutsert, R. A. M. Fouchier, A. D. M. E. Osterhaus, and G. F. Rimmelzwaan, “Functional profile of human influenza virus-specific cytotoxic T lymphocyte activity is influenced by interleukin-2 concentration and epitope specificity.,” *Clin. Exp. Immunol.*, vol. 142, no. 1, pp. 45–52, Oct. 2005.

[190] M. A. Cox, S. M. Kahan, and A. J. Zajac, “Anti-viral CD8 T cells and the cytokines that they love,” *Virology*, vol. 435, no. 1, pp. 157–169, Jan. 2013.

[191] R. A. Seder, P. A. Darrah, and M. Roederer, “T-cell quality in memory and protection: Implications for vaccine design,” *Nat. Rev. Immunol.*, vol. 8, no. 4, pp. 247–258, 2008.

[192] P. Wolint, M. R. Betts, R. A. Koup, and A. Oxenius, “Immediate cytotoxicity but not degranulation distinguishes effector and memory subsets of CD8 + T cells,” *J. Exp. Med.*, vol. 199, no. 7, pp. 925–936, 2004.

[193] A. R. Hersperger, G. Makedonas, and M. R. Betts, “Flow cytometric detection of perforin upregulation in human CD8 T cells,” *Cytom. Part A*, vol. 73, no. 11, pp. 1050–1057, 2008.

[194] G. Makedonas, P. P. Banerjee, R. Pandey, A. R. Hersperger, K. B. Sanborn, G. A. D. Hardy, J. S. Orange, and M. R. Betts, “Rapid up-regulation and granule-independent transport of perforin to the immunological synapse define a novel mechanism of antigen-specific CD8+ T cell cytotoxic activity,” *J. Immunol.*, vol. 182, no. 9, pp. 5560–5569, 2009.

[195] D. C. Ekiert and I. A. Wilson, “Broadly neutralizing antibodies against influenza virus and prospects for universal therapies,” *Curr. Opin. Virol.*, vol. 2, no. 2, pp. 134–41, Apr. 2012.

[196] D. Corti, A. L. Suguitan, D. Pinna, C. Silacci, B. M. Fernandez-Rodriguez, F. Vanzetta, C. Santos, C. J. Luke, F. J. Torres-Velez, N. J. Temperton, R. A. Weiss, F. Sallusto, K. Subbarao, and A. Lanzavecchia, “Heterosubtypic neutralizing antibodies are produced by individuals immunized with a seasonal influenza vaccine,” *J. Clin. Invest.*, vol. 120, no. 5, pp. 1663–1673, 2010.

[197] M. S. Miller, T. Tsibane, F. Krammer, R. Hai, S. Rahmat, C. F. Basler, and P. Palese, “1976 and 2009 H1N1 influenza virus vaccines boost anti-hemagglutinin stalk antibodies in humans,” *J. Infect. Dis.*, vol. 207, no. 1, pp. 98–105, 2013.

[198] G.-M. Li, C. Chiu, J. Wrammert, M. McCausland, S. F. Andrews, N.-Y. Zheng, J.-H. Lee, M. Huang, X. Qu, S. Edupuganti, M. Mulligan, S. R. Das, J. W. Yewdell, A. K. Mehta, P. C. Wilson, and R. Ahmed, “Pandemic H1N1 influenza vaccine induces a recall response in humans that favors broadly cross-reactive memory B cells,” *Proc. Natl. Acad. Sci.*, vol. 109, no. 23, pp. 9047–9052, 2012.

[199] D. J. Dilillo, G. S. Tan, P. Palese, and J. V. Ravetch, “Broadly neutralizing hemagglutinin stalk-specific antibodies require FcR interactions for protection against influenza virus in vivo,” *Nat. Med.*, vol. 20, no. 2, pp. 143–151, 2014.

[200] D. Corti, E. Cameroni, B. Guarino, N. L. Kallewaard, Q. Zhu, and A. Lanzavecchia, “Tackling influenza with broadly neutralizing antibodies,” *Curr. Opin. Virol.*, vol. 24, pp. 60–69, 2017.

[201] G. A. Sautto, G. A. Kirchenbaum, and T. M. Ross, “Towards a universal influenza vaccine: Different approaches for one goal,” *Virol. J.*, vol. 15, no. 1, p. 17, 2018.

[202] H. Ren and P. Zhou, “Epitope-focused vaccine design against influenza A and B viruses,” *Curr. Opin. Immunol.*, vol. 42, pp. 83–90, 2016.

[203] J. H. C. M. Kreijtz, Y. Suezer, G. de Mutsert, G. van Amerongen, A. Schwantes, J. M. A. van den Brand, R. A. M. Fouchier, J. Löwer, A. D. M. E. Osterhaus, G. Sutter, and G. F. Rimmelzwaan, "MVA-based H5N1 vaccine affords cross-clade protection in mice against influenza A/H5N1 viruses at low doses and after single immunization," *PLoS One*, vol. 4, no. 11, p. e7790, Nov. 2009.

[204] J. H. C. M. Kreijtz, Y. Suezer, G. de Mutsert, J. M. A. van den Brand, G. van Amerongen, B. S. Schnierle, T. Kuiken, R. A. M. Fouchier, J. Löwer, A. D. M. E. Osterhaus, G. Sutter, and G. F. Rimmelzwaan, "Recombinant Modified Vaccinia virus Ankara expressing the hemagglutinin gene confers protection against homologous and heterologous H5N1 influenza virus infections in macaques," *J. Infect. Dis.*, vol. 199, no. 3, pp. 405–413, Feb. 2009.

[205] A. N. Aljurayyan, "Characterisation of T follicular helper cell (TFH) in nasopharynx-associated yymphoid tissue and its effect on regulation of immune response to influenza virus," University of Liverpool, 2014.

[206] A. Röth, L. Schneider, H. Himmelreich, G. M. Baerlocher, and U. Dührsen, "Impact of culture conditions on the proliferative lifespan of human T cells in vitro," *Cytotherapy*, vol. 9, no. 1, pp. 91–98, 2007.

[207] M. K. Hoffmann and J. A. Hirst, "Principles of in vitro immunization of human B lymphocytes," in *Human hybridomas and monoclonal antibodies*, Plenum Press, 1985, pp. 279–281.

[208] E. Thorsby, "The role of HLA in T cell activation," *Hum. Immunol.*, vol. 9, no. 1, pp. 1–7, 1984.

[209] A. Aljurayyan, S. Puksuriwong, M. Ahmed, R. Sharma, M. Krishnan, S. Sood, K. Davies, D. Rajashekar, S. Leong, P. S. McNamara, S. Gordon, and Q. Zhang, "Activation and induction of antigen-specific T follicular helper cells play a critical role in live-attenuated influenza vaccine-induced human mucosal anti-influenza antibody response," *J. Virol.*, vol. 92, no. 11, pp. e00114–e00118, Mar. 2018.

[210] S.-E. Bentebibel, S. Lopez, G. Obermoser, N. Schmitt, C. Mueller, C. Harrod, E. Flano, A. Mejias, R. A. Albrecht, D. Blankenship, H. Xu, V. Pascual, J. Banchereau, A. Garcia-Sastre, A. K. Palucka, O. Ramilo, and H. Ueno, "Induction of ICOS+CXCR3+CXCR5+ TH cells correlates with antibody responses to influenza vaccination," *Sci. Transl. Med.*, vol. 5, no. 176, p. 176ra32, 2013.

[211] A. Kamlangdee, B. Kingstad-Bakke, and J. E. Osorio, "Mosaic H5 hemagglutinin provides broad humoral and cellular immune responses against influenza viruses," *J. Virol.*, vol. 90, no. 15, pp. 6771–6783, 2016.

[212] A. N. Aljurayyan, R. Sharma, N. Upile, H. Beer, C. Vaughan, C. Xie, P. Achar, M. S. Ahmed, P. S. McNamara, S. B. Gordon, and Q. Zhang, “A critical role of T follicular helper cells in human mucosal anti-influenza response that can be enhanced by immunological adjuvant CpG-DNA,” *Antiviral Res.*, vol. 132, pp. 122–130, 2016.

[213] J. H. C. M. Kreijtz, Y. Suzer, R. Bodewes, A. Schwantes, G. van Amerongen, R. J. Verburgh, G. de Mutsert, J. van den Brand, S. E. van Trierum, T. Kuiken, R. A. M. Fouchier, A. D. M. E. Osterhaus, G. Sutter, and G. F. Rimmelzwaan, “Evaluation of a modified vaccinia virus Ankara (MVA)-based candidate pandemic influenza A/H1N1 vaccine in the ferret model,” *J. Gen. Virol.*, vol. 91, no. 11, pp. 2745–2752, Nov. 2010.

[214] R. Nachbagauer, T. J. Wohlbold, A. Hirsh, R. Hai, H. Sjursen, P. Palese, R. J. Cox, and F. Krammer, “Induction of broadly reactive anti-hemagglutinin stalk antibodies by an H5N1 vaccine in humans,” *J. Virol.*, vol. 88, no. 22, pp. 13260–13268, 2014.

[215] G. Di Mario, E. Soprana, F. Gubinelli, M. Panigada, M. Facchini, C. Fabiani, B. Garulli, M. Basileo, A. Cassone, A. Siccardi, I. Donatelli, and M. R. Castrucci, “Immunogenicity of modified vaccinia virus Ankara expressing the hemagglutinin stalk domain of pandemic (H1N1) 2009 influenza virus,” *Pathog. Glob. Health*, vol. 111, no. 2, pp. 69–75, 2017.

[216] A. Hessel, M. Schwendinger, G. W. Holzer, K. K. Orlinger, S. Coulibaly, H. Savidis-Dacho, M.-L. Zips, B. A. Crowe, T. R. Kreil, H. J. Ehrlich, P. N. Barrett, and F. G. Falkner, “Vectors based on modified vaccinia Ankara expressing influenza H5N1 hemagglutinin induce substantial cross-clade protective immunity,” *PLoS One*, vol. 6, no. 1, p. e16247, Jan. 2011.

[217] Y. Luo, T. Mohan, W. Zhu, C. Wang, L. Deng, and B. Z. Wang, “Sequential immunizations with heterosubtypic virus-like particles elicit cross protection against divergent influenza A viruses in mice,” *Sci. Rep.*, vol. 8, no. 1, p. 4577, 2018.

[218] C. J. Henry Dunand, P. E. Leon, M. Huang, A. Choi, V. Chromikova, I. Y. Ho, G. S. Tan, J. Cruz, A. Hirsh, N.-Y. Zheng, C. E. Mullarkey, F. A. Ennis, M. Terajima, J. J. Treanor, D. J. Topham, K. Subbarao, P. Palese, F. Krammer, and P. C. Wilson, “Both neutralizing and non-neutralizing human H7N9 influenza vaccine-induced monoclonal antibodies confer protection,” *Cell Host Microbe*, vol. 19, no. 6, pp. 800–813, Jun. 2016.

[219] R. Nachbagauer, A. Choi, R. Izikson, M. M. Cox, P. Palese, and F. Krammer, “Age dependence and isotype specificity of influenza virus hemagglutinin stalk-reactive antibodies in humans,” *MBio*, vol. 7, no. 1, pp. e01996-15, 2016.

[220] J. Wrammert, K. Smith, J. Miller, W. A. Langley, K. Kokko, C. Larsen, N.-Y. Zheng, I. Mays, L. Garman, C. Helms, J. James, G. M. Air, J. D. Capra, R. Ahmed, and P. C. Wilson, “Rapid cloning of high-affinity human monoclonal antibodies against influenza virus,” *Nature*, vol. 453, no. 7195, pp. 667–671, May 2008.

[221] C. M. Trombetta, C. Ulivieri, R. J. Cox, E. J. Remarque, C. Centi, D. Perini, G. Piccini, S. Rossi, S. Marchi, and E. Montomoli, “Impact of erythrocyte species on assays for influenza serology,” *J. Prev. Med. Hyg.*, vol. 59, no. 1, 2018.

[222] I. Stephenson, J. M. Wood, K. G. Nicholson, and M. C. Zambon, “Sialic acid receptor specificity on erythrocytes affects detection of antibody to avian influenza haemagglutinin,” *J. Med. Virol.*, vol. 70, no. 3, pp. 391–398, 2003.

[223] A. Impagliazzo, F. Milder, H. Kuipers, M. V. Wagner, X. Zhu, R. M. B. Hoffman, R. Van Meersbergen, J. Huizingh, P. Wanningen, J. Verspuij, M. De Man, Z. Ding, A. Apetri, B. Kükrer, E. Sneekes-Vriese, D. Tomkiewicz, N. S. Laursen, P. S. Lee, A. Zakrzewska, L. Dekking, J. Tolboom, L. Tettero, S. Van Meerten, W. Yu, W. Koudstaal, J. Goudsmit, A. B. Ward, W. Meijberg, I. A. Wilson, and K. Radoševic, “A stable trimeric influenza hemagglutinin stem as a broadly protective immunogen,” *Science (80-.).*, vol. 349, no. 6254, pp. 1301–1306, 2015.

[224] F. Krammer, I. Margine, G. S. Tan, N. Pica, J. C. Krause, and P. Palese, “A carboxy-terminal trimerization domain stabilizes conformational epitopes on the stalk domain of soluble recombinant Hemagglutinin substrates,” *PLoS One*, vol. 7, no. 8, 2012.

[225] R. Hai, F. Krammer, G. S. Tan, N. Pica, D. Eggink, J. Maamary, I. Margine, R. A. Albrecht, and P. Palese, “Influenza Viruses Expressing Chimeric Hemagglutinins: Globular Head and Stalk Domains Derived from Different Subtypes,” *J. Virol.*, vol. 86, no. 10, pp. 5774–5781, 2012.

[226] A. Vrdoljak, E. A. Allen, F. Ferrara, N. J. Temperton, A. M. Crean, and A. C. Moore, “Induction of broad immunity by thermostabilised vaccines incorporated in dissolvable microneedles using novel fabrication methods,” *J. Control. Release*, vol. 225, pp. 192–204, 2016.

[227] F. Ferrara and N. Temperton, “Chimeric influenza haemagglutinins: Generation and use in pseudotype neutralization assays,” *MethodsX*, vol. 4, pp. 11–24, 2017.

[228] S. F. Andrews, Y. Huang, K. Kaur, L. I. Popova, I. Y. Ho, N. T. Pauli, C. J. H. Dunand, W. M. Taylor, S. Lim, M. Huang, X. Qu, J.-H. Lee, M. Salgado-Ferrer, F. Krammer, P. Palese, J. Wrammert, R. Ahmed, and P. C. Wilson, “Immune history profoundly affects broadly protective B cell responses to influenza,” *Sci. Transl. Med.*, vol. 7, no. 316, p. 316ra192, Dec. 2015.

[229] S. M. Tete, F. Krammer, S. Lartey, G. Bredholt, J. Wood, S. Skrede, and R. J. Cox, “Dissecting the hemagglutinin head and stalk-specific IgG antibody response in healthcare workers following pandemic H1N1 vaccination,” *npj Vaccines*, vol. 1, p. 16001, 2016.

[230] R. Gasparini, D. Amicizia, P. L. Lai, and D. Panatto, “Live attenuated influenza vaccine-a review,” *J. Prev. Med. Hyg.*, vol. 52, no. 3, pp. 95–101, 2011.

[231] MedImmune, “FLUMIST® QUADRIVALENT PRESCRIBING INFORMATION.” [Online]. Available: http://www.fda.gov/downloads/BiologicsBloodVaccines/Vaccines/ApprovedProducts/ucm294307.pdf. [Accessed: 30-Jul-2015].

[232] World Health Organization, “Emergencies preparedness, response.” [Online]. Available: http://www.who.int/csr/don/archive/year/2015/en/. [Accessed: 30-Jul-2015].

[233] F. van Ginkel, H. H. Nguyen, and J. R. McGhee, “Vaccines for mucosal immunity to combat emerging infectious diseases,” *Emerg. Infect. Dis.*, vol. 6, no. 2, pp. 123–132, Apr. 2000.

[234] I. M. Belyakov and J. D. Ahlers, “What role does the route of immunization play in the generation of protective immunity against mucosal pathogens?,” *J. Immunol.*, vol. 183, no. 11, pp. 6883–6892, 2009.

[235] K. G.-I. Mohn, K. A. Brokstad, R. D. Pathirana, G. Bredholt, Å. Jul-Larsen, M. C. Trieu, S. L. Lartey, E. Montemoli, C. Tøndel, H. J. Aarstad, and R. J. Cox, “Live attenuated influenza vaccine in children induces B-cell responses in tonsils,” *J. Infect. Dis.*, vol. 214, no. 5, pp. 722–731, 2016.

[236] J. A. Panapasa, R. J. Cox, K. G. I. Mohn, L. A. Aqrawi, and K. A. Brokstad, “The expression of B & T cell activation markers in children’s tonsils following live attenuated influenza vaccine,” *Hum. Vaccin. Immunother.*, vol. 11, no. 7, pp. 1663–1672, Jul. 2015.

[237] C. S. Rollier, A. Reyes-Sandoval, M. G. Cottingham, K. Ewer, and A. V. S. Hill, “Viral vectors as vaccine platforms: Deployment in sight,” *Curr. Opin. Immunol.*, vol. 23, no. 3, pp. 377–382, 2011.

[238] A. V. S. Hill, A. Reyes-Sandoval, G. O’Hara, K. Ewer, A. Lawrie, A. Goodman, A. Nicosia, A. Folgori, S. Colloca, R. Cortese, S. C. Gilbert, and S. J. Draper, “Prime-boost vectored malaria vaccines: Progress and prospects,” *Hum. Vaccin.*, vol. 6, no. 1, pp. 78–83, Jan. 2010.

[239] S. C. Gilbert, V. S. Moorthy, L. Andrews, A. A. Pathan, S. J. McConkey, J. M. Vuola, S. M. Keating, T. Berthoud, D. Webster, H. McShane, and A. V. S. Hill, “Synergistic DNA–MVA prime-boost vaccination regimes for malaria and tuberculosis,” *Vaccine*, vol. 24, no. 21, pp. 4554–4561, May 2006.

[240] R. R. Amara, F. Villinger, J. D. Altman, S. L. Lydy, S. P. O’Neil, S. I. Staprans, D. C. Montefiori, Y. Xu, J. G. Herndon, L. S. Wyatt, M. A. Candido, N. L. Kozyr, P. L. Earl, J. M. Smith, H.-L. Ma, B. D. Grimm, M. L. Hulsey, H. M. McClure, J. M. McNicholl, B. Moss, and H. L. Robinson, “Control of a mucosal challenge and prevention of AIDS by a multiprotein DNA/MVA vaccine,” *Vaccine*, vol. 20, no. 15, pp. 1949–1955, May 2002.

[241] T. Lambe, J. B. Carey, Y. Li, A. J. Spencer, A. van Laarhoven, C. E. Mullarkey, A. Vrdoljak, A. C. Moore, and S. C. Gilbert, “Immunity against heterosubtypic influenza virus induced by adenovirus and MVA expressing nucleoprotein and matrix protein-1,” *Sci. Rep.*, vol. 3, p. 1443, 2013.

[242] I. Drexler, C. Staib, and G. Sutter, “Modified vaccinia virus Ankara as antigen delivery system: how can we best use its potential?,” *Curr Opin Biotechnol*, vol. 15, no. 6, pp. 506–512, 2004.

[243] J. C. Ramirez, D. Finke, M. Esteban, J. P. Kraehenbuhl, and H. Acha-Orbea, “Tissue distribution of the Ankara strain of vaccinia virus (MVA) after mucosal or systemic administration,” *Arch. Virol.*, vol. 148, no. 5, pp. 827–839, 2003.

[244] M. Corbett, W. M. Bogers, J. L. Heeney, S. Gerber, C. Genin, A. Didierlaurent, H. Oostermeijer, R. Dubbes, G. Braskamp, S. Lerondel, C. E. Gomez, M. Esteban, R. Wagner, I. Kondova, P. Mooij, S. Balla-Jhagjhoorsingh, N. Beenhakker, G. Koopman, S. van der Burg, J.-P. Kraehenbuhl, and A. Le Pape, “Aerosol immunization with NYVAC and MVA vectored vaccines is safe, simple, and immunogenic.,” *Proc. Natl. Acad. Sci. U. S. A.*, vol. 105, no. 6, pp. 2046–2051, 2008.

[245] B. Piet, G. J. De Bree, B. S. Smids-Dierdorp, C. M. Van Der Loos, E. B. M. Remmerswaal, J. H. Von Der Thüsen, J. M. W. Van Haarst, J. P. Eerenberg, A. Ten Brinke, W. Van Der Bij, W. Timens, R. A. W. Van Lier, and R. E. Jonkers, “CD8+ T cells with an intraepithelial phenotype upregulate cytotoxic function upon influenza infection in human lung,” *J. Clin. Invest.*, vol. 121, no. 6, pp. 2254–2263, 2011.

[246] C. Chiu and P. J. Openshaw, “Antiviral B cell and T cell immunity in the lungs,” *Nat. Immunol.*, vol. 16, no. 1, pp. 18–26, 2015.

[247] J. M. Schenkel, K. A. Fraser, and D. Masopust, “Cutting edge: Resident memory CD8 T cells occupy frontline niches in secondary lymphoid organs,” *J. Immunol.*, vol. 192,

no. 7, pp. 2961–2964, 2014.

[248] B. V. Kumar, W. Ma, M. Miron, T. Granot, R. S. Guyer, D. J. Carpenter, T. Senda, X. Sun, S. H. Ho, H. Lerner, A. L. Friedman, Y. Shen, and D. L. Farber, “Human tissue-resident memory T cells are defined by core transcriptional and functional signatures in lymphoid and mucosal sites,” *Cell Rep.*, vol. 20, no. 12, pp. 2921–2934, 2017.

[249] F. Krammer and P. Palese, “Influenza virus hemagglutinin stalk-based antibodies and vaccines,” *Curr. Opin. Virol.*, vol. 3, no. 5, pp. 521–530, 2013.

[250] P. E. Leon, W. He, C. E. Mullarkey, M. J. Bailey, M. S. Miller, F. Krammer, P. Palese, and G. S. Tan, “Optimal activation of Fc-mediated effector functions by influenza virus hemagglutinin antibodies requires two points of contact,” *Proc. Natl. Acad. Sci.*, vol. 113, no. 40, pp. 5944–5951, 2016.

[251] F. Cox, T. Kwaks, B. Brandenburg, M. H. Koldijk, V. Klaren, B. Smal, H. J. W. M. Korse, E. Geelen, L. Tettero, D. Zuijdgeest, E. J. M. Stoop, E. Saeland, R. Vogels, R. H. E. Friesen, W. Koudstaal, and J. Goudsmit, “HA antibody-mediated FcγRIIIa activity is both dependent on FcR engagement and interactions between HA and sialic acids,” *Front. Immunol.*, vol. 7, p. 399, 2016.

[252] N. W. Florek, A. Kamlangdee, J. P. Mutschler, B. Kingstad-Bakke, N. Schultz-Darken, K. W. Broman, J. E. Osorio, and T. C. Friedrich, “A modified vaccinia Ankara vaccine vector expressing a mosaic H5 hemagglutinin reduces viral shedding in rhesus macaques,” *PLoS One*, vol. 12, no. 8, p. e0181738, Aug. 2017.

……

Appendices

Appendix-1: Preparation of reagents and buffers

AEC substrate

AEC substrate is for ELISPOT assay.

1. Prepare 0.1 M acetate solution (pH 5.0)

1.1 Prepare 0.2 M acetic acid and 0.2 M sodium acetate

0.2 M acetic acid

Glacial acetic acid		1.15	ml
Deionised water	added to	100	ml

0.2 M sodium acetate

Sodium acetate (MW 82.03)		1.64	g
Deionised water	added to	100	ml

1.2 Mix 0.2 M acetic acid and 0.2 M sodium acetate and adjust pH to 5.0

0.2 M acetic acid	14.8	ml
0.2 M sodium acetate	35.2	ml
Deionised water	50.0	ml

Note: The solution could be stored at room temperature.

2. Prepare AEC stock solution

3-Amino-9-ethylcarbazole (AEC)	100	mg
N, N-Dimethylformamide, anhuydrous (DMF)	10	ml

Note: 1) The solution could be stably stored at 4°C with tightly sealed and protected from light.

2) Prepare in fume hood using polypropylene tubes (i.e. 15-ml centrifuge tube, Corning) and avoid using any polystyrene containers and disposable pipettes due to their incompatibility to DMF.

3. Dilute AEC stock solution in 0.1 M acetate solution to make working AEC substrate

AEC stock solution	333	μl
0.1 M acetate solution	10	ml

The solution needs filtering through 0.45 μm filter before adding 5 μl of 30% hydrogen peroxide, mixed well. The substrate should be immediately used and protected from light while incubating the plate.

***p*-Nitrophenylphosphate (PNPP) substrate**

PNPP substrate is for ELISA assay.

1. Preparing PNPP substrate diluent solution

Diethanolamine	97	ml
$MgCl_2$. $6H_20$	100	mg
Deionised water	800	ml

The pH was measured and adjusted to 9.8 by adding 10 M hydrochloric acid. Once adjusted, deionised water is added to obtain a final volume of 1000 ml. The solution could be stored at 4°C.

2. Dissolve PNPP substrate (1 mg/ml) in diluent buffer to make PNPP substrate

p-Nitrophenylphosphate tablet	5	mg
PNPP substrate solution	5	ml

The substrate should be immediately used and protected from light while incubating the plate.

0.5% chicken red blood cells

3 ml of chicken blood in Alsever's solution (First link, UK) was pipetted in centrifuge tube. After centrifugation at 1500 rpm for 5 min, supernatant and buffy layer are aspirated, leaving only red blood cells (RBC). RBCs are washed, by adding 10 ml 1XPBS followed by centrifugation at 1,500 rpm for 5 min. The washing is repeated for three times. The end result is packed chicken RBCs. 10% chicken RBCs is prepared by resuspending 0.3 ml of packed RBCs in 2.7 ml. Then 0.5% chicken RBCs is prepared as following

10% chicken RBCs	2.5	ml
1X PBS	47.5	ml

The reagent could be kept at 4°C for 24 hours. It should be gently shaken to homogenously resuspend RBCs before each use.

Standardised influenza virus antigen

1. Each influenza virus antigen (whole inactivated virus) is firstly examined for the HA titre. A HA unit is defined as the amount of virus needed to agglutinate an equal volume of RBCs suspension.
   1.1 Add 50 µl of PBS to two successive row for testing 1 antigen (i.e. A and B)
   1.2 Add 50 µl of standardized antigen to A1, B1 and make two-fold dilution by transferring 50 µl through 11 wells (A11) and discard the final 50 µl. Leave the last well (A12) for negative control.
   1.3 Add 50 µl of 0.5% chicken RBCs in every well.
   1.4 Mix by using a mechanical vibration or manually agitating the plates thoroughly
   1.5 Incubate the microplate for 30 min at room temperature and check the result when the RBCs control completely settle.

   HA titre is determined as the highest dilution that showed positive haemagglutination activity, where the RBCs are suspended in the solution and no RBC button is found at the bottom of the well.

2. When HA titre is measured, the antigen is diluted with 1X PBS to 8 HA units/ 50 µl by calculation. For example;

   HA titre of H1N1 antigen is 320 HA units/ 50 µl.

   The antigen need to be diluted at the ratio of 1:40 to make 8 HA units/ 50 µl.

3. The diluted antigen is performed back titration to verify the correction of HA units. The antigen is 2-fold serial diluted and 3-fold serial diluted in 1X PBS before adding 0.5% chicken RBCs as following steps;
   3.1 Add 50 µl of PBS to two successive row for testing 1 antigen (i.e. A and B)
   3.2 Add 50 µl of standardized antigen to A1, B1 and make two-fold dilution by transferring 50 µl through 5 wells (A6, B6) and discard the final 50 µl
   3.3 Add 25 µl of standardized antigen to A7, B7 and make three-fold dilution by transferring 50 µl through 5 wells (A11, B11) and discard the final 50 µl. Column 12 is left for the RBCs control (negative control).
   3.4 Add 50 µl of 0.5% chicken RBCs in every well.
   3.5 Mix by using a mechanical vibration or manually agitating the plates thoroughly
   3.6 Incubate the microplate for 30 min at room temperature and check the result when the RBCs control completely settle.

4. The standardised antigen must show the complete agglutination in the first three wells of two-fold dilution and the first two wells of three-fold dilution, meaning HA titre is in between 6 and 8 as shown in the following table.

Dilution	2-fold dilution						3-fold dilution					PBS
Row	1	2	3	4	5	6	7	8	9	10	11	12
Result	+	+	+	-	-	-	+	+	-	-	-	-

If the antigen does not have an HA titer of 8, it must be adjusted accordingly by adding more original antigen stock to increase units or by diluting with PBS to decrease units and repeat back titration until obtaining the desired HA unit.

Appendix-2: Measurement of cell viability using propidium iodide

Tonsillar MNCs following 10-day incubation without any stimulation were harvested and resuspended in 100 µl FACS staining buffer then stained with 5 µl propidium iodide solution (eBiosciences, UK) for 5-15 minutes at room temperature with protection from light. Without washing, labeled-cells were acquired their data of cell viability by flow-cytometry.

Gating on the majority of two main populations on FSC-SSC plot, the gate left most debris on the bottom left corner. The selected population was plotted in histogram against propidium iodide, showing three peaks that may refer to three different stage of cell viability within cell population. Cells with lowest intensity of PI (blue) were referred to live cells, whereas cells with increasing intensity of PI (yellow) were referred to dying cells (or in intermediate stage). The cells with the highest PI intensity (red) were dead cells, so they could not resist to dye penetration. With PI staining, it showed that the majority of viable cells were the population on the far right on the FSC-SSC plot, while the dying and dead cells were in the population next to debris at the left corner on the plot.

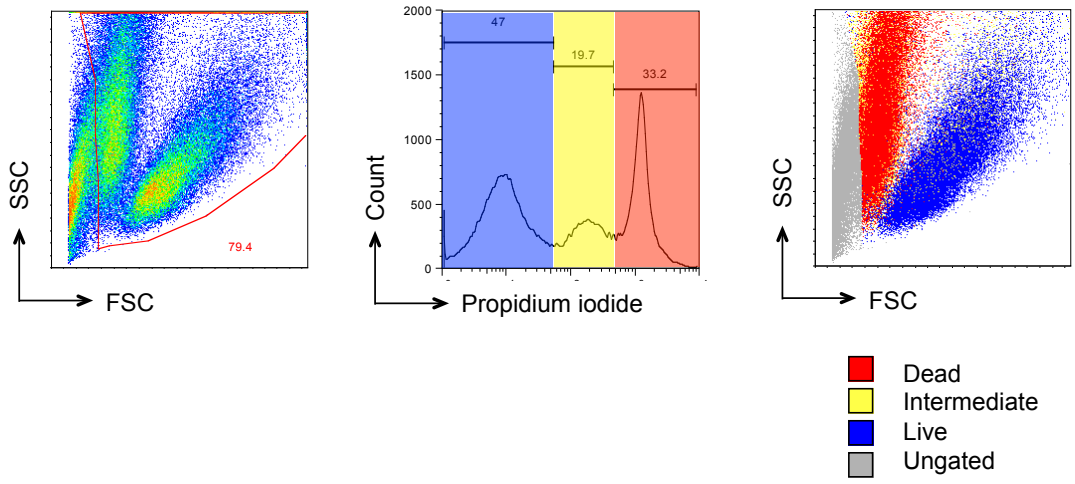

.....